

The Effects of Cyclodextrins and Micelles on some Organic Reactions:
Probes of Supramolecular Catalysis

Ogaritte Jennifer Yazbeck

A Thesis
in
The Department
of
Chemistry and Biochemistry

Presented in Partial Fulfilment of the Requirements
For the Degree of Doctor of Philosophy at
Concordia University
Montréal, Quebec, Canada

December, 2004

© Ogaritte Jennifer Yazbeck, 2004



Library and
Archives Canada

Bibliothèque et
Archives Canada

Published Heritage
Branch

Direction du
Patrimoine de l'édition

395 Wellington Street
Ottawa ON K1A 0N4
Canada

395, rue Wellington
Ottawa ON K1A 0N4
Canada

Your file Votre référence

ISBN: 0-494-04039-4

Our file Notre référence

ISBN: 0-494-04039-4

NOTICE:

The author has granted a non-exclusive license allowing Library and Archives Canada to reproduce, publish, archive, preserve, conserve, communicate to the public by telecommunication or on the Internet, loan, distribute and sell theses worldwide, for commercial or non-commercial purposes, in microform, paper, electronic and/or any other formats.

The author retains copyright ownership and moral rights in this thesis. Neither the thesis nor substantial extracts from it may be printed or otherwise reproduced without the author's permission.

AVIS:

L'auteur a accordé une licence non exclusive permettant à la Bibliothèque et Archives Canada de reproduire, publier, archiver, sauvegarder, conserver, transmettre au public par télécommunication ou par l'Internet, prêter, distribuer et vendre des thèses partout dans le monde, à des fins commerciales ou autres, sur support microforme, papier, électronique et/ou autres formats.

L'auteur conserve la propriété du droit d'auteur et des droits moraux qui protègent cette thèse. Ni la thèse ni des extraits substantiels de celle-ci ne doivent être imprimés ou autrement reproduits sans son autorisation.

In compliance with the Canadian Privacy Act some supporting forms may have been removed from this thesis.

Conformément à la loi canadienne sur la protection de la vie privée, quelques formulaires secondaires ont été enlevés de cette thèse.

While these forms may be included in the document page count, their removal does not represent any loss of content from the thesis.

Bien que ces formulaires aient inclus dans la pagination, il n'y aura aucun contenu manquant.


Canada

ABSTRACT

The Effects of Cyclodextrins and Micelles on some Organic Reactions:

Probes of Supramolecular Catalysis.

Ogaritte Jennifer Yazbeck, Ph.D.

Concordia University, 2004.

The recent interest in non-covalently stabilized molecular assemblies has led to the creation of the field of *supramolecular chemistry*. This thesis is concerned with the effects of supramolecular (host-guest) binding on organic reactivity. Of particular interest is the *catalysis* of organic reactions brought about by *transition state stabilization*, which arises from the binding of substrates (guests) relative to the strength of binding of the transition states to catalytic hosts such as cyclodextrins and micelles. In effect, the work of this thesis is concerned with the origin of *supramolecular catalysis*.

The first area of research discussed in the thesis exploits the principles of supramolecular chemistry (Chapter I, Section 1.1) and hydrophobic effects (Chapter I, Section 1.3) to investigate cyclodextrin-guest inclusion complexes (Chapter II). The effects of cyclodextrins on the reactivity of acid-catalyzed hydrolysis of two acetals and an orthobenzoate in the presence of added ketone guests were studied (Chapter III) as part of a search for improved methods of accurately determining the strength of complexation between cyclodextrins and various guests (eg. ketones). It was shown that *inhibition kinetics* can be employed as a fast reliable methodology to determine the dissociation constants of β -cyclodextrin-ketone complexes under certain circumstances.

The second area of research, which constitutes the bulk of the work in the thesis, focussed on micelles (Chapter IV) and their *catalytic* effects on bimolecular ester cleavage reactions from the perspective of *transition state stabilization* (Chapter I, Section 1.2). The work was initiated after previous research on the alkaline hydrolysis of aryl esters in cetyltrimethylammonium bromide (CTAB) micelles (Chapter V). In those studies it was shown that aryl ester binding to CTAB micelles is independent of the aryl group but it depends on the *hydrophobicity* of the ester chain. The magnitude of catalysis is, however, independent of the ester chain. Following these intriguing results, and in order to clarify the misconceptions about the mechanism of the catalysis by the micelles, it was decided was to investigate the effects of CTAB micelles on ester cleavage by other nucleophiles.

Firstly, the thiolysis of *p*-nitrophenyl alkanoates (acetate to decanoate) in CTAB micelles was studied (Chapter VI). It was found that the magnitude of catalysis is independent of ester chain length, but it depends on the ability of the thiolate anion to transfer from the aqueous phase to the micellar pseudo-phase. The mode and strength of binding of the ester acyl chain to the hydrophobic core of CTAB micelles is the same in both the initial and transition state, and is independent of the ionic nucleophile.

Secondly, the aminolysis of *p*-nitrophenyl esters by neutral amines (mainly *n*-alkylamines) in CTAB micelles was studied (Chapter VII). The reactions of the acetate (pNPA) and hexanoate (pNPH) esters are retarded with the short amines but catalysed with the longer, more hydrophobic ones. The magnitude of catalysis is proportional to *hydrophobic partitioning* of the amine between water and the micelles in the case of pNPA but an additional factor is evident with pNPH. For longer esters and a long amine,

the modes of binding of both the ester and the amine in the transition state are dependent on one another, and the reduced catalysis, despite the concentration effect, was ascribed to the *optimal geometry* for acyl transfer is not readily accessible because of the conflicting demands of binding both the alkyl chain of both reactants in the transition state, as compared to the initial state.

Finally, a study of the cleavage of pNPA and pNPH by amino acid anions (AA^-) in CTAB micelles demonstrated that a *threshold hydrophobicity* dictates the partitioning and binding of the AA^- to the CTAB micelles (Chapter VIII). The mode of transition state binding is independent of the shorter AA^- and is dependent on the longer AA^- . Thus, the results show similarities to those in Chapter VI and to those in Chapter VII.

Micellar catalytic effects on the reactions (Chapters VI - VIII) was discussed from the perspective of transition state stabilization, and Kirby's dissection transition state binding into *passive* and *dynamic* binding was found to be practical for discussion of the micellar-mediated reactions. Future discussions of catalytic processes, in general, should focus more on transition state stabilization by the catalyst in order to find a deeper understanding of mechanisms of catalysis.

ACKNOWLEDGMENTS

First and foremost, I would like to extend immeasurable gratitude to my research supervisor, Professor Oswald S. Tee, for inspiring me to pursue my Ph.D. in Physical Organic Chemistry. His enthusiasm in teaching, knowledge, patience, constant dedication to the research conducted in his laboratory, and optimistic feedback on both professional as well as personal levels, are just a few qualities worth admiring and in the long run emulating. It was an honour to work under his supervision.

I would like to thank Dr. Gilles Peslherbe and Dr. Joanne Turnbull for serving on my yearly committee. Dr. Turnbull's enthusiasm and humbleness leaves a lasting smile on my face every time I see her. I also thank Dr. Heidi Muchall, who served on my proposal committee and for offering her services and accommodating me when I attended the 29th POMS conference in Toronto.

Many thanks to Dr. Louis Cuccia for allowing me to use his privileges at McGill University to use the NMR facilities, and for boosting my confidence after reading my research proposal.

Thanks to Dr. Sébastien Robidoux for having faith in my organic chemistry knowledge, and for recommending me to teach at Champlain College. I thank Dr. Peter Bird for recognizing my dedication to teaching; he indirectly pushed me to tutor general chemistry 205/206 for 3 years, and that greatly improved my teaching style.

I thank the Department of Chemistry at Concordia University for the teaching assistantship and the opportunity to pursue my Ph.D. at this extraordinary unique university.

I would like to express my appreciation to my colleagues in the lab, Alexei Fedorotchenko, Isabelle Turner and Delna Ghadiali and Mike Boyd. A special thanks goes to my good friend Paul Loncke, he sure made my stay at Concordia a memorable one. Good luck to all of them.

I would like to thank my friends for fulfilling my life outside the lab. Ghada Chahrour, Samar Debouk, Sarine Reda, Rana Abbas, Wafa Ataya and Rawan Morani, I was very fortunate to have them all in my life in its good and in its bad. May our friendship last forever.

I thank my extended family of my aunts, uncles, cousins, and my grandparents, who are more anxious than me to finish. I thank my uncle Dr. Adel Hazime, my role model for this life and for the after life. As a teenager I wanted to be just like my uncle; I am still far from it, though I am one step closer.

All this would not be possible without my loving immediate family. Danny, as my young brother following my footsteps, you make me so proud and I sure look up to you now. Marcel, my baby bro, I am learning from you about business, though I think you are too smart and your heart is too white for “that world”. Jamal, you are no less than a brother to me, thank you for escorting me to religious events. Mom and Dad, you put education as the highest priority for us, you instilled in us the drive to succeed, and you were always dedicated to making us happy. I could not have done this without your friendship, trust, faith, patience, and constant support. May God keep you over our head always, and help me give a little back to you. Finally, mom, wherever you are, I hope you can see and be proud of your little girl. I love you.

My best regards to all,
Ogaritte Jennifer Yazbeck

TABLE OF CONTENTS

List of Figures	xiii
List of Schemes.....	xvi
List of Tables	xvii
List of Abbreviations	xx

CHAPTER I. GENERAL INTRODUCTION

1.1 INTRODUCTION TO SUPRAMOLECULAR CHEMISTRY	1
1.1.1 Supramolecular Complexes	3
1.1.2 Molecular Recognition	6
1.1.2.1 Selectivity: Bias versus Recognition	7
1.1.3 Quantifying the Binding Strength of Supramolecular Complexes	8
1.1.4 Supramolecular Reactivity and Catalysis	9
1.1.4.1 Enzyme Mimics	9
1.2 BACKGROUND TO TRANSITION STATE STABILIZATION.....	12
1.2.1 Transition State Theory (TST).....	13
1.2.2 TST Applied to TS Binding and Catalysis	14
1.2.3 What Does K_{TS} Stand For?	15
1.2.4 Application of K_{TS} as a Tool for Predicting Modes of Binding to a Catalyst	20
1.3 BACKGROUND TO THE HYDROPHOBIC EFFECTS.....	21
1.3.1 Definition of Hydrophobicity and the Hydrophobic Effect.....	22
1.3.2 Definition and Explanation of Hydrophobic Interaction	24

CHAPTER II. CYCLODEXTRINS

2.1 INTRODUCING CYCLODEXTRINS	27
2.1.1 Structure of Cyclodextrins.....	27
2.1.2 Requirements for Formation of Cyclodextrin Inclusion Complexes	31
2.1.3 The Driving Force for Complex Formation	33
2.2 EFFECT OF CYCLODEXTRINS ON REACTIONS	36
2.3 OBJECTIVE OF THE RESEARCH	38

CHAPTER III. KINETICS OF ACETAL AND ORTHOBENZOATE HYDROLYSIS AS PROBES OF CYCLODEXTRIN–KETONE BINDING

3.1 INTRODUCTION	40
3.2 RESULTS	44
3.2.1 Mechanism and Probe Reaction.....	44
3.2.2 Effect of Cyclodextrins	47
3.2.3 Effects of Added Guests	49
3.3 DISCUSSION	55
3.3.1 Substrate Binding to CDs.....	55
3.3.2 Transition State Binding and the Reactivity of the CD-Bound Forms	57
3.3.3 Cyclodextrin-Ketone Binding.....	60
a) Assessing the probe reaction for estimating K_G values	60
b) Effect of chain length on the binding of ketones to β -CD.....	63
c) Binding of unsymmetrical ketones to β -CD	66
d) Binding of ketones versus secondary alcohols to β -CD.....	69
3.4 CONCLUSIONS.....	70
3.5 EXPERIMENTAL.....	73
3.5.1 Material	73
3.5.2 Kinetic Apparatus and Solutions	74
3.5.3 Kinetic Analysis.....	75

CHAPTER IV. MICELLES

4.1 INTRODUCING MICELLES	80
4.2.1 Surfactants	80
4.2 MICELLES AND THEIR FORMATION FROM SURFACTANT BUILDING BLOCKS	83
4.2.1 The Critical Micelle Concentration	84
4.2.2 Micellar Aggregation Number.....	87
4.2.3 Thermodynamic Parameters of Micellization	88
4.2.4 Micellar Structure	92
4.3 MICELLAR EFFECTS ON ORGANIC REACTIONS	95
4.3.1 Proximity Effects	95
4.3.2 Medium Effects.....	99

4.5 KINETIC TREATMENT OF REACTIONS MEDIATED BY MICELLES.....	102
4.5.1 The Pseudo-phase Model and Problems with Rate-Surfactant Profiles	103
4.5.2 The Pseudo-phase Ion-Exchange Model and Solving the Problems of Rate-Surfactant Profiles.....	105

CHAPTER V. HYDROLYSIS OF PHENYL ESTERS AND THEIR BINDING IN CATIONIC MICELLES

5.1 INTRODUCTION	111
5.2 EARLY STUDIES.....	112
5.3 FURTHER STUDIES AND TRANSITION STATE STABILIZATION.....	115
5.4 OBJECTIVES OF THE RESEARCH	120

CHAPTER VI. CATALYSIS OF THE THIOLYSIS OF *p*-NITROPHENYL ALKANOATES BY CTAB MICELLES

6.1 INTRODUCTION AND PREVIOUS WORK.....	122
6.2 RESULTS AND KINETIC TREATMENT OF THE DATA	124
6.3 DISCUSSION.....	135
6.3.1 Ester Chain Length Effects: Hydrophobic Interaction.....	135
6.3.2 Nucleophile Effects: Ion-Exchange	139
6.3.3 Transition State Binding	142
6.4 CONCLUSIONS.....	144
6.5 EXPERIMENTAL.....	146
6.5.1 Materials	146
6.5.2 Kinetic Apparatus and Solutions.....	146
6.5.3 Curve Fitting and the <i>cmc</i> Estimate.....	147

CHAPTER VII. CATALYSIS OF THE AMINOLYSIS OF *p*-NITROPHENYL ALKANOATES BY CTAB MICELLES

7.1 INTRODUCTION	150
7.2 RESULTS	152
7.2.1 Ester.CTAB Binding.....	153
7.2.2 Aminolysis of the Unbound Esters	155
7.2.3 Aminolysis of Ester.CTAB Complexes.....	157
7.2.4 Reactivity Ratio k_{cN}/k_N	158
7.2.5 Transition State Dissociation Constants K_{TS}	159
7.2.6 Third Order Reactivity (k_3).....	161
7.2.7 The Aminolysis of a Series of Alkanoate Esters by <i>n</i> -Hexylamine.....	161
7.3 DISCUSSION	
7.3.1 Amine Partitioning into the Micellar Pseudo-phase	164
7.3.2 Transition State Binding Depends on Amine and Ester Hydrophobicity	171
7.3.3 Probing Ester Acyl Chain Length Binding to CTAB Micelles.....	173
7.3.4 Branched and Cyclic Amines.....	176
7.4 CONCLUSIONS.....	177
7.5 EXPERIMENTAL.....	180
7.5.1 Materials	180
7.5.2 Kinetic Measurements	180
7.5.3 pH and Background Hydrolysis.....	182
7.5.4 Concentration Range of Amines	183
7.5.5 Partition Coefficients	183

CHAPTER VIII. CATALYSIS OF THE CLEAVAGE OF *p*-NITROPHENYL ALKANOATES BY AMINO ACID ANIONS IN CTAB MICELLES

8.1 INTRODUCTION	186
8.2 RESULTS	188
8.3 DISCUSSION	198
8.3.1 Amino Acid Anions Ion- Exchange and Partition into CTAB Micelle.	198
8.3.2 Transition State Binding (pK_{TS}) varies with Amino Acid Anion Chain and Ester Chain	205
8.3.3 Comparison of Amines and Amino Acid Anions	209
8.4 CONCLUSIONS.....	211

8.5 EXPERIMENTAL.....	213
8.5.1 Materials, Kinetic Measurements, and pH	213
8.5.2 Hydrophobicity Scales and $P_{o/w}$ Values of Amino Acids.....	214

CHAPTER IX. CONCLUSIONS AND FUTURE PERSPECTIVES

9.1 CONCLUSIONS.....	218
9.2 FUTURE PERSPECTIVES.....	221

REFERENCES.....	226
------------------------	------------

APPENDICES

Appendix A: Data Relevant to Chapter III	244
Appendix B: Data Relevant to Chapter VI	252
Appendix C: Data Relevant to Chapter VII.....	273
Appendix D: Data Relevant to Chapter VIII	288

LIST OF FIGURES

Figure 1.1	From molecular to supramolecular chemistry.....	2
Figure 1.2	The host has a concave binding site, while the guest has a convex binding site	3
Figure 1.3	Fixed (left) and flexible (right) host design	4
Figure 1.4	Some prominent “rigid” hosts	5
Figure 1.5	Schematic representation of the catalytic process	12
Figure 1.6	Gibbs free energy diagram showing transition state stabilization by a catalyst	18
Figure 1.7	a) “Flickering clusters” of water in the bulk phase. b) Highly ordered water molecules form “cages” around a hydrocarbon	24
Figure 1.8	Hydrophobic interactions are entropy driven due to release of “hydration water” into the bulk when hydrocarbon groups aggregate	25
Figure 2.1	Glucopyranose units and the cyclodextrin torus	28
Figure 2.2	A cyclodextrin nano-bucket, where R' can be H or another functional group	29
Figure 2.3	Complementarity based on size is important for CD-guest inclusion.....	33
Figure 2.4	Release of high-energy water from the CD cavity, and breaking of the water cages around the guest, drives complex formation	34
Figure 2.5	Example of the effect of cyclodextrins on reactions	37
Figure 3.1	A guest (G) competes with a substrate (S) for binding to the cyclodextrin and effects the reactivity	41
Figure 3.2	Effects of β -cyclodextrin on rates of hydrolysis of the substrates	47
Figure 3.3	Sample data for the catalysis of the hydrolysis of TMOB in β -CD (1.00 mM) by 2-alkanones	50
Figure 3.4	Sample data for the catalysis of the hydrolysis of TMOB in β -CD (1.00 mM) by 3-alkanones	51
Figure 3.5	Sample data for the catalysis of the hydrolysis of TMOB in β -CD (1.00 mM) by cycloalkanones	51
Figure 3.6	Substrate-cyclodextrin binding	56
Figure 3.7	Comparison of pK_G for CD-ketone binding	62
Figure 3.8	Ketone- β -cyclodextrin binding	63
Figure 3.9	Chain length dependence on the strength of binding of ketones to β -CD	64
Figure 3.10	Comparison of the strength of binding of methyl ketones (RCOMe) and alcohols (ROH) to β -CD	67
Figure 3.11	Comparison of the strength of binding of 2-alkanones and 3-alkanones of the same carbon number to β -CD	67
Figure 3.12	Comparison of the strength of binding of ketones (RCOR') and related alcohols (RCH(OH)R') to β -CD	70
Figure 3.13	Synthesis of L-tryptophan-modified β -CD, and self- and guest-inclusion into cyclodextrin.	73

Figure 3.14	Examples using the quadratic method.....	78
Figure 4.1	An amphipathic surfactant molecule.....	81
Figure 4.2	Surfactant molecules collect on the water surface, but do not form a separate continuous phase in solution	82
Figure 4.3	SDS Surfactant molecules- hydrocarbon tail (green), head group (yellow), counter ion (red) - aggregate in aqueous medium (blue) to form the colloidal micelle	83
Figure 4.4	Changes in physical properties of a solution upon micelle formation.....	85
Figure 4.5	Plot of log <i>cmc</i> versus the alkyl chain length (n) of the amphiphile.....	86
Figure 4.6	Two dimensional schematic representation of the regions of a spherical cationic micelle	93
Figure 4.7	The most probable shapes of micelles.....	94
Figure 4.8	Rate versus micellized surfactant ([D _n]) profiles exhibiting (a) saturation kinetics, (b) rate-maximum	104
Figure 5.1	Mode of TS binding for hydrolysis of <i>p</i> NPAlk esters in CTAB micelles.....	120
Figure 6.1	Variation of <i>k</i> _{obs} for ester cleavage with the concentration of mercaptoethanol ([ME] _o), in the presence of 5.0 mM [NaBr], but no CTAB	127
Figure 6.2	Variation of <i>k</i> _{obs} for ester cleavage with the concentration of [CTAB] _o , above the cmc, in the presence of 20 mM mercaptoethanol, and at a total bromide ion = 5.0 mM	128
Figure 6.3	Variation of <i>k</i> _{obs} for ester cleavage versus the concentration of mercaptoethanol ([ME] _o), in the presence of 5.00 mM of CTAB, and no NaBr	130
Figure 6.4	The dependence of transition state binding (<i>pK</i> _{TS}) and substrate binding (<i>pK</i> _S) to CTAB micelles on the ester chain length (n) of <i>p</i> -nitrophenyl alkanoates	136
Figure 6.5	The acceleration afforded by CTAB (expressed by <i>k</i> _{CN} / <i>k</i> _N) are virtually independent of ester chain length (n) but vary appreciably with the nucleophile	140
Figure 6.6	Modes of TS binding for thiolysis of <i>p</i> NPAlk esters in CTAB micelles and the interactions with CTAB binding domains.....	143
Figure 7.1	Variation of <i>k</i> _{obs} with [CTAB] _o for reaction of: (a) pNPH + <i>n</i> -heptylamine; (b) pNPA + <i>n</i> -heptylamine; (c) pNPH + <i>n</i> -propylamine	154
Figure 7.2	Variation of <i>k</i> _{obs} with [amine] _o for aminolysis of pNPA in the absence of CTAB	155
Figure 7.3	The variation of <i>k</i> _{obs} with [amine] _o for aminolysis of pNPH in the presence of 5.0 mM CTAB	157

Figure 7.4	a) Retardation of the aminolysis of pNPA (■, □) and pNPH (●, ○) by <i>n</i> -butylamine. b) Catalysis of the aminolysis of pNPA and pNPH by <i>n</i> -heptylamine.....	159
Figure 7.5	Variation of k_{obs} for ester aminolysis by <i>n</i> -hexylamine in the absence of CTAB	162
Figure 7.6	Variation of k_{obs} for ester aminolysis by <i>n</i> -hexylamine in the presence of 5.0 mM CTAB	162
Figure 7.7	Correlation between log <i>P</i> in DTAB/water and octanol/water for 28 organic molecules.....	166
Figure 7.8	Dependence of the log ($k_{\text{cN}}/k_{\text{N}}$) on log $P_{\text{o/w}}$, for <i>n</i> -alkyl and <i>iso</i> -alkylamines, and for pNPA and pNPH	167
Figure 7.9	Dependence of the pK_{TS} on amine chain length, for <i>n</i> -alkyl and <i>iso</i> -alkylamines, and for pNPA and pNPH	171
Figure 7.10	The corresponding relationship between TS stabilization for pNPA and pNPH with those same amines.....	173
Figure 7.11	The dependence of transition state binding (pK_{TS}) and substrate binding (pK_{S}) to CTAB micelles on acyl chain length (<i>n</i>)	174
Figure 7.12	Transition State binding for the aminolysis of esters in CTAB micelles	179
Figure 7.13	The correlation between log $P_{\text{o/w}}$ values for amines vs. alcohols	184
Figure 8.1	Observed rate constants for pNPA cleavage vs. the [amino acid] in the absence of CTAB	189
Figure 8.2	Observed rate constants for pNPA cleavage vs. [amino acid] in the presence of 5.0 mM CTAB	193
Figure 8.3	The observed rate constant for pNPH cleavage vs. [amino acid] in the presence of 5.0 mM CTAB	193
Figure 8.4	CTAB catalyzes the reaction between pNPA or pNPH with histidine	196
Figure 8.5	CTAB catalyzes the reaction between pNPA and the anions of the amino acids: norleucine (2-aminohexanoic acid), norvaline (2-aminopentanoic acid), and 2-aminobutanoic acid.....	197
Figure 8.6	The change in the observed rate constant vs. [norvaline], for the cleavage of pNPA and pNPH in the presence of CTAB and in the absence of CTAB	198
Figure 8.7	The reactivity ratio for pNPA cleavage depends on amino acid hydrophobicity (log $P_{\text{o/w}}$) and charge effects	199
Figure 8.8	The relationship between the change in free energies ($\Delta\Delta G$) of transfer from SDS micellar to aqueous phase for X-Tryp-NH ₂ at pH 10.7, relative to X = Gly and those ($\Delta\Delta G_{\text{o/w}}$) of transfer from 1-octanol to water for acetyl-X-NH ₂	202
Figure 8.9	The transition state binding for pNPA + amino acid anions	206
Figure 8.10	Relation between the strength of transition state binding (pK_{TS}) for the reaction of amino acid anions with pNPH and pNPA in CTAB micelles.....	207

Figure 8.11	Comparison of the log ($k_{\text{CN}}/k_{\text{N}}$) for the cleavage of pNPA by amines ($\text{R-CH}_2\text{-NH}_2$) and amino acid anions ($\text{R-CH(NH}_2\text{)(CO}_2^-)$) of the same alkyl carbon chain length (R-C-)	210
Figure 8.12	Transition State binding for the reaction of pNPA and pNPH with <i>n</i> -alkyl amino acid anions in CTAB micelles	212

LIST OF SCHEMES

Scheme 3.1	Acid catalyzed hydrolysis of BDMA.	44
Scheme 3.2	Acid catalyzed hydrolysis of TMOB	46
Scheme 3.3	Inhibition analysis spreadsheet.....	77
Scheme 4.1	The Pseudo-phase Model	103
Scheme 4.2	The Pseudo-phase Ion-Exchange Model	106
Scheme 5.1	Hydroxide ion hydrolysis of aryl esters	111
Scheme 6.1	Thiolysis of <i>p</i> NPAlk esters	112
Scheme 6.2	Worksheet for the analysis of ester cleavage by nucleophiles (thiolate anions), with and without CTAB	149
Scheme 7.1	Aminolysis of <i>p</i> NPAlk esters.....	150
Scheme 7.2	Conformational changes of the cetyl chains produced by solubilization of <i>n</i> -alkyl alcohols or amine additives in CTAB micelles.....	168
Scheme 7.3	In the reaction of a long amine with a long ester, in CTAB micelles, the loss of some hydrophobic binding of the micellar-bound alkylamino and acyl chains is required to attain the transition state	176

LIST OF TABLES

Table 1.1	Factors characteristic of bias versus recognition, extreme types of selectivity	7
Table 2.1	Dimensions and physical properties of natural cyclodextrins.....	30
Table 2.2	Rate constants for acid hydrolysis of β -CD.	30
Table 3.1	Constants for the effect of β -cyclodextrins on acid-catalyzed hydrolysis of BDMA, ADMA and TMOB	49
Table 3.2	Dissociation constants (K_G in mM) of the β -CD-ketone complexes determined using inhibition kinetics and the kinetics of hydrolysis of the probes BDMA, TMOB, and ADMA	54
Table 3.3	Constants for the binding (pK_S) of BDMA, ADMA, and TMOB to cyclodextrins compared to phenyl-substituted guests.....	55
Table 3.4	Structural dependence of the binding of aliphatic guest to β -cyclodextrin. Correlations between pK_G and chain length or ring size (N)	64
Table 4.1	Thermodynamic parameters for micellization of amphiphiles in water	90
Table 5.1	Cleavage of <i>p</i> -nitrophenyl alkanoate esters by hydroxide ion in CTAB micelles analyzed by the pseudo-phase ion exchange model.....	115
Table 5.2	Alkaline hydrolysis of substituted phenyl dodecanoates in CTAB micelles.....	117
Table 5.3	Alkaline hydrolysis of <i>p</i> -nitrophenyl alkanoates in CTAB micelles	118
Table 6.1	Constants for the reaction of the anion of 2-mercaptoethanol (ME), $\text{HOCH}_2\text{CH}_2\text{S}^-$, with <i>p</i> -nitrophenyl alkanoates in the presence and absence of CTAB micelles.....	131
Table 6.2	Constants for the reaction of thiolate ions and other nucleophiles with <i>p</i> -nitrophenyl alkanoates in the presence and absence of CTAB micelles.....	133
Table 6.3	Least squares correlations of substrate binding (pK_S) and transition state binding (pK_{TS}) with acyl chain length (n), and with each other, for the reaction of nucleophiles with <i>p</i> -nitrophenyl alkanoates in the presence CTAB micelles	137
Table 7.1	Some CTAB- <i>p</i> -nitrophenyl alkanoate complex dissociation constants K_S	154
Table 7.2	Second order rate constants k_N for aminolysis of <i>p</i> -nitrophenyl acetate (pNPA) and <i>p</i> -nitrophenyl hexanoate (pNPH).....	156
Table 7.3	Constants for the aminolysis of <i>p</i> -nitrophenyl acetate (<u>p</u> NPA) and <i>p</i> -nitrophenyl hexanoate (pNPH) in the presence of CTAB	160

Table 7.4	Constants for the reaction of <i>n</i> -hexylamine with of <i>p</i> -nitrophenyl alkanoate esters in the absence and presence of CTAB	163
Table 7.5	The logarithms of amine octanol/water partition coefficients and catalytic ratios for aminolysis of pNPA and pNPH	167
Table 8.1	First order rate constants (k_u) and second order rate constants (k_N) for cleavage of <i>p</i> -nitrophenyl acetate (pNPA) and <i>p</i> -nitrophenyl hexanoate (pNPH) by the buffer solution and by the amino acid anions (AA^-) respectively	190
Table 8.2	Constants for the cleavage of <i>p</i> -nitrophenyl acetate (pNPA) by amino acids in the presence of CTAB.....	194
Table 8.3	Constants for the cleavage of <i>p</i> -nitrophenyl hexanoate (pNPH) by amino acids in the presence of CTAB.....	195
Table 8.4	Derived constants for the cleavage of <i>p</i> -nitrophenyl acetate (pNPA) and hexanoate (pNPH) by amino acids in the presence of CTAB	200
Table A.1	Rate constants for the cleavage of $PhCH(OMe)_2$ in the presence of β -CD and various concentrations of ketone (G), and the calculation of K_G values for β -CD-Ketone complexes.....	244
Table A.2	Rate constants for the cleavage of $PhCH(OMe)_3$ in the presence of β -CD and various concentrations of ketone (G), and the calculation of K_G values for β -CD-Ketone complexes.....	246
Table B.1	Rate constants for the cleavage of <i>p</i> -nitrophenyl alkanoates in varying concentration of CTAB, with constant $[Br^-]$ and constant mercaptoethanol ($[ME]_0$).....	250
Table B.2	Rate constants for the cleavage of <i>p</i> -nitrophenyl alkanoates in varying concentration of mercaptoethanol (ME) in the absence or presence of CTAB.....	253
Table B.3	Rate constants for the cleavage of <i>p</i> -nitrophenyl alkanoates in the presence of varying concentration of CTAB, with constant $[Br^-]$ and constant mercaptoacetic acid ($[MAA]_0$).....	255
Table B.4	Rate constants for the cleavage of <i>p</i> -nitrophenyl alkanoates in varying concentrations of mercaptoacetic acid (MAA) in the absence or presence of CTAB.....	257
Table B.5	Rate constants for the cleavage of <i>p</i> -nitrophenyl alkanoates in varying concentration of 3-mercaptopropanoic acid (MPA) in the absence or presence of CTAB.....	259
Table B.6	Rate constants for the cleavage of <i>p</i> -nitrophenyl alkanoates in varying concentration of cysteine (Cys) in the absence or presence of CTAB.....	261
Table B.7	Rate constants for the cleavage of <i>p</i> -nitrophenyl alkanoates in varying concentration glycine (Gly) in the absence or presence of CTAB	262

Table B.8	Rate constants for the cleavage of <i>p</i> -nitrophenyl alkanoates in varying concentration of 2,2,2-trifluoroethanol (TFE) in the absence or presence of CTAB.....	263
Table C.1	Rate constants for the cleavage of <i>p</i> -nitrophenyl acetate (pNPA) in varying concentration of amines in the absence or presence of CTAB	265
Table C.2	Rate constants for the cleavage of <i>p</i> -nitrophenyl hexanoate (pNPH) in varying concentration of amine in the absence or presence of CTAB	268
Table C.3	Rate constants for the cleavage of <i>p</i> -nitrophenyl acetate (pNPA) in the presence of varying concentration of CTAB, constant [Br ⁻], and constant amine concentration	271
Table C.4	Rate constants for the cleavage of <i>p</i> -nitrophenyl hexanoate (pNPH) in the presence of varying concentration of CTAB ₀ , constant total [Br ⁻], and constant amine concentration	272
Table C.5	Rate constants for the cleavage of <i>p</i> -nitrophenyl alkanoates in varying concentration of <i>n</i> -hexylamine in the absence or presence of CTAB.....	273
Table D.1	Rate constants for the cleavage of <i>p</i> -nitrophenyl acetate (pNPA) by amino acid (AA) anions in the absence or presence of CTAB	275
Table D.2	Rate constants for the cleavage of <i>p</i> -nitrophenyl hexanoate (pNPH) by amino acid (AA) anions in the absence or presence of CTAB	278

LIST OF ABBREVIATIONS

TS	Transition State
LFER	Linear Free Energy Relationship
CD	cyclodextrin
CDs	usually referring to α -, β -, and γ - cyclodextrins
BDMA	benzaldehyde dimethylacetal
TMOB	trimethyl orthobenzoate
ADMA	acetophenone dimethylacetal
CTAB	cetyltrimethylammonium bromide
DTAB	dodecyltrimethylammonium bromide
SDS	sodium dodecylsulfate
pNPAIk	<i>para</i> -nitrophenyl alkanoate
pNPA	<i>para</i> -nitrophenyl acetate
pNPH	<i>para</i> -nitrophenyl hexanoate
Ar	substitued phenyl ring
ME	mercaptoethanol
TFE	trifluoroethanol
NMR	Nuclear Magnetic Resonance
<i>cmc</i>	critical micelle concentration
AA ⁻	amino acid anions
S _N Ar	nucleophilic aromatic substitution

CHAPTER I. GENERAL INTRODUCTION

1.1 INTRODUCTION TO SUPRAMOLECULAR CHEMISTRY

Beyond molecular chemistry, based on *covalent bonds*, lies supramolecular chemistry based on *intermolecular interactions*. Since intermolecular interactions are ubiquitous, supramolecular enthusiasts¹⁻⁵ can be concerned with virtually all of Nature and chemistry sub-disciplines. Supramolecular chemistry is an exciting, vast, fast-moving discipline that has resisted all attempts to define and contain it. Lehn⁵ first defined supramolecular chemistry as “the designed chemistry of the intermolecular bond.” Over time, the discipline took under its wings any organized entity in which two or more chemical species are held together by intermolecular forces. Then, when nanotechnology⁶ and self-assembly^a became ‘fashionable’,⁷ supramolecular chemistry immediately embraced it and laid claim to films, gels, liquid crystals, and nanostructures.⁸ Quibbling over definitions, colloidal chemistry has not been completely adopted by supramolecular chemistry.⁹ The point is, today, what is viewed as “supramolecular” seems to lie *in the eye of the beholder*.

One thing is clear, with the development of supramolecular chemistry there has been a simultaneous shift in the mind-set of chemists working in the area. This shift has involved a change in focus from single molecules, often constructed step by step *via* the formation of covalent linkages, towards *supermolecules*, which are “highly structured molecular complexes”¹⁰ or “multi-component molecular assemblies,”¹¹ held together in a unique structural relationship by their weak non-covalent intermolecular contacts. This change in focus is nicely encapsulated in Lehn’s statement that “supermolecules are to

^a Self-assembly has been defined as “the process by which a supramolecular species forms spontaneously from its components”.⁷

molecules and their intermolecular bonds what molecules are to atoms and their covalent bond”⁵ (Figure 1.1). Major functional features of supermolecules include: molecular recognition, supramolecular reactivity and catalysis, and transport processes.

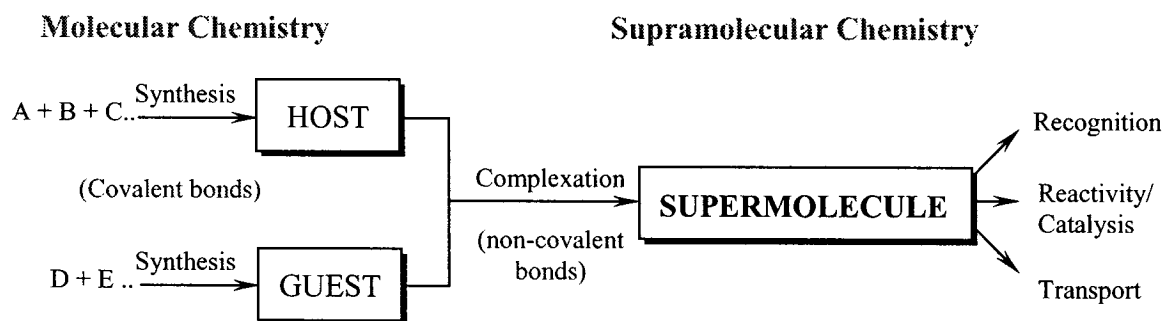


Figure 1.1 From molecular to supramolecular chemistry.⁵

Central to supramolecular chemistry is the use of a variety of weaker (non-covalent) interactions, including hydrogen bonding, π - π stacking, van der Waals forces and hydrophobic interactions, to hold molecular components together. These are the same forces that highly specific biological systems use to bind their molecular assemblies. Enzyme-substrate binding, enzymatic catalysis, immunological responses, intercalation complexes of nucleic acids, storage and retrieval of genetic information, drug action, neurotransmitter processes and import/export across membrane boundaries all involve structural recognition and complexation through such interactions.¹²

Indeed, much of the activity in the area of supramolecular chemistry aims to mimic (but not necessarily copy directly) the way that Nature goes about things. While some quite beautiful examples of self-assembled systems have been synthesized and described as “supramolecular”, in general there is still a long way to go before individual

systems match the biological ones in both intricacy and especially function. Therein lies the challenge.

The research in this thesis is under the supramolecular chemistry umbrella, which reveals no more information content than, for example, the statement that ‘I am a chemist’. This chapter highlights some terminology and functions of supermolecules that are foundations to our research interest.

1.1.1 Supramolecular Complexes

Much attention is currently being paid to the investigation of *supramolecular complexes*, that is, complexes that are bound solely by non-covalent intermolecular forces. In biological systems, examples of supramolecular complex partners are enzyme + substrate, antibody + antigen. In medicinal chemistry, the terms receptor and drug have evolved. Complexation between synthetic organic entities has been given the terms host and guest.

The host–guest convention, largely derived from Cram’s work on macrocyclic chemistry,^{10,13,14} was defined at the outset as representing species with concave and convex binding sites, respectively (Figure 1.2). Although sometimes used within the limit

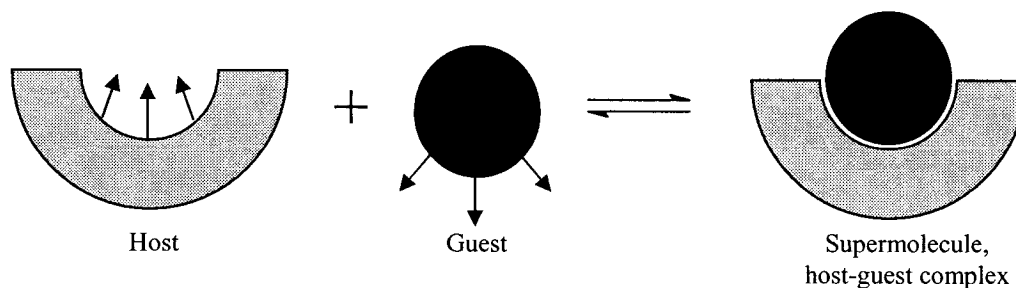


Figure 1.2 The host has a concave binding site, while the guest has a convex binding site.

of their original meanings, the convention is not necessarily appropriate for describing the components of all individual supermolecules or self-assemblies. At the present there is no universal consensus on the catalogue of criteria to be met by molecular hosts. In a definition with very broad scope, “all compounds capable of binding another species with a somewhat higher affinity than what must be expected from their fundamental molecular properties can be adopted as hosts.”^{15,b} What is meant by a “host” has thus become increasingly problematic.

There are two opposing concepts of host design,¹⁶⁻¹⁸ “fixed” versus freely “flexible”, as illustrated in Figure 1.3.

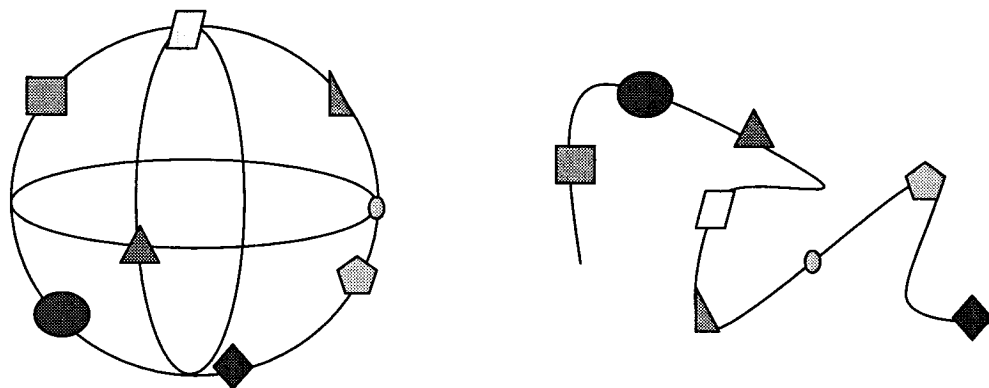


Figure 1.3 Fixed (left) and flexible (right) host design.¹⁸

The fixed, more or less “rigid” host and its anchor-points would have to be placed in predetermined topology and orientation in space. The convergence of binding sites toward a binding centre generally requires construction of macrocyclic framework.¹⁷ Such an assemblage is inherently difficult to build or even modify, that is why the study of natural analogs and their derivatives has received wider attention. Moreover, rigid skeletons run the risk of slow guest exchange kinetics, which are undesirable if the

^b Under this broad definition, the host does not have to have a unique covalent structure or a convergent binding sites, even though receptor sites of biological molecules generally have concave surfaces.

application requires equilibration of the complexes and their components. Prominent fixed cyclic hosts with a proven ability in a broad range of guest binding are crown ethers, cryptands, calixarenes, cavitands, and spherands (Figure 1.4).¹³ Over the last 10 years our research group has studied and continues to study the host-guest complexes and supramolecular function of natural and synthetic cyclodextrins.¹⁹ The first part of this thesis involved an investigation of cyclodextrin-guest complexes (Chapters II and III).

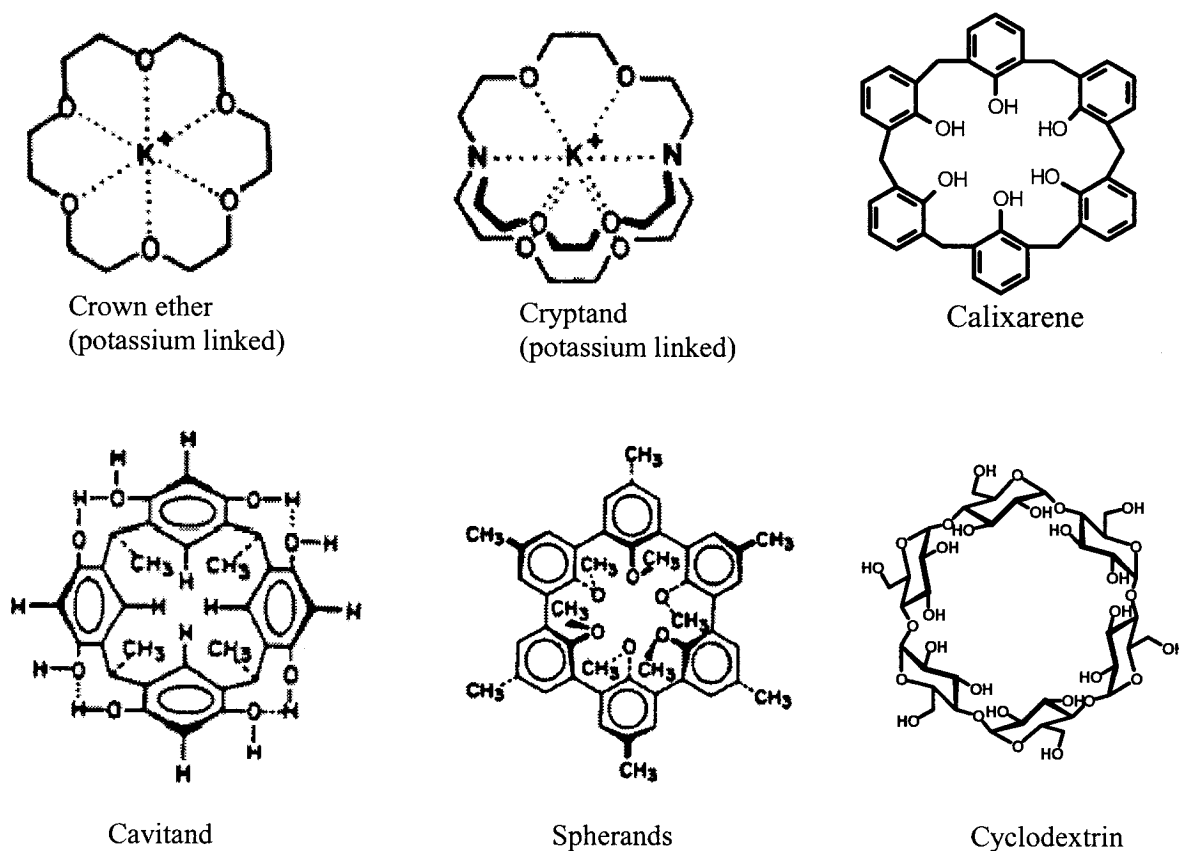


Figure 1.4 Some prominent “rigid” hosts.¹³

An alternative to the fixed host is the “flexible” host. In flexible host design, various anchor groups may be placed on a linear or branched chain molecule and left to fold or ‘aggregate’, arranging the binding functions in the appropriate layout in space

(Figure 1.3, right). From a practical standpoint, foldable hosts have a closer analogy to biological systems such as proteins, nucleic acids, polysaccharides, which are all linear polymers acquiring a distinct tertiary structure by informed folding. Such hosts have the virtue of being comparatively easy to synthesize and modify, by shortening or extending of the chain or by altering of their anchor groups. Also, generally they do not suffer from the problem of slow guest exchange rates. A difficulty, however, is that analysis of host-guest interactions, in particular the correlation of binding data and complex structures, is not as obvious as with fixed host systems. Flexible hosts will also display inferior selectivity towards competing guests. The bulk of research described in the thesis explores micelles as flexible aggregate hosts, examining their supramolecular ability, in particular, supramolecular catalysis (Chapters IV-VIII). The incorporation of designed functionality into micelles will undoubtedly attract increased attention in future studies.

1.1.2 Molecular Recognition

Molecular recognition, extreme selectivity of a guest, results from the ‘readout’ of specific information concerning the guest to be bound.^{2,20} This information is stored at the molecular level within the structure of the molecular host. Quantification of this selectivity, ascertaining the driving forces for complexation, and estimating the strength of the complex are facets that we are engaged in researching.

1.1.2.1 Selectivity: Bias versus Recognition

Traditionally, it is mandatory for a supramolecular host to show discrimination between various guests offered for association. The selectivity observed is thought to

emerge from complementary molecular interactions of the binding partners, along with a balance of flexibility and rigidity of the host. The question remains: does the host truly ‘*recognize*’ the guest that it selects?²¹ Or, does it just exhibit ‘*bias*’ for one guest over the other? Some of the distinguishing features of bias and recognition are compared in Table 1.1. One should consciously avoid the term recognition when only bias is indicated. The terms selectivity, preference, or discrimination will be treated as all-inclusive throughout the thesis.

Table 1.1 Factors characteristic of bias versus recognition, extreme types of selectivity.²²

Selectivity Type	
Bias	Recognition
Monotonic trend	Peak preference
Little geometrical preference	Geometry sensitive
Physical variables important	Bonding character important
Solvation important	Shielding from solvent
Minimal host-guest interactions	Multiple host-guest interactions
Simple guest	Multifunctional guest

Achievement of a particular selectivity is amenable to characterization and optimization by the prudent engineering of the host or the changing of the guest. In retrospect, as we shall see in the thesis, it is arguable that cyclodextrins do entail some aspects of guest selectivity based on recognition; however, simple micelles are more primitive in this regard and discrimination between guests primarily involves bias and not recognition. Certainly, more functionalization of either cyclodextrins or micelles can bring about departures from the simple bias type of selectivity.

1.1.3 Quantifying the Binding Strength of Supramolecular Complexes

Host-guest complexes are simple to form in principle, but measuring the strength of interaction of the two binding partners (determining their association or binding constant) is not quite as elementary. Binding constants of supramolecular complexes association depend on all direct mutual non-covalent interactions, structure complementation, as well as the changes in the environment, solvent, and the host conformational reorganization upon complexation. The total interaction energy between supramolecular complexes will increase the greater the number of recognizable binding forces. More specifically, complexes are held together by hydrogen bonding, ion pairing, π -acid to π -base attractions, van der Waals attractive forces, solvent-liberation driving forces, or partially made and broken covalent bonds (as in transition states). Nonetheless, the energy donated by each one of these forces is rarely enough to hold the complex together. Also, the binding strength in complexation reflects structural complementarity in binding. Thus, binding constants depend on the degree to which the geometry of the host binding site, its size, and its stereochemistry matches the guest.

Even though extensive research on different supramolecular complexes has been carried out, the intimate understanding of the interdependence of structure and complex stability remains obscure. This obscurity has fostered a pursuit of more methodologies to determine the binding strengths of complexes in order to ascertain meaningful interpretations of the correlation between structure, forces of interaction and complex stability. Most methods to estimate host-guest binding constants make use of NMR, IR, UV, fluorescence, circular dichroism, titration, as well as molecular mechanics calculation.²³ We, as will be described in more detail later on, use the kinetics of well-

known organic reactions to estimate the strength of guest (or substrate) binding to cyclodextrin and micelle hosts. The discrepancies between binding constants from different sources give us reason to exercise a fair measure of caution or even scepticism when interpreting published binding constants. We believe that the most significant and reliable data arise from trend analysis of guests or host series of purposefully and systematically induced variation of structure of interacting partners. If then a consistent picture of all binding events can be advanced, the principles derived there-from have a higher reliability and greater predictive power than direct structural studies of a single example.

1.1.4 Supramolecular Reactivity and Catalysis

The formation of supramolecular complexes can result in a change in the *supramolecular reactivity* of the guest (substrate); the host modifies the chemical and/or physical properties of the bound substrate or transition state.¹ *Supramolecular catalysis* results when the rate of the chemical transformation of the host-guest complex is promoted relative to the uncomplexed species.¹

1.1.4.1 ‘Enzyme mimics’

Chemists long to reveal and understand how enzymes work.²⁴⁻²⁶ Who would not be envious of the enzymes impressive ability to catalyze reactions, achieving rates of 10^6 - 10^{17} faster than the uncatalyzed reaction, at ambient temperature and modest pH? To top it off, they often do this with high substrate selectivity, regioselectivity and enantioselectivity.^{19,27} Enzyme catalysis depends on subtle combinations of effects that

are difficult to separate and quantify. Early on in the history of supramolecular chemistry, it was realized that an enzyme and its substrate were a type of host-guest system, and that enzyme action almost certainly results from supramolecular behaviour and especially *supramolecular catalysis*.²⁷

Since then, molecular architects have been inspired and challenged to look for and design artificial catalytic hosts with the main goal being to mimic some key aspect of enzyme function on more easily accessible and modifiable structures.^{4,10,13,28-30} In general, an enzyme model should fulfill a three-fold purpose: (a) it should provide a reasonable simulation of the enzyme mechanism, (b) it should identify particular factors responsible for the catalytic efficiency, and (c) it should lead to an explanation of the observed rate enhancement in terms of structure and mechanism. In order to achieve analogous quantitative performance which simulate those of the natural archetype a good enzyme model should fulfill the following requirements:²⁸

1. The key to biological flexibility and specificity are non-covalent interactions, and thus the model host should have a well-oriented hydrophobic auxiliary region for good binding site for the substrate.
2. To help in the orientation of the substrate binding the mimic should provide the possibility of forming electrostatic and/or hydrogen bonds to it.
3. Catalytic groups are selected and properly attached or somehow bound to the model to effect the reaction.
4. It is hoped that complementary intermolecular interactions will allow for appropriate substrate orientation and chiral discrimination if need be, and this usually dictates that the model be of rigid and well-defined structure.

5. The mimic host should preferably be water soluble and catalytically active under physiological conditions of pH and temperature.
6. It is of prime importance in catalysis that the transition state of the reaction be stabilized. This point will be described in detail in the next section of this chapter.

Cyclodextrins and micelles form a variety of supramolecular complexes and can fit into the catalogue of ‘artificial catalysts’ that ‘mimic enzymes’. Surely, this adds motivation to study their catalytic effects. Actually it was an interest in catalytic effects on organic reactions that prompted our research with cyclodextrins and micelles as hosts. In particular, we have been studying organic reactions, mostly hydrolytic, where systematic variations in the structure of the substrates (or guests) in the presence of the hosts, causes alteration in the rate retardation and acceleration, in an attempt to better understand some of the origins of supramolecular catalysis, principally from the perspective of transition state stabilization.¹⁹ The bulk of the research described in the thesis aims to uncover factors responsible for supramolecular reactivity/catalysis of micellar aggregates by studying their effects on esterolytic reactions (Chapters V-VIII).

1.2 BACKGROUND TO TRANSITION STATE STABILIZATION

Ascertaining the origins of supramolecular catalysis presents a great challenge. Explanations of the extraordinary power of enzymes to accelerate chemical reactions have been sought ever since this behavior was observed. To date, substrate recognition and selective stabilization of the transition state (TS) relative to the ground state are regarded as being at the heart of enzyme catalysis.

A catalyst can collect and orient reactants through complexation, a relationship that converts potentially reacting groups into neighboring groups.^{27,31} In layman's terms, as seen in Figure 1.5, the catalyst (e.g. enzyme) recognizes and binds to a substrate (*lock in key*) or changes in shape to induce binding (*induced fit*). The bound substrate is then

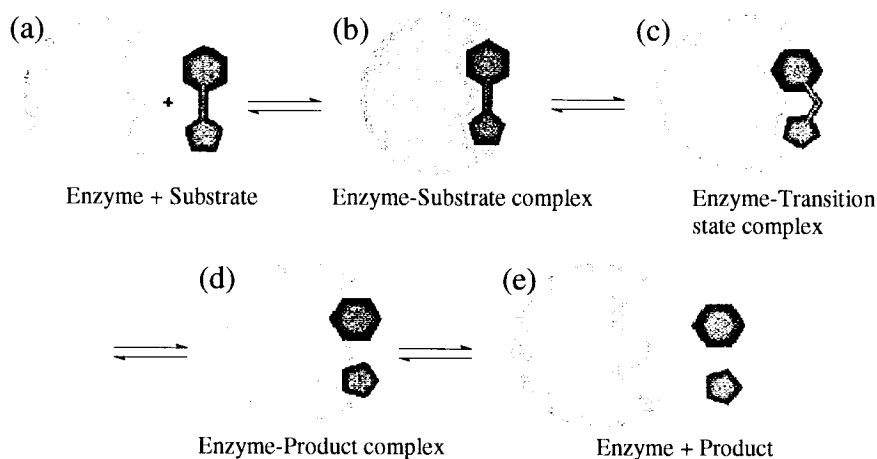


Figure 1.5 Schematic representation of the catalytic process.

converted into the catalyst-transition state complex before forming products and releasing the catalyst, as first suggested by Haldane in 1930.³² The function of an enzyme, like that of any catalyst, is to make the transition state (TS) for a reaction easier to reach. It is difficult to imagine how this could be achieved if the enzyme did not possess an affinity

for the altered substrate in the TS which exceeds that for the substrate itself. Pauling³³ originally advanced this view of selective TS stabilization to elucidate the underlying principle of enzyme catalysis, but it took a while for this idea to gain widespread acceptance.

1.2.1 Transition State Theory

Transition-state theory (TST) has a long history and it is discussed in standard texts on physical chemistry, kinetics and physical organic chemistry.³⁴⁻³⁸ The TST, also referred to as the *absolute reaction-rate theory*, furnishes a basis for the calculation of rate constants at equilibrium and the correlation of the rate and equilibria. Despite the success of this theory, many physical chemists regard the TST with suspicion, if not outright opposition.^{39,40}

The TST rests on some basic assumptions. 1) There exists a potential energy surface in phase space that divides into the reactant region and the product region. An energy barrier, at a saddle point on the surface, separates the regions. It is assumed that this saddle point is located at the *transition state* (TS).^c The TS is defined as the molecular configuration of maximum potential energy value, on the minimum potential energy path, along the *reaction coordinate*. 2) “Trajectories in the products direction originated at the reactants will not reach the surface again before being captured in a product state.”⁴⁰ This is called the *dynamical bottleneck* assumption or non-recrossing rule. 3) The TS is assumed to be in equilibrium with reactants, and both reactants and TS maintain a Boltzmann energy distribution. This assumption is often the stumbling block

^c The *activated complex* more realistically corresponds to any of the states in the vicinity of the saddle point that cross over from reactant to product.

for acceptance of the TST. 4) The rate of a reaction is determined by the rate of decomposition of the TS.

Henry Eyring⁴¹ was instrumental in the development of the TST. His classical fundamental equation [1.1] describes the experimental (observed) rate constant k in terms a transmission coefficient, κ (lumping all correction factors, including tunneling, the barrier recrossing correction, and solvent frictional effects), ν is the frequency of the “normal mode” oscillation of the transition state complex along the reaction coordinate (or the average frequency of barrier crossing), and K^\ddagger is the quasi-equilibrium constant for formation of the transition state complex from reactants.

$$k = \kappa \nu K^\ddagger \quad [1.1]$$

Other derived forms of the Eyring equation (eq. [1.2] and [1.3]) are more often used to interpret the rate constant in term of energy.

$$k = \kappa (k_B T/h) (Q^\ddagger/Q_R) \exp (-E_0^\ddagger/RT) \quad [1.2]$$

$$k = (k_B T/h) \exp (-\Delta G^\ddagger/RT) \quad [1.3]$$

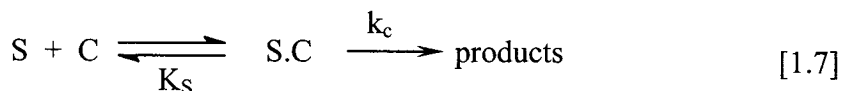
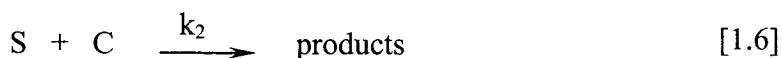
$$k = (k_B T/h) \exp (-\Delta H^\ddagger/RT) \exp (\Delta S^\ddagger/R) \quad [1.4]$$

Here k_B is the Boltzmann constant, T is the absolute temperature, and h is Planck's constant, Q is the partition functions of the TS or reactants, ΔG^\ddagger is the free energy of the TS. In turn, ΔG^\ddagger can be divided into contributions from enthalpy of activation, ΔH^\ddagger , and entropy of activation, ΔS^\ddagger (eq. [1.4]). In many references, derivations of the basic equation of the TST are deceptively simple, sometimes incorrect or at best misleading. Fortunately, these errors probably do not make a difference for the principle of transition state binding that follows from the basic equation.²⁴

1.2.2 TST Applied to TS Binding and Catalysis

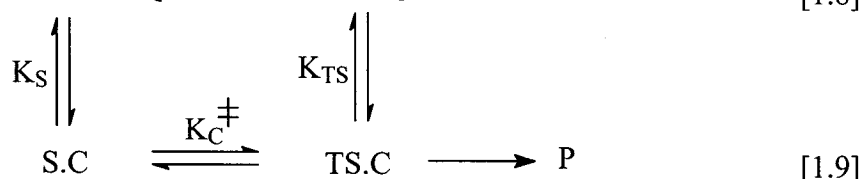
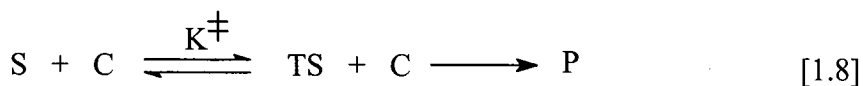
Transition State Theory (TST) extends beyond its use in the context of chemical kinetics, though this is the field with which this theory is most closely applied. TST laid the ground for the later suggestion by Pauling,³³ already mentioned above, that the catalytic powers of enzymes resulted from their highly specific binding of the TS. The quantitative relationship between TS stabilization and catalysis was first formulated by Kurz.^{42,43} Later, Wolfenden⁴⁴⁻⁴⁶ and Lienhard⁴⁷ elaborated on the Kurz approach to transition state analogs and multi-substrate reactions.

The Kurz method relies on TST and a thermodynamic cycle to estimate the energy of stabilization of the TS by catalysts.^{42,43} Consider two reactions, one of which is ‘uncatalyzed’ with a rate constant k_u (eq. [1.5]) and the other which is influenced, ‘catalyzed’, by some ‘catalyst’ (C) with a rate constant k_2 (eq. [1.6]). The two reactions are essentially in competition. The catalyzed reaction can go through a substrate-catalyst complex before being transformed to products, as shown in equation [1.7]. Equations [1.6] and [1.7] are kinetically equivalent.



Following from TST, a reaction is assumed to involve the attainment of a transition state that goes on to product irreversibly at extremely rapid rate. This route is depicted in equations [1.8] and [1.9]. The transition states (TS and TS.C) for both uncatalyzed and catalyzed reactions are considered to be in equilibrium with their

component molecules, and K^\ddagger and K_C^\ddagger are the equilibrium constants for the formation of the two transition states from the corresponding reactants. The position of the equilibrium is related to the free energy of activation required for attainment of the transition state.



As depicted in the above thermodynamic cycle, since there is equilibrium between the transition states and the reactants (according to the TST), and also $S + C$ and $S.C$ are in equilibrium, then $TS.C$ should be in equilibrium with $TS + C$. There is, of course, no direct dynamic equilibrium between these transition states. Note that K_S and K_{TS} are the equilibrium constants for the dissociation of the $S.C$ and $TS.C$.

According to the basic equation of the TST, for reactions whose transmission coefficients are near unity, the rate constant k_u can be written in the form of equation [1.10] and k_c by equation [1.11].

$$k_u = \nu K^\ddagger = \nu [TS]/[S] \quad [1.10]$$

$$k_c = \nu K_C^\ddagger = \nu [TS.C]/[S.C] \quad [1.11]$$

As a starting point, for simplification of mathematical and thermodynamic considerations, the transition state for the uncatalyzed reaction (TS) is assumed to be the same as that bound to the catalyst (TS.C) for the catalyst mediated process. Furthermore it is assumed that the average frequency of barrier crossing (ν) is the same for both

reactions [1.8] and [1.9]. With these assumptions, which may not always be valid,²⁴ simply dividing equation [1.10] by [1.11] furnishes expression [1.12].

$$\frac{k_u}{k_c} = \frac{[\text{TS}][\text{S.C}]}{[\text{TS.C}][\text{S}]} = \frac{K^\ddagger}{K_C^\ddagger} \quad [1.12]$$

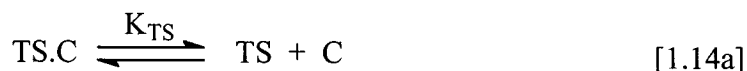
But, from the thermodynamic cycle $K^\ddagger/K_C^\ddagger = K_{\text{TS}}/K_S$ (eq. [1.13a]) and so,

$$k_u/k_c = K_{\text{TS}}/K_S \quad [1.13a]$$

If the relative rates of a reaction in the presence and absence of a catalyst are known, a “conservative semi-quantitative”²⁴ estimate of the tightness of binding of the altered substrate in the transition state may be made.

1.2.3 What Does K_{TS} Stand For?

The quasi-equilibrium constant, K_{TS} , for hypothetical dissociation of the transition state bound to the catalyst, TS.C, is depicted separately in equations [1.14].



$$K_{\text{TS}} = \frac{[\text{TS}][\text{C}]}{[\text{TS.C}]} \quad [1.14b]$$

It is important to note that the derivation of K_{TS} makes *no assumption about the mechanism of either the catalyzed or uncatalyzed reactions*.¹⁹ A purist in thermodynamics would argue that reversible dissociation of TS.C into TS and catalyst is unlikely, if not impossible, rendering K_{TS} a constant of questionable significance. Granted, K_{TS} does not represent a “true” equilibrium constant but it does correspond to an energy difference of indisputable importance: the relative Gibbs energy difference,

$\Delta G^\circ_{\text{TS}}$, between the transition states of the normal (uncatalyzed) and catalyzed reactions under standard conditions (eq. [1.15]).¹⁹

$$\Delta G^\circ_{\text{TS}} = -RT \ln K_{\text{TS}} = 2.303 RT \text{ p}K_{\text{TS}} \quad [1.15]$$

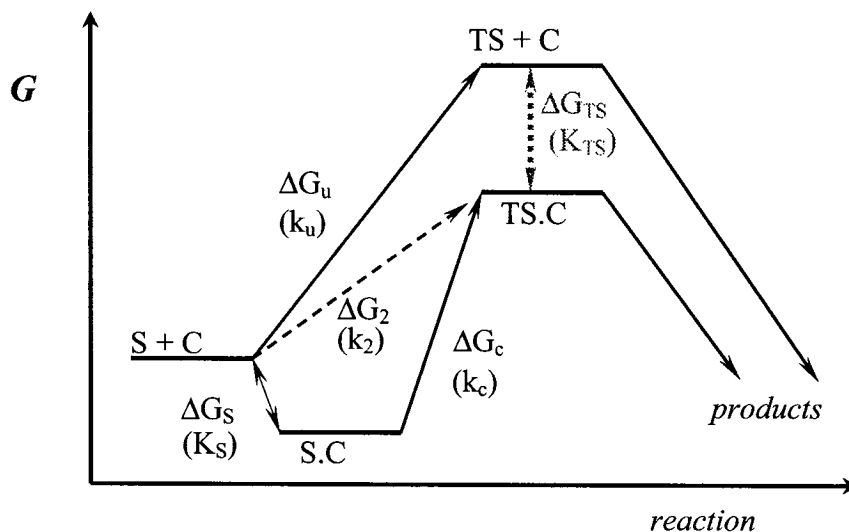


Figure 1.6 Gibbs free energy diagram showing transition state stabilization by a catalyst.^{19,48}

The Gibbs energy diagram (Figure 1.6) illustrates how the energetics of the TS of the uncatalyzed and of the catalyzed processes are linked by the measurable quantity k_u (the overall rate constant for the reaction in the absence of the catalyst), k_2 (the overall rate constant for the reaction in the presence of the catalyst), K_S (the dissociation constant of the S.C complex) and k_c (the rate constant for the decomposition of the complex into products). Together these parameters are used to derive another expression for K_{TS} (eq. [1.13b]).

$$K_{\text{TS}} = k_u / k_2 = (k_u / k_c) K_S \quad [1.13b]$$

The quantity, k_2 , has the same significance as does k_{cat}/K_M for enzymes in that it is a measure of the substrate selectivity of the catalyst, and measures the net efficiency of the catalyst at *non-saturating* concentrations. The term k_c/k_u measures the magnitude that the uncatalyzed reaction is accelerated (or retarded) at *saturating levels* of the catalyst. Since rate constants frequently vary with the pH of the medium, temperature, buffer, ionic strength, etc., the ratios k_c/k_u and k_2/k_u , are more reliable estimates of *catalytic efficiency* for comparative purposes, canceling out external influences other than catalysis (or inhibition) by a catalyst (or host). Variation in these two ratios with structure can provide insight regarding TS binding.¹⁹

The Gibbs energy diagram (Figure 1.6) also emphasizes that stabilization of the transition state by the catalyst is responsible for any rate enhancement. From the rearrangement of eq.[1.13b] to eq. [1.13c], it is apparent, that the catalysis ($k_c/k_u > 0$), or retardation ($k_c/k_u < 0$), reflects the stabilization (or destabilization) afforded by “catalyst” to the transition state relative to stabilization of the substrate.

$$\frac{k_c}{k_u} = \frac{K_S}{K_{TS}} \quad [1.13c]$$

“rate ratio” “binding ratio”

The dissociation constant of the altered substrate in the transition state is therefore expected to be lower than the dissociation of the substrate from the catalyst-substrate complex by a factor – the “*binding ratio*”, at least as large as the ratio of the limiting rates in the presence and absence of the catalyst – the “*rate ratio*”. Simply, catalysis arises from the preferential binding of the TS over the substrate, whereas the reverse is true for retardation.

1.2.4 Application of K_{TS} as a Tool for Predicting Modes of Binding to a Catalyst

Estimation of transition state stabilization by the Kurz approach provides a general explanation of substrate specificity: as Richard Wolfenden⁴⁵ puts it, “*when two substrates of comparable chemical reactivity but differing catalytic reactivity are compared, the more reactive substrate is simply the one which the catalyst possesses stronger forces of attraction in the transition state*”. Obviously, substrate binding to the catalyst may bring it into closer proximity to another potential reactant, it may orient the substrate favorably or unfavorably, or it may even alter the geometry towards that of the TS, in all cases affecting the reaction. Such binding effects are inherently difficult to probe since they depend on the reaction at hand, the catalyst and on the mechanism of the reaction. The usefulness of Brønsted plots, Hammett plots, isotope effects, pH-rate profiles, all depend on variations in kinetic parameters which physical organic chemists employ to discuss the mechanisms of organic reactions.^{35,37,49} Estimation of TS binding, using $pK_{TS} = -\log(K_{TS})$, is based solely on measurable quantities k_u , k_c and K_S (or k_u and k_2), “*without making any assumptions about the reaction mechanism.*”^{19,48} It is for precisely this reason that our research group uses “ *K_{TS} and its variation with structure as a criterion of mechanism.*”^{19,48} Of course, if the mechanisms of the catalyzed and uncatalyzed reaction are quite different, then complications may occur.

Kurz’s approach to quantify TS stabilization^{42,43} has been applied for catalytic antibodies, enzymes, acid base catalysis and metal ion catalysis.^{24,45,47,50,51} In this thesis, we continue to use K_{TS} and its variation with structure as a focal point to probe reactions mediated by potential enzyme mimics.^{52,53} Many examples of the use of K_{TS} to probe modes of transition state binding to cyclodextrins can be found in publications from this

laboratory and others over the last 10 years.^{19,48,54-57} To our knowledge, our research group first suggested to extend this methodology to reactions mediated by micelles.¹⁹ Since then we^{58,59} and other researchers⁶⁰⁻⁶³ have reformulated a sensible description of mechanism of micellar catalysis for a number of well-studied organic reactions in terms of TS stabilization. The ultimate objective of research in this area is to eventually fine tune the origins of supramolecular catalysis and to furnish insight to manipulating it according to demand.

1.3 BACKGROUND TO THE HYDROPHOBIC EFFECTS

We do not at present possess a sufficient handle on intermolecular forces, the heart and soul of supramolecular chemistry, to predict reliably the structure of many supramolecular complexes. Non-covalent bonds are not as strong (stable) and directional as covalent bonds. Hydrogen bonds display only weakly preferred orientations and hydrogen-bonding sites are often swamped by water (usually the solvent of interest). Hydrophobic forces, although operative in water, are even more uncontrollable because they lack simple rules for directionality.

Hydrophobic effects are important in many biological phenomena of interest such as protein folding,⁶⁴ enzyme-substrate interactions, and lipid bilayer assembly. There is a direct relationship between hydrophobic parameters and enzyme action, it is manifested in their conformational features (folding of polypeptide chains) and in their ability to bind substrates and catalyze reactions. Formation of supramolecular complexes between cyclodextrins and the reaction substrates (or guests) depend on hydrophobicity (Chapters II and III). Micelle formation^{65,66} is partly due to hydrophobic interactions between

individual surfactant molecules (Chapter IV). Hydrophobic effects influence reaction rates and catalysis by micelles (Chapter V-VIII). Despite intensive experimental and theoretical work, the hydrophobic effect is not well understood on the molecular level, and the physical origins are still a topic of much controversy.⁶⁷⁻⁷⁰

1.3.1 Definition of Hydrophobicity and the Hydrophobic Effect

Traditionally, the reluctance of apolar compounds (eg. oil, hydrocarbon, chlorocarbons) to dissolve in water has been attributed to their “fear” for water, or *hydrophobicity*. In fact, the London dispersion interactions between water and apolar compounds are favorable and quite substantial. So, the meaning of the term hydrophobicity is somewhat misleading.⁷¹ As described by Hartley in 1936, hydrophobicity is the antipathy of the paraffin chain for water, but “there is no question of actual repulsion between individual water molecules and paraffin chains, nor is there any very strong attraction of paraffin chains for one another. There is, however, a very strong attraction of water molecules for one another in comparison with which the paraffin-paraffin or paraffin-water are slight.”⁷²

Broadly defined, the *hydrophobic effect* is a term used to describe the unusual behavior of hydrophobic solutes in aqueous solution. There is an up-surge of reviews on the thermodynamic models describing hydrophobic effects, which are beyond our purpose here. In 1993 Blokzijl and Engberts⁶⁸ defined the hydrophobic effect on the basis of the thermodynamics of the transfer of apolar compounds either from their liquid state, or from a solution in an apolar solvent, to water. This process involves i) the disruption of interactions between apolar molecules and its apolar environment, ii) refilling of the

vacancy in the apolar medium, iii) the creation of a cavity in water, iv) the initiation of water-solute interactions, and v) the concomitant reordering of the water molecules in the near vicinity of the solute.

Thermodynamically, the overall transfer of a hydrophobic compound from a reference state, organic solvent, into water, experiences a change in free energy.

$$\Delta G_{tr} = \Delta H_{tr} - T \cdot \Delta S_{tr}$$

The signature of the hydrophobic effect is (1) a large, positive change in free energy dominated by entropy at room temperature, and (2) a large, positive change in heat capacity (C_p).⁷³ At room temperature, the enthalpy of transfer is negligible, since the interaction enthalpies are approximately the same in organic and aqueous phase. The entropy of transfer is, however, negative.

Frank and Evans⁷⁴ presented the first, and still most commonly accepted, molecular interpretation for the large unfavorable (negative) entropic contribution in the celebrated paper in 1945. They argued that water molecules arrange into more ordered “cages” around non-polar molecules, that is in effect, a solute is surrounded by a microscopic “iceberg” (Figure 1.7). The iceberg (clathrate) picture thus assigns the origins of hydrophobicity to the unique ability of liquid water to form a highly-structured network of hydrogen bonds surrounding the hydrophobic solute.⁷⁵ This interpretation is undoubtedly appealing, but direct evidence was limited. Recent calculations⁷⁶ have shown that nonpolar solutes cause a concerted decrease in the average length and angle of water-water hydrogen bonds in the first hydration shell.⁷³ Meanwhile, the large positive heat capacity change was considered an indication of the ability of the iceberg to absorb heat as it melts. In spite of the serious and growing doubts about the validity of the

iceberg model (and the general concept of structure making),⁷⁷ its explanation of hydrophobic effects still prevails in the literature.^{77d} However, ‘whether or not the hydrogen bond structure in the hydrophobic hydration shell is significantly different from that in water?’ is still not fully answered.^{78,79}

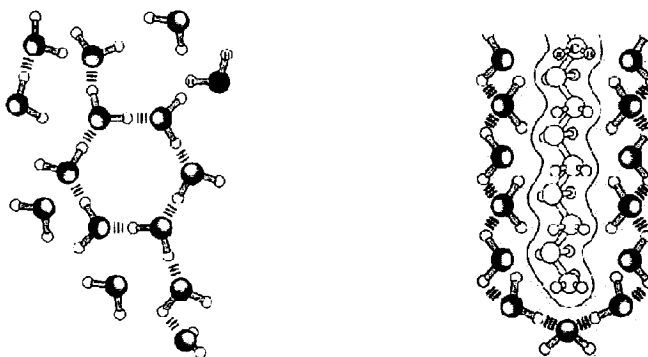


Figure 1.7 a) “Flickering clusters” of water in the bulk phase. b) Highly ordered water molecules form “cages” around a hydrocarbon. Adopted from reference ⁸⁰.

At higher temperature the role of ‘hydrophobic entropy’ in the hydrophobic effect vanishes.⁸¹ At a temperature ≈ 110 °C water cages are no longer any stronger than bulk water, and the entropic contribution tends to zero. The enthalpy of transfer, however, is now positive (unfavorable). Because the temperature dependence of entropy and enthalpy are not the same, there is some temperature at which the hydrophobic effect is strongest.

1.3.2 Definition and Explanation of Hydrophobic Interaction

Hydrophobic interactions, a type of hydrophobic effect, refer to the alleged solvent-induced forces acting between two or more non-polar solutes, causing them to

^d Another explanation is as follows: water molecules in water solution have an average of about 3.5 hydrogen bonds and nearly 6 degrees of freedom. The degrees of freedom add to the entropy and the hydrogen bonds add to the enthalpy. Solvation of extended hydrophobic surfaces disrupts the structure of water molecules. The water molecules become “energetically frustrated”, because they cannot maintain a hydrogen bond network and their freedom is severely restricted.⁷⁷

aggregate.⁶⁸ The term hydrophobic interaction or “hydrophobic bond”, has received much use, particularly in the field of protein chemistry.²⁸

Initially, chemists were genuinely uncomfortable with the notion that hydrophobic interactions between apolar solutes in aqueous medium are entropically driven. Normally clustering of groups corresponds to an increase in the order of the system (negative entropy). Back in 1959 Kauzmann⁸² suggested that the attractive interaction between apolar molecules in aqueous solution are prompted by the solvent as a result of the release of “energetically frustrated” water into the bulk. An illustration of hydrophobic interaction is shown below (Figure 1.8).⁸⁰

(a) Consider hydrocarbon groups well apart surrounded by water. To accommodate hydrophobic groups, the water molecules adjust their hydrogen-bonded arrangements and form a cavity. The net effect is the reduction in the disorder of the system as the water molecules forms a clathrate-like cage around each hydrocarbon group.

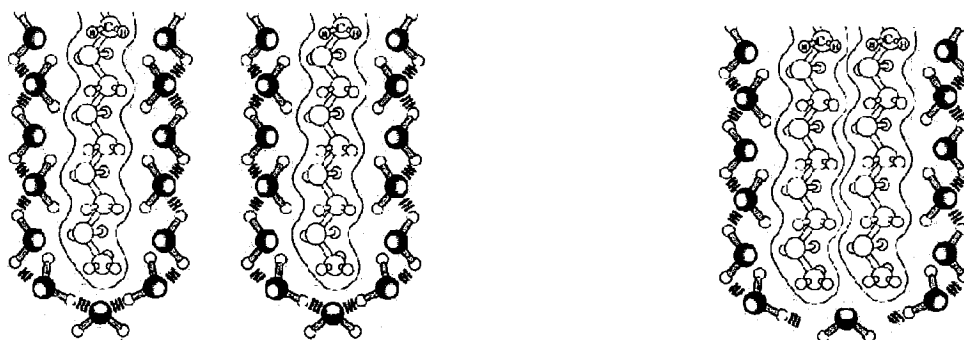


Figure 1.8 Hydrophobic interactions are entropy driven due to release of “hydration water” into the bulk when hydrocarbon groups aggregate. Adopted from reference ⁸⁰.

b) Now consider the arrangement when the hydrocarbon groups aggregate. They occupy a single bigger cavity, of smaller total surface area, and fewer water molecules need to become organized into the cage-like structure. Regardless of enthalpy, the net increase in entropy when the hydrocarbon groups come together results in a favorable change in free energy.

Later we shall discuss the thermodynamics of micelle formation in terms of the hydrophobic interaction between surfactant molecules (Chapter IV, Section 4.2.3).

CHAPTER II. PART 1: CYCLODEXTRINS

2.1 INTRODUCING CYCLODEXTRINS

Cyclodextrins (CDs), bottomless “nano-buckets”, were first isolated in the late nineteenth century.⁸³ Soon after, on account of their relatively hydrophobic interiors, their ability to form *inclusion complexes* with suitable organic molecules was discovered.⁸⁴ With the development of the field of supramolecular chemistry, their host-guest inclusion complexes and supramolecular ability have received even greater interest.⁸⁵⁻⁸⁸ Cyclodextrin chemistry and applications are sought in various areas including enzyme mimics, catalysis, analytical separations, pharmaceutical encapsulation of drugs, food, cosmetic and agriculture industry.^{86,89-91}

2.1.1 Structure of Cyclodextrins

Cyclodextrins (CDs) are cyclic oligosaccharides of D(+)-glucose linked together through α -(1 \rightarrow 4)-glycosidic bonds. Natural CDs are classified as α -, β -, or γ -cyclodextrin according to whether they have six, seven or eight glucose units respectively.^{83,90,91} They are produced by the action of the enzyme *cycloglucosyltransferases* (CGTase or cyclodextrinase) of bacteria⁹² (eg. *Bacillus macerans*) on starch to give a mixture of α -, β -, and γ -CDs, along with small amounts of higher homologues.^{83,90,93} There are no cyclodextrins with less than six glucopyranose units due to steric strain and hindrance.⁹⁴

CDs resemble a dough-nut or torus ring in two dimensions (Figure 2.1), but they are not perfectly cylindrical molecules, their overall 3-dimensional shapes being reminiscent of truncated hollow cones (Figure 2.2).⁹⁵ All of the glucopyranose units have

a relatively undistorted C1 chair conformation, and based on this architecture, the secondary hydroxyl groups on the C2 and C3 atoms automatically line one rim of the torus (the wider CD opening), while the primary hydroxyl groups on the C6 atoms line the other rim (the narrower CD opening) (Figure 2.2).^{83,90,91}

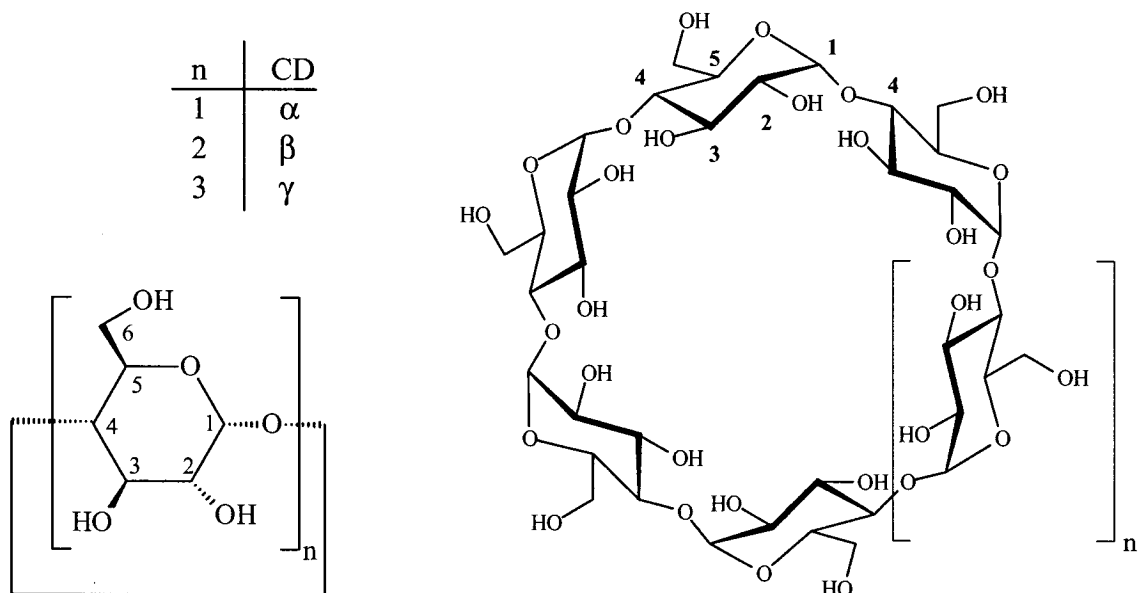


Figure 2.1 Glucopyranose units and the cyclodextrin torus.

The outside of the cyclodextrin cavity is relatively hydrophilic because of the hydroxyl groups. A network of intramolecular hydrogen bonding between the secondary hydroxyl groups on the C2 and C3 atoms of adjacent glucose units, contribute to the overall stability and provide rigidity to the CD “bucket” structure,^a and at the same time it can influence the CD solubility in water.⁹⁴ This hydrogen bonding also makes the secondary hydroxy groups more acidic ($pK_a \approx 12.2$) such that the CD can be more reactive as a nucleophile.⁹⁶ The primary hydroxyl groups can rotate to partially block the

^a According to calculations by Sundararajan and Rao, hydrogen bonding between C2 and C3 results in a lowering of energy by 20 kcal/mole in α -CD and 30 kcal/mol in β -CD.⁹⁴

smaller primary opening of the cavity whereas the secondary hydroxyl groups are on the rings and cannot rotate to block the wider secondary opening.

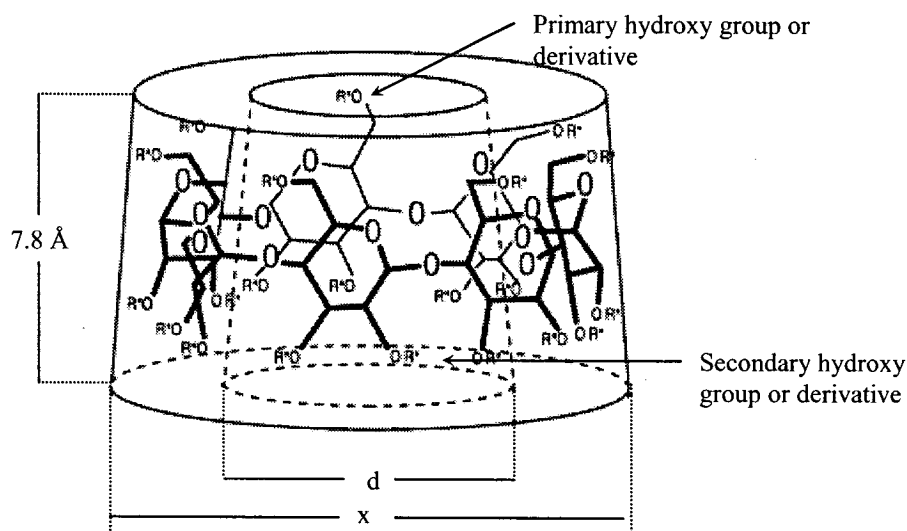


Figure 2.2 A cyclodextrin nano-bucket, where R' can be H or another functional group.

The most important feature of cyclodextrins is the presence of a central cavity. Inside the bucket is a ring of glycosidic oxygens between two rings of methine hydrogens. This feature renders the interior of the cyclodextrin to be less polar than water and relatively hydrophobic. Some authors have suggested that the polarity of the CD cavity is similar to that of oxygenated solvents such as dioxane,^{83,97} ethanol,⁹⁸ or isopropyl ether.⁹⁹ The apparent polarity of the CD cavity is critical for binding of a variety of organic molecules in aqueous solution to the CD cavity. Many literature sources suggest that the non-bonding electron pairs of the glycosidic oxygen bridges are directed towards the inside of the cavity generating a high electron density and thus gives the CD some degree of Lewis-base character.^{83,90,91} However, this feature is not reflected in CD

reactivity and the binding of cationic guests which is much poorer than that for anionic guests.

The dimensions and some physical properties of natural CDs are shown in Figure 2.2 and Table 2.1. The cavity depth is essentially the same for all CDs, whereas, the cavity width increases from α -CD < β -CD < γ -CD.

Table 2.1 Dimensions and physical properties of natural cyclodextrins.^{84,95}

CD	Molecular Weight	Solubility (g/100 ml H ₂ O)	D (Å)	X (Å)	Volume (Å)	# of water molecules in cavity*
α	972	14.5	5.7	13.7	176	6
β	1135	1.85	7.8	15.3	346	11
γ	1297	23.2	9.5	16.9	516	17

* Taken from Bergeron *et al.*⁸⁷

Cyclodextrins are insensitive to base hydrolysis but do undergo partial hydrolysis in strong acidic aqueous solution, at elevated temperatures (Table 2.2),⁹⁰ to yield glucose along with a series of linear maltosaccharides and/or oligosaccharides.

Table 2.2 Rate constants for acid hydrolysis of β -CD.⁹⁰

T, °C	[HCl], N	10 ⁵ k, s ⁻¹	T _{1/2}
100	1.15	137	500 sec
80	1.15	13.7	84.3 min
60	1.15	1.25	15.4 hrs
40	1.15	0.0533	15.1 days
26	5.00	0.617	1.3 days

Data taken from Szejtli in reference (90).

Terminal glycosidic bonds of acyclic polysaccharides are cleaved much faster than their non-terminal members. Since CDs do not have terminal glycosidic bonds, and for entropic reasons, the acid-catalyzed hydrolysis of CDs is very slow. For example, the half-life of β -CD in 1.15 N aqueous HCl at 25 °C is over two weeks (Table 2.2).⁹⁰

2.1.2 Requirements for Formation of Cyclodextrin Inclusion Complexes

The appeal of cyclodextrins to chemists stems from their ability to form supermolecular inclusion complexes, which, in turn, derives from the gross geometrical form of the CD molecules being truncated hollow cones which are capable of accommodating (hosting) a variety of compounds (guests). CDs are indeed “traditional” hosts since their binding sites converge on the guest in the inclusion complex. The structure and formation of CD inclusion complexes may be quite different in crystalline state from that in solution. Since the work in this thesis was conducted in aqueous media we will briefly introduce CD complexes in aqueous solution.

A supermolecular complex requires a minimum of one host and one guest component. In most cases, the cyclodextrin to guest ratio is 1:1,^{83,90,91,93,100} though 2:1 binding can be significant at higher concentration of cyclodextrin with longer aliphatics,^{101,102} aromatics,¹⁰³ azo dyes⁸³ and aryl-alkyl guests.^{19,104,105,106} There are also reports of 1:2 binding,¹⁰⁷ as well as of 1:1:1 binding of a cyclodextrin with two different guests;^{19,88,108,109} this usually occurs with γ -cyclodextrin.

Host-guest complementarity is involved in structural recognition since it increases the area of contact and the number of non-covalent interactions involved. For strong binding the CD and guest should complement each other both in terms of polarity and

size. The cyclodextrin interior affords a less polar hydrophobic cavity, while the exterior is hydrophilic. A property that is of interest for applications in medicine is the complexation of hydrophobic guests (drugs) in a CD cavity to improve their solubility in water and to aid their transport and absorption. Based on polarity, there is an inverse correlation between solubility in water and complex formation, and while additional methyl groups on a guest promote complex formation, cationic groups impede it. The guest will tend to bind in a way to optimize interaction between its hydrophobic parts and the CD cavity. The hydrophilic groups of a guest are kept further away and in contact more with the solvent water or with the hydrogen bond network of the secondary hydroxyls of the CD bucket.

Does size really matter? Even though CDs have been labeled “promiscuous” for their propensity to act as hosts to a wide variety small to medium sized guests,¹⁹ size is a vital determining factor for ‘complete tight inclusion’ of a guest in the CD. The guest must fit into the CD cavity, either partially or fully. However, a guest can form a supermolecular complex with the CD by binding *in* the cavity, *through* the cavity, or requiring two cavities for binding, or just remain at the *interface* of the CD cavity.¹³ A common rule of thumb, is that α -, β -, or γ -cyclodextrin can accommodate benzene, naphthalene and anthracene, respectively (Figure 2.3).^{103,110} It has been repeatedly shown that molecules that are significantly larger than the CD cavity either do not bind or they form a complex with only a side chain (or group) of the guest included into the CD cavity.^{83,90,93,111} Conversely, if the guest is too small, it will bind weakly or not at all. Irrespective of size, sometimes the shape of the guests and steric interactions affect inclusion of guests in CDs. Some guests which are not size nor shape compatible with the

cavity may form a complex by hydrogen bonding to hydroxyl groups on the exterior of the cyclodextrin.⁸³

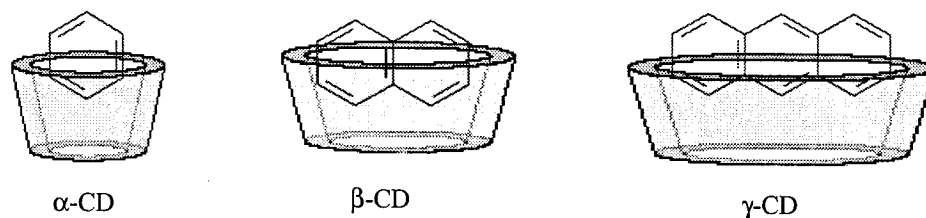


Figure 2.3 Complementarity based on size is important for CD-guest inclusion.

Incidentally, guest molecules have been varied in size from fatty acid coenzyme A derivatives, small and medium-sized aliphatic hydrocarbons, aromatic hydrocarbons, aromatic dyes acids, amines, alcohols, ketones (vide infra), and to a smaller extent, small ions such as ClO_4^- , SCN^- , halide anions, as well as neutral noble gases.^{83,90}

2.1.3 The Driving Force for Complex Formation

The driving force for the inclusion of guests in the CD cavity is governed by several factors, acting synchronously to bring about a favorable decrease in the overall free energy of the system.¹¹² The most important factors are non-classical hydrophobic effects and the extrusion of ‘enthalpy rich’ water molecules from the CD cavity to the bulk, van der Waals and hydrogen bonding interactions, and conformational changes or strain release of the cyclodextrin molecule upon complexation.^{83,87,90,91,113}

In aqueous solution, according to the “iceberg” model, water molecules form highly ordered clusters around the apolar guest but not inside the apolar cyclodextrin cavity - because it is too small. Experts believe that the water molecules enclosed in the CD cavity (and to a lesser extent those surrounding the guest) cannot satisfy their full

potential for forming tetrahedral hydrogen bonds, as they can in bulk aqueous solution, and so they are "enthalpy rich".^{83,87,90,91,113} When the guest enters the CD cavity from the aqueous solution there is a decrease in the relative freedom of the guest and host and so their combined entropy is reduced. Working against this reduction are entropy increases due to the break-up of those 'water cages' around the apolar guest and to the release of water molecules from inside the cyclodextrin cavity. Consequently, the net change in *entropy* is small. At the same time, enthalpy is decreased as the water molecules liberated from around the guest and inside the CD cavity are better able to form hydrogen-bonded water clusters in the bulk medium.

In keeping with the previous paragraph, most of the thermodynamic data available on cyclodextrin complexation indicate that the overall ΔG° for the process is negative because of favorable (negative) ΔH° changes, but only small (negative or positive) changes in ΔS° .^{107,114,115}

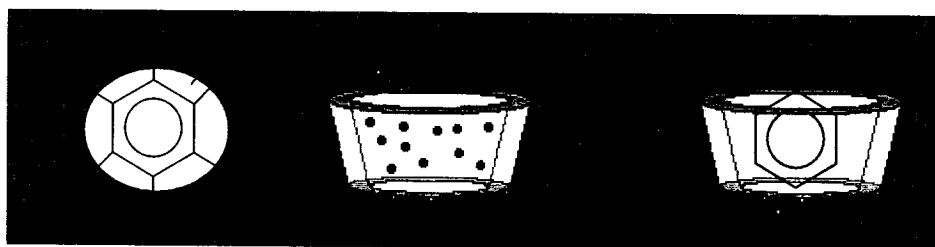


Figure 2.4 Release of high-energy water from the CD cavity, and breaking of the water cages around the guest, drives complex formation.

The extrusion of the enthalpy rich water molecules from the cavity upon inclusion of the apolar guest also results in the removal of the unfavorable polar-apolar interactions between water molecules and the CD cavity, and between water molecules and the guest. They are replaced by more favorable apolar-apolar interactions between the guest and CD cavity and polar-polar interactions between liberated water molecules and those in the

bulk aqueous medium. As a result, substitution of the "high-energy" water molecules by guests result in the high negative *enthalpy* change. As the size of the CD increases from α -CD, to β -CD, to γ -CD, the number of water molecules that can be enclosed in the CD cavity increases (Table 2.1).^{84,87} Because of the greater size each water molecule is better able to acquire complementary hydrogen bonds, and so the water molecules are less "enthalpy rich", on average.

Van der Waals interactions, which include permanent dipole-induced dipole interaction and London dispersion forces, may contribute to favorable host-guest binding. The strength of these interactions is approximately proportional to the reciprocal of the distance between two components raised to the sixth power, and to the polarizability of these two components. Thus, bulkier guests that fit into a cyclodextrin have stronger van der Waals interactions with the CD cavity, and thus they form more stable complexes.⁸³

Some guests, are capable of forming hydrogen bonds with the hydroxyl groups of cyclodextrins.^{115,116} For example, phenol,¹¹⁷ *p*-hydroxylphenol,¹¹⁷ and substituted phenyl propionates¹¹⁴ are capable of forming hydrogen bonds with the hydroxyl groups of α -CD and β -CD. These H-bonds may contribute to the stability of the complexes formed especially when geometrically convenient. However, sometimes such H-bonding weakens the binding of the complex relative to the parent compound because of enhanced unfavorable (negative) entropic contribution.¹¹⁴ It has also been suggested that increasing the hydrogen bond acceptor basicity of some guests leads to destabilization of the complex with a cyclodextrin because of stronger hydrogen bond interaction with the water in the aqueous medium.¹¹⁸

X-ray crystallographic studies and potential energy calculations have shown that one of the glucose rings of α -cyclodextrin is more or less orthogonal to the others in aqueous solution.¹¹⁹ When a substrate is included in α -CD, the gluocpyranose unit that is canted inward relaxes to a more normal state, and the cyclodextrin becomes more symmetrical. These observations have led to the suggestion that strain energy is associated with α -CD in aqueous solution and upon inclusion of a guest some of this strain energy is alleviated. However, the release of strain energy does not contribute to the driving force in complexation of a guest to hydrated β -CD¹²⁰ and γ -CD¹²¹ since the "doughnut" arrangements of the glucose rings in these CDs are more or less symmetrical.

2.2 EFFECT OF CYCLODEXTRINS ON REACTIONS

Because cyclodextrin "hosts" can form complexes with a wide variety of "guest" molecules, CDs may catalyze and retard chemical reactions in aqueous solution. CDs exhibit two basic forms of catalysis: "non-covalent" and "covalent".⁸³ *Covalent catalysis* arises when there is a distinct covalent interaction (formation or rupture of a covalent bond) between a functional group of the substrate and the CD during the rate-limiting step of the reaction. Hydrolytic cleavage of a number of aryl esters,^{19,54,55,111} amides,¹²² and phosphates¹²³ are well-studied examples under this category.^{19,83} In all these reactions, the substrate, which may or may not be bound to one or more cyclodextrins, undergoes nucleophilic attack by an ionized secondary hydroxyl group of the CD, as depicted below in Figure 2.5.

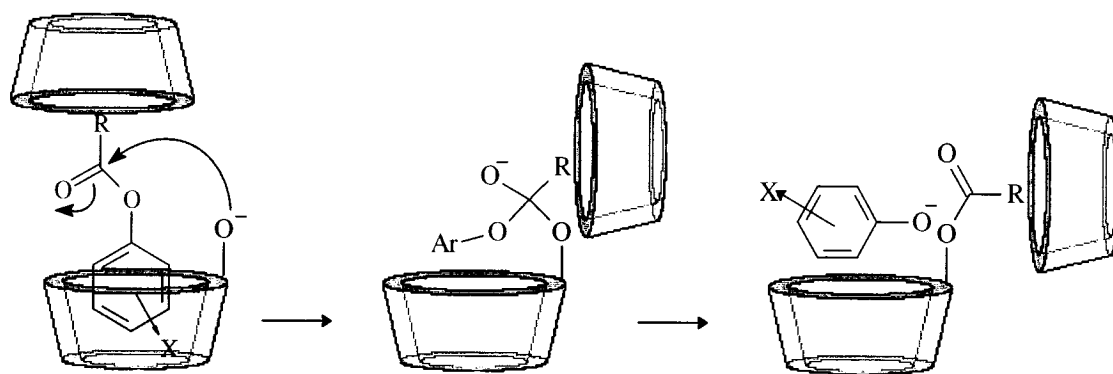


Figure 2.5 Example of the effect of cyclodextrins on reactions. The mode of cleavage of X-phenyl alkanoate esters by an ionized secondary hydroxyl group of the CD in aqueous base depends on the aryl substituent X-, the alkanoate chain and the CD. The ester may be bound to the CD by aryl or alkyl group inclusion, or even both.¹¹¹

Cyclodextrins can alter the rate of reactions by various non-covalent means. In *non-covalent catalysis*, inclusion of the substrate(s) into the CD cavity provides a new medium for the reaction (microsolvent effect), and the effect is seen most in reactions which are highly solvent dependent such as Diels-Alder,¹²⁴ decarboxylation,¹²⁵ and bromination-debromination reactions.^{48,126,127} Alternatively, the cyclodextrin may bind a guest in one conformer rather than another, for geometrical reasons.^{54,83,128,129} Such complexation by a cyclodextrin may help to bring reactants into a more reactive geometry. Non-covalent catalysis may also arise from a differential solvation effect at the interface of the CD cavity with the bulk aqueous medium.^{19,48,126,130,131} There is a differential effect because part of the guest (the reaction transition state) is in the environment of the CD and the rest of it is in "water".

2.3 OBJECTIVE OF THE RESEARCH

Due to the ability of cyclodextrins (CDs) to form inclusion complexes, they can influence the rate and selectivity of certain chemical reactions, either by simply sequestering one or both of the reactants or, in some cases, the deprotonated cyclodextrin hydroxyl group catalyzes the conversion of reacting molecules. Catalytic processes of this kind, either covalent or non-covalent,⁸³ have been regarded as models of enzyme action.

The kinetic effect of cyclodextrins on certain organic reactions has led us to intensify research on their complexation properties (structure and strength), and their ability to stabilize the transition states of reactions.¹⁹ The values of the strength of binding of the transition state (K_{TS}) can be useful for differentiating between the modes of binding in the S.CD complex and TS.CD complex. It is also possible to use the values of K_{TS} to differentiate between the two types of cyclodextrin catalysis.¹⁹

Various techniques can be utilized to study cyclodextrin-guest complexes depending on the type of information sought. The method of choice to gain structural information about complexes between CDs and guests is NMR spectroscopy.¹¹⁶ Because the CD cavity is chiral it induces circular dichroism in the UV-visible spectra of non-chiral guests, upon complexation. Apart from providing evidence of the inclusion of a guest, this induced circular dichroism signal can give information about the orientation of a guest in a cavity.¹³²

Although the CDs are almost transparent in the UV-visible region, moving a guest from bulk water to the hydrophobic cavity of a cyclodextrin may have a large influence on the spectroscopic properties of the guest due to changes in polarity. Absorbance and

fluorescence spectroscopy have therefore long been used to study complexation by CDs of probes with suitable chromophores or fluorophores.^{83,133} Unfortunately, there is no guarantee that all methods will give the same structure of the complex; even worse, the equilibrium constants reported for CD-guest complexation are not always reproducible.¹³⁴ The work presented in the thesis is an extension of the earlier studies on determining the dissociation constants and binding of non-reactive guests such as alkylcarboxylate ions, alkanesulfonate ions, aliphatic alcohols, and other aliphatics to CDs using different methodologies.^{113,135,136} We have used and will continue to use ‘inhibition kinetics’ to determine these dissociation constants. This research is part of the ongoing search for improving the facility, speed, and reliability of the methods used for estimating the dissociation constants of host-guest complexes formed by CDs.

The specific objective of the study described in Chapter III of the thesis is 1) to study the effect of cyclodextrins on the rate of acetal/orthoester hydrolysis, 2) to see the binding mode of the substrates in the CD cavity, 3) to use the acid-catalyzed hydrolysis of acetals/orthoesters as a probe reaction in order to estimate the binding strength of CD-ketone complexes, 4) to ascertain the binding forces of ketones with cyclodextrins, and most importantly 5) to evaluate ‘inhibition’ kinetics as a methodology for estimating the binding strength of CD-guest complexes.

CHAPTER III. KINETICS OF ACETAL AND ORTHOBENZOATE HYDROLYSIS AS PROBES OF CYCLODEXTRIN–KETONE BINDING

3.1 INTRODUCTION

Our interests in cyclodextrins (CDs) are mainly associated with the varied kinetic effects they can have on organic reactivity, causing alteration in rates (retardation or acceleration) due to their ability to form host-guest complexes of different strength with the substrate and transition state.¹⁹ Competitive inhibition kinetics^{26,27,137} are widely used in enzymology to quantify the binding of substrate analogues and transition state analogues to enzymes.^{45,46} To a limited extent, similar methodology has been employed for assessing the binding of guests to CD hosts.^{129,136,138-141}

In aqueous solution, cyclodextrin-substrate complexes (CD.S) are not static species. There is a rapid exchange (dissociation and association in equilibrium) between CD-bound and free substrate. The substrate will re-accommodate with a favorable orientation in the CD that maximizes binding interactions. A dissociation constant (K_s) measures this equilibrium and represents the strength of binding of a substrate to a CD.



The Gibbs energy of dissociation of the CD.S complex is given by:

$$\Delta G^\circ = -2.303 RT \log K_s = 2.303 RT \text{p}K_s \qquad [3.2]$$

In some cases, it is possible to determine the orientation of a substrate in the cyclodextrin cavity by looking at how dissociation constants vary with structure.

The basis of “normal” competitive inhibition kinetics method,^{26,27,137} is that presence of a guest molecule (G, potential inhibitor), which competes with the substrate

for binding to the CD (Figure 3.1), reduces the concentration of free CD catalyst, and thereby reduces (inhibits) the rate of the catalyzed reaction. Appropriate analysis of the rate reductions in terms of the amount of added guest (G) then affords an estimate of the CD.G dissociation constant (K_G).

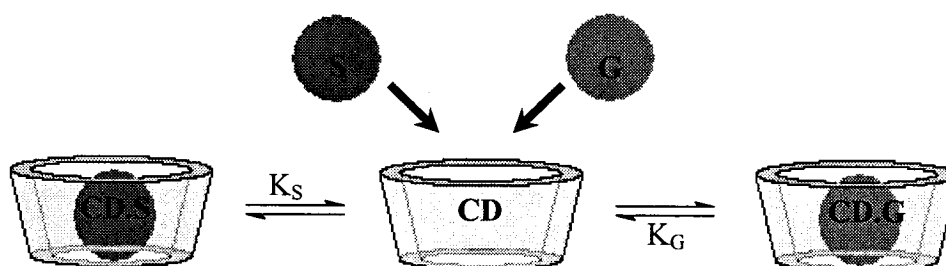


Figure 3.1 A guest (G) competes with a substrate (S) for binding to the cyclodextrin and effects the reactivity.

The use of “inhibition” kinetics approach to estimate K_G values has been successfully used with phenyl ester cleavages that are catalyzed by CDs as the probe reactions. VanEtten and co-workers¹²⁹ demonstrated the use of competitive inhibition of the reaction of m-nitrophenyl acetate (mNPA) with α -CD by various carboxylate and sulfonate anions to find their binding constants ($K_I = 1/K_G$).

Later, Tee and co-workers^{19,111,136,138,140,141} have used a similar approach on many occasions, although with a different form of data analysis from that of VanEtten,¹²⁹ to find dissociation constants of non-reactive guests such as alkylcarboxylate ions, alkanesulfonate ions, aliphatic alcohols, ketones other aliphatics to CDs.^{113,135,136} Our research group has since showed that binding of a guest (potential inhibitor = PI) to a

cyclodextrin (α -, β -, hp- β -, or γ) may alter its reactivity toward ester cleavage and not necessarily ‘inhibit’ it. For example, the cleavage of p-nitrophenyl acetate and hexanoate (pNPA and pNPH) by cyclodextrins was not severely inhibited, and in some cases was even catalyzed, by concomitant binding of the guest (PI) and the substrate.^{19,136} It was proposed that the PI acted more like an inert spacer or ‘spectator’ which can bind in the CD cavity without affecting the mode of transition state binding where the ester moiety is largely outside the CD cavity. In some cases, the spectator guest can even have a modest stabilizing effect on the TS for acyl transfer and lead to additional catalysis.¹³⁶ The latter effect has been termed “spectator catalysis”.¹⁰⁹ Such behavior stands in contrast to that of acyl transfer with mNPA for which substrate binding and transition state binding are quite similar (aryl inclusion), so that ‘spectators’ are not tolerated, and guests of the CD act as true inhibitors.¹²⁹ However, with m-nitrophenyl hexanoate and β -CD a ‘mode switch’ was exhibited when simple aliphatic alcohols suppressed the normal favored mode of reaction, which occurs through aryl inclusion into the CD cavity, and promoted reaction by a different mode, acyl inclusion through an alcohol-mediated ternary complex (PI.CD.ester).¹⁴¹ The examples above provided a model for primitive allosteric effects by enzymes,^{25,27,142} in which binding of a guest (allostere) at a site on a host (cyclodextrin) causes a change in reactivity or mode of the reaction at more or less the same site.

The vast majority of studies of the influence of cyclodextrins (CDs) on guest binding and reactivity, especially those which made use of ‘inhibition’ kinetics to estimate K_G values, had been carried out in basic aqueous solution. The reason for the choice of basic medium is probably because CDs, being glycosides, are presumed to labile in aqueous acid media. In fact, as remarked earlier, CDs are reasonably robust, and

moderately strong acids (or elevated temperatures) are required to destroy them quickly.⁹⁰ Thus, the effects of CDs on reactions that are fast in dilute acid, such as the bromination of activated aromatics,^{19,48} can be studied without the CDs undergoing appreciable degradation.

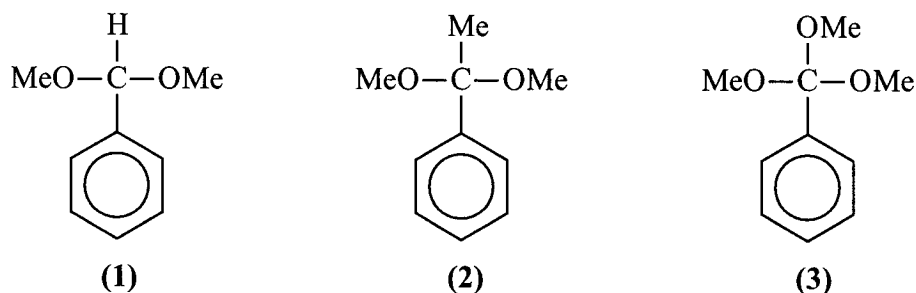
Recently, our research group has studied the effects of cyclodextrins on the hydrolysis of a simple acetal (benzaldehyde dimethylacetal) in aqueous acid, and evaluated the use of this reaction as a probe for determining CD.Guest dissociation constants (K_G).¹⁴³ This probe reaction was *slowed down* substantially by CDs, and the addition of inert guests causes it to speed up. The general features and analysis will be reiterated later. Unfortunately, using the methodology of “inhibition kinetics” to assess the K_G values of aliphatic alcohols to the CDs only worked well for β -CD and *hp*- β -CD and not for α -CD or γ -CD.¹⁴³

In the research presented in this thesis, further examples of acid-catalyzed acetal and orothobenzoate hydrolysis are tested as probe reactions that are inhibited rather than catalyzed by CDs. These were studied in order to determine the feasibility of using such reactions to find the dissociation constants (K_G) for complexes formed in dilute acid aqueous solution (rather than dilute base) between various ketone guests and CDs. The results have been published already.¹⁴⁴

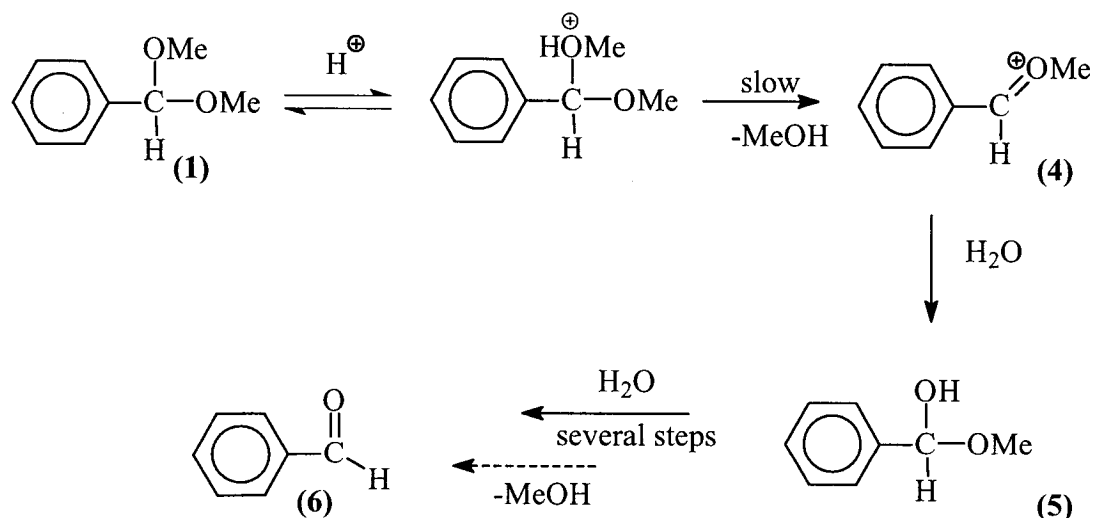
3.2 RESULTS

3.2.1 Mechanism and Probe Reaction

Acid-catalyzed hydrolysis reactions of benzaldehyde dimethylacetal (BDMA, **1**), acetophenone dimethylacetal (ADMA, **2**), and trimethyl orthobenzoate (TMOB, **3**) were



chosen as the kinetic probe reactions because they are fast in dilute aqueous acid and can be monitored easily. Their products have carbonyl chromophores (C=O), which make them suitable for stopped-flow experiments, with UV-visible spectroscopic detection. A simplified mechanism of BDMA hydrolysis is shown in Scheme 3.1 below:

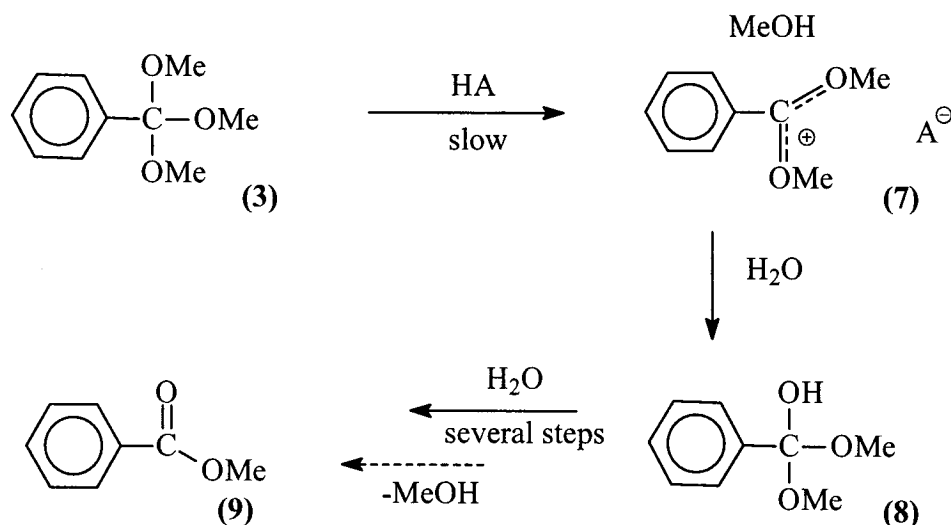


Scheme 3.1 Acid catalyzed hydrolysis of BDMA.

The mechanism of acetal cleavage has been extensively studied.¹⁴⁵⁻¹⁵¹ In general, it is accepted that first the acetal (**1**) undergoes specific hydrogen-ion catalysis¹⁵¹ in an equilibrium protonation followed by rate-limiting loss of alcohol to yield an oxonium ion (**4**) that, in water, converts rapidly to the hemiacetal (**5**). A subsequent number of fast steps, having another elimination of a molecule of alcohol from the hemiacetal (**5**) facilitated by acid or base catalysis, yield the final products.

BDMA (**1**) hydrolysis is followed by the appearance of benzaldehyde (**6**), and the reaction is essentially complete in 2 s, having a half-life of 0.2 s, in 0.10 aqueous HCl at 25 °C.¹⁴³ At short times (<100 ms) the absorbance trace shows a distinct induction period that is indicative of a two-step, consecutive reaction.^{150,152} In the case of BDMA the decomposition of the hemiacetal is faster having a rate constant of $75.5 \pm 4.4 \text{ s}^{-1}$; the first step, hemiacetal formation, with a rate constant of $3.55 \pm 0.01 \text{ s}^{-1}$, is largely rate-limiting, and the increase in absorbance, after omitting the first 10%, can be treated as a single exponential due to this step.¹⁴³

The hydrolysis of ADMA (**2**), also known as 1,1-dimethoxyethyl benzene, which was monitored by the absorbance increase due to acetophenone (PhCOMe) production, proceeds by the same mechanism as BDMA. The hydrolysis of the orthoester TMOB (**3**), shown in scheme 3.2, is general-acid-catalyzed,^{146,153} and it was monitored by the production of methyl benzoate (**9**).



Scheme 3.2 Acid catalyzed hydrolysis of TMOB.

Releasing strain in the tetrahedral ground state in formation of the transition state and enhancing the stability of the oxocarbenium ion (7), that has additional resonance stabilization by another methoxy substituent, induces general-acid catalysis.^{151,154} The greater the bulk in (3) inhibits protonation, but accelerates C-O cleavage, so that the first two steps become ‘concerted’. The production of (7) is still rate-limiting. In what follows, the observed rate constants (k_{obs}) for hydrolysis of BDMA, ADMA and TMOB were all obtained from non-linear analysis of the final 90% of the absorbance trace collected over 2 seconds, so they refer to the slower step (acetal/orthoester to hemiacetal/hemiorthoester).

3.2.2 Effect of Cyclodextrins

Tee and coworkers^{143,144} have established that four cyclodextrins (α -, β -, hp- β -, and γ -CD) all retard the acid-catalyzed hydrolysis of the three substrates. Figure 3.2 illustrates the decrease in k_{obs} for the hydrolysis of TMOB, ADMA, and BDMA brought about by added β -CD.¹⁴³

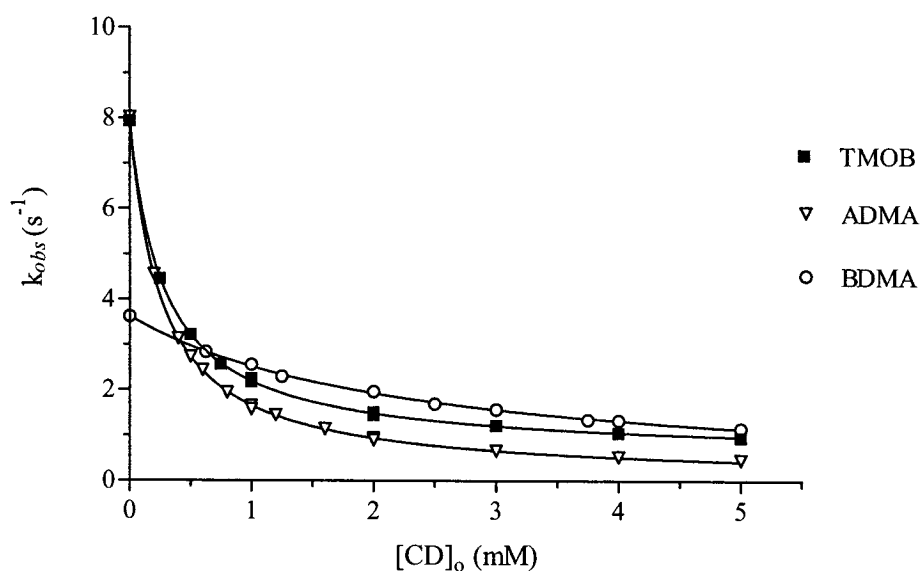
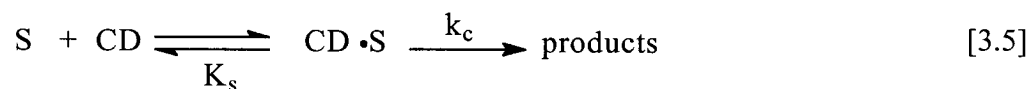


Figure 3.2 Effects of β -cyclodextrin on rates of hydrolysis of the substrates. The curves are calculated from equation [3.6] with constants from Table 3.1.

For all three substrates, the decrease in k_{obs} brought about by hp- β -CD^a was not all that different from that by β -CD. For α -CD and γ -CD, the binding of the substrates is weaker and care was taken to vary $[CD]$ over a wide enough range to make the curved dependence of k_{obs} quite evident.¹⁴⁴ Other researchers,^{155,156} before the start of this study, found the dissociation constants K_S for those substrates and the cyclodextrins.

^a Hydroxypropyl- β -cyclodextrin (hp- β -CD) is β -CD, dissolved in basic solution, that has been reacted with propylene oxide so that most of its primary hydroxyl groups are alkylated.

The decreases of k_{obs} with $[CD]$ are consistent with simple saturation kinetics, arising from 1:1 binding between the substrate (S) and the CD, according to the following model:



$$k_{obs} = \frac{(k_u K_s + k_c [CD])}{(K_s + [CD])} \quad [3.6]$$

The model allows for the reaction of the free substrate (S) in the medium (eq. [3.4]), and the reaction through a complex (CD.S) (eq. [3.5]). The predicted variation of k_{obs} with CD is given by eq. [3.6] assuming that $[CD] \gg [CD.S] < [S]_0$, which was valid for all experiments. Equation [3.6] is normally associated with reactions where k_{obs} increases with $[CD]$ (because $k_c > k_u$) but it is equally applicable for rate retardation (where $k_c < k_u$) and for outright inhibition ($k_c = 0$). As long as the observed data corresponding to eq. [3.6] have sufficient curvature values of K_s and k_c can be estimated with reasonable confidence.

Table 3.1 contains parameters k_u , k_c and K_s for BDMA, ADMA and TMOB with β -CD. The parameters for substrate binding to the other CDs are known but are not required for the research presented in this thesis, which is concerned mainly with finding ketone dissociation constants (K_G) to β -CD using ‘inhibition’ kinetics of the probe reactions.

Table 3.1 Constants for the effect of β -cyclodextrins on acid-catalyzed hydrolysis of BDMA, ADMA and TMOB.^a

Substrate	k_u (s ⁻¹)	K_S (mM)	k_c (s ⁻¹)	r	N
BDMA ^b	3.62 ± 0.02	2.26 ± 0.05	0 ^e	0.9992	12
ADMA ^c	8.02 ± 0.04	0.247 ± 0.006	0.0507 ± 0.0296	0.9999	7
TMOB ^d	7.94	0.281 ± 0.004	0.573 ± 0.018	0.9999	11

^a At 25 °C. Values of K_S and k_c were obtained by non-linear fitting of equation [3.6], usually with k_u fixed at the observed value. Where k_u is presented with errors, it was fitted. N is the number of data points, and r is the correlation coefficient. Examples of the data and fitted curves is shown in Figure 3.2.

^b In 0.100 M aqueous HCl. From data collected by A. Fedortchenko.¹⁵⁶

^c In 0.010 M aqueous HCl. From data collected by S. Hussein.

^d In 0.100 M aqueous HCl. From data collected by I. Turner¹⁵⁵ and O.J. Yazbeck.^{143,144}

^e Value fixed at zero. With k_c treated as a parameter, fitting gave values indistinguishable from zero, and closely similar values of K_S .¹⁴³

3.2.3 Effects of Added Guests

In this study, the author of the thesis mainly looked at the effects of ketone guests on β -CD retarded hydrolysis of BDMA and TMOB.¹⁴⁴ As remarked in the introduction, with “normal” CD-catalyzed reactions, the addition of a guest inhibitor will reduce the concentration of free CD catalyst, which should effectively reduce the rate of the reaction. This was observed with the addition of ketones and alcohols to cyclodextrin-mediated ester cleavage.^{140,141} Since acetal hydrolyses are probe reactions which are slowed down by CDs, not accelerated ($k_c < k_u$), addition of a guest, which competes with the substrate for the CD (eq. [3.3], Fig. 3.1), effectively lowers the free CD concentration, and leads to an *increase* in the observed rate of acetal hydrolysis (k_{obs}), rather than a decrease. This indeed was observed, and some examples involving the hydrolysis of TMOB in the presence of β -CD at various concentration of ketone are shown in Figures

3.3-3.5 (data necessary for calculation of K_G are tabulated in Appendix A). Comparable rate increases were also seen with ADMA and BDMA, though the fits were not as good, due to spectral interference. Turner and other researchers in our group looked at the effects of alcohols as guests on these acid-catalyzed hydrolysis reactions in the presence of all CDs, and similar rate enhancements were observed.^{143,144}

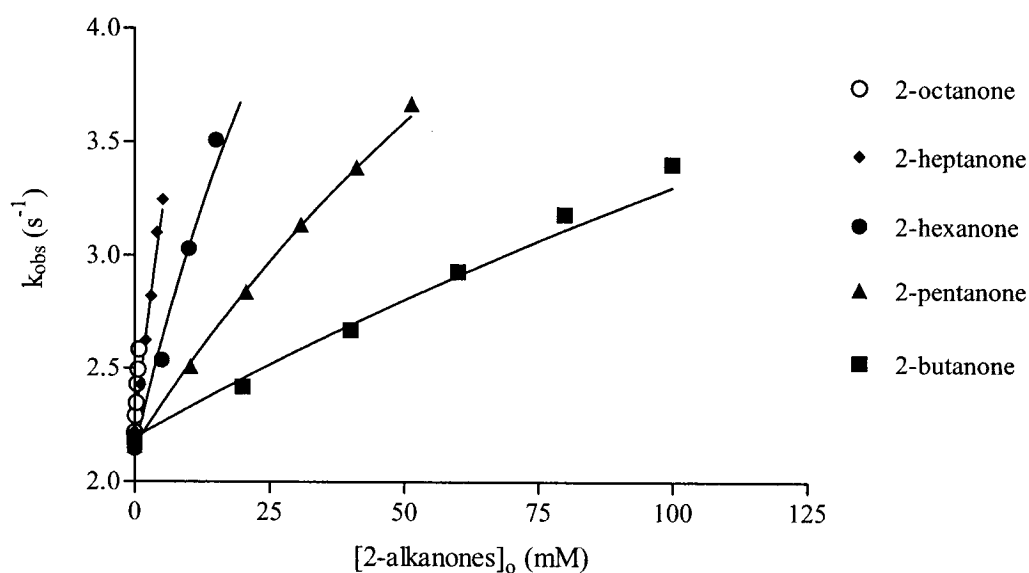


Figure 3.3 Sample data for the catalysis of the hydrolysis of TMOB in β -CD (1.00 mM) by 2-Alkanones. The curves are splines through points calculated with the relevant dissociation constants K_G in Table 3.2.

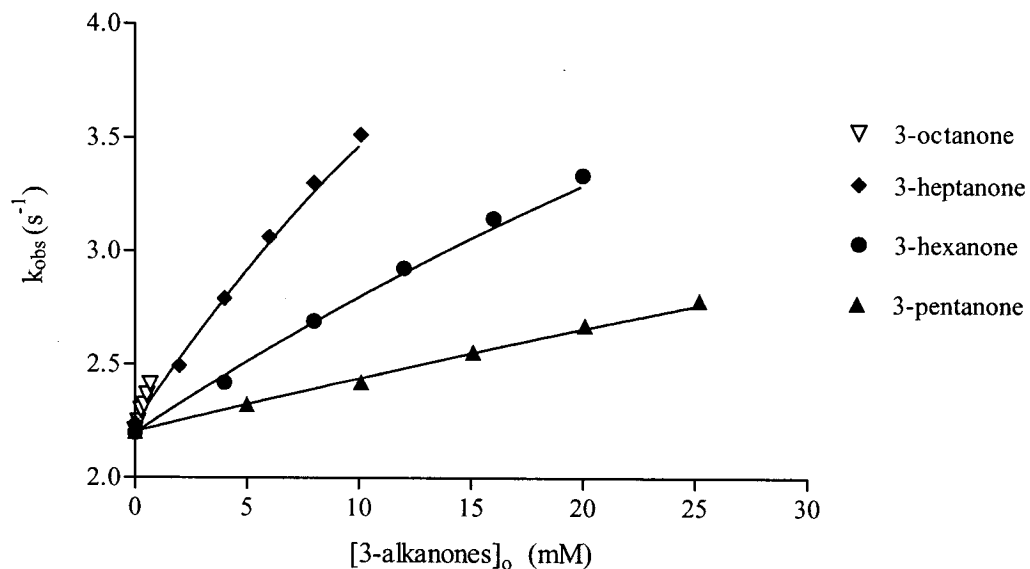


Figure 3.4 Sample data for the catalysis of the hydrolysis of TMOB in β -CD (1.00 mM) by 3-alkanones. The curves are splines through points calculated with the relevant dissociation constants K_G in Table 3.2.

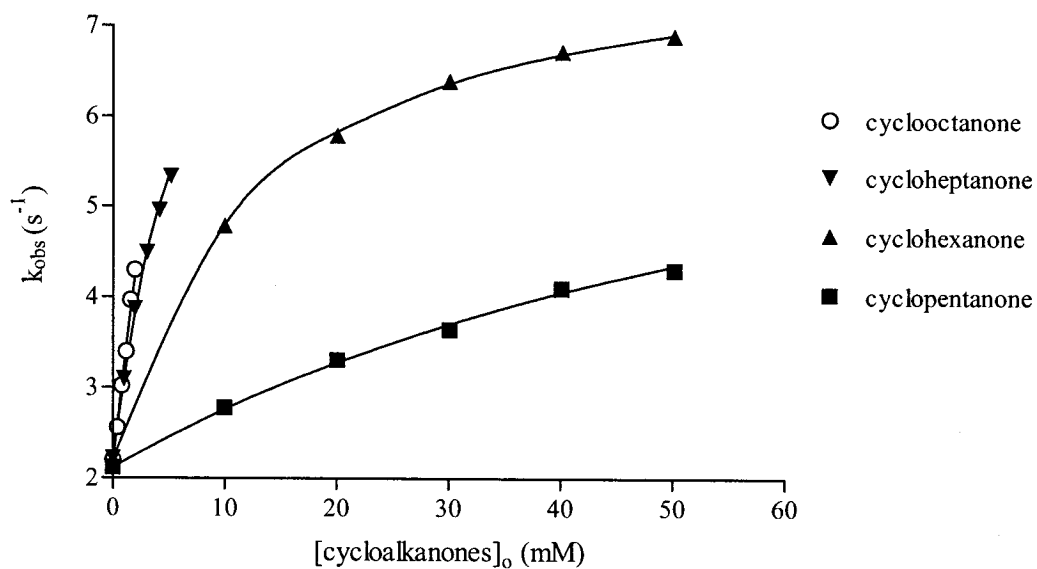


Figure 3.5 Sample data for the catalysis of the hydrolysis of TMOB in β -CD (1.00 mM) by cycloalkanones. The curves are splines through points calculated with the relevant dissociation constants K_G in Table 3.2.

Analysis of the substantial rate increases as a function of [ketone]_o, such as those displayed in Figures 3.3-3.5, can be used to estimate the dissociation constants (K_G) of cyclodextrin–ketone (CD·G) complexation, by utilization of a slightly modified ‘inhibition’ kinetics approach that was developed some years ago.^{136,143,155} The basis of the approach is to exploit eq. [3.7], derived from a rearrangement of eq. [3.6], to find the concentration of unbound CD from k_{obs} measured in the presence of an added guest, G.

$$[CD] = \frac{(k_{obs} - k_u) K_s}{(k_c - k_{obs})} \quad [3.7]$$

Using established parameters k_u , k_c and K_s (Table 3.1), which are measured at the same conditions as this work, the free [CD] are calculated for several [G]_o.

Remember, by definition, K_G is given by

$$K_G = \frac{[CD] [G]}{[CD \cdot G]} \quad [3.3]$$

Knowing the initial concentration [G]_o, and also [CD] from eq. [3.7], then [CD·G] and [G] can be calculated from mass balance equations, eq. [3.8] and [3.9]:

$$[CD \cdot G] = [CD]_o - [CD] \quad [3.8]$$

$$[G] = [G]_o - [CD \cdot G] = [G]_o - ([CD]_o - [CD]) \quad [3.9]$$

Then, estimates of K_G are evaluated for several [G]_o, through the use of eq. [3.10], and averaged. Such calculations are carried out in a spreadsheet (see Experimental Section for a sample spreadsheet).

$$K_G = \frac{[CD] \{ [G]_o - ([CD]_o - [CD]) \}}{([CD]_o - [CD])} \quad [3.10]$$

Table 3.2 contains the dissociation constants K_G for 15 ketones with β -CD, determined using the hydrolysis reaction of BDMA, ADMA and TMOB as kinetic probes and data analysis based on equation [3.7] and [3.10]; along with literature values determined in our laboratory by one or more other methods.

Attempts by other researchers to use ADMA and TMOB hydrolysis to probe guest binding to α -CD gave results that were not particularly reproducible and therefore unreliable, as was found previously for BDMA.¹⁴³ In all three cases, the difficulty is due to the low sensitivity of k_{obs} to $[\alpha\text{-CD}]$ which arises because the values of k_c and k_u are not greatly different from one another, unlike the situation with β -CD. As a consequence, relatively small errors in k_{obs} translate to larger errors in $[\alpha\text{-CD}]$ and even larger errors in estimates of K_G .

Equally disappointing, experiments on guest binding to γ -CD were unsuccessful since small *decreases* in the rates of hydrolysis of the probes were observed, instead of the increases that are required for simple 1:1 CD–guest binding. As suggested previously,¹⁴³ γ -CD is large enough to accommodate the substrate and guest, and the further decrease in rate could arise from the formation of an unreactive ternary complex. Thus, K_G values for ketones with α -CD or γ -CD could not be accurately evaluated.

Table 3.2 Dissociation constants (K_G in mM) of the β -CD-ketone complexes determined using inhibition kinetics and the kinetics of hydrolysis of the probes BDMA, TMOB, and ADMA.^a

Guest	BDMA ^c	TMOB	ADMA ^{b,e}	Literature
Acetone	142 \pm 38	224 \pm 29		367 \pm 42 ^c 200 ^d
2-butanone	61.4 \pm 19.6 48.9 \pm 21.1 56.0 \pm 12.9	91.7 \pm 9.1		107 \pm 2 ^c
2-pentanone	34.4 \pm 3.3 27.6 \pm 3.4	32.2 \pm 0.9		39.0 \pm 1.7 ^c
2-hexanone	10.0 \pm 3.1 10.3 \pm 1.8 6.73 \pm 3.09	11.2 \pm 1.8		16.4 \pm 0.7 ^c
2-heptanone		5.07 \pm 0.32		4.94 \pm 0.50 ^c 4.76 \pm 0.21
2-octanone		1.87 \pm 0.13		1.73 \pm 0.03
3-pentanone		51.1 \pm 2.3		56.9 \pm 2.3
3-hexanone	19.7 \pm 0.2 ^f	21.8 \pm 1.0 18.4 \pm 1.4	19.8 \pm 0.3 ^f	21.2 \pm 0.4
3-heptanone		7.88 \pm 0.52		9.62 \pm 0.66
3-octanone		3.37 \pm 0.27		3.76 \pm 0.33
4-heptanone		8.84 \pm 0.23		8.79 \pm 0.12
cyclopentanone	18.4 \pm 1.5	16.2 \pm 0.6	20.0 \pm 0.4 ^f	19.6 \pm 0.6
cyclohexanone	2.88 \pm 0.14 2.82 \pm 0.05 ^f	2.50 \pm 0.06 2.63 \pm 0.17	2.30 \pm 0.24 ^f 2.56 \pm 0.05 ^f	2.51 \pm 0.05 1.96 ^d
cycloheptanone		0.801 \pm 0.040		0.635 \pm 0.085
cyclooctanone		0.530 \pm 0.040		0.484 \pm 0.025

^a The acid catalyzed hydrolysis of BDMA and TMOB were conducted in the presence of 5.00 or 1.00 mM β -CD, respectively, and 0.100 M aqueous HCl at 25 °C. Multiple entries for a particular guest reflect separate results from different experiments under the same conditions or different researchers.

^b The acid catalyzed hydrolysis of ADMA were conducted in the presence of 1.00 mM β -CD and 0.010 M aqueous HCl at 25 °C, and the data was collected by S. Hussein in our laboratory.

^c Literature values determined using a fluorescence probe displacement method; the rest are from the inhibition of β -CD-induced ester cleavage.¹⁴⁰

^d Binding constants K_I ($=1/K_G$) for acetone are from Taraszewska¹⁵⁷ and for cyclohexanone from Rekharsky *et al.*¹⁵⁸

^e There are fewer entries for ketones and ADMA or BDMA, because of spectral interference by the ketone at the wavelength used to monitor the hydrolysis reaction (see text).

^f Data collected by other researchers in our lab, using the same methodology of this study.

3.3 DISCUSSION

The present work expands greatly on initial studies and reaffirms that acid-catalyzed hydrolysis of BDMA, ADMA, and especially TMOB can be used as a kinetic probes for finding CD–guest dissociation constants, in particular for β -CD and ketones. Before discussing the details of ketone binding to β -CD, we will first affirm what we know about the substrate binding and transition state binding to CDs and how it relates to the rate reductions.

3.3.1 Substrate Binding to CDs

Re-iterating previous findings, the hydrolysis of the acetals is slowed down, and in some cases substantially, by added CDs. The trend in strength of binding (pK_S) of all three substrates to CDs, presented in Table 3.3, follows the order α -CD < β -CD \approx hp- β -CD > γ -CD, as expected, and the trend has been attributed to the cavity sizes of the CDs.

Table 3.3 Constants for the binding (pK_S) of BDMA, ADMA, and TMOB to cyclodextrins compared to phenyl-substituted guests.^a

Ph-X	α -CD	β -CD	hp- β -CD	γ -CD
Ph-CH (OMe) ₂	1.33	2.65	2.44	1.29
Ph-CMe(OMe) ₂	1.31	3.61	3.33	1.91
Ph-C(OMe) ₃	1.76	3.55	3.34	2.03
Ph-X (mean) ^b	1.40 \pm 0.25	1.98 \pm 0.67		1.34 \pm 0.35

^a At 25 °C. The $pK_S = -\log K_S$, units of molarity. All pK_S values are from data collected by other researchers in our laboratory.^{143,144}

^b A mean value for Ph-X, calculated by Gadre *et al.*¹⁵⁹

This order is typical for benzenoid compound derivatives. Tee *et al.*¹⁴⁴ compared the strength of binding (pK_S) of these phenyl-substituted substrates to the four

cyclodextrins to mean values of pK_s determined by Gadre *et al.*¹⁵⁹ for Ph-X derivatives binding through their phenyl groups (Table 3.3). From such comparisons, the binding mode to the CDs was deduced, as illustrated in Figure 3.6.

For binding to α -CD, the studied substrates bind by their phenyl groups, but the cavity is too narrow (~ 0.6 nm) to encapsulate all of the phenyl ring with ease and so the aromatic substrate sits more or less “perched” in the mouth of the α -CD cavity, **(10)**. By contrast, the strength of the substrates binding to β -CD happen to be stronger than that of the mean of other phenyl derivatives, particularly for PhCMe(OMe)_2 and PhC(OMe)_3 ; suggesting the involvement of some additional interactions. Conceivably, the substrates sit more deeply and “snugly” in the β -CD cavity (width ~ 0.8 nm), with some attractive interactions between the rim and the substituents, **(11)**. Alternatively, the stronger binding may arise from binding of the substrates to β -CD with their substituents deep inside the

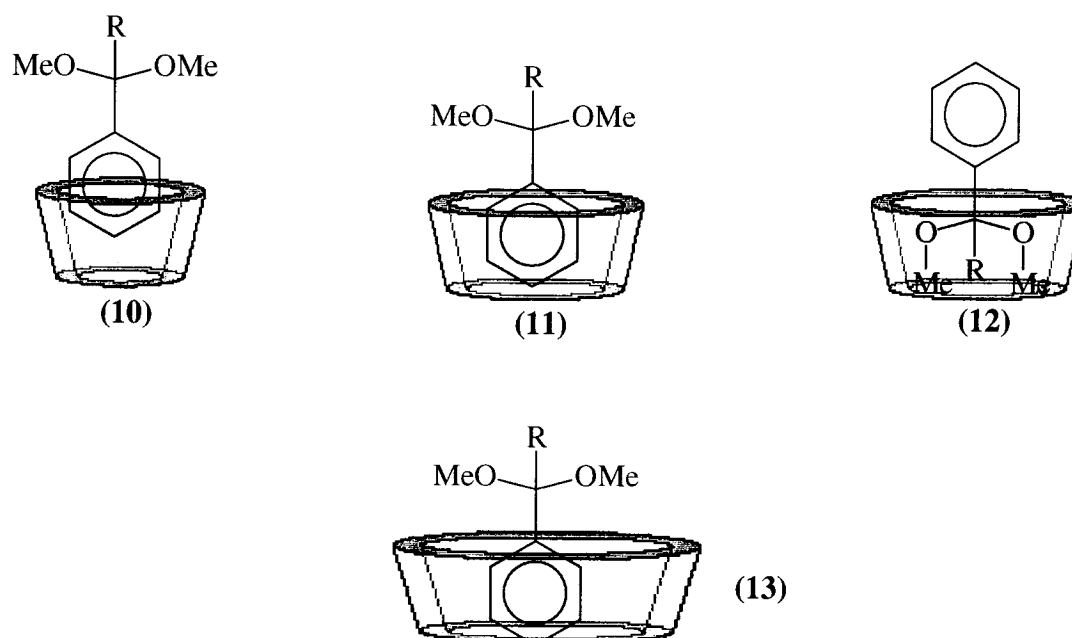


Figure 3.6 Substrate-cyclodextrin binding.

CD cavity, (12).^b Because of the wider cavity of γ -CD (~ 1.0 nm), these aromatic substrates can sit deep in the cavity but with a “looser fit”, (13), so that they show weaker binding than with β -CD (or hp- β -CD). In the case of ADMA and TMOB, their binding to γ -CD is stronger than expected relative to the mean value. Thus, the binding mode might well be similar to that of β -CD having some additional interaction with the cavity rim, (13), or that the substituents are buried inside the CD cavity (12).

3.3.2 Transition State Binding and the Reactivity of the CD-Bound Forms

There is a significant decrease in the reactivity of the cyclodextrin bound substrates for acid-catalyzed hydrolysis. For example, the complexation of TMOB and ADMA to β -CD attenuates the rate by a factor of 14 and of more than 270, respectively; for BDMA, the bound form is essentially unreactive ($k_c = 0$) (see Table 3.1) Such sizable rate reductions can be attributed to a combination of factors.

In terms of the transition state stabilization model, described in Chapter I, which we have employed extensively to describe reactions mediated by CDs,¹⁹ the substantially low reactivity of the CD-substrate complexes mean that the hydrolysis transition states are bound less strongly (less favorably) than the substrates to the CDs ($k_u/k_c = K_{TS}/K_S > 1$). As was noted previously for BDMA hydrolysis,¹⁴³ since the transition state (TS) is cationic for these acid-catalyzed hydrolysis reactions,¹⁴⁶ then the TS binding to the CD is very much less favorable than the substrate binding because the CDs do not bind simple cations well as neutrals or anions. Whereas the binding of anions of many types (eg.

^b In Figure 3.6, structure (12), this binding mode is perhaps less likely because the two methoxyl groups are somewhat hydrophilic and so would prefer to be directed towards the aqueous bulk medium, while the phenyl ring is hydrophobic and would have favourable interactions with the hydrophobic CD cavity.

phenolate anions, alkanoate anions, benzenesulfonate ions) by CDs have been observed, and it can be quite strong,^{83,134} the binding of cations has rarely been observed,¹⁶⁰ except with large organic dyes,^{90,161} long chain cationic surfactants,¹⁰¹ and metal ions with organic ligands.¹⁶² The binding of simple cations like anilinium ion (PhNH_3^+) to CD appears to be relatively unfavourable, and it binds only in combination with a counterion.¹⁶⁰ Iglesias and coworkers have adopted the same factor, destabilization of a cationic TS relative to the substrate, in order to explain the rate-retarding effects of β -CD on the acid-catalyzed hydrolysis of phenylpropyl nitrites¹⁶³ and on the nitrosation of the enol of benzoylacetone.¹⁶⁴

Acetal, ketal and orthoester reactivity toward hydrolysis do not always parallel the stability of the corresponding cation, and reactivity also depends on the basicity of the substrate and on steric factors.¹⁴⁹ For example, in the absence of cyclodextrin, ADMA is 10 times more reactive than TMOB and some 20 times more reactive than BDMA towards acid-catalyzed hydrolysis.¹⁴⁴ Then again, the relative reactivity of the cyclodextrin-bound acetals and orthoesters greatly depends on the stability of the corresponding intermediate TS cation in the CD and the mechanism of hydrolysis. From the mechanism of the specific-acid-catalyzed hydrolysis of BDMA (Scheme 3.1) the transition state (TS) for the rate-limiting step is intermediate in structure between the protonated acetal and the α -methoxybenzyl cation (**4**) plus methanol. The TS of the general-acid-catalyzed hydrolysis of TMOB (Scheme 3.2) is intermediate in structure between neutral TMOB + hydronium ion and α,α -dimethoxybenzyl cation (**7**). Inductive effects and hyperconjugation by the methyl group of ADMA can play a role in the stabilization of its specific-acid catalyzed hydrolysis transition state. Without exception,

for acetals bearing polar substituents in the aryl moiety, the second order rate constants for the hydrolysis correlate with σ and not σ^+ , and with large negative ρ values.^{146,147,165} However, the hydrolysis of orthobenzoates is less sensitive to polar substituents, having smaller negative ρ values, indicating that the TS for TMOB hydrolysis may have less cation character than that for acetal hydrolysis.¹⁴⁶ It has also been suggested, from α -deuterium isotope effects, that little C-O bond cleavage occurs at the TS for TMOB hydrolysis, i.e. the TS is earlier on the reaction coordinate in the direction of C-O bond cleavage.¹⁶⁶ It may then be argued that the TS destabilization by the cyclodextrin will be less for TMOB hydrolysis than for the acetal hydrolysis, because the former TS has less cationic character, and this is reflected in higher reactivity of TMOB.CD complex (higher k_c value). Since the substrate binding to β -CD (pK_s) hardly varies between TMOB and ADMA,^c the magnitude of retardation by β -CD which has the order BDMA ($k_c/k_u = 0$, complete inhibition) \gg ADMA ($k_c/k_u = 0.00632$) $\gg\gg$ TMOB ($k_c/k_u = 0.0722$) (Table 3.1) may be a consequence of the relative cationic character of the hydrolysis transition states.

Another possibility for the inhibitory effect of CDs is that the cyclodextrin severely impedes the separation of a molecule of methanol from the initially-formed 'encounter complex', eg. $\{\text{PhCR}=\text{O}^+-\text{Me}/\text{MeOH}\}$, which has been suggested to be the rate-limiting step in some acetal hydrolysis.^{148,167} Slowing down the separation effectively promotes reformation of the starting acetal and retardation is most severe when the 'encounter complex' is sequestered within the CD cavity.

^c Actually BDMA is least tightly bound, and one would have thought that it would have been least affected by the CD relative to ADMA and TMOB.

In the case of α -CD, the substrates are most likely bound with their reactive groups exposed to the aqueous medium (10), which is most probably the reason that the rate reductions are relatively modest for α -CD as compared with the other CDs. However, in the case of the β -CDs and γ -CD, the much larger reductions in reactivity may result because the substrates are bound deeper within the CD cavities (11), and possibly with their reactive groups buried (12) and completely screened from the aqueous acidic medium, rendering them quite unreactive.

3.3.3 Cyclodextrin-Ketone Binding

a) Assessing the probe reaction for estimating K_G values

Previously, our research group estimated the binding of ketones to CDs using a method based on displacement of a fluorescent probe, 1-anilino-8-naphthalenesulfonate (ANS), from the CD by the guests.¹⁴⁰ This method worked reasonably well for small ketones, but was not successful with larger ketones that had to be used in low concentrations due to their poor solubility. The method was also impractical with α -CD because the binding of ANS to this CD is very weak, and the change in fluorescence upon binding of the ketone guests is therefore relatively small.¹¹¹ Additionally, our group has used 'normal' inhibition kinetics, employing m-nitrophenyl acetate (mNPA) hydrolysis in basic aqueous medium as a CD-catalyzed probe reaction, and they found CD-ketone dissociation constants for α -, β - and hp- β -cyclodextrin for 22 ketones.¹⁴⁰ In basic solution, ketones may undergo enolate formation and base-catalyzed condensation,^{35,49,168} which are much slower than the cleavage of mNPA in the presence of CDs, and so should not have complicated measurements. Surprisingly, aside from our

research group, there were no decent compilations of ketone binding to CDs to compare K_G values.^{134,157,158}

For the purposes of comparison, and as preparation for future studies of the effects of CDs on the chemistry of ketones, the dissociation constants of various β -CD-ketone complexes (K_G) have been determined in acidic medium, rather than basic solution. Use was made of the rate increases of the CD-retarded hydrolysis of BDMA, ADMA and TMOB upon inclusion of the ketone guests (see Table 3.2, page 54). Obviously, ketones are a very important class of organic compounds and reliable determination of their complexation to CDs in aqueous solution could have many potential uses.

The estimated K_G values obtained with TMOB hydrolysis as the probe reaction agreed very well with those obtained from previous studies,¹⁴⁰ taking account the experimental error, as can be appreciated from Figure 3.7 and Table 3.2. There is a very good correspondence between pK_G values from hydrolysis of TMOB in acid medium and pK_G from the cleavage of mNPA in basic medium, with almost all the points lying on the line of unit slope passing through the origin, which means that the binding strength of the ketones to β -CD is independent of the substrate and the aqueous medium. The apparent discrepancies, which were generally small, may just simply reflect systematic differences between the different methodologies used. The only sizeable deviations in Figure 3.7 are for two quite small, volatile ketones, acetone and 2-butanone, which must be added in high concentrations because they bind weakly. Their K_G values are large and less easily determined, and there is the possibility that these ketones not completely impede the binding of the substrate.¹⁴⁰

Experiments of the effects of added alkyl ketones on the β -CD-retarded hydrolysis of BDMA and ADMA were more disappointing and gave data which did not analyze particularly well. They provided variable K_G values with higher margins of error (Table 3.2) and so fewer experiments were carried out with these two probes. The problem arises because their hydrolysis products, benzaldehyde ($\lambda_{\max} = 252$ nm) and acetophenone ($\lambda_{\max} = 244$ nm), absorb in the same general region (250-290 nm) as the ketone guests, and so the guests interfere with monitoring the hydrolysis reactions. Generally speaking, the problem was less severe with BDMA than with ADMA, and there is no comparable spectral interference when using the hydrolysis of TMOB as the probe reaction because then the product is an ester that was monitored at a lower wavelength (228 nm). Note that such spectral problems are not encountered when the guests are alcohols, and all three probe reactions were equally efficient for estimating K_G for alcohol-CD complexes.¹⁴⁴

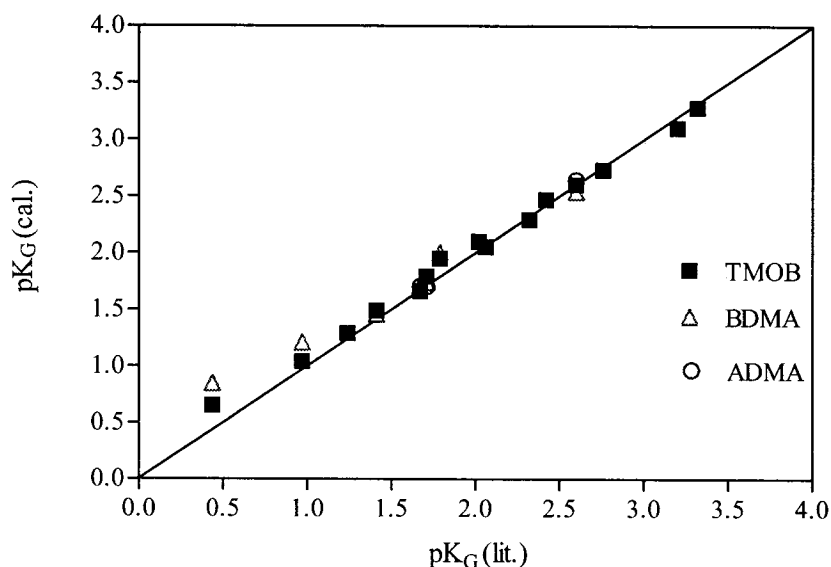


Figure 3.7 Comparison of pK_G values for CD-ketone binding, plotted as pK_G (lit.) vs. pK_G (cal.), where the latter are from the present work (Table 3.2) and the former from Tee *et al.*¹⁴⁰ The diagonal line through the origin with a slope of one corresponds to pK_G (cal.) = pK_G (lit.).

b) Effect of chain length on the binding of ketones to β -CD

It is by now well-established, by our group and others, that the strength of binding of simple n-alkyl derivatives (alcohols, alkanes, amines, alkanoate ions, alkanesulfonate ions, alkanoate esters, etc.) to CDs increases more or less monotonically with chain length, up to about 8 carbon atoms.^{19,111,135,139,140} The chain length dependences of pK_G for binding of the 2-alkanones (MeCO-R) and 3-alkanones (EtCO-R) are illustrated in Figure 3.9 (overleaf). These correlations may be considered as linear free energy relationships (LFERs),^{34,35,49,169} and the slopes of the LFERs for 2-alkanone and 3-alkanones (Table 3.4) are similar to those obtained for other alkyl derivatives (Table 3.4).¹⁴⁰ These similarities indicate analogous sensitivity to structural changes, and the response of binding to β -cyclodextrin by increasing chain length of the different n-alkyl derivatives is the same. This concurs with the general view that the binding of these n-alkyl guests is determined by inclusion of the n-alkyl moiety of the ketone in the β -CD cavity while the hydrophilic portion resides in the bulk aqueous medium (Figure 3.8, 14). Minor variations in the slopes with different n-alkyl derivatives may be due to differences in the solvation requirements of the hydrophilic head groups and possibly to weak interactions with hydroxyl groups on the rims of CDs.

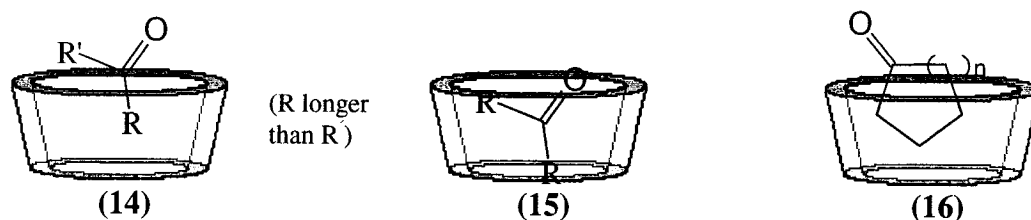


Figure 3.8 Ketone- β -cyclodextrin binding.

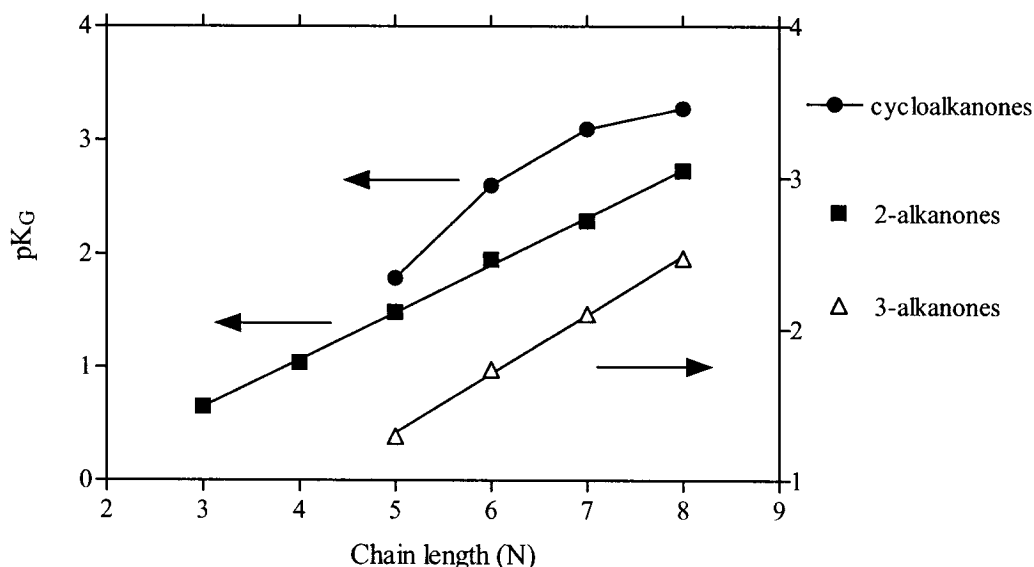


Figure 3.9 Chain length dependence on the strength of binding of ketones to β -CD. pK_G values are taken from hydrolysis of TMOB as the probe reaction. The sets of pK_G values are offset for clarity. Note that for ketones of the same total number of carbon atoms, the pK_G values have the order cycloalkanones > 2-alkanones > 3-alkanones.

Table 3.4 Structural dependence of the binding of aliphatic guest to β -cyclodextrin. Correlations between pK_G and chain length or ring size (N).^a

Guests	N	Slope \pm sd	R	Note
2-alkanones	3-8	0.417 ± 0.007	0.999	b
3-alkanones	5-8	0.391 ± 0.013	0.999	b
cycloalkanones	4-8	0.653 ± 0.092	0.961	b
2-alkanones	3-8	0.459 ± 0.010	0.999	c
3-alkanones	5-8	0.388 ± 0.011	0.999	c
cycloalkanones	4-8	0.617 ± 0.083	0.974	c
1-alkanols	1-8	0.547 ± 0.016	0.997	d
2-alkanols	5-8	0.502 ± 0.022	0.996	e
cycloalkanols	4-8	0.539 ± 0.087	0.963	e
RSO_3^-	4-8	0.479 ± 0.041	0.989	f
RNH_2	3-7	0.524 ± 0.008	0.999	f

a) In aqueous solution, at 25 °C. The slope, standard deviation (sd) and correlation coefficient (r) are taken from the linear least square analysis of pK_G against N. b) Based on K_G values given in Table 3.2.¹⁴⁴ c) Based on values taken from Tee *et al.*¹⁴⁰ d) Values taken from Tee *et al.*^{143,144} e) Based on values taken from Matsui and co-workers^{113,135} with additional values from Tee *et al.*¹⁴⁰ f) Taken from Tee *et al.*^{139,140}

Except for the cyclic derivatives, the slopes of pK_G vs. chain length (N) (Table 3.4) fall in the range of 0.39 - 0.55, which correspond to free energy increments of free energy increments^d of 2.0 - 2.9 kJ mol⁻¹ for each methylene group that is sequestered from the aqueous medium by inclusion in the β -CD cavity. These values are approaching the range (2.8 - 3.6 kJ mol⁻¹) for the free energy of transfer of CH₂ groups from water to various organic media (including micelles) and are typical for systems where hydrophobic effects are operative.^{65,75} Consequently, it appears that hydrophobic effects⁶⁸ are a primary factor to the binding of simple aliphatics and alkyl ketones to β -CDs. However, the size and surface area of the n-alkanones also increase with the number of carbon atoms (chain length), which means that van der Waals forces between the ketones and CDs increase, and these interactions significantly contribute to complexation as well.^{116,170,171}

Furthermore, it is noteworthy that pK_G vs. the carbon number for the cyclic ketones is decidedly curved downward and not linear (Figure 3.9). It is reasonable to assume that as the ring size increases, it is not only hydrophobicity but also size that influence binding strength. Cyclic ketone inclusion into the CD cavity leads to expulsion of more high energy water molecules from the cavity, better snugness of fit, and more van der Waals interactions as compared with the inclusion of the corresponding linear ketone, thus increasing the driving force for complexation and strength of the complex. However, the larger cyclic ketones ($\geq C_7$) may no longer completely “fit” into the cavity of β -CD (Figure 3.8, 16), as reflected in the lower pK_G than anticipated had there been a linear correlation between pK_G and ring size (Figure 3.9). So the larger size of the ring

^d $\Delta G_s^0 = 2.303 RT pK_s$, where $R = 8.314 \text{ J K}^{-1} \text{ mol}^{-1}$, and $T = 273 \text{ K}$.

will constrain the cyclic ketone to sit higher in the cavity of β -CD, resulting in weaker hydrophobic and van der Waals interactions. Binding of cycloalkanones to α -CD do not vary much with ring size past cyclobutanone, and their K_G values are much higher than those with β -CD.¹⁴⁰ Cyclic ketones ($> C_4$) are too bulky to penetrate far enough into the narrower cavity of α -CD, and are constrained to 'perch' on top, while β -CD can accommodate cycloalkanones more readily.

c) Binding of unsymmetrical ketones to β -CD

This study confirms that unsymmetrical alkanones ($RCOR'$) bind to β -CD by inclusion of the longer of the two-alkyl fragments (Figure 3.8, **14**).¹⁴⁰ Following the same analysis, the strength of binding to β -CD (pK_G) of methyl ketones ($RCOMe$) and primary alcohols (ROH) bearing the same alkyl group are plotted and compared in Figure 3.10. A linear correlation, with a slope of 0.73 ± 0.04 ($r = 0.997$, 4 points) for n-alkyl groups (propyl to hexyl), reveals that binding of methyl ketones has a comparable, though diminished, sensitivity to the changes in R. In addition, and as expected, the methyl group of the $RCOMe$ makes an unmistakable positive contribution to ketone binding strength judged by their overall larger pK_G values than the corresponding ROH (Figure 3.10). It is quite rational that the $-COMe$ head group of the methyl ketones is more hydrophobic than the $-OH$ group of the corresponding alcohols, and therefore would interact more strongly with the hydrophobic CD, where the OH group would tend to interact more strongly with the aqueous medium. At the same time, the presence of the methyl group reduces the sensitivity (somewhat) of the binding to the structure of the alkyl group, R.

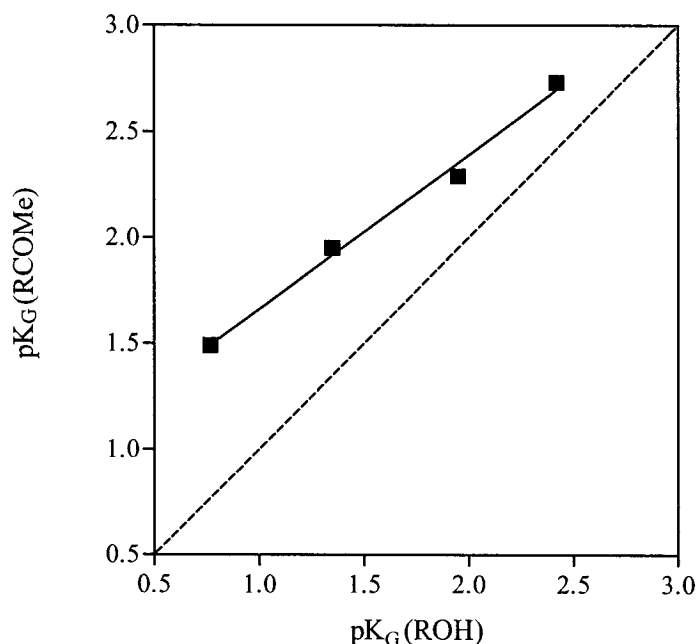


Figure 3.10 Comparison of the strength of binding of methyl ketones (RCOMe) and alcohols (ROH) to β -CD. pK_G ($= -\log K_G$) for the 2-alkanones from TMOB hydrolysis, are taken from our data in table 3.2, those for primary alcohols are taken from Tee *et al.*⁵⁹ under the same conditions and the same orthoester. The dashed line corresponds to the $pK_G(RCOMe) = pK_G(ROH)$.

The 2-alkanones have smaller dissociation constants than the corresponding 3-alkanones of the same overall carbon number (Table 3.2), again supporting the idea that alkanones bind to β -CD mainly by inclusion of the larger alkyl group. There is a reasonable correlation (slope = 0.962 ± 0.03 ; $r = 0.999$, 4 points) for the complexation of these ketones with an overall carbon number ranging from 5-8 (Figure 3.11), which suggests that there are no major differences in the manner in which these ketones bind to β -CD, although in general the binding of 3-alkanones is weaker.

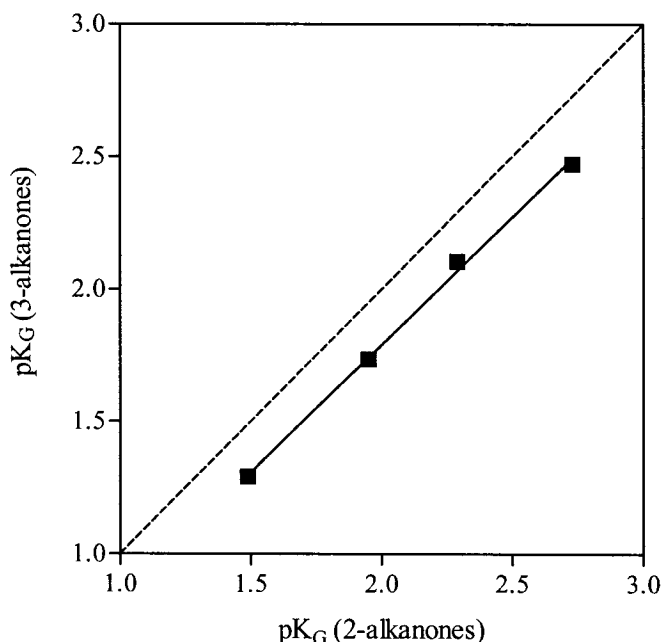


Figure 3.11 Comparison of the strength of binding of 2-alkanones and 3-alkanones of the same carbon number to β -CD. The dashed line corresponds to the pK_G (3-alkanones) = pK_G (2-alkanones).

Although our data support the idea that unsymmetrical alkanones bind to CDs mainly by inclusion of the larger alkyl group, we cannot infer that the larger group is the sole determinant. When we compare the K_G values for a few unsymmetrical ketones ($RCOR'$), we find that increasing the n -alkyl chain length of the shorter portion causes an increase in the strength of binding, also. For instance, the K_G values decrease appreciably along the series 2-pentanone ($MeCOPr$), 3-hexanone ($EtCOPr$), and 4-heptanone ($PrCOPr$) (Table 3.2). Similarly, 3-pentanone ($EtCOEt$) and 3-heptanone ($EtCOBu$) bind more strongly than 2-butanone ($MeCOEt$) and 2-heptanone ($MeCOBu$), respectively. Analogous to the rationale given for methyl ketones binding stronger than primary alcohols, increasing the length of either alkyl fragment flanking the ketone carbonyl group will increase the hydrophobicity of the whole molecule, gradually overcoming the

hydrophilicity of the carbonyl group. Where size permits, there could be an increase in the depth of inclusion of the whole ketone molecule in the CD cavity (Fig. 3.8, 15) and hence, an increase in the binding strength.

d) Binding of ketones versus secondary alcohols to β -CD

Because of their structural similarities, it is of interest to compare the strength of binding of ketones (RCOR') by β -CD to that of the corresponding secondary alcohols, $\text{RCH(OH)R}'$, bearing the same alkyl groups. On the whole the binding of the ketones to β -CD is slightly weaker than that of the alcohols, with the difference increasing with chain length, but the two sets of values are fairly correlated, as shown in Figure 3.12, and the slope is 0.901 ± 0.046 ($r = 0.984$, 14 points), even though the correlation includes cyclic derivatives as well as linear ones. The correlation and slope suggest that the geometry and mode of binding of ketones and of related secondary alcohols to β -CD are similar. However, the binding is a slightly different with α -CD.¹⁴⁰ In that situation, all the alcohols bind appreciably more strongly than their ketone analogues, $\text{pK}_G(\text{alcohol}) \gg \text{pK}_G(\text{ketones})$, and it was suggested that there may be hydrogen-bonding between the hydroxy groups of alcohols and those on the rim of α -CD which strengthens complexation.¹⁴⁰

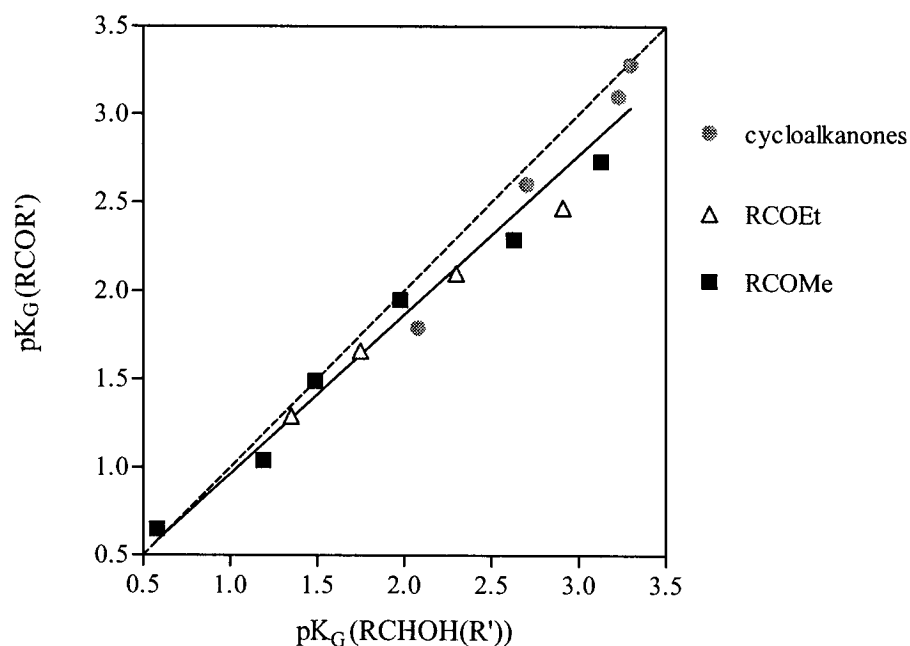


Figure 3.12 Comparison of the strength of binding of ketones (RCOR') and related alcohols (RCH(OH)R') to β -CD. pK_G for the ketones are taken from TMOB hydrolysis (Table 3.2), those for alcohols are taken from Matsui *et al.*^{113,135} and a few missing values from Tee *et al.*¹⁴⁰ The dashed line corresponds to the pK_G (RCOR') = pK_G (RCH(OH)R'), and the solid one to the correlation for all the ketones and alcohols.

3.4 CONCLUSIONS

Cyclodextrins cause appreciable retardation of the acid-catalyzed hydrolysis of benzaldehyde dimethylacetal (BDMA), acetophenone dimethylacetal (ADMA), and trimethyl orthobenzoate (TMOB). The acid hydrolysis of TMOB, and to a lesser extent that of BDMA and ADMA, were used successfully as probe reactions for estimating dissociation constants of β -CD-ketone complexes by 'inhibition' kinetics. The speed and simplicity of these hydrolysis reactions in dilute acidic medium renders them to be good kinetic probes for finding CD-guest dissociation constants, especially for non-reactive guests which may be sensitive to basic medium. The K_G values for CD-ketones

complexes were very similar to literature values, obtained in other ways, demonstrating the reliability of this procedure in calculating these constants.

Using the three hydrolysis reactions as quantitative probes of CD–guest binding works very well for β -CD (and hp- β -CD)^{143,144} because these CDs bind the substrates tightly and cause drastic reductions in their rates of hydrolysis. By contrast, the approach works poorly for α -CD because it does not bind the substrates strongly or reduce their reactivities greatly.¹⁴³ With γ -CD the approach is not applicable because added guests cause further reductions in the rates of hydrolysis, not increases, possibly due to formation of ternary (substrate·CD·guest) complexes.¹⁴³ The findings also serve to emphasize that to be successful, competition methods for estimating host–guest binding must involve a host and probe that bind together tightly, so that little host or probe need be used, and that the host–probe binding should evoke a large response in some easily measurable property.

The results and discussion presented are essentially a verification and backup to earlier research performed in our laboratory, dealing with estimation of dissociation constants of CD-ketone complexes, using inhibition kinetics combined with different probe reactions. Hydrophobic interactions and van der Waals forces are the primary factors involved in β -CD-ketone complexation whereas hydrogen-bonding plays only a minor role. For ketones having linear alkyl groups, the strength of binding increases monotonically with chain length, the slopes corresponding to free energy increments per methylene group which are appropriate for hydrophobic effects contributing to the binding. For cyclic ketones the change in surface area and size alter the van der Waals interactions and determine the depth of penetration inside the β -CD cavity and hence

affect the binding constant. We maintain the idea that unsymmetrical alkanones bind to β -CD mainly by inclusion of the larger of their two alkyl groups but still the shorter alkyl group does make some small contribution to the binding of these complexes. This study provides a valuable background for further study of the effect CDs on ketone chemistry.

We have also showed, using correlation plots, that the mode of inclusion of ketones is similar to that of alcohols. Comparing primary alcohols, ROH, to ketones RCOMe, the greater hydrophobicity of the methyl group of the ketones causes stronger binding to β -CD. By contrast, secondary alcohols tend to bind a little stronger to β -CD than their ketone counterparts but the differences are too small to suggest hydrogen bonding between the alcoholic OH and the CD hydroxyl group.

For future studies, one could diversify these acetals and orthobenzoates by modifying substituent groups on the phenyl ring in order to get better insight into the modes of binding of the acetals and orthoesters to CDs, and the factors involved in complexation of these substrates and their hydrolysis transition states with CDs.

Recently, several modified cyclodextrins bearing a spectroscopically active group or a fluorescence probe, have been synthesized and their complexation behaviors have been investigated;^{172,173} and this overcomes the spectroscopic transparency of the CD.^{172,173} The various changes in the self-inclusion behavior of this type of molecule upon the binding of an external guest into the CD cavity enable the optical detection of spectroscopically inactive guests. For example, Liu and coworkers¹⁷³ synthesized L-tryptophan-modified β -CD (Figure 3.13) and investigated the self-inclusion of the indole group of tryptophan and the inclusion of various alcohols (Figure 3.13) by fluorescence and circular dichroism spectrometry, and complex stability constants were

then determined. This approach can become the next wave of methodology used to harvest reliable estimates of guest dissociation constants to cyclodextrins.

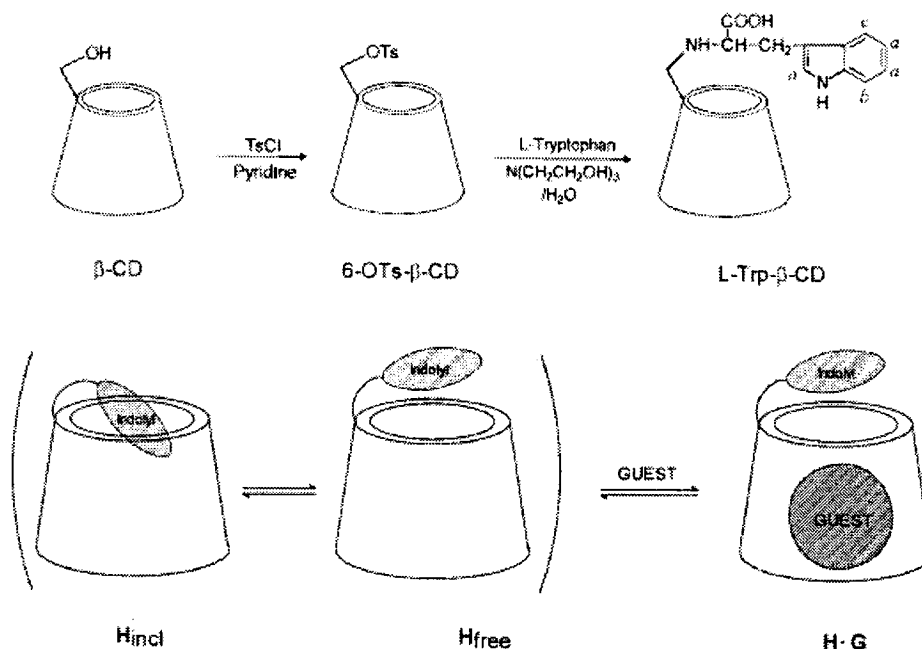


Figure 3.13 Synthesis of L-tryptophan-modified β -CD, and self- and guest-inclusion into cyclodextrin. The figure is taken from reference ¹⁷³.

3.5 EXPERIMENTAL

3.5.1 Materials

The cyclodextrins were purchased from the Aldrich Chemical Co. or Wacker-Chemie (Munich), and were used as supplied. Benzaldehyde dimethylacetal (BDMA), ADMA (1,1-dimethoxyethylbenzene), and trimethyl orthobenzoate (TMOB) and ketones were all of the best grade available at Aldrich. Hydrochloric acid solutions were made by dilution of standard 1.00 M solution obtained from American Chemicals Ltd (Montreal).

3.5.2 Kinetic Apparatus and Solutions

The hydrolysis of BDMA, ADMA, and TMOB was followed by monitoring the appearance of their products in the UV-visible region: benzaldehyde at 252 nm, acetophenone at 244 nm, methyl benzoate at 228 nm. Pseudo-first-order rate constants were calculated from absorbance increases, measured using an Applied Photophysics SX17MV stopped-flow spectrophotometer (Leatherhead, U.K.). The observation cell of the apparatus was kept at 25.0 ± 0.1 °C by circulating water from a thermostatted water bath. Absorbance traces consisting of 400 points spanning 7 to 15 half-lives were collected, with the first 10% of the absorbance trace was ignored to allow for the induction period that is a feature of acetal hydrolysis – See: section 3.2.1. A first-order rate constant was estimated from non-linear least squares fitting of an exponential increase, using computer software supplied with the stopped-flow apparatus. The recorded rate constants (k_{obs}) were taken as the average of 5-10 determinations differing by less than 5%.

Hydrolysis reactions were initiated by 1:1 mixing in a stopped-flow spectrophotometer. To minimize the effect of the slow substrate hydrolysis in water, the substrate solutions were made up fresh for each set of kinetic runs and made slightly basic with a drop of concentrated aqueous NaOH solution. These substrate (S) solutions (100 μM) were made by 1000 fold dilution of a 0.1 M stock solution of substrate in spectral grade acetonitrile, so as to give $[\text{S}]_0 = 50$ μM , after the 1:1 mixing. For the kinetics experiments with varying $[\text{CD}]_0$ (eg. Figure 3.2), one syringe of the stopped-flow apparatus contained 2 x 0.100 M aqueous HCl, and the other syringe held the substrate

(BDMA or TMOB, 100 μ M) and the CD at twice the concentration desired in the final reacting solution.

For the competition experiments, with fixed $[\text{CD}]_0$ and varying $[\text{ketone}]_0$, one syringe contained $2 \times [\beta\text{-CD}]_0$ and 0.200 M aqueous HCl and the other had the substrate (100 μ M) and $2 \times [\text{ketone}]_0$. The values for $[\beta\text{-CD}]_0$ after mixing was 5.00 mM with BDMA and 1.00 mM with TMOB. In general, as in previous studies involving the same guests,¹⁴⁰ we attempted to use ketone concentrations up to 2-5 times the expected K_G value, based on the binding of the similar alkyl-bearing compounds to the CD, but this was often not possible. Depending on their alkyl substituents, ketones have quite a range of solubility, and the upper limits for the ketone concentration used can be judged from the examples in Figures 3.3-3.5. Acetone, which is very soluble in water, binds only weakly to cyclodextrins, and so requires large concentrations to elicit a significant effect on the probe reactions. However, its concentration was kept ≤ 0.25 M to avoid any substantial ‘solvent effect’, which could obscure the effect under investigation. At the other extreme, the larger ketones (eg. 1-heptanone and 1-octanone) have quite limited solubilities in water, and it is not always possible to get a sufficient amount of the guest into solution to provide enough of a variation in k_{obs} , to give reliable estimates of K_G . This problem is less acute for the cyclic ketones which are more soluble than their linear counterparts.

3.5.3 Kinetic Analysis

Non-linear least squares fitting¹⁷⁴ of equations [3.7] and [3.11] was carried out with commercial software: GraphPad Prism, version 2.01. The estimation of dissociation

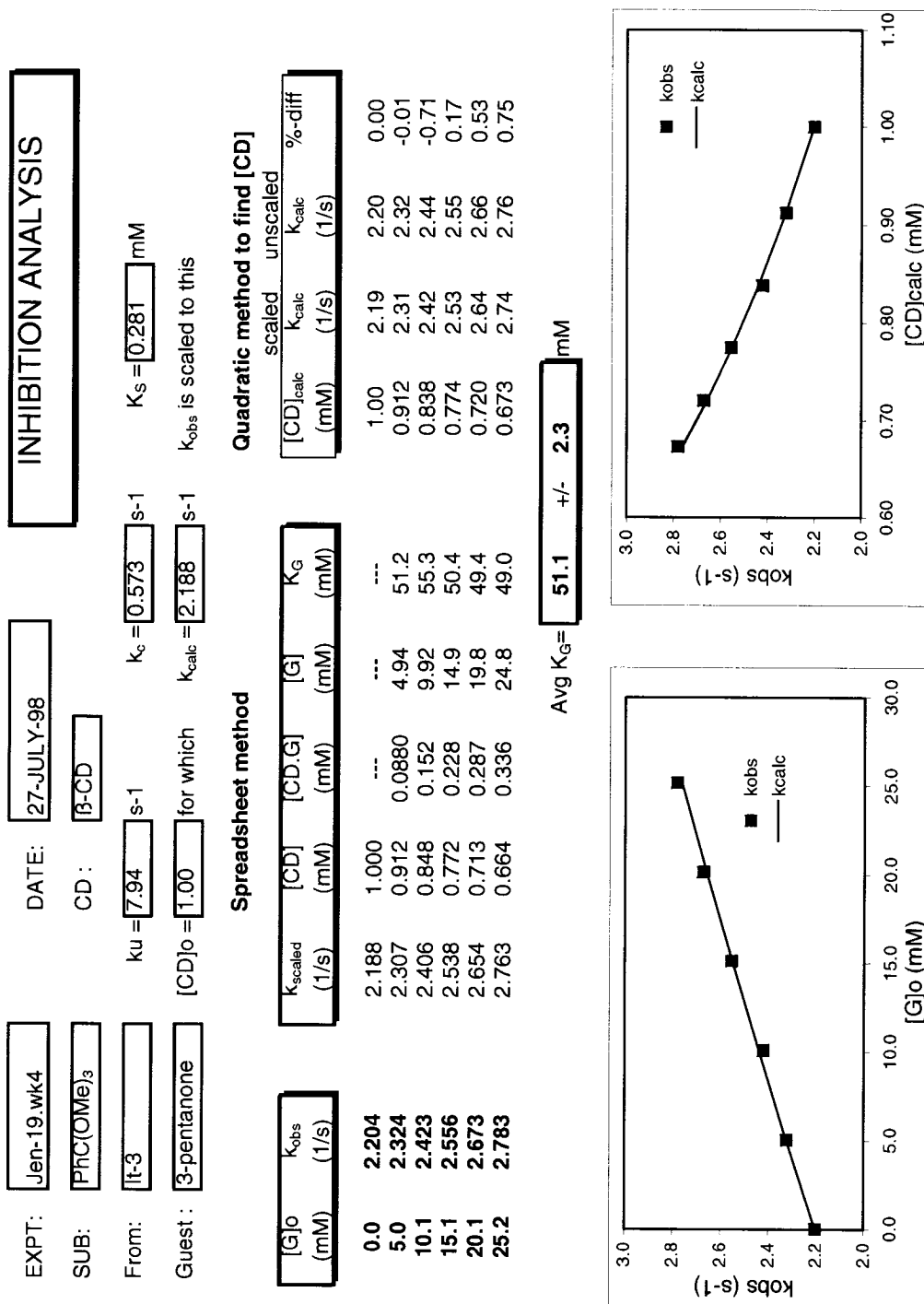
constants of the CD-ketone complexes using inhibition kinetics is conveniently carried out using a LOTUS 123 spreadsheet. An example of such a spreadsheet is shown in Scheme 3.3.

The k_{obs} value at $[\beta\text{-CD}]_0$ ($= 1.0 \text{ mM}$ or 5.0 mM) obtained for each substrate, at $[G]_0 = 0$, in different experiments were found to differ slightly from each other, probably due to subtle differences in the pH of the buffer. In order to minimize the effect of pH variations, the observed rate constants (k_{obs}) for each experiment were scaled to master runs for each substrate, with $k_{\text{calc}} = (k_u K_S + k_c [\text{CD}]_0) / (K_S + [\text{CD}]_0)$, where k_u , K_S , and k_c are known for each substrate (Table 3.1).

$$k_{\text{scaled}} = \frac{(k_{\text{obs}} \text{ at each } [\text{CD}]) (k_{\text{calc}})}{(k_{\text{obs}} \text{ at each } [\text{CD}]_0)}$$

As was explained in the results, $[\text{CD}]$ comes directly from eq. [3.7], but using k_{scaled} instead of k_{obs} . $[\text{CD} \cdot \text{G}]$ and $[\text{G}]$ are found using mass balance equations [3.8] and [3.9] (section 3.2.3). Then separate K_G values, from eq. [3.10], for different $[G]_0$ are found. Average K_G values and the standard deviation are those that appear in Table 3.2.

The observed rate constants are compared (graphically and by % difference) to calculated rate constants, where $[\text{CD}]$ in k_{calc} comes from eq. [3.11] (explained below). The use of ‘inhibition’ method to estimate the K_G values is best fitted when all values of k_{obs} are on the k_{calc} curve, with the % diff $= (k_{\text{obs}} - k_{\text{calc}}) \times 100 / k_{\text{calc}}$ approaching zero.



Scheme 3.3 Inhibition analysis spreadsheet

In addition to the “spreadsheet” analysis,^{136,138-141} we have examined the use of an expression that relates [CD] to the initial concentration of the guest.¹⁴⁴ Expansion of eq. [3.10] leads to a quadratic in [CD] whose solution is given by eq. [3.11]. For several different [G]₀, non-linear fitting of eq. [3.11] to the values of [CD]_{calc}, can be used to get an estimate of K_G. Figure 3.14 shows examples of the variation of [CD]_{calc} with [ketone]₀ along with fitted curves described in equation [3.11].

$$[\text{CD}]_{\text{calc}} = \{-b + (b^2 + 4K_G \cdot [\text{CD}]_0)^{1/2}\} / 2 \quad [3.11]$$

$$\text{where } b = ([G]_0 - [\text{CD}]_0 + K_G)$$

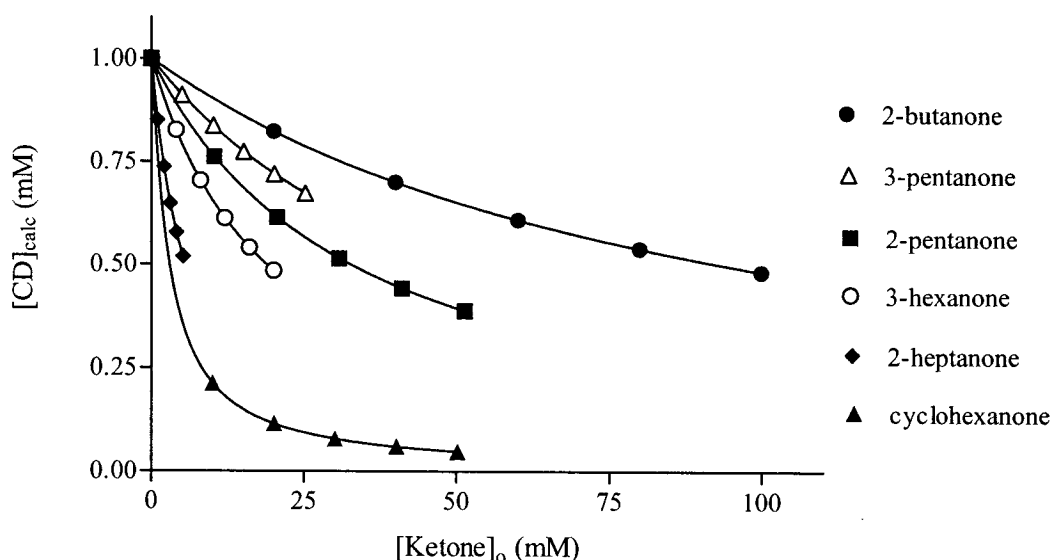


Figure 3.14 Examples using the quadratic method. Variation of the [CD]_{calc} with [Ketone]₀, calculated from the variation of the rate of hydrolysis of TMOB in the presence of total [β-CD]₀ = 1.00 mM. The curves are drawn using the quadratic solution, eq. [3.11], and fitted K_G values.

Table. 3.5 Dissociation constants (K_G , in mM) of β -CD-Ketone complexes, as calculated by the quadratic method and spreadsheet method.^a

Ketone	Quadratic method	Spreadsheet method
2-butanone	92.5 ± 0.05	91.7 ± 9.1
3-pentanone	51.1 ± 0.07	51.1 ± 2.27
2-pentanone	32.1 ± 0.02	32.2 ± 0.9
3-hexanone	18.3 ± 0.007	21.8 ± 1.0
2-heptanone	5.06 ± 0.03	5.07 ± 0.32
cyclohexanone	2.49 ± 0.002	2.50 ± 0.06
3-hexanone ^d	19.7 ± 0.2	19.8 ± 0.3
cyclopentanone ^d	20.0 ± 0.2	20.0 ± 0.4
Cyclohexanone ^d	2.51 ± 0.09	2.30 ± 0.24
	2.54 ± 0.01	2.66 ± 0.05

^a At 25 °C, in aqueous acidic solution. From the effect of added ketone on the kinetics of hydrolysis of TMOB in the presence of β -CD.

^d From the effects of added ketone on the kinetic of hydrolysis of ADMA in the presence of β -CD. These values were found by other researchers in our lab.

The K_G values that resulted from fitting to the quadratic solution, which are presented in Table 3.5, are very close to those obtained from the “spreadsheet” treatment, though with smaller standard errors. The quadratic method was tested for finding dissociation constants of alcohols to β -CD also, and again it gave K_G values which were essentially identical to those obtained in the spreadsheet method.¹⁴⁴

CHAPTER IV. MICELLES

4.1 INTRODUCING MICELLES

Micelles are supramolecular aggregates formed by surfactant molecules in aqueous solution, normally.^{65,175} Micellar solutions are used widely in numerous technical applications such as detergency, pharmaceuticals (eg. for solubilization and delivery of drugs),¹⁷⁶ enhanced oil recovery, and in surfactant-based separation techniques (eg. micellar electrokinetic capillary chromatography, micellar-enhanced ultrafiltration)¹⁷⁷ - to name only a few. Micelles have been a subject of interest to chemists because of their catalysis of reactions¹⁷⁸⁻¹⁸³ and to biochemists because of their similarity to biological membranes.^{65,184} Micelles can provide a reaction medium, a restricted volume where hydrophobic molecules may collide and react, within a largely water solvent, which is a 'green solvent' of great economical potential.^{79,185} One focus of research in our laboratory is to try to understand the role that micelles can play in altering rates, equilibria and the pathways of organic reactions. The major portion of this thesis is concerned with the effects of cationic micelles on acyl transfer reactions (Chapters V-VII). It is a significant extension of some earlier work in this laboratory in which we applied ideas about transition state binding and stabilization¹⁹ (Section 1.2) to micelle-catalyzed reactions for the first time.⁵⁸

4.1.1 Surfactants¹⁷⁵

Detergents are *amphipathic* molecules,¹⁷⁵ consisting of a structural tail group that has very little attraction for the solvent, known as a *lyophobic group*, together with a head group that has strong attraction for the solvent, called the *lyophilic group* (Figure 4.1).

Detergents are also known as *surfactants*, which stand for surface-active agents.^a At low concentration these agents tend to migrate and adsorb to the surfaces or interfaces of the system they are present in, and consequently alter the surface or interfacial properties.¹⁷⁵

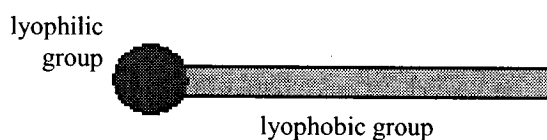


Figure 4.1 An amphipathic surfactant molecule.

Surfactants reduce the surface (or interface) free energy of water rather than increase it.¹⁷⁵ When a surfactant is dissolved in water (or a largely aqueous solvent), the presence of the surfactant's lyophobic (hydrophobic) group in the interior of the solvent causes distortion of the "water structure" and an increase in the free energy of the system (see section Section 1.3). This increase means that less work is needed to bring a surfactant molecule rather than a water molecule to the surface. The surfactant therefore concentrates at the surface, decreasing the surface free energy per unit area, and thereby the surface tension of water. However, surfactants are prevented from being expelled completely from the solvent, to form a separate continuous phase in solution, because this would require dehydration of the lyophilic (hydrophilic) group. The amphipathic nature of the surfactant therefore causes not only the concentration of the surfactant at the surface and reduction of the surface tension of the water, but also orientation of the molecules at the surface with their hydrophilic head groups in the aqueous phase and their hydrophobic tails oriented away from it, as shown in Figure 4.2.

^a For background on surfactants see the web site [<http://Surfactant.net>].

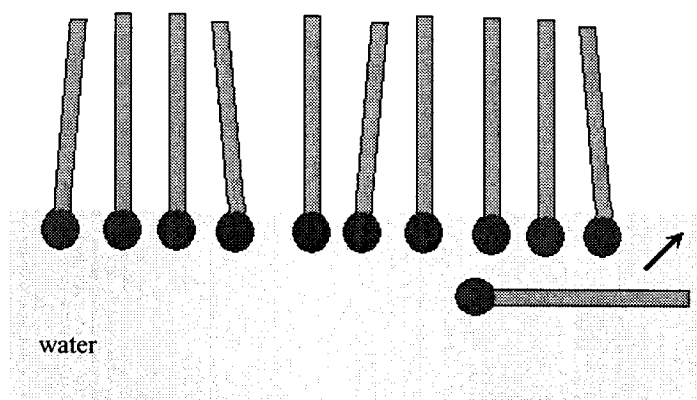


Figure 4.2 Surfactant molecules collect on the water surface, but do not form a separate continuous phase in solution.¹⁷⁵

Generally, the hydrophobic group of a surfactant is composed of long hydrocarbon chains (less often halogenated or oxygenated analogues), both straight and branched, or aromatic. Four main classical types of surfactants are recognized according to the nature of their hydrophilic head group: neutral (non-ionic), anionic, cationic, and zwitterionic.¹⁷⁵

Neutral (non-ionic): the surfactant bears no apparent ionic charge, for example, $\text{RCOOCH}_2\text{CHOHCH}_2\text{OH}$ (a monoglyceride of long-chain fatty acid), $\text{RC}_6\text{H}_4(\text{OC}_2\text{H}_4)_x\text{OH}$ (a polyoxyethylated phenol).

Anionic: the surfactant bears a negative charge, for example, $\text{RCOO}^- \text{Na}^+$ (a soap), $\text{RSO}_4^- \text{Na}^+$ (an sodium alkylsulfate, e.g. sodium dodecylsulfate, SDS).

Cationic: the surfactant bears a positive charge, for example, $\text{RNH}_3^+ \text{Cl}^-$ (a salt of a long-chain amine), $\text{RN}(\text{CH}_3)_3^+ \text{Br}^-$ (a quaternary ammonium bromide, e.g. cetyltrimethylammonium bromide, CTAB).

Zwitterionic: Both positive and negative charges may be present in the surfactant molecule, for example, $\text{RNH}_2^+ \text{CH}_2\text{COO}^-$ (a long chain amino acid) and $\text{RN}(\text{CH}_3)_2^+ \text{CH}_2\text{CH}_2 \text{SO}_3^-$ (sulfobetaine).

There is a new class of surfactants called "gemini" surfactants, which are compounds with hydrocarbon-ion-spacer-ion-hydrocarbon, which have stimulated a great deal of group interest due to their versatility, potential applications and better

resemblance to phospholipid membranes.¹⁸⁶⁻¹⁸⁸ Also chiral surfactants, with a chiral head group or amino acid head group, have been synthesized to promote stereoselectivity in micelles.¹⁸⁹⁻¹⁹⁵

4.2 MICELLES AND THEIR FORMATION FROM SURFACTANT BUILDING BLOCKS

The story is told,^{79,196} of how McBain's original proposal concerning the possibility that surfactants might aggregate in water was met with the reply 'Nonsense, McBain'. Of course, it is now recognized that in a polar solvent, a specific number of molecules of a surfactant begin to aggregate into clusters called *micelles* (Figure 4.3).

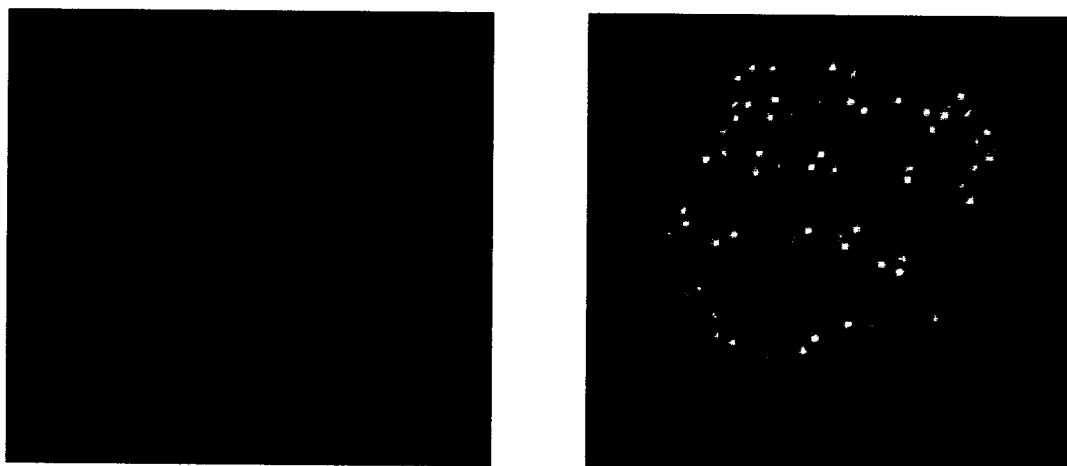


Figure 4.3 SDS Surfactant molecules-hydrocarbon tail (green), head group (yellow), counter ion (red) - aggregate in aqueous medium (blue) to form the colloidal micelle. The pictures are used with permission from Alexander Mackerell.¹⁹⁷

As mentioned, surfactant molecules tend to adsorb and concentrate at the surface of water, where they orient themselves so that their hydrophobic groups are directed away from the solvent, in order to minimize the distortion of the water by the hydrophobic groups. However, another means of reducing the free energy is for

surfactant molecules to aggregate into a colloidal micelle (Figure 4.3), directing the hydrophobic tails towards the interior of a cluster and the hydrophilic groups on the exterior, close to the solvent. *Micellization* is therefore an alternative mechanism to adsorption at the interfaces, which removes hydrophobic groups from contact with water; the distortion of the solvent structure is minimized, thereby reducing the free energy of the system (*vide infra*). If there is little distortion of the structure of the solvent structure by the lyophobic group (e.g. in water, when the hydrophobic group of the surfactant is short), then there is little tendency for micellization to occur.¹⁷⁵

4.2.1 The Critical Micelle Concentration¹⁷⁵

There exists a certain concentration of surfactant, more precisely a narrow range of concentrations, at which the onset of micellization occurs. This is called the *critical micelle concentration (cmc)*. The *cmc* has also been defined as the maximum chemical potential (concentration) of monomer attainable.¹⁷⁵ Implicit in that definition is the concept that all surfactant molecules added to a solution already at the *cmc* will be incorporated into micelles. A surfactant solution above the *cmc* is therefore composed of micelles in equilibrium with monomer surfactants at a concentration equal to the *cmc*. Sometimes micellization can occur over a broad concentration range, and variation in monomer concentration can exist above the *cmc*. Thus the designation of a *cmc* is somewhat arbitrary and actually inappropriate because there is no ‘critical’ phenomenon.

Many methods are available to measure the *cmc*, all of which depend on changes in the concentration-dependant properties upon micellization.^{198,199-203} Values of *cmc* have been measured by changes in electromotive force, conductivity, surface tension,

light scattering, NMR,²⁰¹ quenching of fluorescence probes,¹⁹⁹ dye solubilization,²⁰³ and predicted by computational approaches.²⁰⁴ The point of inflection on the plot of an observed property versus [surfactant] corresponds to the *cmc*, three examples are shown in Figure 4.4. The results of extrapolations of quasi-linear regions above and below the breakpoint depend on the range of data points taken, and different graphical or mathematical procedures may give more than one estimate of the *cmc*. In our research we have estimated the *cmc* under our reaction conditions from abrupt changes in kinetic rates (see Section 6.5). For the majority of surfactants the *cmc* falls into the range 10^{-6} – 10^{-1} M.

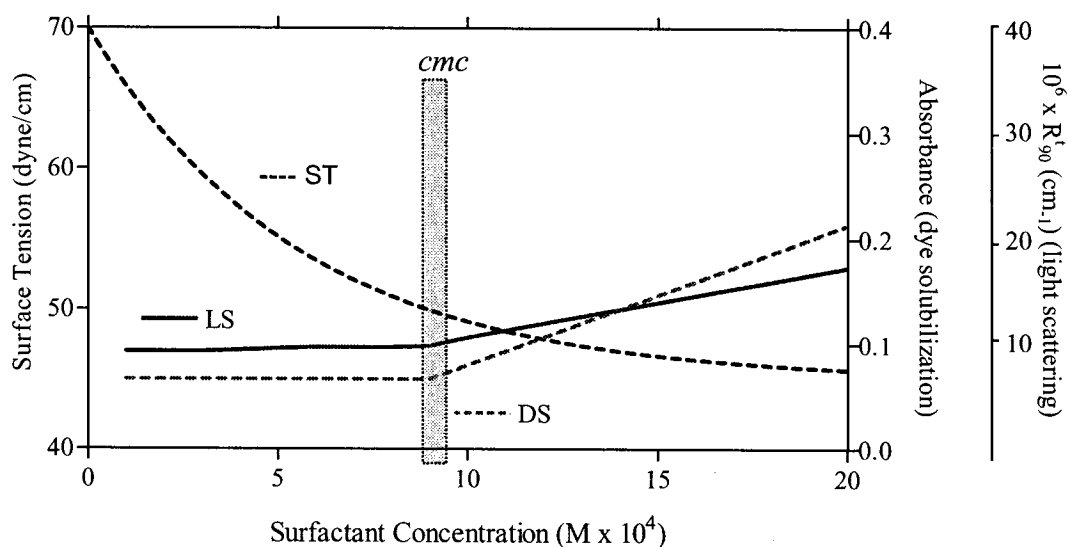


Figure 4.4 Changes in physical properties of a typical surfactant solution upon micelle formation.¹⁷⁵ The *cmc* is determined from surface tension (ST), light scattering (LS), and absorbance of hydrophobic dyes (DS). The *cmc* is about 0.9 mM.²⁰⁰

A great deal of work has been done on elucidating the various factors that determine and affect the *cmc*.^{175,205} Observed *cmc* values depend strongly on the structure of the surfactant and on experimental conditions, including temperature, pH, ionic strength and the presence of additives or impurities.²⁰⁶ An extensive compilation of *cmc*s of surfactants in aqueous media, at varied conditions and temperature, may be found in

Rosen's book and references therein.¹⁷⁵ In aqueous medium, ionic surfactants have much higher *cmc* values than non-ionic surfactants containing equivalent hydrophobic groups. Increase in the binding of the counterion to the micelles, or adding an external salt (increasing the ionic strength of the medium), causes decreases in the *cmc* of ionic surfactants.^{65,175} This depression of the *cmc* is due mainly to the decrease in the thickness of the ionic atmosphere surrounding the head groups and the consequent decreased repulsion between them in the micelle. For nonionic and zwitterionic surfactants the changes in *cmc* is attributed to the "salting out" of the hydrophobic groups in the aqueous solvent by the electrolyte.²⁰⁷ A predominant and regular feature for simple surfactants is the dependence of the *cmc* on the length of the hydrophobic alkyl chain of the surfactant, regardless of whether the surfactant is ionic or non-ionic (Figure 4.5).⁶⁵

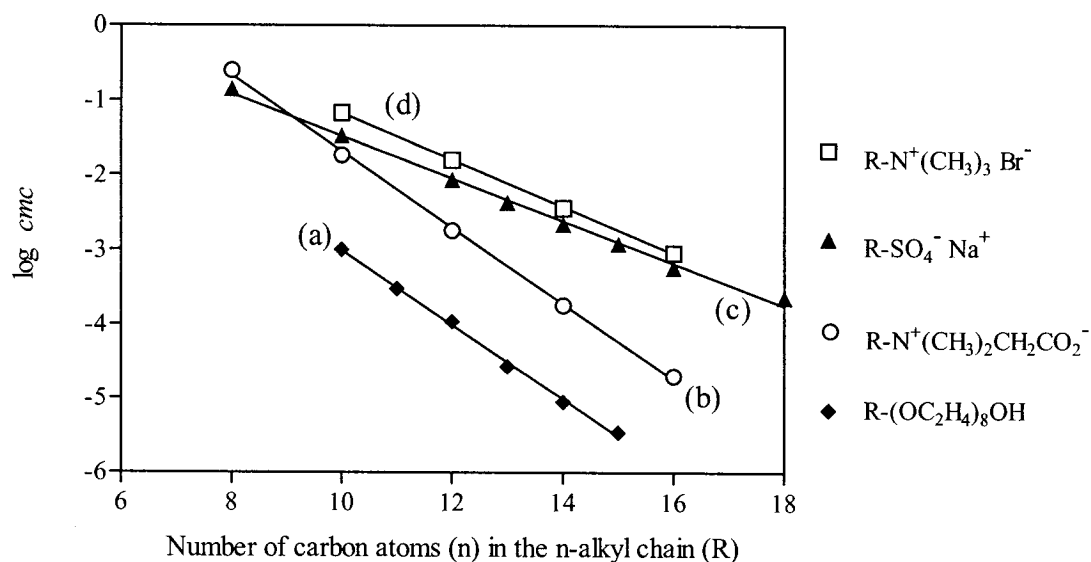


Figure 4.5 Plot of $\log cmc$ versus the alkyl chain length (n) of the amphiphile. The *cmc*s are taken from Rosen,¹⁷⁵ in water solvent. (a) alkyl-octaoxyethylated alcohols (at 25 °C); (b) N-alkyl-betaines (at 23 °C); (c) sodium alkylsulfates (at 40 °C); (d) alkyltrimethylammonium bromides (at 25 °C). The slopes are around -0.3 for the anionic and cation amphiphiles, and about -0.5 for the neutral and zwitterionic surfactants.

For homologous series of straight chain surfactants, the dependence of the *cmc* on *n* (Figure 4.5) can be written in the form of the linear equation [4.1]:

$$\log cmc = A - B.n \quad [4.1]$$

Where A and B reflect the change in free energy of transferring the surfactant from the aqueous environment to the micelle (*vide infra*). For example, for n-alkyltrimethylammonium bromide, from the intercept of the line in Figure 4.5, $A = 2.01$ (which is a constant for the ammonium head group, at 25 °C), and from the slope, $B = 0.32$ (a constant ≈ 0.3 ($\log 2$)). If 0.1 M NaCl is added, B remains constant but $A = 1.23$, and the *cmc* decreases.¹⁷⁵

For ionic surfactants (type 1,1 electrolyte), in the absence of added salt, a smaller dependence of the *cmc* on chain length is observed than that for anionic and neutral and zwitterionic surfactants.⁶⁵ The reduced slopes (Figure 4.5) are ascribed to the fact that the ionic strength of the solution is determined by the concentration of free ionic amphiphile, which is, essentially equal to the *cmc*. The ionic strength is then decreasing as the alkyl chain is lengthened, partially counteracting the decrease in the *cmc* that would be expected at a constant ionic strength.

4.2.2 Micellar Aggregation Number^{65,175}

A designated *aggregation number* (N) for the number of surfactant molecules contained in a single micelle furnishes an image of well-defined, static aggregates suspended in solution. In contrast (and in fact), micelles are dynamic structures, in some cases partially penetrated by water,²⁰⁸ with monomer exchange between micellar phase and the bulk solution occurring constantly. The aggregation number quoted for a

particular surfactant is therefore just a reflection of the average micellar composition over a period of time and it may be strictly valid only within a certain concentration range since micelles can exhibit concentration dependent size.

Ionic surfactants containing a single long alkyl chain generally show aggregation numbers of less than 100 in aqueous solution and these vary slightly with surfactant concentration.^{65,175} At high salt content, however, N increase sharply with the concentration of surfactant. Closer packing of head groups is permitted upon the addition an electrolyte due to the compression of the electrical double layer and reduced repulsion between the ionic heads, with a consequent increase in N .¹⁷⁵ Aggregation numbers of non-ionic surfactants can be in the thousands.

If small amounts of hydrocarbons or long-chain polar compounds are added to an aqueous solution of a surfactant above its *cmc*, the normally water-insoluble material may be solubilized in the micelle. Such addition generally causes an increase in N , and as the amount of material solubilized by the micelle is raised, N continues to increase (and micelle shape changes) until solubilize limit is reached and a phase separation occurs.

4.2.3 Thermodynamic Parameters of Micellization

Aggregation of the hydrophobic chains of monomeric surfactants in polar media, followed by dehydration, leads to a decrease in the free energy of the system. Such classical hydrophobic interactions, as discussed in Section 1.3, are normally associated with *positive entropy* changes, which are considered to be the main driving force for micelle formation. Yet, many factors increase the free energy of the system and thus oppose micellization. A surfactant molecule, in transferring from the bulk solvent to the

micelle, may experience some loss of freedom by being confined to the micelle, decreasing the entropy. Also, in the case of ionic surfactants, electrostatic repulsion from other similarly-charged surfactant molecules within the micelle limits its size. In the case of neutral surfactants, the preference for hydration of a head group opposes the self-association. Whether micelles form in a particular case, and at what *cmc*, depends therefore on the balance between the factors promoting micellization and those that are opposing it.

Many thermodynamic descriptions of the equilibrium between micelles and surfactant monomers in solution have been derived but all of them are generally based on either the mass action model or phase separation model.^{65,79,175,206,209-213} The *mass action (closed association) model* expresses micelle formation in terms of an equilibrium constant for association of monomeric surfactant [D] into micelles [D_N] in the aqueous phase:^{65,211}

$$K = [D_N (aq)] / [D (aq)]^N \quad [4.2]$$

and the Gibbs free energy of micellization in solution is just $\Delta G_{mic} = - RT \ln K$.

According to the *phase separation model*, micelles form a separate phase in the aqueous system with surfactant in the micellar phase in equilibrium with surfactant in the aqueous phase at the *cmc*. From this model, the standard Gibbs free energy of micellization per monomer $\Delta G_{mic}^0(aq;mon)$ can be approximated by equations [4.3] and [4.4], where X_{cmc} is the *cmc* in mole fraction units.

$$\Delta G_{mic}^0 (aq;mon) \approx RT \ln X_{cmc} \quad (\text{for non-ionic micelles}) \quad [4.3]$$

$$\Delta G_{mic}^0 (aq;mon) \approx 2RT \ln X_{cmc} \quad (\text{for ionic micelles}) \quad [4.4]$$

The handling of the aggregation number (N) and the counterion contribution (for ionic surfactants), is where thermodynamic analysis of micellar systems becomes difficult.^{79,212} Further, the thermodynamic parameters for micellization from the different models are not always evaluated on the basis of a single standard state, and so the results are not always comparable.^{65,175,206,211-214} Some values of cmc , ΔG_{mic}^0 , the molar standard enthalpies, ΔH_{mic}^0 , and molar standard entropies, ΔS_{mic}^0 , of micellization are listed below in Table 4.1.

Table 4.1 Thermodynamic parameters for micellization of amphiphiles in water.

Amphiphile	Temp (°C)	cmc (mM)	ΔG_{mic}^0 (kJ/mol)	ΔH_{mic}^0 (kJ/mol)	$T\Delta S_{mic}^0$ (kJ/mol)
$C_{10}H_{21}SO_3^- Na^+$	25 ^a	43	-34.9	+8	34
$C_{12}H_{25}SO_3^- Na^+$	25 ^a	12.4	-39.7	+5	46
$C_{12}H_{25}(OC_2H_4)_8 OH$	25 ^a	1.8	-32.6	+9	43
$C_{16}H_{33} N(CH_3)_3^+ Br^-$	25 ^b	0.90	-16.5	-4.8	11.7
$C_{16}H_{33} N(CH_3)_3^+ Br^-$	40 ^b	0.97	-20.1	-7.6	12.5

^a Values taken from Rosen,¹⁷⁵ using a phase separation model that accounts for micelle head group charge and aggregation numbers.

^b Values taken from Singh, *et al.*²⁰⁶ using a phase separation model that does not account for micelle aggregation number or ionic head group.

The negative values of ΔG_{mic}^0 in the Table 4.1 indicate that micelle formation in aqueous solution is spontaneous. Values of ΔH_{mic}^0 in the literature may be positive but they have been found to be negative in many cases. The destruction of hydrogen bonding (from released water) will give *positive enthalpy* changes, which will increase the free energy, however *negative enthalpy* (promoting micellization) will occur when a substantial number of water molecules surrounding the small hydrophilic head-group

becomes more important than those destroyed. Whatever the case, with some exceptions, according to Rosen¹⁷⁵, $\Delta H_{\text{mic}}^{\circ}$ values are usually smaller in magnitude than the values of $T.\Delta S_{\text{mic}}^{\circ}$ (which are always positive) and so they contribute less to $\Delta G_{\text{mic}}^{\circ}$. Therefore, micellization is governed primarily by the *positive entropy* gain associated with it,⁶⁵ which is essentially due to hydrophobic interaction (aggregation) of the surfactant chains.

Investigators have developed theoretical equations relating the free energy change ΔG_{mic} to various structural units in the surfactant.¹⁷⁵ As shown in eq. [4.5], ΔG_{mic} can be broken into contributions from component parts of the surfactant molecule, $\text{CH}_3(\text{CH}_2)_m\text{W}$, where W is the hydrophilic head group.

$$\Delta G_{\text{mic}} = \Delta G_{\text{mic}}(-\text{CH}_3) + m.\Delta G_{\text{mic}}(-\text{CH}_2-) + \Delta G_{\text{mic}}(-\text{W}) \quad [4.5]$$

$$\Delta G_{\text{mic}}(-\text{CH}_3) = \Delta G_{\text{mic}}(-\text{CH}_2-) + k, \text{ where } k \text{ is a constant.}$$

From the relationship between $\log cmc$ and the number of carbon atoms in the hydrophobic group ($n = m + 1$) in equation [4.1], by rearrangement of eq. [4.3],

$$\text{the intercept} \quad A = [-\Delta G_{\text{mic}}(-\text{W}) + k] / 2.3 RT \quad [4.6]$$

$$\text{and the slope} \quad B = [-\Delta G_{\text{mic}}(-\text{CH}_2-)] / 2.3 RT \quad [4.7]$$

Thus, A and B in equation [4.1] reflect the free energy changes involved in transferring the end hydrophilic group and a single methylene unit of the alkyl chain, respectively, from an aqueous environment to the micelle.¹⁷⁵ Studies with structural variation in the surfactant (such as those in Figure 4.5, above) indicate that the free energy change $\Delta G_{\text{mic}}(-\text{CH}_2-)$ involved in the transfer of a methylene unit of the alkyl group from an aqueous environment to the interior of the micelle fall in the range -2.8 to -3.3 kJ mol^{-1} for many types of surfactants.⁶⁵ Such values are typical for the transfer of methylene groups from water to organic media.^{65,75,215}

4.2.4 Micellar Structure

It is important to remember that a micelle is a dynamic species in constant equilibrium with its surfactant monomers. For precisely this reason, the structures of simple micelles are still elusive after several decades of research. As Menger has pointed out, "...unless a small organic compound assembles into a crystalline array, the task of determining its colloidal properties and structure at the molecular level often presents a major challenge."¹⁸⁸ There are multitude of publications, both experimental and theoretical, attempting to resolve the questions of the micelle shape, water penetration, interior viscosity, chain conformation, and solubilization sites.

An idealized model of an ionic spherical micelle^{196,216} (Figure 4.6) describes it as having a sharp interface between a hydrocarbon core (10-30 Å) and a *Stern layer* (a few Å thick). The inner hydrophobic hydrocarbon core is believed to be "dry",^{216,217} however the aqueous phase can penetrate into the micelle beyond the hydrophobic chain, up to the first few methylene groups from the head group.^{208,218} Thus, an outer hydrophobic core is often considered within the "hydration sphere" of the micelle.¹⁸² In addition, it is believed that folding of surfactant tails in the interior is not extensive because the diameter of a typical spherical micelle is roughly twice that of the fully extended surfactant molecule. The Stern layer is the region filled with the surfactant head groups, some counterions, and water. It has been shown to contain hydrophobic pockets as well, due to back folding of long alkyl chains.^{196,216,217} Some authors prefer to use the term "Stern region" instead of "Stern layer". The Stern region thus has variable polarity, being more polar at the head groups and less polar at the back-folded alkyl chains of the surfactants.²¹⁶

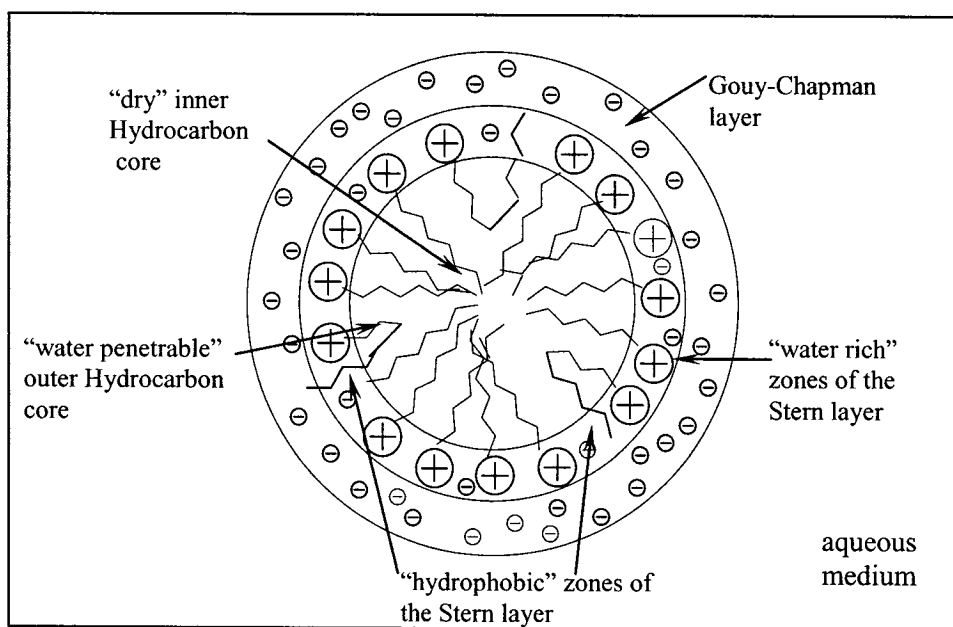


Figure 4.6 Two dimensional schematic representation of the regions of a spherical cationic micelle.¹⁸² The figure does not reflect the relative size of each region.

Both the core and Stern region are surrounded by an electrical double layer, called the *Gouy-Chapman layer* (reaching up to several hundred Å), into which counterions for the head groups are attracted. Some authors prefer the use of the term *diffuse layer*, to distinguish between the Gouy-Chapman model (double layer model) and the planar triple layer model for describing the distribution of counterions as a function of the distance from charged surface.^{219,220} Also, some authors refer to a *palisade layer* as the region that includes the head groups and the first few methylene groups of a surfactant, especially for non-ionic micelles.¹⁸² Polarity and water content in different regions of the micelle play an important role in determining the rates of reactions in these regions. With that said, experimental evidence for the extent of water penetration into a micelle are contradictory.^{182,221}

Several models have been proposed for the configuration adopted by surfactant units and their arrangement.^{196,222} Some possible shapes of micelles (Figure 4.7) are: (1) relatively small, spherical structures (aggregation number <100 usually); (2) elongated cylindrical micelles; (3) rod-like micelles with hemispherical ends (prolate ellipsoids), (4) Hexagonal, (5) large, flat lamellar micelles.¹⁷⁵

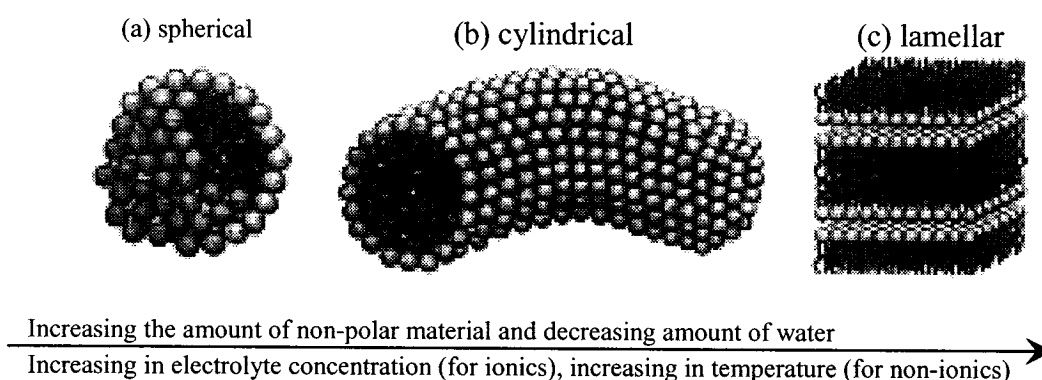


Figure 4.7 The most probable shapes of micelles, pictures taken from Soler-Illia *et al.*²²³ and effects of solubilization taken from Rosen.¹⁷⁵

In aqueous media, surfactants with bulky or loosely-packed hydrophilic groups and long, thin hydrophobic groups tend to form spherical micelles, while those with short, bulky hydrophobic groups and small, close-packed hydrophilic groups tend to form lamellar or cylindrical micelles. Also, the size and shape of the micelle may change when non-polar material is solubilized by the micelle and by change in environmental factors.^{175,224} Continued addition of non-polar material may result in the conversion from normal micelle to reverse micelles.¹⁷⁵

Knowing the gross morphology (i.e., whether the micellar assembly is a sphere, rod, cylinder, etc.) is less problematic today. Even if the assembly is dynamic, one can now capture a picture of a transient morphology by using rapid freezing methods, in

conjunction with microscopy.^{186,188} This technique has been used for polymer morphology studies and, more recently, colloid imaging,¹⁸⁶ and it will likely spread to capture an instantaneous picture of other supramolecular assemblies.¹⁸⁸

The definition of the micellar boundary and shape is an arbitrary one, and even though each layer (or region) has a specific environment, the micelle as a whole is considered as a distinct entity, surrounded by the aqueous medium. Frequently, the totality of all the micelles in solution is referred to as a “pseudo-phase” because an organic solute may be distributed between the aqueous (bulk) solvent and the micelles. For the purpose of analysis, as discussed later, it is easier to consider the micelles collectively, even though they are dispersed through the aqueous medium.

4.3 MICELLAR EFFECTS ON ORGANIC REACTIONS

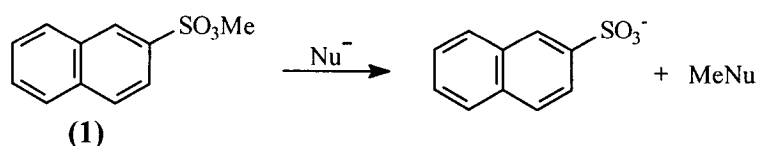
In solutions of micelles, reactions can be accelerated, inhibited, or unaffected, compared to reactions in pure water.^{216,225-238} Exactly how micelles do this remains obscure and depends on the nature of the substrate(s), the reaction, and the micelle. There are some monographs and several review articles which have many examples on the effect of micelles on organic reactions, organometallic reactions, enzymatic reactions, and polymerisation.^{178-183,239-247} Broadly speaking, micellar effects on organic reactions have been attributed to *proximity effects* and *medium effects*.

4.3.1 Proximity Effects

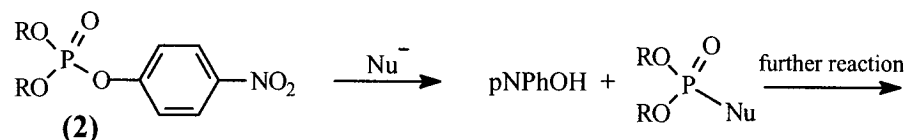
Normal (non-functional) micelles act as a “marriage broker” providing an environment that is conducive for the reaction without the micelle itself becoming

involved covalently in a the reaction. For bimolecular reactions, the *concentration effect* (a proximity effect) refers to bringing two potential partners into closer proximity within the confined volume of the micelle, and this compartmentalisation may promote the reaction between the reactants (partners). As a prerequisite for micellar “catalysis” of a reaction, all reacting partners must be incorporated, through hydrophobic interactions^{65,67,68,75} or electrostatic attractions (and ion-exchange)^{247-249,250} or a combination of the two, into the micellar pseudo-phase. Many examples are given in Taşciolğu’s review,¹⁸² and *observed rate increases* ranged from 5-fold to 100-fold and even up to a million fold.

In general, “catalysis” by micelles is *observed* for bimolecular reactions involving a reactive ion and a non-polar substrate when the charge of the head groups of the ionic micelle is opposite to the charge of the reactive ion. The electrostatic basis of the concentration effect may be appreciated on the basis of the following examples. The attack of anionic nucleophiles on carboxylate esters is “catalyzed” by cationic micelles but inhibited by anionic ones, as will be discussed in detail in Chapters V and VI. Anionic micelles inhibit S_N2 of methyl naphthalene-2-sulfonate (**1**) with anionic nucleophiles,²⁵¹ but zwitterionic (e.g. $RN^+R_2CH_2CO_2^-$) and cationic micelles generally increase the observed rate of these reactions with “soft” anions.²³⁵ The spontaneous hydrolysis of (**1**) is inhibited by all micelles with the order anionic \gg zwitterionic $>$ cationic.^{234,235}

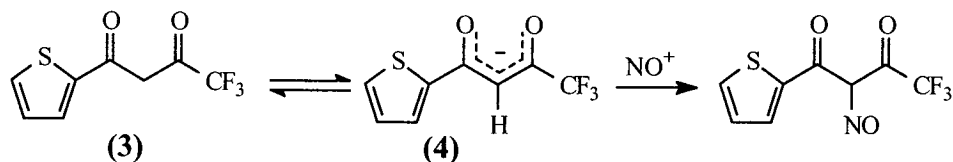


The hydrolysis of some phosphate esters (2) is promoted by cationic (eg. CTAB) micelles, but the reaction is unaffected by anionic or non-ionic micelles.^{230,238,252,253}



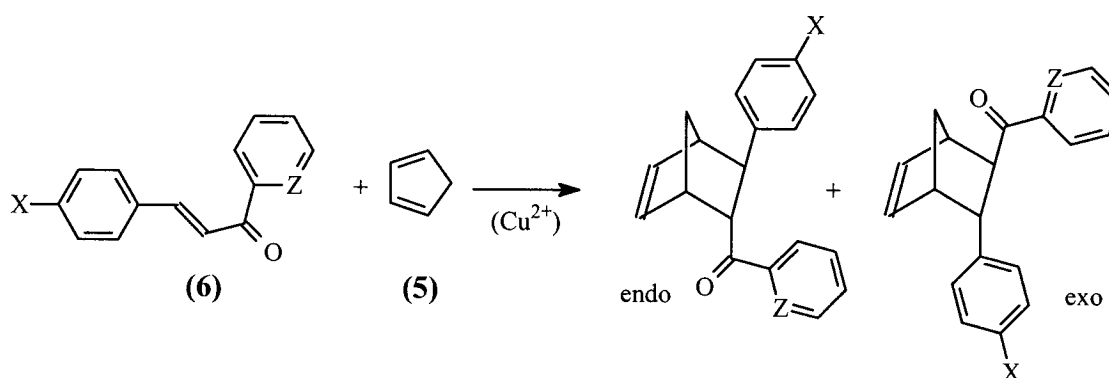
On the other hand, anionic micelles, such as of sodium dodecylsulfate (SDS), “catalyze” the acid-catalyzed hydrolyses of acetals and methyl orthobenzoates (the mechanism of these reactions was discussed in Chapter III), while cationic micelles inhibit them.^{156,165,254,255} Generally, for all the above examples, the extent of the rate enhancement (or retardation) depends on the strength of the interactions between the reactive ion and the substrate with the micelle.

While the list of reactions that can be viewed as above can be extended,²⁵⁶ not all reactions fit neatly into the categories discussed. For example, the higher than 30-fold rate enhancements of nitrosation of a diketones (3) in cationic micelles,²²⁹ in mild acid medium, would not be expected on the basis on the previous generalization. Iglesias²²⁹ partially attributed this rate enhancement to the more rapid formation of the delocalized enolate anion (4) in the region of the positively charged micellar interface.



When both reactants are non-ionic, they must be hydrophobic enough to partition (or bind preferentially) into the micellar pseudo-phase. But such binding still does not ensure catalysis. It has been found that micelles may separate reactants not only

i) between the micellar pseudo-phase and the aqueous phase, but also ii) in different micelles within the micellar pseudo-phase, or iii) in different binding domains of the micelle itself. A ‘mismatch’ in the binding sites of non-ionic reactants usually results in “inhibition” or “retardation” of the reaction. For example, Engberts and coworkers²⁵⁷ reported a million-fold acceleration of a Diels-Alder reaction in water and copper dodecylsulfate $\text{Cu}(\text{DS})_2$, due to the combined Lewis acid (Cu^{2+}) and micellar catalysis. However, in the absence of the catalytically active metal ion, SDS and CTAB micelles (independently) retard the reaction, by up to a factor of 10, compared to water as the medium. By probing the binding site of the reactants, using ^1H NMR, they found that, on average, the diene (**5**) would be bound preferentially into the interior of the micelle, while the dienophile (**6**) favors the outer regions of the micelle. So even though the micelles are able to bind both reactants efficiently, inhibition results due to the different binding locations in the micelle.²⁵⁷



More recently, Rispens and Engberts²³⁷ studied a number of different Diels-Alder reactions, and compared the micellar rate constants with rate constants in water/1-propanol mixtures. They suggested that, rather than the “mismatch” in the binding of the reactants between micellar regions, a more probable explanation for the inhibition

caused by micelles is the “poorer” water concentration (~10-15 M) at the reaction site, which is between the core and Stern layer.²³⁷

In fact, there has been much controversy over the time-averaged *local concentration* of different reactants in the micelle and how it may affect reactivity in micelles.^{196,253,257-259} It is important to note that the location and orientation of reactants within the micelle is determined mainly by their *polarity* (or hydrophobicity) and less by their geometry or size. Generally, an ionic or polar reactant will preferentially stay at the surface of the micelle. However, a hydrophobic molecule may move rapidly inside a micelle, spending a great percentage of its time in the hydrophobic core of a micelle, but that does not preclude its fleeting presence in the more aqueous regions of the micelle.¹⁹⁶ How deep a hydrophobic substrate is buried into the micelle may well affect its reactivity. The location of a molecule may be controlled by pH and ionic strength.²⁶⁰ Even though the local concentration of reactants in the micellar pseudo-phase is important in discussing micellar catalysis, the solubilization of substances may well be *stochastic*, distributed among several sites within a single micelle, or rapidly exchanging between different micelles, or between the micellar pseudo-phase and the aqueous phase.^{261,262}

4.3.2 Medium Effects

Together with the proximity effect, micelles also exert a medium effect on reactions. Reactions taking place in the *microenvironment* of the micellar pseudo-phase, relative to those taking place in the aqueous phase, will experience changes in polarity, water content, solvation, or hydrogen-bond donor capacity, much like a solvent effect.

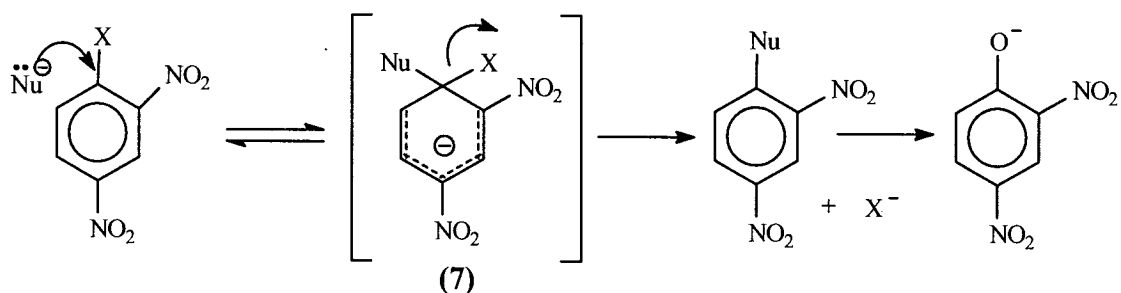
The differences in rates and equilibria will be most evident if the reaction takes place in the non-polar micellar core, rather than in the largely aqueous Stern region which has a polarity that can be mimicked by a concentrated salt solution.²¹⁶ The concentration of water in Stern layer for CTAB micelles is estimated to be 45 M.²¹⁶ Most organic bimolecular reactions take place in the interfacial region between the aqueous medium and the “palisade layer” of the micelle.

Reaction in the micellar pseudo-phase medium may result in major changes in the reactivity of both ionic reagents and non-polar substrates.²⁶³ For example, nucleophilic anions may form ‘hydrophobic ion-pairs’^{264,265,266} with the head groups of cationic micelles, and the reactivity of anions may be enhanced by desolvation. The reactivity of reagents may also be augmented or diminished by pK_a shifts caused by the effect of the micelles on anion stability.^{255,267,268}

A micelle may solubilize a substrate in a specific orientation (*preorientational effect*),¹⁸² depending on the substrate polarity. This may change the substrate reactivity and could provide control over the regioselectivity and stereoselectivity of the reaction.¹⁸² Also, when the substrate is an aromatic anion (or cation), an interaction between positive (or negative) head groups of the micelle and the π -system of the aromatic ring may affect the reactivity of the substrate, as in the example below.

The micellar medium can also lead to changes in the relative free energy of the ground state and the transition state. Micelles that catalyze a reaction decrease the activation energy (E_a), while the inhibitory micelles increase E_a . Nucleophilic aromatic substitution (S_NAr) in cationic micelles^{253,269-273} is the most pronounced example of a bimolecular reaction where medium effects play a major role in the catalysis. “True

catalysis” of S_NAr by cationic micelles was attributed to stabilization of the transition state, resembling a Meisenheimer complex of delocalized negative charge (7), relative to the initial state, and to possible cation- π interaction of the aromatic ring with the positive head group of the micelle.



Alkene bromination in CTAB micelles, is an example where the great inhibition by the micelles has been ascribed to medium effects.²⁷⁴ Despite the fact that both alkene and Br_2 were incorporated effectively into CTAB micelles, the reaction involves charge separation and it readily occurs in water. So, inhibition by the micelles was ascribed partially to the lower polarity of the micellar surface, compared to water. Inhibition was also ascribed to the stabilization of Br_3^- in the initial state.²⁷⁴ Tribromide ion (Br_3^-) is formed from Br_2 and Br^- in a rapid equilibrium:



and in the presence of CTAB the formation of more Br_3^- is promoted by the micelle. A similar situation occurs with aromatic bromination in the presence of α -cyclodextrin which sequesters the substrates, and also promotes the formation of Br_3^- , generally leading to large rate reductions.^{19,275}

Various authors have discussed the role micelles may play in stabilization of the transition states of reactions. In 1994, Tee¹⁹ first pointed out that the Kurz^{42,43} approach to

estimate the pseudo-transition state stabilization equilibrium constant (K_{TS}), which was derived and discussed in detail in Chapter I, Section 1.2, may be applied to micellar catalysis. Since then, the estimation of the stabilization of the transition state relative to initial state stabilization by micelles has appeared more often in the literature to interpret micellar effects on reaction rates.^{60,216}

Our research has focused on the ‘catalytic’ effect that cationic cetyltrimethyl ammonium bromide (CTAB) micelles have on the cleavage of *p*-nitrophenyl alkanoate ester by nucleophiles (Chapter V-VIII). We will address both the proximity and medium effects that these cationic micelles have on these reactions. These effects will be ascertained from the magnitude of “catalysis” and its relationship to nucleophile(s), from the ester-micelle binding strengths and their variations with ester structure, and from the transition state stabilization relative to initial state stabilization by the micelle.

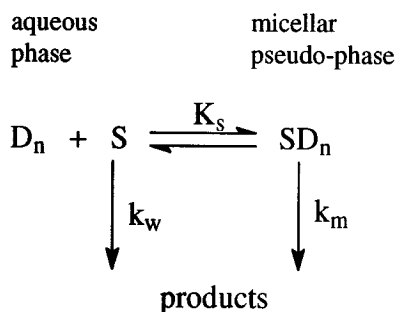
4.4 KINETIC TREATMENT OF REACTIONS MEDIATED BY MICELLES

Various models have been investigated to quantify micellar-modified reaction kinetics. Among the most widely applied models are Pseudo-phase Model (PP)²⁷⁶ and the Pseudo-phase Ion-Exchange Model (PPIE).^{181,244,247,249,277} Both of these quantitative models involve the assumptions that: i) the totality of micelles in solution act as a separate phase, a “pseudo-phase”, distributed evenly throughout the aqueous phase, ii) the reactants bind independently to the micellar pseudo-phase, and iii) the effect of reactant binding on micellar structure are relatively unimportant. These models have imperfections and failures have been recognized.²⁷⁷⁻²⁸¹ The way we have analyzed our kinetic data is very different from the models normally used for micellar kinetics. To

appreciate our method, and to be able to compare our results to previous work, it is important for us to briefly discuss the PP model and the PPIE model.

4.5.1 The Pseudo-phase Model and Problems with Rate-Surfactant Profiles

Surfactants affect reaction rates by incorporating the substrate(s) into the micellar aggregate. In 1967, Menger and Portnoy²⁷⁶ devised the Pseudo-phase Model (PP) to explain data for unimolecular reactions in the presence of micelles. According to this model (Scheme 4.1) the substrate (S) is distributed between the aqueous phase and the micellar pseudo-phase. The rate constant for the reaction in the aqueous phase is k_w , and the rate constant for the micellar-bound substrate is k_m .



Scheme 4.1 The Pseudo-phase Model

$$k_{\text{obs}} = \frac{(k_w + k_m K_s [D_n])}{(1 + K_s [D_n])} \quad [4.8]$$

For Scheme 4.1, equation [4.8] was derived assuming that the reactions in the two phases occur independently. Here, the equilibrium constant K_s is for the association of the substrate with the micellized surfactant, and it is given by $K_s = [S.D_n]/[S][D_n]$. The concentration of micellized surfactant is $[D_n] = ([\text{Surf}]_T - \text{cmc})$. Sometimes the

concentration of micelles ($[D_n]/N$) is used instead of micellized surfactant $[D_n]$, where N is the aggregation number.

Much like the Michaelis-Menten equation of enzyme kinetics,^{27,50} equation [4.8] implies saturation kinetic behavior [Figure 4.8 (a)]. In other words, the overall rate versus $[D_n]$ profile should increase with surfactant concentration and should reach a plateau once essentially all the substrate is bound in micelles.²⁴⁶ This levelling off occurs at a value of k_m when $K_S[D_n] \gg 1$ and $k_m > k_w$.

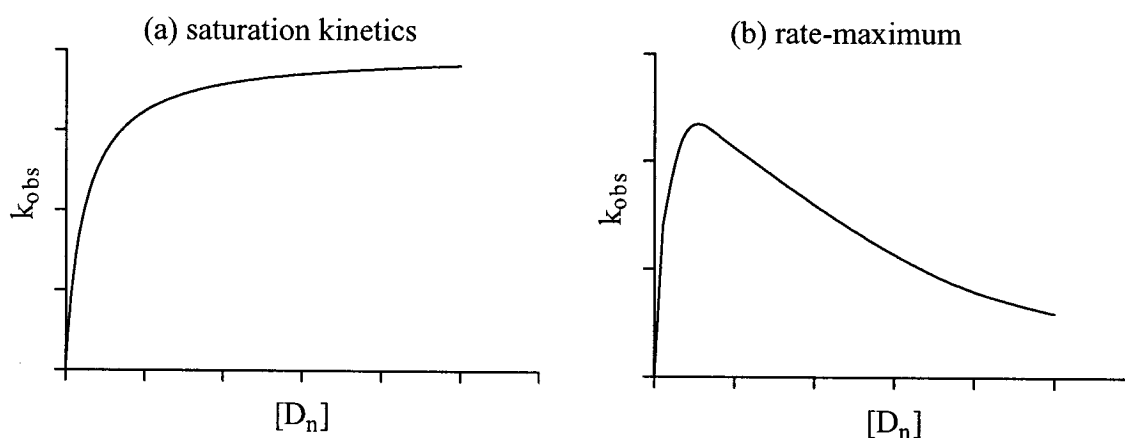


Figure 4.8 Rate versus micellized surfactant ($[D_n]$) profiles exhibiting (a) saturation kinetics, (b) rate-maximum.

Most unimolecular reactions show saturation kinetics and can be successfully described using the PP model.^{178,243} However, for most bimolecular reaction data there are features that are not adequately described using this model.^{246,282,283} Most notably, rate-maxima [Figure 4.8(b)], instead of saturation kinetics [Figure 4.8(a)], are frequently observed for ion-molecule reactions catalyzed by ionic micelles.^{181,246} Other common features are that added salts decrease rate-maxima, and counterions of the surfactant with stronger affinity for the Stern region of the micelle show the rate-maxima at lower detergent concentration.

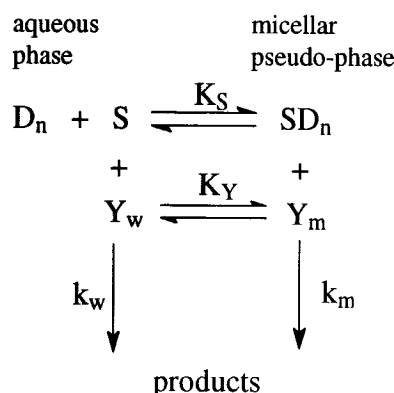
These features have been attributed to: 1) additional surfactant dilutes reactants (ionic or non-ionic) by increasing the total volume of the micellar pseudo-phase, and a consequent decrease in the rate of the reaction at high $[D_n]$; 2) dilution of the reactive-ion concentration in the vicinity of the completely micellar bound substrate due to an increase in the concentration of the inert-counterion of the surfactant at higher $[D_n]$; 3) a negative salt effect due to competition between reactive ions and the salt ions for binding to the Stern layer. The last two reasons are under the assumption that there are limited numbers of ion binding sites in the Stern region of an ionic micelle.^{247-249,283-284} Another suggestion for the *negative salt effect*, is that there is an increase in the aggregation number (and a decrease in *cmc*) of the micelle with increasing ionic strength, resulting in a reduction in the number of micelles present at a given $[D_n]$.

Rate-maxima were also observed with non-ionic micelles and non-ionic reactants. In these cases, when virtually all of one reactant is sequestered in the micellar pseudo-phase, additional micelles will take up the other reactant and reduce the rate because of the lower probability the two reactants meeting one another when they are in different micelles.^{244,247,249}

4.5.2 The Pseudo-phase Ion-Exchange Model and Solving the Problems of Rate-Surfactant Profiles

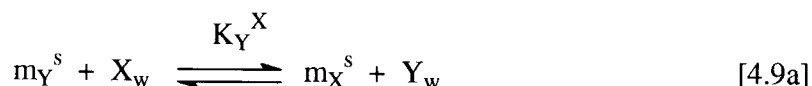
The major shortcomings of the PP model are its inability to account for the negative salt effects, the counterion effect, or the rate-maxima observed for bimolecular reactions.²⁷⁷ In 1975, Romsted^{246,282} devised the Pseudo-phase Ion-Exchange Model (PPIE) to treat reactions between molecules and nucleophilic ions, following an advance by Berezin and coworkers,^{285,286} who treated reactions between two non-ionic reactants in

micelles. The PPIE model (illustrated in Scheme 4.2) attempts to account for the distribution of ionic solutes into the micellar pseudo-phase.^{180,181,244,247,249,277}



Scheme 4.2 The Pseudo-phase Ion-Exchange Model .

The Stern region acts like an ‘ion-sink’ or ‘ion-exchange resin’,^{180,247,249} and the reactant Y (assuming that it is ionic) competes with the inert ion X (the counterion in the surfactant) for binding sites in the Stern region. An empirical ion-exchange constant, K_Y^X (eq. 4.9), describes the selectivity between various pairs of ions.^{287,288,246-248}



$$K_Y^X = \frac{[Y_w] m_X^s}{[X_w] m_Y^s} \quad [4.9b]$$

The concentrations of ions in solution are $[X_w]$ and $[Y_w]$, and the ratio of micellar bound ions in the Stern layer are m_X^s and m_Y^s . These *ratios* are taken because there is no simple or rigorous way for computing local ionic concentrations (in molarities) at the interfacial region of associated colloids, and the various approaches used all depend on assumptions.^{280,289}

A major underlining assumption of the PPIE model is that the extent of charge neutralization of micellar head groups by ions, β (eq. [4.10]), is constant.^{180,249,277} In the

original PPIE model, equations [4.10] and [4.9b] are combined with a number of mass balance equations for Y and X to derive equation [4.11] under limited conditions.

$$m_Y^s + m_X^s = \beta \quad [4.10]$$

$$m_Y^s = \frac{[Y_T]}{[Y_T] + K_Y^X [X_T]} \quad [4.11]$$

Mathematical analysis of Scheme 4.2 yields equation [4.12] to describe the overall, observed second order rate constant of the reaction.

$$k_{\text{obs}} = \frac{k_w [Y_w] + k_m K_s m_Y^s [D_n]}{1 + K_s [D_n]} \quad [4.12]$$

From equations [4.11] and [4.12], the effect of added concentration of counterions is easy to visualize. Increasing $[X_T]$ (through $[D_n]$) reduces m_Y^s (eq. [4.11]) and so, according to equation [4.12], k_{obs} decreases at high $[D_n]$.

This treatment fits much kinetic data for bimolecular reactions in micelles, quantitatively accounting for the observed maxima in rate-surfactant profiles [Figure 4.7(b)]. However, it is important to note that the rate constants, k_w and k_m , have *different dimensions*. For example, the units of k_w would normally be $M^{-1} s^{-1}$, whereas the corresponding units for k_m would be simply reciprocal seconds because the concentration of Y is expressed as a *molar ratio*, m_Y^s . So, k_m is corrected to account for the molar volume of reaction within the micelles, $k_2^m = k_m V_M$, where V_M is the conversion factor between interfacial molarity and the molar ratio concentration units. Inevitably, the estimate of a molar volume of the micellized surfactant that is available for the reaction is somewhat arbitrary, and V_m is taken to be either the molar volume of the Stern layer or

the molar volume of the micelle, depending on the research group.¹⁸⁰ For example, V_m is estimated to range from 0.14 to 0.37 L/mol for CTAB.¹⁸⁰

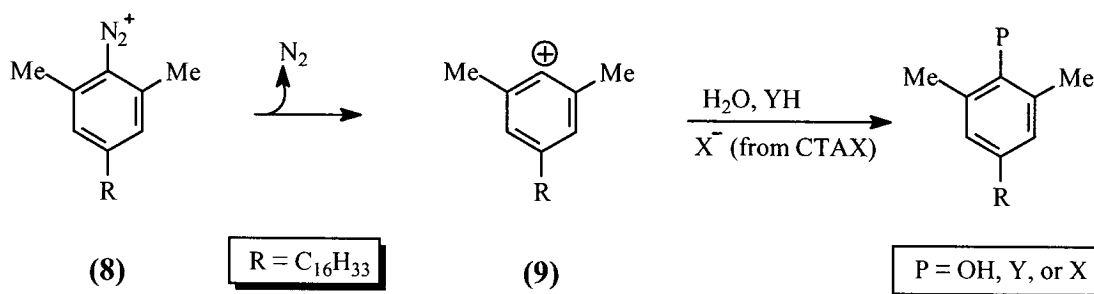
Remarkably, when the concentration effect is taken into account in kinetic data analysis, as is the case of the PPIE model, the corrected second-order rate constants for reaction within the micellar pseudo-phase are often very similar to those for reaction in aqueous phase (i.e. $k_2^m \sim k_w$) for the majority of bimolecular reactions.^{180,244,249,277,290}

While the PPIE model can quantitatively account for the observed rate-surfactant profiles of a variety of bimolecular reactions in ionic micelles containing a mixture of reactive and inert counterions, it still has limitations.^{225,226,277,278,291-293} The assumption that the *cmc* marks the onset of a second phase does not account for observed interactions between micelles and organic additives near the *cmc*. In dilute micellar solutions, the PPIE model gives reasonable, but seldom perfect, fits of the observed changes in rate and equilibrium constants for a wide range of chemical reactions.²⁴⁷ Also, when strongly hydrophilic counterions of the surfactant are involved, (eg. OH^- , F^- , and AcO^-), the PPIE did not qualify as a suitable model.^{246,277,278,281} In addition, the prediction of k_{obs} for bimolecular reactions in reactive-counterion surfactants (i.e. for the reaction between a completely-bound-substrate and the surfactant counterion in the absence of inert-counterion) by the PPIE model often fails.^{230,278,294} In some micellar solutions containing large excesses of a reactive ion, k_{obs} increases linearly with the concentration of the ion. This observation is inconsistent with the PPIE model, since k_{obs} should be constant ($k_{\text{obs}} = k_2^m \beta/V_m$) and independent of [surfactant] and the [reactive counterion] when the organic substrate is completely micellar bound.

The reasons for these failures have been suggested to be the breakdown of the assumptions that the Stern region has limited ionic binding sites (i.e. β is constant) and that V_m is constant.^{280,281,295} Analysis of the data using the PPIE model depends on constants that are often taken *arbitrarily*. For example, the values of K_Y^X , which have been estimated by different methods (kinetic fitting, spectral analysis, fluorescence quenching, ion-exchange chromatography, electrochemistry, and ultrafiltration), often differ greatly depending on the method used.^{244,249,277,290} Ion-association in the Stern-region (as expressed by β) also varies greatly depending on the micelle structural model and the method used to calculate it.^{219,220,296}

Since neither the PP nor the PPIE model are flawless, improvements have been forthcoming regularly. Quina and coworkers^{287,288} further developed the PPIE model for ionic micelles in order to be suitable for buffered systems. Micellar distribution of ionic solute, counterions²¹⁹ and external salt ions are treated by using the Poisson-Boltzmann Equation (PBE),^{249,259} which considers both Coulombic attraction and other specific interactions. Nome *et al.*,²⁷⁹ Romsted and co-workers,^{280,289} and Iglesias²³³ have added another reaction pathway to the original PPIE formulation, accounting for the reaction of completely-micelle-bound-substrate to the reactive-ion in the aqueous phase. Romsted and coworkers^{280,289} have used “chemical trapping” to estimate interfacial concentrations of nucleophiles in cationic micelles and other associated colloids. The basis of their method is the use of dediazonation of arenediazonium salts. Thermal loss of nitrogen from the diazonium ion **8** gives a highly reactive aryl cation **9** that is trapped extremely rapidly by any available nucleophile in its vicinity, so the product yields, which are measured by HPLC, are proportional to micellar interfacial concentrations of ions.²⁸⁰ It is

assumed that the long alkyl group, R, of the ion **8** anchors it within the micellar pseudo-phase, and its charge orients the reactive diazonio group within the interfacial region of the micelles. Using this method, for example, Soldi *et al.*²⁸⁰ found that with the increasing concentration of CTAB micelles from 0 to 0.2 M, the concentration of bromide ion increases, while the concentration of water decrease, in the interfacial region (Stern region). This result goes to show that β may not be constant.

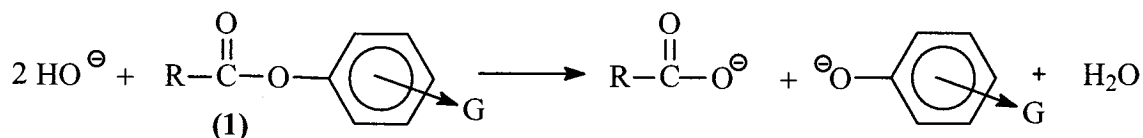


Today, it is becoming increasingly clear that conventional “two domain” micellar models are an approximation. Davies^{60,61} “multi-state” model and Engberts²¹⁶ “three-domain” model seem to be more accurate representatives of true multi-region micellar media. Suffice it to say, these models have yet to be tested extensively.

CHAPTER V. HYDROLYSIS OF PHENYL ESTERS AND THEIR BINDING IN CATIONIC MICELLES

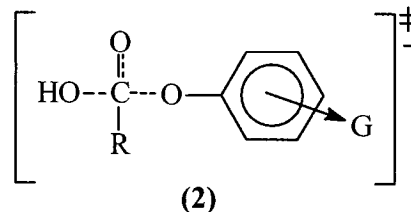
5.1 INTRODUCTION

The effect of surfactants on alkaline hydrolysis of aryl esters (1) (Scheme 5.1) was one of the first cases studied in the field of micellar catalysis.^{178,180,255,263,276,297,298} Generally, it was found that cationic micelles accelerate the observed rate for this bimolecular reaction²⁹⁷ while anionic micelles retard it.²⁹⁹ This is as expected due to simple electrostatic inclusion or exclusion of OH⁻ into the area of the head groups of micelles (see section 4.3).



Scheme 5.1 Hydroxide ion hydrolysis of aryl esters.

The mechanism of alkaline hydrolysis of phenyl esters involves initial attack of the hydroxide ion on the carbonyl carbon, leading to the formation of a tetrahedral intermediate, which further decomposes into products. The rate-limiting step of this addition-elimination reaction depends on the leaving phenoxide ion,^{168,300,301} but it is usually hydroxide ion attack. Irrespective of the details in the mechanism, with hydroxide ion as the nucleophile the transition state (2) has a substantial tetrahedral geometry with the negative charge delocalised on the three oxygens.



For many types of kinetic studies, the most popular choice of substrates are *p*-nitrophenyl alkanoate esters.³⁰² With these substrates, the probe reaction has more favourable reaction times, one of the hydrolysis products (the *p*-nitrophenoxide anion) can easily be monitored spectrophotometrically, catalysis of the reaction can attain enzyme-like accelerations, and the hydrophobicity of **1** may be changed by increasing acyl chain length, such that the hydrophobic interactions can be probed.

All kinetic studies, without exception, showed a significant acceleration in the *observed rate* for the hydrolysis of *p*-nitrophenyl alkanoates esters in the presence of cationic micelles, such as cetyltrimethylammonium bromide (CTAB) micelles [C₁₆H₃₃N⁺(CH₃)₃Br⁻]. However, authors credited this “catalysis” to different effects. The majority of authors ascribed the origin of this “micellar catalysis” to the *concentration* of the reactants into the micellar pseudo-phase and not to *medium effects* on the reaction, as we shall discuss in detail in the next section. Even though the kinetic treatments at the time considered the micellar pseudo-phase a “homogeneous solution”, discussions often necessitated knowing the binding forces and localization of reactants and transitions states within the different binding domains of the micelle.

5.2 EARLY STUDIES

In the 1960s various researchers studied the effect of *n*-alkyltrimethylammonium micelles on the alkaline hydrolysis of a limited number *p*-nitrophenyl alkanoate esters (*p*NPAlk).^{178,180,181,,276,297} In 1965, Cordes and co-workers^{181,242,255} looked at the effect of micelles on several reactions including the hydroxide ion induced hydrolysis of *p*-nitrophenyl acetate (pNPA) and *p*-nitrophenyl hexanoate (pNPH) in CTAB micelles.

Afterwards, Menger and Portnoy²⁷⁶ introduced the pseudo-phase model and compared the basic hydrolysis of pNPA and *p*-nitrophenyl octanoate (pNPO) in the presence of dodecyltrimethylammonium bromide, among other surfactants. In the same period, Romsted and Cordes²⁹⁷ studied the effect of various *n*-alkyltrimethylammonium salts on the cleavage of pNPH and *p*-nitrophenyl laurate (dodecanoate) (pNPL). In all cases, the catalytic effectiveness was more evident for esters with longer acyl chains and micelles of longer surfactants. Therefore, it was reasonable for authors to conclude that the catalytic effect is chain length dependent, presumably because an ester with a longer acyl chain is more readily incorporated into the micelle. Without data from a comprehensive series of esters, and faced with the difficulty of estimating ester-micelle association constants from the rate-surfactant profiles,²⁷⁶ authors merely presumed the importance of hydrophobic interactions of the esters with the cationic micelles.²⁹⁷

It was still questionable how changing the *reaction medium*, going from water to the micellar pseudo-phase of lower polarity, which is expected to have a mild retarding effect resulted in a catalytic effect on the reaction. The transition state for deacylation is negatively charged and should be stabilized by hydrogen bonding to water molecules, which may be less available at the surface of an ionic micelle than in the bulk. It was thus hypothesised, that the observed catalysis may result, in part at least, from the *electrostatic stabilization* of the negatively charged tetrahedral transition state (**2**) by the cationic hydrophilic head groups on the micellar surface. At the time, it was also reasoned that the inhibitory effect of added salts and the observed rate drop at higher surfactant concentration, are a consequence of weakening this electrostatic stabilization. In that period, the magnitude of the catalytic effect was estimated from the *maximum observed*

rate for ester cleavage in the presence of micelles, since plots of observed rate constant *versus* the concentration of micellized-surfactant $[D_n]$ gave rate-maxima (refer to Section 4.4, and Figure 4.8) rather than saturation-type plots.

Later, in the late 1970s, inhibition by added salts and the rate drop at high surfactant concentration were explained in terms of the displacement of reactive ions by unreactive ones in the binding sites within the region of the surfactant head groups (the Stern layer). After Bunton and coworkers¹⁸⁰ developed the PPIE model (Chapter IV), in 1980 Quina *et al.*³⁰³ used the concepts of ion-exchange in micellar solutions to analyse the cleavage of pNPA and pNPO by hydroxide ion in CTAB micelles, in a buffered system. They showed that the diminished rate of CTAB-catalyzed hydrolysis of the esters at high [CTAB] (> 1 mM) can be explained by the preferential exchange of bromide ions for hydroxide ions in the Stern layer of the micelles. They, as well as other authors^{180,245,298,304} who used a slight modification to their treatment of the kinetic data, concluded that the *second order rate constant in the micellar pseudo-phase* (k_2^m) is smaller than the second order rate constant for ester cleavage by hydroxide ion in the aqueous phase (k_w), as illustrated in Table 5.1. It should be noted, that the values of k_2^m ($= k_m V_m$) depend on the value chosen for V_m , the volume of the micelle or Stern layer, and k_2^m is thus a composite of the reactivity in the volume element within which *both* the ionic nucleophile and the substrate are incorporated and said to be “bound” to the micelle. As seen from Table 5.1, values of K_{OH}^{Br} , measured differently in each case, are not consistent and thus their reliability is questionable. Obviously, different research groups’ estimates of the *binding constants* of pNPAIk esters to CTAB micelles (K_s) did not coincide with one another. We envision the problem is mainly due to the rate-

surfactant plots giving rate-maxima, not reaching saturation, rendering estimates of K_S that are very sensitive to experimental conditions – pH, buffer, salts, concentrations.

Table 5.1 Cleavage of *p*-nitrophenyl alkanoate esters by hydroxide ion in CTAB micelles analyzed by the pseudo-phase ion exchange model.^a

Ester	K_S, M^{-1}	K_{Br}^{OH}	K_{OH}^{Br}	k_2^m/k_w	Reference
Acetate	54	12.5		0.14	303
Acetate	50	40		0.6	298
Acetate ^b	22.6		2	0.104	304
Propanoate ^b	23.11		15.05	0.198	304
Butanoate ^b	29.39		3.62	0.0841	304
Butanoate	530	10		0.13	245
Octanoate	15,000	12.5		0.11	303

^a Constants are discussed in the PPIE model (Chapter IV). The value of K_S here is a *binding constant*.

^b K_S hardly very with acyl chain length which is peculiar. The values of K_{Br}^{OH} were kept as a “variable” rather than as a “constant”.

Irrespective of the inconsistent kinetics, from these studies,^{245,304} the origin of “observed micellar catalysis” for alkaline hydrolysis of pNPAlk esters was attributed to the *concentration* of reactants into the micellar pseudo-phase, and *not* to providing a more favourable medium for the reaction, so the reaction must be taking place in water rich pools of the micellar pseudo-phase.

5.3 FURTHER STUDIES AND TRANSITION STATE STABILIZATION

In order to better understand the origin of catalysis of alkaline hydrolysis of aryl esters by CTAB micelles, and to help clear up misconceptions about them, it is essential to know how the reactants and their transition state are bound within the micellar pseudo-

phase. There is no dispute that hydroxide ions will be concentrated in the Stern region of CTAB micelles by *electrostatic attraction* and that they undergo *ion exchange* with the bromide counterions of CTAB. Despite the debate over the binding site(s) of aryl esters in micelles, there is now a general agreement that the site of ester cleavage (reactive centre) is at the predominately water rich region of the micelle (the Stern region), especially following the work of Al-Awadi and Williams.³⁰⁵

These authors³⁰⁵ studied the basic hydrolysis of nine substituted phenyl laurates (dodecanoates) in CTAB micelles. Their kinetic data were obtained under conditions of constant $[\text{Br}^-]$ to avoid dilution of the hydroxide ion in the Stern layer, as $[\text{CTAB}]$ is increased. Under these conditions, rate vs. $[\text{CTAB}]$ plots showed clean saturation kinetics (as illustrated in Figure 4.8a and as will be seen later). The observed rate constant for ester consumption obey a Michaelis-Menten-like rate law, eq. [5.1]:

$$k_{\text{obs}} = \frac{(k_{\text{OH}} K_{\text{eq}} + k_{\text{OH}}^{\text{cat}} [\text{CTAB}]) [\text{OH}^-]}{(K_{\text{eq}} + [\text{CTAB}])} \quad [5.1]$$

where $k_{\text{OH}}^{\text{cat}}$ is the second-order rate constant for the reaction of the micelle-bound ester with *bulk* hydroxide ion, K_{eq} is an equilibrium constant for *dissociation* of the ester from the micelle-bound ester, and k_{OH} is the second-order rate constant for the reaction of free ester with hydroxide ion.³⁰⁵ From the rate constants, shown in Table 5.2, CTAB micelles clearly “catalyze” the alkaline hydrolysis of the esters. Remarkably, their values of the parameter K_{eq} exhibit no significant change with the substituent on the phenyl group, within experimental error (Table 5.2, overleaf).

The Brønsted plots of the logarithms of the rate constants ($\log k_{\text{OH}}$ or $\log k_{\text{OH}}^{\text{cat}}$) vs. the $\text{p}K_{\text{a}}$ of the leaving phenol are both linear, with negative slopes (*Brønsted* β_{lg}

values). Al-Awadi and Williams³⁰⁵ found that the sensitivity of the micelle-catalyzed reaction to the leaving group ($\beta_{lg} = -0.51 \pm 0.06$) is virtually the same as that for the hydrolysis in basic aqueous solution ($\beta_{lg} = -0.56 \pm 0.05$). This situation arises because the binding of the esters (and of their transition states, as will be pointed out later) to the micelles is independent of the substituent on the phenyl group. The corresponding *Hammett* ρ values, from the slope of the logarithms of the rate constants vs. Hammett substituent constant σ , indicate that the effective *negative charge development* on the hydrolysis transition state in the CTAB micelles ($\rho = +0.19$) is almost the same as in the bulk aqueous solution ($\rho = +0.14$).³⁰⁶ These results are direct evidence that the catalyzed reaction takes place in an aqueous-rich region of the micelles (i.e. the Stern region). The results may also indicate that there is no additional electrostatic stabilization of the anionic hydrolysis transition state by cationic micelles, which rules out cation- π interaction with the aryl ring and the ammonium head groups of CTAB.

Table 5.2 Alkaline hydrolysis of substituted phenyl dodecanoates in CTAB micelles.^a

Substituent (G)	$k_{OH} \cdot 10^3$ $M^{-1} s^{-1}$	k_{OH}^{cat} $M^{-1} s^{-1}$	K_{eq} , mM	K_{TS} , ^b μM
2-NO ₂ -4-Cl	46	5.8	0.39	3.1
4-NO ₂	18	4.8	0.41	1.5
2-NO ₂	14	4.5	0.41	1.3
4-CN	13	3.3	0.40	1.6
3-NO ₂	6.3	0.55	0.43	4.9
3-Cl	1.8	0.30	0.38	2.3
4-Cl	1.0	0.28	0.39	1.4
H	0.39	0.101	0.40	1.5
4-Me	0.22	0.088	0.42	1.1

^a Data from Al-Awadi and Williams.³⁰⁵ Values of k_{OH}^{cat} and K_{eq} were found at constant $[Br^-] = 0.09$ M, borate buffer at 0.01 M and pH=11.66.

^b Values of $K_{TS} = k_{OH}K_{eq}/k_{OH}^{cat}$ were calculated afterwards by Tee.¹⁹

Subsequently, Tee¹⁹ pointed out that the above findings “mean that the transition state stabilization afforded by the micellar environment is essentially constant for esters with a 200-fold range of reactivity” (Table 5.2). Since the transition state (TS) stabilization by CTAB micelles is independent of the phenoxide leaving group of the ester, it was suggested that it most probably depends on the chain length of the ester. To test this suggestion, Tee and Fedortchenko⁵⁸ studied the alkaline hydrolysis of a series of *p*-nitrophenyl alkanoate (*p*NPAlk) esters (from acetate to octanoate) in CTAB micelles, in order to probe the *hydrophobic interactions*.^{65,68,75} Following Williams,³⁰⁵ their kinetic study was carried out with constant [Br[−]] and at constant pH, which resulted in rate vs. [CTAB] profiles also showing saturation kinetics, with good data fits to equation [5.2].

$$k_{\text{obs}} = \frac{(k_u K_S + k_c[\text{CTAB}])}{(K_S + [\text{CTAB}])} \quad [5.2]$$

Non-linear least squares fitting of eq. [5.2] over a range of [CTAB], provided the parameter k_c , the rate constant for the cleavage of the micellar-bound ester, as well as K_S , the *dissociation constant* for the ester bound to CTAB; the rate constant k_u is for hydrolysis of the free ester in the medium. Their results are shown in Table 5.3.

Table 5.3 Alkaline hydrolysis of *p*-nitrophenyl alkanoates in CTAB micelles.^a

Ester	k_u (s ^{−1})	k_c (s ^{−1})	K_S (mM)	k_c/k_u	K_{TS} (mM) ^b
Acetate	0.110	0.301	11.4	2.73	4.17
Propanoate	0.107	0.236	5.29	2.21	2.39
Butanoate	0.0693	0.161	1.96	2.33	0.844
Pentanoate	0.0697	0.160	0.769	2.30	0.335
Hexanoate	0.0649	0.160	0.257	2.47	0.104
Heptanoate	0.0630	0.162	0.0819	2.56	0.0319
Octanoate	0.0591	0.147	0.0423	2.48	0.0170

^a Data from Tee and Fedortchenko.⁵⁸ Total [Br[−]] = 5.0 mM, phosphate buffer pH = 11.6. ^b $K_{TS} = k_u K_S / k_c$.

We have discussed, in Chapter I (Section 1.2) of the thesis, the derivation of the pseudo-equilibrium constant for hypothetical dissociation of the transition state bound to the catalyst (K_{TS}),^{42,43} and the general use of pK_{TS} ($= -\log K_{TS}$) and its variation with the structure as a means for probing mechanisms of catalysis by host systems.¹⁹ Tee and Fedortchenko⁵⁸ applied this approach to their data, and found that transition state stabilization, expressed by K_{TS} , varied systematically with ester chain length, as does K_S for ester binding (Table 5.3). Surprisingly, they found that the limiting acceleration $k_c/k_u = K_S/K_{TS}$, that is the extent of catalysis, is *independent of the acyl chain length* of the ester (Table 5.3), which is a direct consequence of the *parallelism* between ester (substrate) binding and TS binding to CTAB micelles. Thus, contrary to earlier beliefs, catalysis is not greater for longer esters, but the binding of the esters *and of their transition states* to CTAB micelles is stronger. Linear free energy relationship (LFER) plots of pK_S (and pK_{TS}) versus acyl chain length are linear and *parallel*, with the *same* slopes of 0.42. It was thus concluded that the incorporation (and binding) of the substrates and their transitions in CTAB micelles are determined by the *same effects*, namely, hydrophobic interactions.⁵⁸ This assertion is based on the knowledge that many phenomena associated with hydrophobicity of n-alkyl derivatives vary linearly with chain length and with slopes ~ 0.4 .^{65,75,175,215} For example, the $\log (cmc)$ against chain length (n) of surfactants are straight lines with slopes ranging from 0.3–0.5 (see Chapter IV, Figure 4.5). Thus, the sensitivities of pK_S and pK_{TS} to chain length are consistent with dominant hydrophobic effects.

In conclusion, the catalysis of the alkaline hydrolysis of the esters by CTAB micelles is due to the *concentration* of the ester and the hydroxide ion into the cationic

micelles by hydrophobic interactions and ion-exchange, respectively. From the studies of Al-Awadi and Williams,³⁰⁵ and of Tee and Fedortchenko,⁵⁸ one can construct Figure 5.1, which shows that, in the transition state, the *reaction centre* (the ester carbonyl group and associated aromatic ring, -COOAr) is localized at the Stern layer, with the alkyl portion of the acyl group of the ester extending into the hydrocarbon core of the micelle, where it is bound.

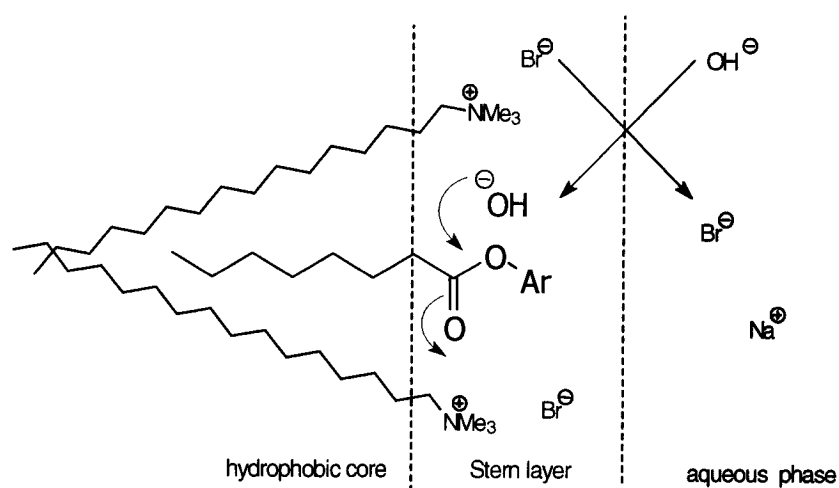


Figure 5.1 Mode of TS binding for hydrolysis of *p*NPAlk esters in CTAB micelles.

5.4 OBJECTIVES OF THE RESEARCH

The motivation for our studies of micellar reactions stems from four general objectives: first, to further the understanding of those factors which influence the rates and course of organic reactions in micellar media; second, to modify experimental procedures and explore the utility of a kinetic model which is not based on too many assumptions; third, to apply transition state binding relative to the initial state binding, and their variation in structure of the reacting species, as a prime focal point for

discussing “micellar catalysis”; and finally, to gain additional insight into the exceptional catalysis of enzymatic reactions.

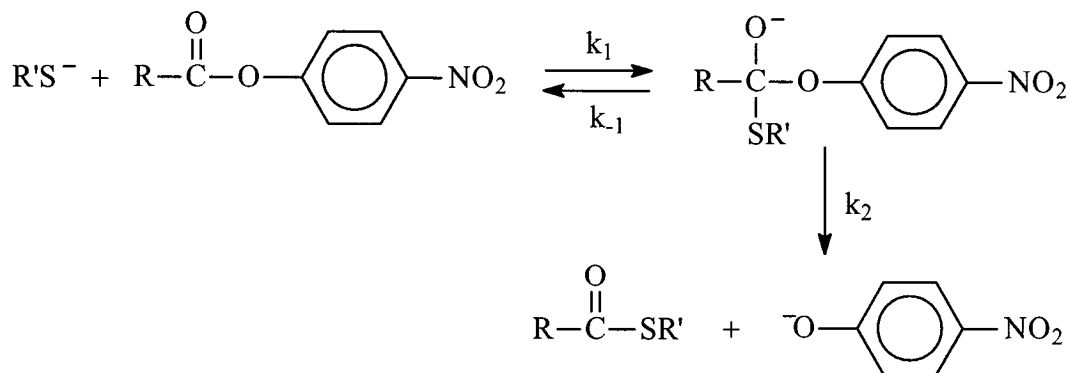
Specifically, we were intrigued by the controversial results on the “catalysis” of aryl ester hydrolysis within CTAB micelles, and perhaps we were even initially sceptical about the constant magnitude of this catalysis with ester chain length.⁵⁸ So we wanted to verify previously executed research, as well as address the effects of changing the nucleophile on the catalysis. Thus, we have revisited the cleavage of *p*-nitrophenyl alkanoate esters (*p*NPAlk, from acetate to decanoate) in CTAB micelles by anionic nucleophiles, mainly thiolate ions (Chapter VI). Following on that study, we then turned to neutral alkylamines of varying chain length as the nucleophiles (Chapter VII). Finally, we concluded our research by studying the cleavage of the *p*NPAlk esters by amino acids of varying ionic charge and hydrophobicity (Chapter VIII), which to the best of our knowledge has never been systematically investigated before in CTAB micelles. This research was conducted under “constant ionic atmosphere”,^{62,305} as well as constant buffer concentration.^{236,307} The research was conducted bearing in mind the following questions: 1) How does the TS binding and ester binding to CTAB micelles depend on the ester chain length? 2) How and to what extent does the nucleophile affect the magnitude of catalysis by CTAB micelles? 3) Does the nucleophile affect the strength of ester or TS binding to the micelle?

CHAPTER VI. CATALYSIS OF THE THIOLYSIS OF *p*-NITROPHENYL ALKANOATES BY CTAB MICELLES

1.1 INTRODUCTION AND PREVIOUS WORK

There have been a few previous studies of the effect of cationic surfactants on ester thiolysis.^{308,309,310} None of those studies were carried out under the controlled experimental conditions discussed in Chapter V, with a homologous series of esters, and none have focussed on “transition state stabilization” and binding within CTAB micelles. In this chapter, we present a study of the catalysis by cetyltrimethylammonium bromide (CTAB) micelles of the thiolysis of *p*-nitrophenyl alkanoates (*p*-NPAlk, acetate to decanoate). This work has already been published.⁵⁹

The general mechanism of acyl-transfer to sulfur nucleophiles was investigated in the late 70s.^{301,311} The mechanism of thiolysis of *p*-NPAlk esters, under basic conditions, is illustrated in Scheme 6.1. In this, the addition of the thiolate ion to the ester produces a metastable tetrahedral intermediate that may revert back to reactants or breakdown into the thiolate ester and *p*-nitrophenoxide ion:



Scheme 6.1 Thiolysis of *p*NPAlk esters.

The Brønsted-type plot for this type of system is bent because there is a change in rate-limiting step. The break in the plot of $\log k_{\text{obs}}$ against pK_{a} of RSH appears when the breakdown of the tetrahedral intermediate by forward and backward routes are as fast as each other, i.e. when $k_{-1} = k_2$. When $k_{-1} < k_2$, loss of *p*-nitrophenoxide ion is relatively fast and thiolate attack is rate-limiting; on the other hand when $k_{-1} > k_2$, then departure of the leaving group is rate-limiting. We studied thiolate ions having a pK_{a} range between 9.5-10.6, which are past the break point of the Brønsted plot for *p*-nitrophenyl acetate, that occurs at $\text{pK}_{\text{a}} \sim 7.8$, and thus, in all cases, the first step (thiolate attack) is rate limiting.

Correia *et al.*²⁶⁸ showed that the mechanism and rate-limiting step of the thiolysis of some benzoate esters (eg. *p*-nitrophenyl *p*-X-benzoate) may be modified by micellar media. For the reaction in CTAB micelles, the Brønsted plot is *linear*, not bent, in the region close to the pK_{a} of the leaving group, while for reaction in water the plot is bent. This indicated that either the mechanism or the rate-limiting step in the aggregates is different from that in water. Using α -toluenethiol, PhCH_2SH ($\text{pK}_{\text{a}} = 9.43$ (in water), 10.6 (in micelle)), as the source of thiolate, the Hammett plots are linear with in both water and CTAB micelles. However, the micelles increase the sensitivity of the reaction to substituent electronic effects, with $\rho_{\text{m}} (+2.65) > \rho_{\text{w}} (+2.08)$. Correia *et al.*²⁶⁸ suggested that the increased sensitivity to polar effects in the micelles is due to a reduction in charge stabilization by the solvent. For the reaction of these substrates with phenylthiolate ion, PhS^- , in water, the $\log(\text{rate})$ is linear with σ^- , and the value of ρ_{w} is 0.87 which is lower than that obtained for the rate limiting attack step. The corresponding Hammett plot in CTAB micelles is linear with σ and the value of ρ_{m} is 2.83. These results clearly show

that the micelles bring about a change in rate-limiting step, leading exclusively rate-determining thiolate attack on the benzoate esters.

The above results of Correia *et al.*²⁶⁸ are not like those of Al-Awadi and Williams³⁰⁵ for the alkaline hydrolysis of substituted phenyl laurate esters, where the ρ values in the aqueous and in micellar media are the same (Chapter 5). This may mean that in the transition state, the benzoate ring of the *p*-nitrophenyl *p*-X-benzoates is either in the more hydrophobic regions of the Stern layer, or even in the palisade layer of CTAB micelles.

Previously, Cuccovia *et al.*³⁰⁹ had shown that hexadecyltrimethylammonium bromide (CTAB) micelles result in a rate increases of 50-fold in the thiolysis of *p*-nitrophenyl acetate by thiophenoxide anions. The micelles were shown to affect the acid dissociation constants of thiols substantially, and contrary to what was expected, the pK_a values of the thiophenols were lowered upon their incorporation into the micellar phase. The rate increases were entirely explained on the basis of concentration of the reagents in the micellar pseudo-phase.³⁰⁹

6.2 RESULTS AND KINETIC TREATMENT OF THE DATA

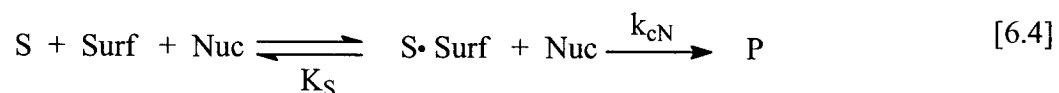
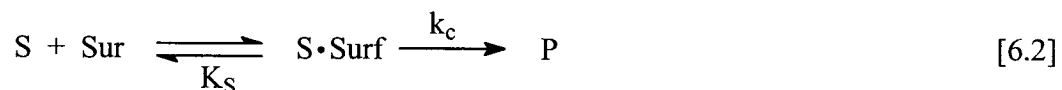
The present studies were more demanding than the previous study of hydroxide ion induced cleavage of the *p*NPAIk esters in CTAB micelles⁵⁸ because they required more than one series of experiments. We have studied reaction of the esters with several thiolate nucleophiles in the absence and in the presence of CTAB, and the data are tabulated in Appendix B. Detailed kinetic analysis of this data will be described for the results of the reaction between the anion of 2-mercaptoethanol (ME) and the esters in

CTAB micelles. Analogous experiments with the dianion of mercaptoacetic acid (MAA), with the dianions of 3-mercaptopropionic acid (MPA) and cysteine (CYST), and, for comparison, with the anion of glycine (GLY), an amine nucleophile, and the anion of 2,2,2-trifluoroethanol (TFE), an oxyanion.

The kinetics of the ester cleavage was followed by monitoring the pseudo first-order appearance of *p*-nitrophenoxide ion. The model used to analyze data for the variation of k_{obs} with [CTAB] and with [Nuc] is not exactly based on the pseudo-phase assumption and is not like any model used before to quantify bimolecular reactions in micelle-mediated processes (Chapter IV). We have treated the partitioning of the ester into the micellar pseudo-phase as if it were regular 1:1 complexation process, which is basically the same as that developed earlier for some cyclodextrin-mediated bimolecular reactions.^{54,55,57,131} This treatment is acceptable under the conditions where the concentration of surfactant (1-5 mM) far exceeds that of the ester (2-50 μM), such that the probability of more than one ester molecule interacting with the same micelle is small. The concentrations of nucleophile are also kept higher (15-20 mM) than that of the ester or surfactant, because under these conditions the concentration of unbound and micellar-bound nucleophile remains a constant, embedded in the second order rate constant. To maximize thiolysis and to limit basic hydrolysis, the reaction medium for these studies was chosen to be an aqueous carbonate buffer, adjusted to pH 10.6. The pK_a of the thiols is between 9-10, and thus the thiols are more than 50% ionized at that pH. Finally, as suggested by Romsted²⁹⁷ and by Williams,³⁰⁵ to avoid added complications arising from variable bromide ion exchange into the micelles,^{245,248,288,290} and to be

consistent with our previous work,⁵⁸ the total bromide ion concentration was kept constant at 5.0 mM.

With these experimental conditions, for the analysis of the nucleophilic cleavage of the esters in CTAB micelles, four competing reactions were considered: (i) basic hydrolysis of the ester (S) in the aqueous medium (eq. [6.1]); (ii) basic hydrolysis of the micellar-bound ester (eq. [6.2]); (iii) nucleophilic attack in the aqueous medium (eq. [6.3]); and (iv) nucleophilic attack on the micellar-bound ester (eq. [6.4]).



For these four processes together, the expected variation of the rate constant (k_{obs}) for ester cleavage with the concentration of nucleophile [Nuc] and with micellized surfactant [Surf] = ([Surf]₀ – cmc) is given by equation [6.5], provided that the concentration of the ester is low enough not to affect micellization. The [Nuc] in equation [6.5] is equal to the initial concentration of the nucleophile since [Nuc]₀ >> [S]₀. Note that the binding of the ester to the micellized surfactant is characterized by a dissociation constant $K_S = [S][\text{Surf}]/[S \cdot \text{Surf}]$.

$$k_{\text{obs}} = \frac{(k_u K_S + k_c [\text{Surf}]) + (k_N K_S + k_{cN} [\text{Surf}]) [\text{Nuc}]}{(K_S + [\text{Surf}])} \quad [6.5]$$

As written, it is difficult to fit equation [6.5] to the acquired data because the equation is non-linear and bivariant, having a dependence on the concentration of both the nucleophile and the surfactant. At pH 10.6, the two background processes [6.1] and [6.2] are not too significant (see Experimental Section) and simplifications to equation [6.5] can be made to estimate the required parameters k_N , K_S and k_{cN} from three series of experiments in the absence and presence of CTAB.

From the first series of experiments, in aqueous buffer in the *absence* of CTAB, the dependence of k_{obs} on added nucleophile (here ME) is strictly linear (Figure 6.1). Similar linear dependence was found with other nucleophiles. This behaviour adheres to equation [6.6], which comes from equation [6.5] when $[Surf] = 0$. The second order rate constants for nucleophilic attack on the free ester, k_N , (eq. [6.3]) are simply obtained from the slopes of the plots of k_{obs} vs $[Nuc]$.

$$k_{obs} = k_u + k_N [Nuc] \quad [6.6]$$

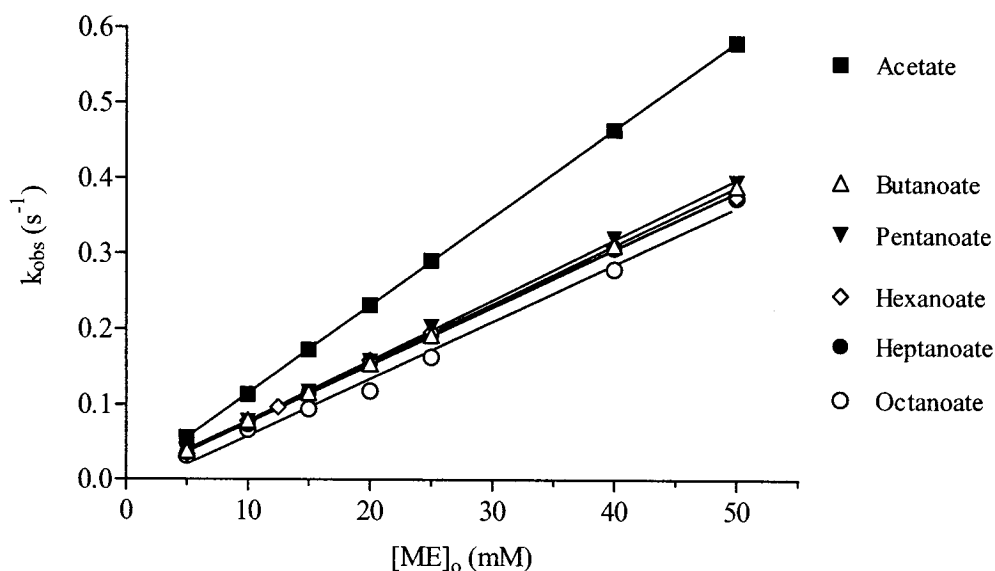


Figure 6.1 Variation of k_{obs} for ester cleavage with the concentration of mercaptoethanol ($[ME]_o$), in the presence of 5.0 mM NaBr, but not CTAB.

The values of k_N are shown later in Table 6.1. Note that it is difficult to reproduce observed rate constants for the decanoate ester, due to its aggregation even at very low concentrations³¹² and its poor solubility in water. Accordingly, k_N for this ester was taken to be the same as found for the octanoate (Table 6.1). Note that much the same rate constants k_N are obtained for all the esters butanoate – octanoate, as found previously for cleavage by hydroxide ion.⁵⁸

From a second series of experiments, the variation of k_{obs} with $[CTAB]$, at a fixed $[Nuc]$ and at a constant *total* $[Br^-]$ shows catalysis and saturation behaviour (Figure 6.2), due to binding of the ester substrates to the micelles, and the data adhere to equation [6.7]. Equation [6.7] is derived from equation [6.5], when $[Nuc]$ is constant, where $k_o = (k_u + k_N [Nuc]_o)$ and $k_{mic} = (k_c + k_{cN} [Nuc]_o)$, and $[Surf] = [Surf]_o - cmc$, assuming that the

$$k_{obs} = \frac{k_o K_S + k_{mic} [Surf]}{K_S + [Surf]} \quad [6.7]$$

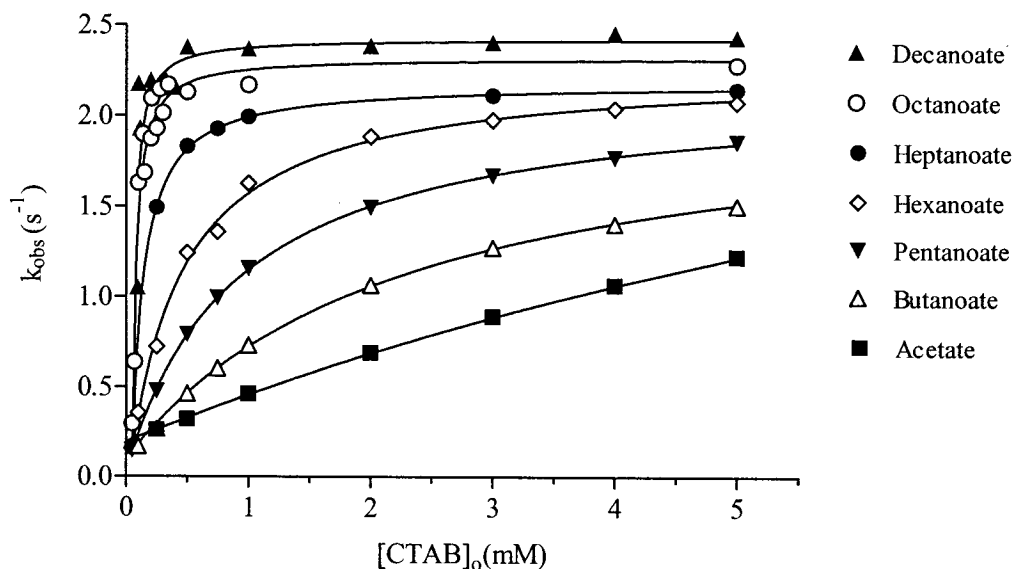


Figure 6.2 Variation of k_{obs} for ester cleavage with the concentration of $[CTAB]_o$, above the cmc, in the presence of 20 mM mercaptoethanol, and at a total bromide ion = 5.0 mM.

added nucleophile does not alter K_S or the micellization of CTAB. Non-linear least square regression analysis of the data affords estimates of K_S as well as of k_o and k_{mic} . One can see that k_o is the sum of the processes occurring in aqueous solution, and k_{mic} is the sum of processes occurring in the micellar pseudo-phase. *Saturation kinetic* behaviour, not *rate-maxima*, are observed and the degree of curvature reflects the strength of ester binding in the micelles. The units of the ester-micelle dissociation constant K_S are in molar concentrations of micellized-surfactant rather than the molar concentration of the micellar aggregates because this would require an accurate knowledge of the aggregation numbers. If the micelle were to be treated as a molecule the molar dissociation constant would be given by the term K_S/N , where the aggregation number N ranges from 70-100 for CTAB.¹⁷⁵ The estimates of the values of the ester-micelle dissociation constant, K_S , are shown in Table 6.1.

For a third series of experiments, in the presence of a *fixed* concentration of surfactant ($[CTAB] = 5.0$ mM), the variation of k_{obs} with the concentration of nucleophile ($[ME]$) also comes out to be linear (Figure 6.3) which indicates that even though thiolate ions exchange into the Stern layers of micelles, their effects do not show saturation. Note the slope becomes steeper with the longer esters. At *constant* $[Surf]$, equation [6.5] can be divided into two terms, one that is independent of the concentration of nucleophile and another that is not (eq. [6.8]).

$$k_{obs} = \frac{(k_u K_S + k_c [Surf])}{(K_S + [Surf])} + \frac{(k_N K_S + k_{cN} [Surf]) [Nuc]}{(K_S + [Surf])} \quad [6.8]$$

$$k_{obs} = \text{intercept} + \text{slope} \cdot [Nuc] \quad [6.8b]$$

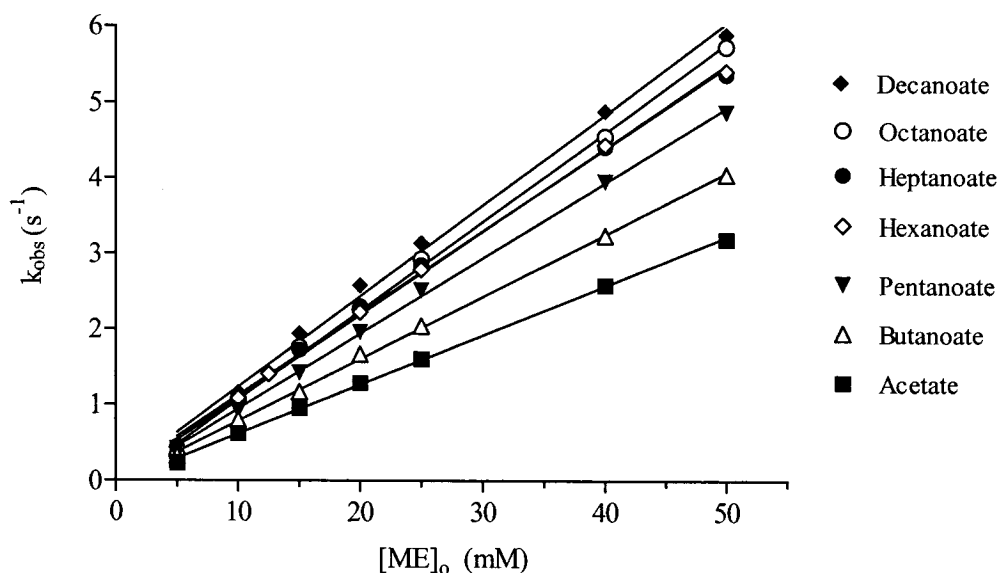


Figure 6.3 Variation of k_{obs} for ester cleavage with the concentration of mercaptoethanol ($[\text{ME}]_o$), in the presence of 5.0 mM of CTAB, and no NaBr. Note that, because of micellar catalysis, the vertical scale here is 10 times that in Fig.6.1.

Knowing k_N and K_S , from the analysis of the other two series of experiments, the second order rate constants of nucleophilic attack on the bound-ester micelle complex, k_{cN} (eq. [6.4]), are estimated from the **slopes** $= (k_N K_S + k_{cN} [\text{Surf}]) / (K_S + [\text{Surf}])$ of the plots in Figure 6.3. Values of k_{cN} are shown in Table 6.1.

For the present purposes, K_{TS} (eq. [6.9]) is defined to be the dissociation constant the micelle-bound transition state (TS.Surf) into the transition state of normal cleavage (TS) and the micellized surfactant (Surf).^{19,42,48} Background derivations of equation [6.9] are in Section 1.2 of the thesis.

$$K_{TS} = [\text{TS}][\text{Surf}] / [\text{TS.Surf}] = k_N K_S / k_{cN} = k_N / k_3 \quad [6.9]$$

$$k_{cN} / k_N = K_S / K_{TS} \quad [6.10]$$

According to rearrangement of equation [6.9], the catalytic ratio k_{cN} / k_N (eq. [6.10]) is a consequence of the relative strength of TS and substrate binding to CTAB. Values of this ratio are also presented in Table 6.1.

In equation [6.9], k_3 stands for the third order rate constant corresponding to the overall process shown in equation [6.11], which is kinetically equivalent to that shown earlier in equation [6.4]. Hence, $k_3 = k_{cN}/K_S$.



Table 6.1 Constants for the reaction of the anion of 2-mercaptoethanol (ME), $\text{HOCH}_2\text{CH}_2\text{S}^-$, with *p*-nitrophenyl alkanoates in the presence and absence of CTAB micelles. ^a

Ester	k_N $\text{M}^{-1} \text{s}^{-1}$	k_{cN} $\text{M}^{-1} \text{s}^{-1}$	K_S mM	k_{cN}/k_N	K_{TS} mM
Acetate	11.7 ± 0.02	202 ± 3	12.7 ± 0.5	17.3	0.736
Butanoate	7.77 ± 0.04	117 ± 2	2.34 ± 0.10	15.0	0.155
Pentanoate	7.99 ± 0.08	118 ± 2	0.975 ± 0.015	14.8	0.0660
Hexanoate	7.59 ± 0.13	120 ± 2	0.465 ± 0.030	15.8	0.0294
Heptanoate	7.64 ± 0.06	110 ± 3	0.0995 ± 0.0040	14.4	0.00691
Octanoate	7.56 ± 0.31	118 ± 3	0.0323 ± 0.0065	15.6	0.00207
Decanoate	7.56^b	120 ± 4	0.00585^c	15.9	0.000369

^a At 25 °C, in an aqueous carbonate buffer of pH 10.60, with the total bromide concentration ($[\text{CTAB}] + [\text{Br}^-]$) kept at 5.00 mM.

^b Difficult to determine accurately and so assumed to be the same as for the octanoate.

^c Obtained by extrapolation of the linear plot of $\text{p}K_S$ vs. *n*.

The above results, obtained for the anion of 2-mercaptoethanol, will be discussed later, along with those for other nucleophiles.

6.2.1 Other Nucleophiles

Analogous experiments with the dianion of mercaptoacetic acid (MAA) gave results similar to those found for the anion of mercaptoethanol (ME). However, plots of k_{obs} vs [MAA] at fixed [CTAB] showed very slight downward curvature at the high end of [MAA] = 0 to 25.0 mM, and to minimize its effect, values of k_{cN} were estimated from the data points in the concentration range 0 to 15.0 mM, where the variation in k_{obs} is quite linear. This weak curvature at high [MAA] may indicate the onset of saturation of the micelles with the MAA dianions which probably bind stronger to CTAB micelles than the monoanion of ME - see Discussion. Alternatively, high thiolate concentrations may start to alter the micellization parameters – shape, size, aggregation numbers. The K_{S} values found from the experiments with the anions of ME (Table 6.1) and MAA (Table 6.2) differ little from each other, or from those found earlier during studies of ester cleavage by hydroxide ion,⁵⁸ despite differences in pH, buffer, and ionic strength.

Experiments were also carried out with the dianions of 3-mercaptopropionic acid (MPA) and cysteine (CYST), and, for comparison, with the anion of glycine (GLY), an amine nucleophile, and the anion of 2,2,2-trifluoroethanol (TFE), an oxyanion. For the experiments with TFE, the medium was a 0.20 M phosphate buffer of pH 11.60, as used for previous studies of ester cleavage by hydroxide ion.⁵⁸ Again, for the dianions, the plots of k_{obs} against [Nuc], at constant [CTAB], showed slight curvature at the high [Nuc], and so k_{cN} values were estimated from the linear dependence in the range [Nuc] = 0 to 15.0 mM. Since the values of K_{S} do not appear to be significantly sensitive to the nucleophile, the values found from the experiments with MAA were used in the analyses to find k_{cN} values for the anions of MPA, CYST and GLY. For the anion of TFE, the

values of K_S that were found earlier from reaction with hydroxide ion in the same phosphate buffer were used.⁵⁸ Values of k_N and k_{cN} obtained for the anions of MAA, MPA, CYST, GLY, and TFE are collected in Table 6.2, along with the apparent “equilibrium constants”, K_{TS} , and other derived quantities.

Table 6.2 Constants for the reaction of thiolate ions and other nucleophiles with *p*-nitrophenyl alkanoates in the presence and absence of CTAB micelles.^a

Ester	k_N $M^{-1} s^{-1}$	k_{cN} $M^{-1} s^{-1}$	K_S mM	k_{cN}/k_N	K_{TS} mM
Dianion of mercaptoacetic acid (MAA)			${}^{-}O_2CCH_2S^{-}$		
Acetate	15.6 ± 0.2	1780 ± 100	24.6 ± 4.0	114	0.216
Butanoate	10.4 ± 0.2	774 ± 26	2.60 ± 0.23	74.4	0.0349
Pentanoate	10.4 ± 0.2	776 ± 39	1.06 ± 0.07	71.2	0.0149
Hexanoate	11.0 ± 0.2	776 ± 24	0.374 ± 0.009	70.5	0.00530
Heptanoate	11.2 ± 0.2	915 ± 20	0.141 ± 0.009	81.7	0.00173
Octanoate	10.1 ± 0.1	886 ± 7	0.0539 ± 0.0032	87.7	0.000614
Decanoate	10.1^b	867 ± 14	0.00664^c	85.8	0.0000774
Dianion of 3-mercaptopropionic acid (MPA) ^d			${}^{-}O_2CCH_2CH_2S^{-}$		
Acetate	11.8 ± 0.2	786 ± 96	24.6	66.8	0.368
Butanoate	8.64 ± 0.07	453 ± 25	2.60	52.4	0.0497
Pentanoate	8.44 ± 0.19	435 ± 24	1.08	51.5	0.0205
Hexanoate	8.08 ± 0.25	462 ± 16	0.374	57.2	0.00654
Heptanoate	8.11 ± 0.11	421 ± 18	0.141	51.9	0.00271
Octanoate	7.62 ± 0.39	395 ± 25	0.0539	51.8	0.00104

Continued overleaf

Ester	k_N $M^{-1} s^{-1}$	k_{cN} $M^{-1} s^{-1}$	K_S mM	k_{cN}/k_N	K_{TS} mM
Dianion of cysteine (CYST) ^d $^{-}O_2CCH(NH_2)CH_2S^{-}$					
Acetate	9.78 ± 0.08	812 ± 17	24.6	83.0	0.296
Butanoate	6.01 ± 0.07	362 ± 16	2.60	60.3	0.0431
Hexanoate	5.70 ± 0.03	364 ± 16	0.0374	63.8	0.00586
Octanoate	6.91 ± 0.01	370 ± 9	0.0539	53.5	0.00101
Anion of glycine (GLY) ^d $^{-}O_2CCH_2NH_2$					
Acetate	1.51 ± 0.03	2.55 ± 0.05	24.6	1.69	14.6
Butanoate	0.561 ± 0.025	0.711 ± 0.12	2.60	1.27	2.05
Hexanoate	0.573 ± 0.007	0.856 ± 0.068	0.0374	1.49	0.250
Octanoate	0.477 ± 0.041	0.639 ± 0.055	0.0539	1.34	0.0402
Anion of 2,2,2-trifluoroethanol (TFE) ^e $CF_3CH_2O^{-}$					
Acetate	13.1 ± 0.08	531 ± 19	11.4	40.5	0.282
Butanoate	7.25 ± 0.09	196 ± 3	1.96	27.1	0.0723
Hexanoate	7.67 ± 0.02	178 ± 5	0.257	23.2	0.0111
Octanoate	7.00 ± 0.21	176 ± 2	0.0423	25.4	0.00167

^a At 25 °C, in an aqueous carbonate buffer of pH 10.60, with the total bromide concentration ($[CTAB] + [Br^{-}]$) kept at 5.00 mM.

^b Difficult to determine accurately and so assumed to be the same as for the octanoate.

^c Obtained by extrapolation of the linear plot of pK_S vs n .

^d For the experiments with the anions of MPA, CYST, and GLY the values of K_S were to be taken to be the same as those found with the mercaptoacetate dianion.

^e For TFE, the medium was a 0.20 M phosphate buffer of pH 11.60, as used for previous studies of ester cleavage by hydroxide ion. The values of K_S were to be taken to be the same as those found earlier with hydroxide ion.

6.3 DISCUSSION

6.3.1 Ester Chain Length Effects: Hydrophobic Interaction

The cleavages of *p*-nitrophenyl alkanoates by various nucleophilic anions are *all catalyzed* by CTAB micelles. From Table 6.1 it is immediately apparent that beyond the acetate ester, the rate constants k_N and k_{cN} both show almost no variation with ester chain length within experimental error, and where variation is evident, there is no particular trend in that variation. Correspondingly, and remarkably, the *limiting accelerations* (k_{cN}/k_N) brought about by CTAB micelles are virtually *constant* for each nucleophile and independent of ester acyl chain length (Tables 6.1 and 6.2). Similar behaviour was found earlier for cleavage of the same series of esters by hydroxide ion (Chapter V, Table 5.3). Thus, as described in Chapter V, and contrary to previous belief, the magnitude of the micellar catalysis does not change with ester chain length.

It should be remembered that the “catalytic” ratio, $k_{cN}/k_N = K_S/K_{TS}$ (eq. [6.10]), is determined by the relative strengths of *transition state binding* and *substrate binding*. Seen from this point of view, the nearly constant k_{cN}/k_N ratios for each nucleophile, from acetate to decanoate, arise because the substrate binding and transition state binding to CTAB micelles have exactly the same sensitivity to elongation of the ester chain. For the catalytic ratio to increase significantly with chain length would require that the TS binding be more sensitive to the acyl chain length than the initial state binding, which is not the case.

In actuality, the dissociation constants K_S and K_{TS} both *vary* appreciably with ester chain length (Tables 6.1 and 6.2). Moreover, the strengths of both ester binding ($pK_S = -\log K_S$) to CTAB and transition state binding ($pK_{TS} = -\log K_{TS}$) to CTAB

increase linearly with chain length (Figure 6.4) and the two are closely *parallel*. The slopes of the linear plots of pK_{TS} vs. chain length (n) and of pK_S vs. n , are all essentially the same, at 0.43 ± 0.02 , for the thiolate nucleophiles, and they are barely different for the other three nucleophiles (Table 6.3). Even more to the point, pK_{TS} values (for transition state binding) are very strongly correlated with pK_S values (for substrate binding), with slopes very close to *unity* (see correlations in Table 6.3).

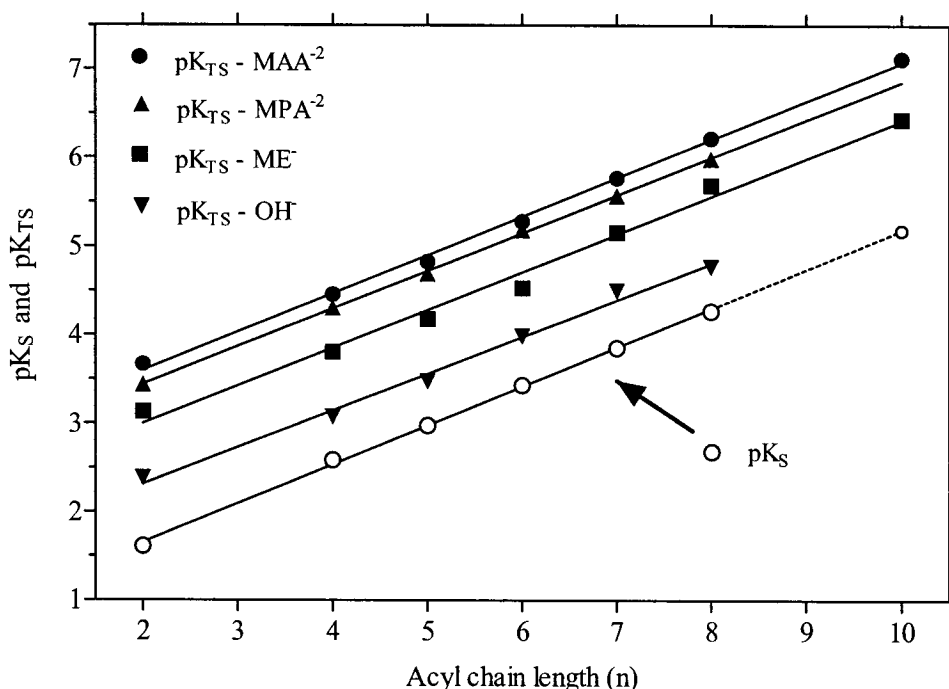


Figure 6.4 The dependence of transition state binding (pK_{TS}) and substrate binding (pK_S) to CTAB micelles on the ester chain length (n) of *p*-nitrophenyl alkanoates. The values of pK_{TS} (closed symbols) are for various nucleophiles, as indicated; the values of pK_S are those found with MAA. The pK_{TS} points for CYST and TFE (not shown) are close to those for MPA, and those for GLY are barely different from pK_S because k_{CN}/k_N values are almost one (Table 6.2). The corresponding plot of pK_{TS} against pK_S are linear, with slopes very close to one (Table 6.3).

In contrast to the effect of CTAB micelles, the cleavage of *p*-nitrophenyl alkanoates by hydroxide ion is strongly retarded by sodium dodecylsulfate (SDS) micelles.¹⁵⁶ Inhibition occurs because the nucleophile, hydroxide ion, is largely excluded

from the anionic SDS micellar pseudo-phase where the esters are bound. Reactivity ratios ($k_c/k_u \sim 0.01$) are also independent of ester chain length.

Table 6.3 Least squares correlations of substrate binding (pK_S) and transition state binding (pK_{TS}) with acyl chain length (n), and with each other, for the reaction of nucleophiles with *p*-nitrophenyl alkanoates in the presence CTAB micelles.^a

Nucleophile	Plot	Slope	"r"	number of points
Anion of ME	pK_S vs. n	0.43 ± 0.03	0.9924	6
	pK_{TS} vs. n	0.43 ± 0.02	0.9950	7
	pK_{TS} vs. pK_S	0.99 ± 0.01	0.9998	7
Dianion of MAA	pK_S vs. n	0.44 ± 0.01	0.9994	6
	pK_{TS} vs. n	0.43 ± 0.01	0.9990	7
	pK_{TS} vs. pK_S	0.98 ± 0.03	0.9981	7
Dianion of MPA	pK_S vs. n	0.44 ± 0.01	0.9994	6 ^b
	pK_{TS} vs. n	0.43 ± 0.01	0.9996	6
	pK_{TS} vs. pK_S	0.97 ± 0.02	0.9995	6 ^b
Dianion of CYST	pK_S vs. N	0.44 ± 0.01	0.9993	4 ^b
	pK_{TS} vs. N	0.41 ± 0.01	0.9997	4
	pK_{TS} vs. pK_S	0.94 ± 0.02	0.9994	4 ^b
Anion of GLY	pK_S vs. n	0.44 ± 0.01	0.9993	4 ^b
	pK_{TS} vs. n	0.43 ± 0.01	0.9997	4
	pK_{TS} vs. pK_S	0.97 ± 0.03	0.9992	4 ^b
Anion of TFE	pK_S vs. n	0.41 ± 0.01	0.9996	4 ^c
	pK_{TS} vs. n	0.38 ± 0.02	0.9972	4
	pK_{TS} vs. pK_S	0.92 ± 0.04	0.9980	4 ^c
Hydroxide ion ^d	pK_S vs. n	0.42 ± 0.01	0.9983	7
	pK_{TS} vs. n	0.42 ± 0.02	0.9963	7
	pK_{TS} vs. pK_S	1.00 ± 0.02	0.9994	7

^a Using the values of K_S and K_{TS} presented in Table 6.1 and 6.2. "Slope" is the slope of the least squares line, "r" is the correlation coefficient. ^b The values of K_S were taken to be the same as those found with the mercaptoacetate dianion. ^c The values of K_S were taken to be the same as those found with hydroxide ion under the same conditions.⁵⁸ ^d From previous experiments carried out in an aqueous phosphate buffer of pH 11.60 taken from ref.⁵⁸

Analysis of inhibition curves gives K_S values for binding of the esters to SDS micelles, with the slope of the plot of pK_S vs. n being 0.40 ± 0.01 ($r = 0.9986$, 5 points, (acetate to hexanoate), much like the values we have found with CTAB micelles (Table 6.3).

These slopes of about 0.4 for linear free energy (LFER) plots, such as those in Figure 6.4, are completely consistent with free energy of transfer of a methylene group from aqueous solution to a largely hydrocarbon medium.^{65,68,75} Many times over, it has been shown that free energies of transfer (water \rightarrow micelle, water \rightarrow organic medium, and water \rightarrow gas phase) for organic solutes vary linearly with solute chain length.^{65,215} Likewise, the hydrophobicity of n -alkyl derivatives varies linearly with chain length. For example, a plot of $-\log(cmc)$ against chain length ($n = 10, 12, 14, 16$) for micellization of n -alkyltrimethylammonium bromides is a straight line ($r = 0.9998$), with a slope of 0.313 ± 0.004 (See Chapter IV, Figure 4.5).¹⁷⁵ Other n -alkyl ionic surfactants show similar behaviour, with slopes actually closer to what observe here (slope ~ 0.5).³¹³

From another angle of comparison, our own research group has shown that the strength of binding of many n -alkyl derivatives to cyclodextrins, is sensitive to chain length, with slopes of pK_S vs. n falling in the range 0.3-0.6, due in part to hydrophobic effects. Interestingly, the cleavage of esters, including $pNPAlk$, by hydrolytic enzymes (lipases, chymotrypsin, trypsin, horse liver esterase)³¹⁴ also shows distinct chain length dependence, with plots of $\log(k_{obs})$ vs. n having slopes of 0.3 - 0.4. These values are consistent with acyl binding site of the enzymes being quite hydrophobic.

Thus, for $pNPAlk$ cleavage by anions in CTAB micelles, the parallelism, linearity, and LFER slopes suggest that *transition state binding* and *ester binding* (and

stabilization) are governed by the same structural feature(s) of the esters, and that they are partially or largely determined by similar hydrophobic effects.

6.3.2 Nucleophile Effects: Ion-Exchange

A key feature of current models of the effects of micelles on reactivity is the exchange of anions between the Stern layer of the cationic micelle and the bulk aqueous medium. With respect to the present results, the catalytic ratios $k_{\text{cN}}/k_{\text{N}}$ vary widely from ~1.5 to ~80 with the nucleophiles studied (Tables 6.1 and 6.2, above; Figure 6.5, below) and they presumably reflect the ability of the anionic nucleophiles to *ion exchange* with bromide counter ions in the Stern layer of the CTAB micelles. This exchange is determined by a combination of factors including the hydrophobicity, the hard/soft character, the solvation, and the overall charge of the anions. To quote Bunton and coworkers, for cationic micelles, "large, weakly hydrated polarizable anions displace hydrophilic anions."²⁴⁹ For example, bromide ions are bound more strongly than hydroxide ions. Among other things, this factor explains why added bromide ion depresses the rate of CTAB-catalyzed hydroxide ion attack on esters (and other substrates) and why high concentrations of CTAB are less catalytic than moderate ones. Also, it explains why cetyltrimethylammonium chloride (CTAC) micelles are better catalysts for hydroxide ion attack on esters than are CTAB micelles – because chloride ions are bound less strongly.

Hydroxide ion is a small, "hard" anion that is strongly solvated in water,^{315,316} and for its CTAB-catalyzed reaction with *p*-nitrophenyl esters the catalytic ratio $k_{\text{cN}}/k_{\text{N}}$ is

only 2.4 ± 0.3 , when the total bromide ion is kept at 5.0 mM.⁵⁸ This ratio is low because the heavily hydrated hydroxide ion does not compete well with bromide ion in the Stern

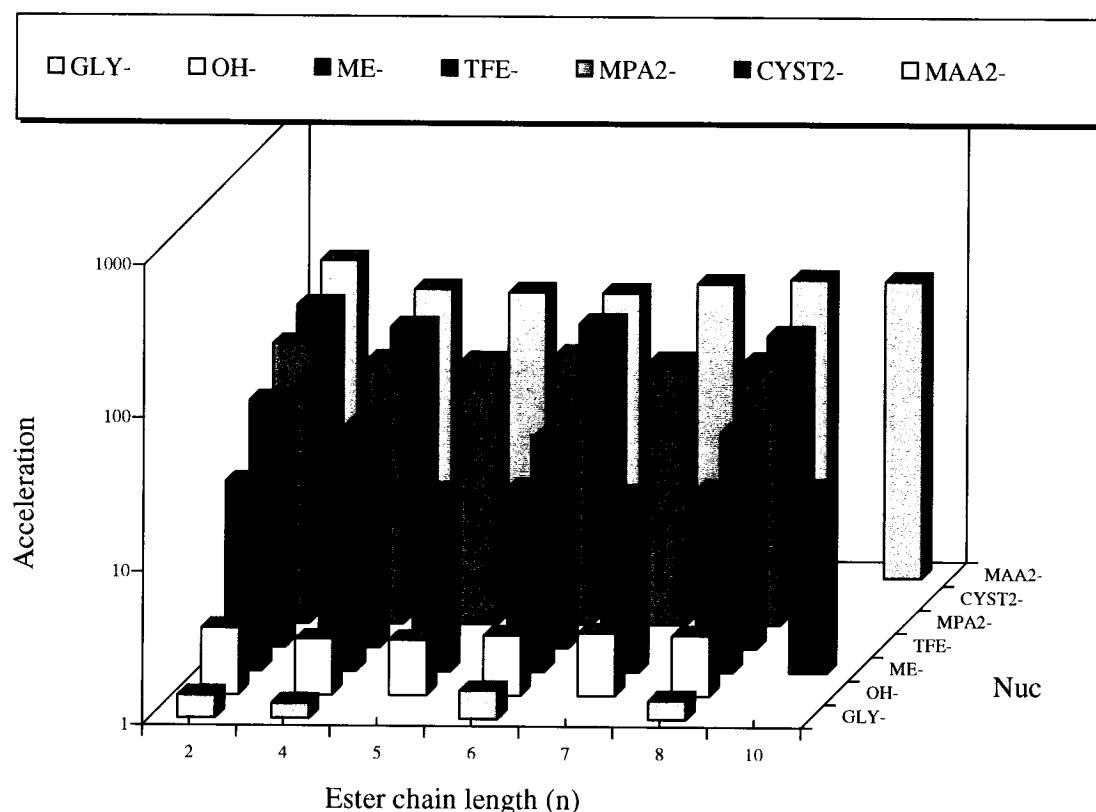


Figure 6.5 The accelerations afforded by CTAB (expressed by k_{cN}/k_N) are virtually independent of ester chain length (n) but they vary appreciably with the nucleophile.

layer. Thiolate ions, which are “softer”,³¹⁶ more polarizable, and much less strongly solvated, interact more strongly with CTAB micelles, and so they exchange much more readily with bromide ions. Consequently, CTAB catalysis of ester thiolysis is appreciably stronger. For the anion of 2-mercaptoethanol, the catalytic ratio is larger than that for hydroxide ion and remarkably constant at 15.3 ± 0.6 , for esters beyond the acetate (Table 6.1). For the mercaptoacetate dianion this ratio is larger still, at 79 ± 7 (Table 6.2), presumably because the double negative charge on the nucleophile enhances its ion exchange into the CTAB micelles. The catalytic ratios are not quite as large for the

3-mercaptopropionate dianion (53 ± 2) or the cysteine dianion (59 ± 4), perhaps because in these larger ions the doubly-negative charge is more spread-out or because they are hydrated slightly more strongly than the dianion of MAA.

In contrast to the high ratios found for the thiolate dianions, for the glycinate anion, which is an amine nucleophile, the catalytic ratio is barely greater than one, at ~ 1.4 (Table 6.2). This much lower value is presumably due to a combination of factors: the lower overall charge, the harder, nitrogen nucleophile, and stronger hydration in the bulk aqueous medium. Interestingly, the TFE anion has a much higher catalytic ratio (~ 25) than hydroxide ion (~ 2.4), even though both are oxyanions. Almost certainly, the TFE anion is appreciably more hydrophobic and *less strongly hydrated* than hydroxide ion, so that it exchanges into CTAB micelles more readily.

The third order rate constants $k_3 = k_{cN}/K_S$ (eq. [6.11]) increase substantially with ester chain length: (i) 1300-fold for the anion of ME and 1800 for the dianion of MAA (going from acetate to decanoate ester), (ii) 200-fold for the dianions of MPA and CYST, and (iii) 100-fold for the anions for Gly and TFE (going from acetate to octanoate). Previously, k_2 for hydroxide ion cleavage of the same esters was found to increase 130 fold (from acetate-octanoate). These increases occur not because k_{cN} increases with chain length, but because K_S decreases considerably (and systematically) with chain length. It is worth noting that the substrate dissociation constants (K_S) for each ester were more or less the same for all the anionic nucleophiles, and so ester binding is essentially independent of the nucleophile exchanging into the micellar pseudo-phase, at the concentrations used. Since the magnitude of k_{cN} is greatly influenced by ion-exchange,

the differences in the overall rate constants k_3 not only reflect differences in ester binding but they also reflect difference in the ion-exchange of the nucleophiles into the micelles.

6.3.3 Transition State Binding

Kirby⁵³ has proposed that the “recognition” of transition states (TSs) by enzymes involves “passive binding” and “dynamic binding”. By his definition, *passive binding* refers to ordinary “molecular recognition” of the TS which usually involves non-covalent forces, such as those entailed in normal host-guest complexation. In contrast, *dynamic binding* refers to interactions between the catalyst and the TS at the reaction centre. Dynamic interactions are a major contribution to catalytic efficiency, and they are the most obvious difference between the binding of the substrate and that of the TS. These interactions involve partially formed or broken covalent bonds, and they change substantially as a reaction proceeds from reactants to product.

It is not always obvious where TS binding starts and finishes, and there may be no clear-cut distinction between *passive* and *dynamic* binding of the TS. Therefore, the division between the two types of binding can be simplistic and artificial, especially for catalysts as complex as enzymes and catalytic antibodies. Nevertheless, Kirby’s approach seems to provide a useful framework for the interpretation of our studies.

Based on our discussion of the results of the thiolysis⁵⁹ (and hydrolysis⁵⁸) of *p*NPAlk esters in CTAB micelles, and Kirby’s approach, we recognize two types of transition state binding:

- (i) A *passive component* of TS binding is *similar* to ester acyl chain binding and it is independent of the nucleophile; it involves *hydrophobic interaction* of the *TS acyl chain*

with the *hydrocarbon core* of CTAB micelle (Figure 6.6). This conclusion is supported by the work of Buurma *et al.*,²¹⁶ who probed the nature of the Stern region of micelles (cationic, anionic and neutral) using the kinetics of two pH-independent hydrolysis reactions, and who concluded "... that the stabilisation by the hydrophobic parts of the micelle is similar for the reactant state and for the activated complex."

(ii) A *dynamic component*⁵³ of TS binding is primarily associated with interactions accompanying *acyl transfer* in the *Stern layer* of CTAB. The *delocalized charge* developed in the TS will be the same for a given nucleophile, rendering the dynamic component constant for each anion. However, this dynamic component varies with the anions since the rate constant for nucleophilic attack on the micelle-bound ester is greatly influenced by the extent of *ion exchange* of the nucleophiles into the micelles. These binding interactions are illustrated below in Figure 6.6.

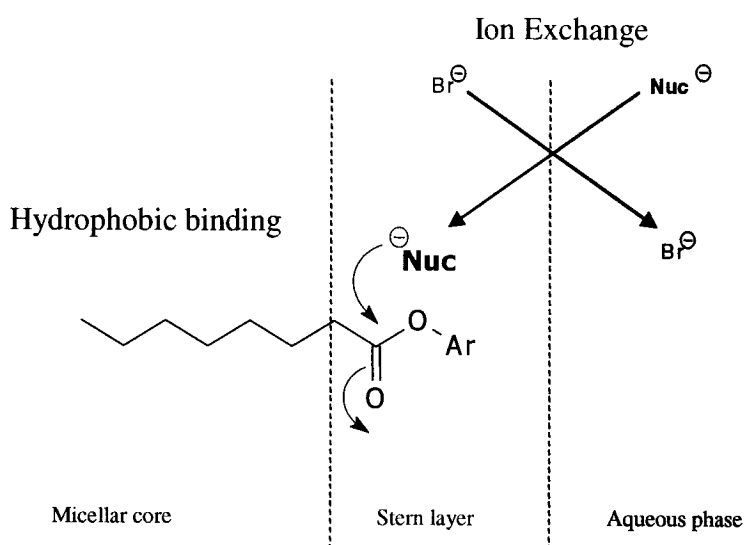


Figure 6.6 Modes of TS binding for thiolysis of *p*NPAalk esters in CTAB micelles and the interactions with CTAB binding domains.

6.4 CONCLUSIONS

CTAB micelles *catalyze* the cleavage of *p*-nitrophenyl alkanoate by *all* anionic nucleophiles studied, especially thiolate ions. Unlike what was believed previously, the magnitude of this catalysis is *independent* of the ester chain length, and the “catalytic ratios” reflect the efficiency of ion-exchange of the anionic nucleophiles with bromide ion in the Stern region of CTAB micelles. The nearly constant ratios, k_{cN}/k_N , for each nucleophile are quite understandable if they are determined almost solely by the accessibility of the nucleophile to the micelle-bound ester. Nonetheless, the observed rate constants (k_{obs}) in the presence of CTAB micelles do appear to increase with ester chain length (Fig. 6.2), but this is due to the increase in the strength of ester binding to the micelles (as measured by the K_S values), and not to an increase in the catalysis afforded to the reaction by the micelles.

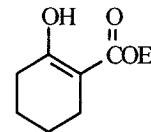
As observed previously,^{58,305} the rate of ester cleavage *versus* the concentration of micellized surfactant ($[CTAB - cmc]$) showed *saturation* behaviour at constant ionic atmosphere (including constant bromide ion, buffer concentration). Under these conditions, and at a “constant” nucleophilic ion concentration, the kinetic model which was used to estimate ester binding to CTAB micelles from the saturation plots is simpler than the pseudo-phase ion exchange model,²⁴⁶ and it does not depend on any arbitrary constants (see Chapter IV). We found that the strength of *p*-NPAlk binding to CTAB micelles, as expressed by pK_S , increases linearly with acyl chain length, but it hardly varies with the anionic nucleophile.

In a similar way, for CTAB-catalyzed cleavage of *p*-NPAlk esters by anionic nucleophiles, transition state binding (pK_{TS}) varies with acyl chain length and closely

parallels ester binding to the micelles (Figure 6.4 and Table 6.3). This behaviour suggests that the passive TS binding component is basically the *same* as substrate binding, and both are more or less totally hydrophobic in origin, since the slopes of the plots of pK_{TS} vs. n , and pK_S vs. n are ~ 0.4 , irrespective of the ionic nucleophile used. The dynamic TS binding component, however, is associated with nucleophilic attack on the micelle-bound ester and it is greatly influenced by exchange of the nucleophile into the CTAB micelles. Thiolate ions show significant catalysis because they exchange readily with bromide ion in the Stern layer of CTAB micelles.

Catalysis of thiolate attack by cationic micelles has been observed before.^{267,268,308-310,317} Moreover, spectral measurements have shown that there are very strong interactions between thiophenoxide ions and CTAB micelles.³¹⁸ Correspondingly, CTAB micelles catalyze the reaction of thiophenoxide ion with *p*-nitrophenyl acetate by 50-fold³⁰⁹ and its reaction with 2,4-dinitrofluorobenzene even more so.^{267,268,309} Obviously in this latter case there are additional factors beside ion exchange, contributing to the dynamic component of transition state stabilization. Micelles of the thiol functionalised surfactant, $n\text{-C}_{16}\text{H}_{33}\text{N}^+(\text{CH}_3)_2\text{CH}_2\text{CH}_2\text{SH Cl}^-$, have been reported to be a good micellar esterolytic agent when compared to other micelles.¹⁸² Indeed, these functional micelles cleave pNPA and pNPH with second-order catalytic rate constants which are at least 100-fold greater than the ester cleavage by anion of mercaptoethanol or even by CTAB + ME (Tables 6.1). In contrast to our results however, the rate constant in the presence of these functional micelles, greatly depended on the ester chain length, and are decidedly higher for the longer ester.

After our article on this present work was published,⁵⁹ Iglesias²²⁹ showed that for the hydrolysis and nitrosation of the enol-ester (right), the binding of that substrate to a number of ionic micelles (including CTAB and SDS) is insensitive to both the counterion of the micelles and the electrolyte in the water phase. This is similar to our results, where ester binding of the acyl chain to the CTAB micellar core is essentially independent of the anionic nucleophile.



6.5 EXPERIMENTAL

6.5.1 Materials

The *p*-nitrophenyl esters were purchased from Sigma Chemical Company, except for the heptanoate which was synthesized as previously.^{54,55} Cetyltrimethylammonium bromide (hexadecyltrimethylammonium bromide, CTAB) was obtained from ICN Biochemicals and purified by extraction with diethyl ether in a Soxhlet apparatus for 4 hours to remove any residual amines,³¹⁹ followed by drying overnight. The other chemicals were the best grades available from the Aldrich Chemical Company, except for standard NaOH solutions which were obtained from A & C Chemicals (Montreal).

6.5.2 Kinetic Apparatus and Solutions

The kinetics of the ester cleavage were followed by monitoring the pseudo-first order appearance of the *p*-nitrophenolate ion at 405 nm, using an Applied Photophysics Ltd. SX17MV Stopped-flow Spectrophotometer, with the cell temperature kept at 25.0 ± 0.1 °C. From 5 to 10 absorbance traces were acquired and computer averaged before estimation of k_{obs} by non-linear least squares fitting of an exponential growth curve.

Small aliquots of stock ester solutions (0.1 M in spectral grade acetonitrile) were added to solutions of NaBr + requisite amount of CTAB in distilled water to give ester solutions of twice the desired final concentrations. The ester + CTAB solutions were sonicated for 10-20 minutes to facilitate complete solubilization of the ester and dispersal of the surfactant. The dilute substrate solutions were mixed 1:1 in the stopped-flow apparatus with a solution containing carbonate buffer + Nuc, brought to pH 10.60. The final reacting solutions contained 0.10 M carbonate buffer, CTAB (0 to 5.00 mM), NaBr (5.00 mM - [CTAB]₀), and ester concentrations as follows: acetate to pentanoate, 50 μ M; hexanoate, 25 μ M; heptanoate, 5 μ M; octanoate, 2.5 μ M; decanoate, 1.5 μ M. Note that generally [ester] \ll [CTAB]₀, so the micelles would not be significantly affected by the presence of the esters. Experiments with TFE were carried out with a 0.20 M phosphate buffer, at pH 11.60, instead of the carbonate buffer.

Recently it has been shown that catalysis of benzoate esters by phosphate buffers (where H_2PO_4^- or HPO_4^{2-} are the catalytically active species) can be general base or nucleophilic.³²⁰ More recently Bunton, Nome and coworkers demonstrated the esterolysis of 2,4-dinitrophenyl acetate in the presence of micellar benzyltrimethylammonium *n*-decylphosphate shows nucleophilic catalyses by phosphate buffers.³²¹ In our work, by analysis of the ratios $k_{\text{CN}}/k_{\text{N}}$, we are concentrating on the catalysis due to the micelles and how it varies with nucleophile and ester; any buffer effects should be relatively constant.

6.5.3 Curve Fitting and the *cmc* Estimate

Non-linear fitting of equation [6.7] was carried out with GraphPad Prism software. When using equation [6.5] and [6.7] in data analysis, one has to decide how to handle the critical micelle concentration (*cmc*). In Fedortchenko's previous work⁵⁸, the

value of the *cmc* was neglected since its influence on the estimated kinetic parameters was minimal. For CTAB, the *cmc* is 0.92 mM at zero ionic strength, but it is appreciably lower at high salt concentrations¹⁷⁵ (see Section 4.2.3) and the lowering effect of less hydrophilic anions like thiolate ions is greater still. For example, the addition of only 40 μ M thiophenolate ion, in a 0.010 M borate buffer at pH 10, lowers the *cmc* of CTAB to 0.08 mM.³²² In the present work, taking $[\text{Surf}] = ([\text{Surf}]_0 - \text{cmc})$, and treating *cmc* as a fitting parameter in eq. [6.7] for the data obtained for each of the seven esters reacting with 20.0 mM ME in 0.10 M carbonate buffer, gave values of *cmc* that were close to an average of 0.05 mM. Accordingly, for consistency we have taken the *cmc* to be equal to this value throughout.

According to the literature, the pK_a s of the thiols at zero ionic strength are: cysteine, 8.39;³²³ 2-mercaptoethanol, 9.72;³²⁴ mercaptoacetic acid, 10.56;³²³ 3-mercapto-propionic acid, 10.84,³²⁴ but they are lower at high ionic strength. For example, at $\mu = 1.0$ M, the pK_a of ME is 9.61,³²⁵ and at $\mu = 0.2$ M, the second pK_a of MAA drops from 10.56 to 9.84.³²³ Thus, at the working pH of 10.60, in the 0.10 M carbonate buffer, the thiols will exist to a considerable extent as their reactive thiolate anions. The exact fractions of the anions are not important to the discussion above because they are the same for all the esters in the series, and they cancel out in the ratios $k_{\text{cN}}/k_{\text{N}}$ and in $K_{\text{TS}} = k_{\text{N}}K_{\text{S}}/k_{\text{cN}}$. The relevant pK_a of glycine is 9.78,³²⁶ and that of TFE is 12.4.^{325, 327}

A sample ExcelTM worksheet for the analysis of kinetic data (Appendix B) for ester (eg. *p*-nitrophenyl butanoate) cleavage by thiolate anions (eg. 2-mercaptoethanol) in the presence and absence of CTAB, is shown in Scheme 6.2 (overleaf).

EXPT: Jen-44
 DATE: 18-Sep-99
 ESTER: pNPBut
 CAT: CTAB
 NUC: 2-ME

Analysis for Non Binding Nucleophiles

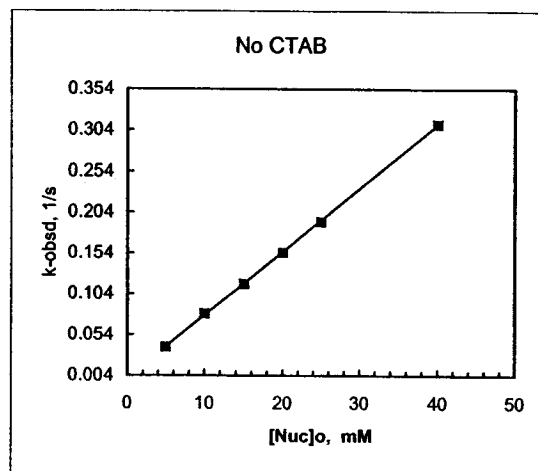
$K_s = 2.34 \text{ mM}$

$[CTAB] = 4.95 \text{ mM}$

No CTAB Jen-44		
[Nuc]o (mM)	k(obsd) (s ⁻¹)	k(calcd) (s ⁻¹)
5.00	0.0390	0.0389
10.0	0.0798	0.0778
15.0	0.1163	0.1166
20.0	0.1547	0.1555
25.0	0.1923	0.1944
40.0	0.3112	0.3110
50.0	0.3896	0.3887

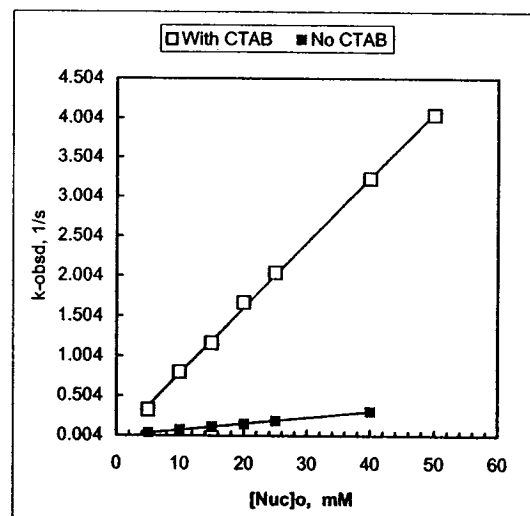
Slope = $7.77\text{E-}03 \pm 3.54\text{E-}05$
 Intercept = 0.00002 ± 0.00099
 $R^2 = 0.99990$
 $R = 0.99995$

$k_N = 7.77 \pm 0.04 \text{ M}^{-1} \text{ s}^{-1}$



With CTAB Jen-45		
[Nuc]o (mM)	k(obsd) (s ⁻¹)	k(calcd) (s ⁻¹)
5.00	0.326	0.37666
10.0	0.803	0.78629
15.0	1.169	1.19592
20.0	1.672	1.60555
25.0	2.042	2.01518
40.0	3.233	3.24407
50.0	4.042	4.06333

Slope = $(k_N K_s + k_{CN} [CTAB]) / (K_s + [CTAB])$
 $= 8.19\text{E-}02 \pm 1.08\text{E-}03$
 Intercept = -0.0330 ± 0.0303
 $R^2 = 0.99913$
 $R = 0.99956$



$k_{CN} = 117 \pm 2 \text{ M}^{-1} \text{ s}^{-1}$

$K_{TS} = 0.156 \text{ mM}$

$k_{CN}/k_N = 15.0$

$pK_{TS} = 3.81$

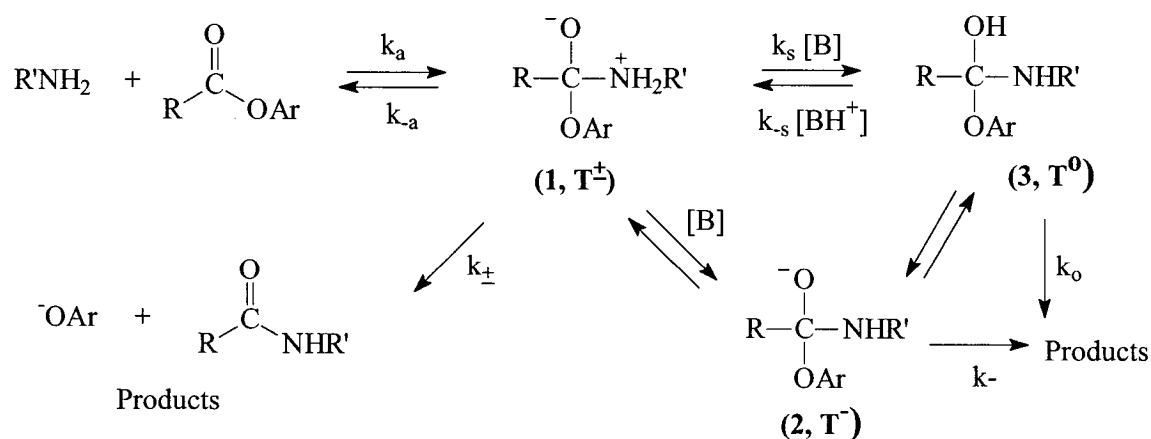
Scheme 6.2 Worksheet for the analysis of ester cleavage by nucleophiles (thiolate anions), with and without CTAB.

CHAPTER VII. CATALYSIS OF THE AMINOLYSIS OF *p*-NITROPHENYL ALKANOATES BY CTAB MICELLES

7.1 INTRODUCTION

Prompted by our findings on ester hydrolysis⁵⁸ and thiolysis,⁵⁹ we have studied the effects of CTAB micelles on the kinetics of aminolysis of *p*-nitrophenyl alkanoates. We were interested to see how the behaviour observed for anionic nucleophiles is affected by changing to neutral nucleophiles, and ones with a range of hydrophobicity. Accordingly, we have studied a series of primary aliphatic amines, as well as looking at the effect of structural variation in the alkanoate esters.

The overall mechanism of ester aminolysis,³²⁸⁻³³¹ which is suited for our basic reaction conditions, is as depicted in Scheme 7.1. Amine attack on the ester is reversible and a tetrahedral intermediate is formed. Through a number of proton transfer steps, the tetrahedral intermediate can exist in many forms, zwitterionic (**1**, T^{\pm}), anionic (**2**, T^{-}), or neutral (**3**, T^0).^{331,332} The final step in the reaction is the elimination of the leaving aryloxide group from the tetrahedral intermediate(s) to produce an alkylamide.



Scheme 7.1 Aminolysis of *p*NPAIk esters

For a good leaving group, such as *p*-nitrophenoxide ion, the first addition step (k_a) is normally rate limiting. The Brønsted slopes of the logarithmic plots of the rate constant for the aminolysis of *p*-nitrophenyl acetate against the pK_a of the protonated amine nucleophiles are linear and show β_{nuc} values close to 0.8, and the slope is similar for other esters.³³⁰ This suggests that there is no change in mechanism or in rate-determining step for the reaction of phenyl acetate (with pK of leaving group = 10) with amines with protonation of pK_a s of 3.5 - 11. Values of β_{lg} for varying the leaving groups are close to 1.0 for most ester aminolysis reactions, indicating a large change in the charge on the leaving group in the transition state. Such results do not discriminate unequivocally between a concerted mechanism or one involving a metastable tetrahedral intermediate. The similarity in behaviour of primary, secondary and tertiary amines was argued to mean that proton transfers are not required in these reactions and that amine attack and leaving-group expulsion can occur through transition state(s) of zero net charge.³³⁰

Where reversible proton transfer steps occur, they are normally fast relative to other steps, and they are expected to be faster still in cationic micelles.³³³ For example, Menger and Lynn³³⁴ found that water-catalyzed N-H exchange of $R'NH(CH_3)_2^+$ is about 30-fold greater for $R' = \text{dodecyl}$ in its own cationic micelles than for the case where $R' = \text{hexyl}$, which does not form a micelle. Since the tetrahedral intermediates are in rapid equilibrium, the barriers between them are small, and their transition states are not very different in structure. Then, as a corollary to Hammond's Postulate,³³⁵ factors which stabilize the intermediates will tend also to stabilize the transition states adjacent to them, and so lower the overall activation barrier. In CTAB-mediated aminolysis, we envisage that *hydrophobic interactions* of the alkyl groups R and R' (Scheme 7.1) with the

micellar core could play a role in stabilizing the initial states(s), intermediate(s) and/or their transition state(s). Also, it is possible that the cationic micelles stabilize the anionic intermediates and their associated transition states for electrostatic reasons. If the stabilization were to be greater for the overall transition state than for the initial state then catalysis should result.

After our studies were commenced, we became aware of recent Russian work describing the reaction of a number of *n*-alkylamines with *p*-nitrophenyl acetate and with *p*-nitrophenyl octanoate in cetylpyridinium bromide (CPB) micelles,^{336,337} and for the same reactions in “oil-water” microemulsions.³³⁸ We will mention this work again later in the discussion. As a matter of fact, studies on ester aminolysis and micellar effects date back to the 1970s,^{329,339} and all authors reported catalysis arising from hydrophobic interactions between the long hydrocarbon chains of the ester and the alkylamine (or alkylimidazole) micelles. However, the validity of the comparisons of rate constants in some of those early studies was challenged by Guthrie³¹² on grounds that the initial concentration of the long esters (octanoate, decanoate, and dodecanoate) was high enough for the esters to have been aggregated. So, it was suggested that the apparently very large rate enhancements in aminolysis are at least partly due to the unusually low rate constants for ester hydrolysis. To our knowledge, none of the previous research on aminolysis attempted to probe initial state or transition state binding to CTAB micelles.

7.2 RESULTS

Berzin and co-workers²⁸⁵ were the first to quantify the kinetics of two non-ionic reactants according to the pseudo-phase model (Chapter IV). For our aminolysis studies

we have used the same model, experimental conditions, and data analysis as was used for the thiolysis work (Chapter VI).

Kinetic experiments were carried out for the aminolysis of *p*-nitrophenyl acetate (pNPA) and *p*-nitrophenyl hexanoate (pNPH) by amines: *n*-alkylamines (*n*-propyl to *n*-octyl), two branched (*iso*-butyl and *iso*-pentyl) and two cyclic amines (cyclopentyl and cyclohexyl). Again, the reaction was monitored by the first order rate of production of the *p*-nitrophenoxide anion (Scheme 7.1). The bulk medium was aqueous carbonate buffer of pH 10.6, with a constant total bromide ion concentration of 5.00 mM, as used for the thiolysis studies.⁵⁹ At this pH, the background hydrolysis is not very important, and the constant bromide ion minimizes complications due to ion exchange into the micelles.^{181,246,247-249, 297,305}

7.2.1 Ester.CTAB Binding

From our previous studies^{58,59} the binding of the alkanoate esters to CTAB micelles is well-established, and it manifests itself in aminolysis, also. Figure 7.1 shows examples where the variation of k_{obs} with $[\text{CTAB}]_0$, at constant [amine], exhibit *catalysis* for longer chain amines and *retardation* for shorter amines. The curvature reflects the strength of the ester binding, and from the saturation kinetic curves {Ester.CTAB} dissociation constants (K_S) for pNPA and pNPH were estimated, as before (Chapter VI, eq. [6.7]). The values of K_S from this work are shown in Table 7.1.

The K_S values for the acetate and hexanoate esters are very close to those found in the previous studies of hydrolysis⁵⁸ (Table 5.3) and thiolysis⁵⁹ (Table 6.1 and Table 6.2), and to ones found by other research laboratories,^{62,340,341} which means that the initial state

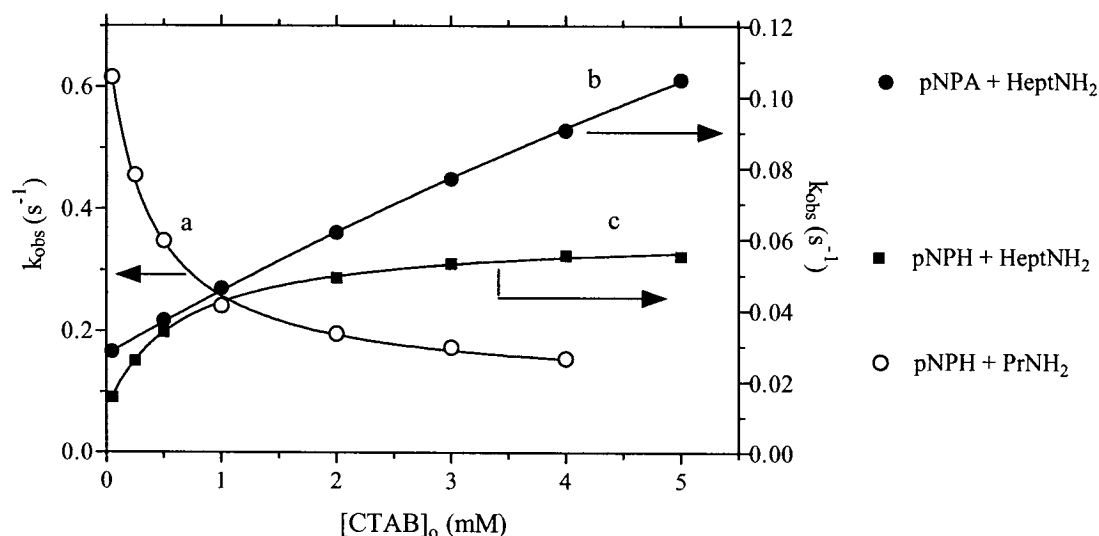


Figure 7.1 Variation of k_{obs} with $[\text{CTAB}]_o$ for reaction of: (a) pNPH + *n*-heptylamine; (b) pNPA + *n*-heptylamine; (c) pNPH + *n*-propylamine. Data for the reaction of pNPA with *n*-propylamine was also obtained but k_{obs} hardly changed with $[\text{CTAB}]$ and the plot did not analyze as well as those shown.

Table 7.1 Some CTAB - *p*-nitrophenyl alkanoate complex dissociation constants K_S .

Ester	Nucleophile	K_S (mM)	Reference
Acetate ^a	5mM <i>n</i> -heptylamine	22.3 ± 3.1	This work
Acetate ^{b,c}	0.1 M imidazole	19.6 ± 3.7	Williams <i>et al.</i> ⁶²
Acetate ^d	Hydroxide ion	18 ± 0.68	Williams <i>et al.</i> ⁶²
Acetate ^e	Myristoylhistidine	33.2	Gitler ³⁴⁰
Hexanoate ^a	250 mM <i>n</i> -propylamine	0.397 ± 0.027	This work
Hexanoate ^a	5 mM <i>n</i> -heptylamine	0.684 ± 0.33	This work
Hexanoate ^c	0.1 M imidazole	0.303 ± 0.007	Williams <i>et al.</i> ⁶²
Hexanoate ^e	Myristoylhistidine	0.500	Gitler ³⁴⁰

^a Our experiments work was carried under out with bromide ion concentration maintained at 5.0 mM with NaBr, 0.01 M carbonate buffer adjusted to pH =10.60.

^b Williams' and coworkers⁶² have bromide ion concentration maintained at 5.0 mM with KBr.

^c Imidazole buffered at pH 7.04 ± 0.02 .

^d pH 10.06 maintained with 0.025 M borate buffer.

^e Experiments were done in a 0.05 M TRIS buffer at pH 7.2.³⁴⁰

binding of the esters to the CTAB micelles is not noticeably affected by the nucleophile. Also, it was shown that that minor variations in K_S do not greatly affect the ratios k_{cN}/k_N or alter the trends in them. Consequently, where K_S values were needed later for data analysis, we took those obtained from the studies of CTAB-catalyzed thiolysis by mercaptoacetate dianion in the same medium (Chapter VI).

7.2.2 Aminolysis of the Unbound Esters

The aminolysis of *p*NPA (and of *p*NPH) in the absence of CTAB, shows a strictly linear dependence of k_{obs} on $[amine]_o$ (e.g. Figure 7.2), the second order rate constants (k_N) for the aminolysis of the free ester are estimated as the slopes of equation [7.1]:

$$k_{obs} = k_u + k_N [amine]_o \quad [7.1]$$

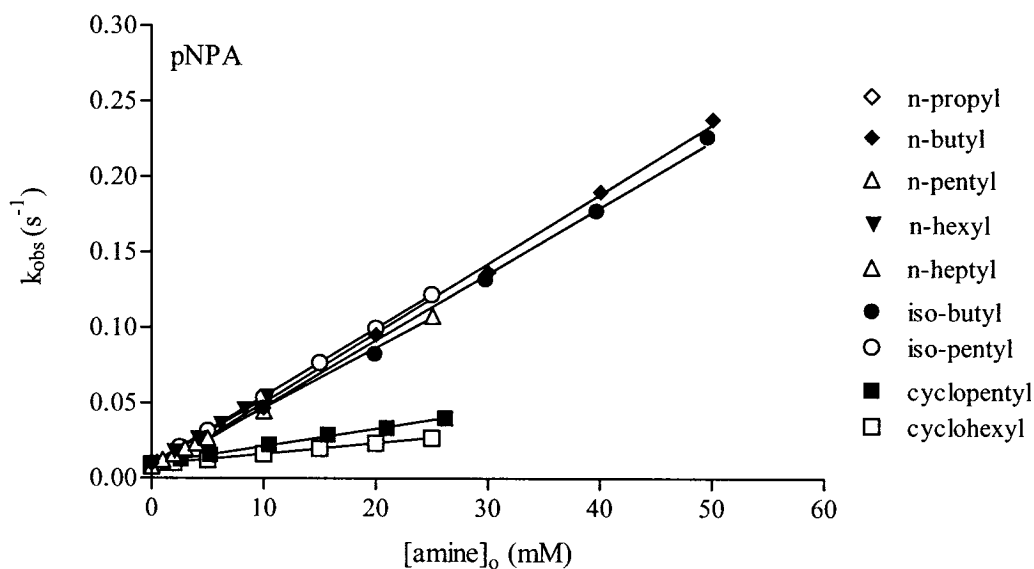


Figure 7.2 Variation of k_{obs} with $[amine]_o$ for aminolysis of *p*NPA in the absence of CTAB. A comparable plot was observed with *p*NPH.

Table 7.2 Second order rate constants k_N for aminolysis of *p*-nitrophenyl acetate (pNPA) and *p*-nitrophenyl hexanoate (pNPH).^a

Amine	[amine] ₀ (mM)	k_N (M ⁻¹ s ⁻¹)	
		pNPA	pNPH
<i>n</i> -propyl	0 – 100	4.86 ± 0.07	2.14 ± 0.09
<i>n</i> -butyl	0 – 50 (100)	4.60 ± 0.11	2.20 ± 0.07
<i>n</i> -pentyl	0 – 25	3.99 ± 0.09	1.97 ± 0.05
<i>n</i> -hexyl	0 – 10	4.38 ± 0.05	2.26 ± 0.05
<i>n</i> -heptyl	0 – 5	3.71 ± 0.04	1.83 ± 0.17
<i>n</i> -octyl	0 – 2	3.71 ^b	1.83 ^b
<i>iso</i> -butyl	0 – 50	4.40 ± 0.14	2.27 ± 0.07
<i>iso</i> -pentyl	0 – 25	4.50 ± 0.02	2.28 ± 0.29
cyclopentyl	0 – 25	1.17 ± 0.03	0.545 ± 0.015
cyclohexyl	0 – 25	0.728 ± 0.01	0.273 ± 0.13

^a Rate constants obtained at 25 °C, in an 0.10 M aqueous carbonate buffer of pH 10.60, with [NaBr] = 5.0 mM. The range of amine concentrations are those used to find k_N as well as k_{cN} .

^b Low solubility of *n*-octylamine in aqueous buffer renders absorbance plots which are difficult to analyze, thus k_N was assumed to be the same as for *n*-heptylamine.

Table 7.2 contains rate constants k_N for reaction of the free esters (pNPA and pNPH) with the various amines. These values are smaller than those reported by other workers in our lab, even after correcting for the difference in pH,¹³¹ and differences are probably due to different buffer medium and different ionic strength. As found earlier,¹³¹ the k_N values for each particular ester do not vary appreciably with *n*-alkyl and *iso*-alkyl amines, which is reasonable since the steric (and electronic) parameters of the alkyl substituents hardly vary.³⁴² By contrast, for the cyclic amines, the reactivity is much lower, presumably due to their lower basicity and their steric bulk being close to the amino group. As observed with other nucleophiles (Chapter VI), the k_N values for aminolysis of pNPH are roughly half those for pNPA for normal steric reasons.

7.2.3 Aminolysis of the Ester.CTAB Complex

In the presence of a fixed concentration of the surfactant ($[\text{CTAB}] = 5.0 \text{ mM}$), the variation of k_{obs} with $[\text{amine}]_0$ also comes out to be linear, over the concentration of amine used. Figure 7.3 shows data for reaction of pNPH with several amines; analogous data was observed for reaction with pNPA (see Appendix C). This linearity was somewhat surprising since curved plots would have indicated strong amine binding to CTAB.⁵⁷ The lack of downward curvature at high $[\text{amine}]$, is evidence against the onset of saturation of the micelles with amines, at least for the range of $[\text{amine}]$ used in the experiments. Moreover, the linear behaviour allows a relatively easy analysis of the variation of k_{obs} with $[\text{CTAB}]$ and $[\text{amine}]$ with the same model used for studies of thiolysis catalyzed by CTAB micelles (Chapter VI).

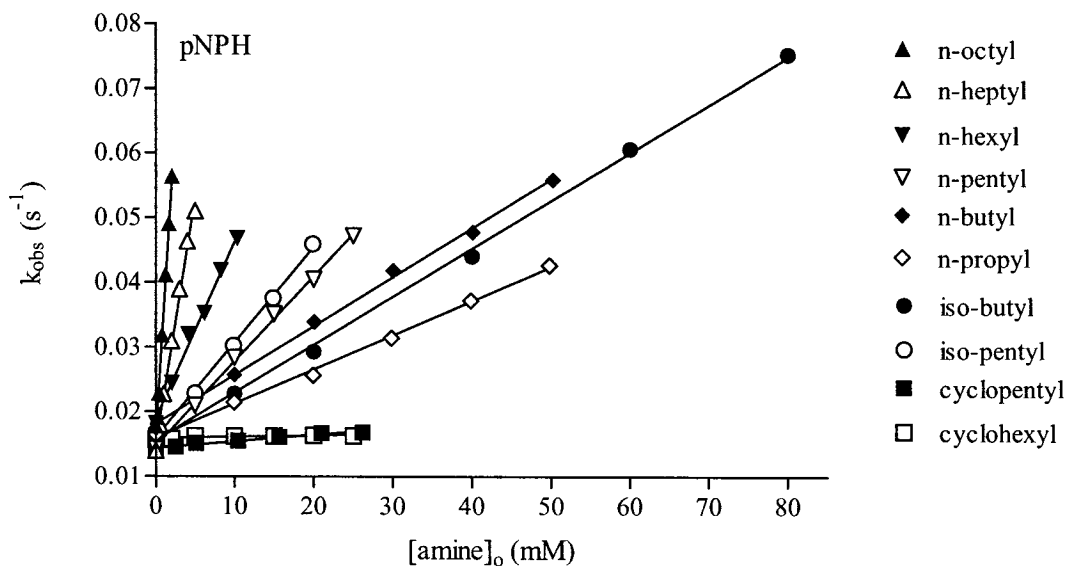


Figure 7.3 The variation of k_{obs} with $[\text{amine}]_0$ for aminolysis of pNPH in the presence of 5.0 mM CTAB. A comparable plot was observed with pNPA.

The second order rate constants of amine attack on the ester-CTAB complex, k_{cN} , are estimated from the slopes of Figure 7.3, which are equal to $(k_N K_S + k_{cN} [\text{Surf}]) / (K_S + [\text{Surf}])$, knowing k_N and K_S from the other experiments, as in Chapter VI. These k_{cN} values are collected in Table 7.3, along with other parameters. Note that the slopes in Figure 7.3 become steeper with increasing amine chain length since k_{cN} increases (Table 7.3), as $[\text{Surf}]$ is constant, K_S is constant for each ester, and k_N is essentially the same for all non-cyclic amines.

7.2.4 Reactivity Ratio k_{cN}/k_N

The reactivity ratio k_{cN}/k_N is a measure of the relative rates of reaction of the CTAB-bound and free forms of the ester with the amine, assuming that the micelle-mediated reaction takes place between the bound ester and free amine. For *p*NPA, the ratios k_{cN}/k_N increase from 0.25 to 71 (*n*-propylamine to *n*-octylamine), and from 0.19 to 12 for *p*NPH (for the same amines) (Table 7.3, below), spanning the range from 5-fold retardation to appreciable (70-fold) catalysis.

Retardation (Figure 7.4 a), $k_{cN}/k_N < 1$, is exhibited by short amines (*n*-propyl and *n*-butyl), and for each amine the value of k_{cN}/k_N is slightly lower for *p*NPH than for *p*NPA. Catalysis (Figure 7.4 b), $k_{cN}/k_N > 1$, was found for both esters reacting with amines longer than *n*-pentylamine, but with the longer amines there is larger difference between the values of k_{cN}/k_N for *p*NPA and *p*NPH. For example, with *n*-octylamine $k_{cN}/k_N = 71.2$ for *p*NPA whereas it is 11.5 for *p*NPH. We therefore questioned what might be causing this difference in the magnitude of the reactivity ratio between the two esters especially for the longer chain amines, as will be discussed later on.

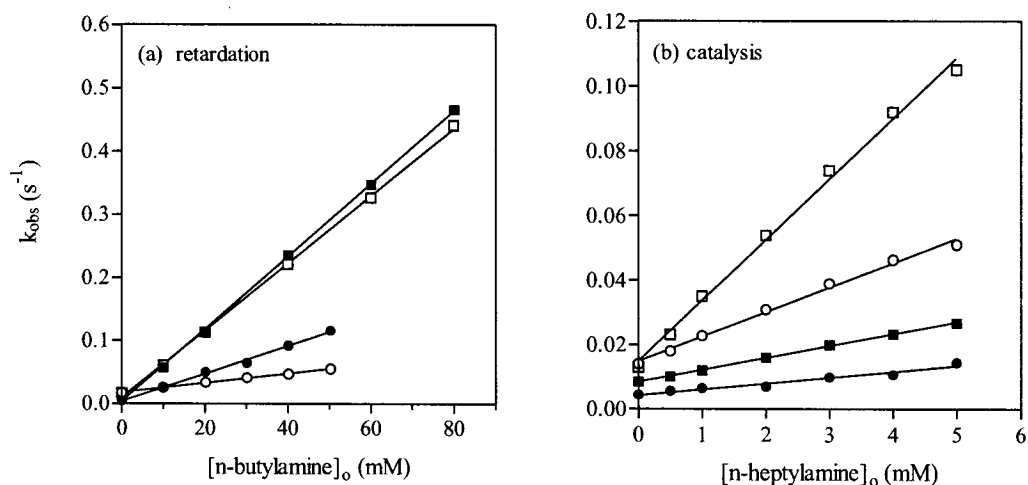


Figure 7.4 a) Retardation of the aminolysis of pNPA (■, □) and pNPH (●, ○) by *n*-butylamine. b) Catalysis of the aminolysis of pNPA and pNPH by *n*-heptylamine. Solid symbols are for the reactions in the absence of CTAB and open symbols are for those in the presence of 5.0 mM CTAB.

7.2.5 Transition State Dissociation Constant K_{TS}

A cursory view of the K_{TS} ($= K_{\text{S}}k_{\text{N}}/k_{\text{cN}}$) results clearly shows that the transition state dissociation constant varies with the amine structure, Table 7.3. The strength of transition state binding, reflected in the $\text{p}K_{\text{TS}} = -\log(K_{\text{TS}})$, *increases* with amine chain length and there are differences for pNPA and pNPH. As will be discussed latter, from the homologous series of amines we can probe transition state binding of the amine to CTAB, and in order shed light on ester binding a necessary extension is to investigate the aminolysis of a series of esters.

Table 7.3 Constants for the aminolysis of *p*-nitrophenyl acetate (pNPA) and *p*-nitrophenyl hexanoate (pNPH) in the presence of CTAB.^a

Amine	k_{cN} $\text{M}^{-1} \text{s}^{-1}$	$k_{\text{cN}}/k_{\text{N}}$	K_{TS} mM	k_3 $\text{M}^{-2} \text{s}^{-1}$
pNPA + CTAB ($K_{\text{S}} = 24.6 \text{ mM}$) ^b				
<i>n</i> -propyl	1.20 ± 0.84	0.247	100	48.8
<i>n</i> -butyl	3.85 ± 0.41	0.837	29.4	157
<i>n</i> -pentyl	10.8 ± 0.3	2.71	9.09	439
<i>n</i> -hexyl	43.4 ± 1.0	9.91	2.48	1764
<i>n</i> -heptyl	93.8 ± 3.5	25.3	0.973	3813
<i>n</i> -octyl	264 ± 5	71.2	0.346	10732
<i>iso</i> -butyl	3.55 ± 0.93	0.807	30.5	144
<i>iso</i> -pentyl	11.8 ± 0.3	2.62	9.38	480
cyclopentyl	1.17 ± 0.03	1.04	27.7	48.0
cyclohexyl	10.4 ± 0.8	14.3	1.72	423
pNPH + CTAB ($K_{\text{S}} = 0.374 \text{ mM}$) ^b				
<i>n</i> -propyl	0.407 ± 0.014	0.190	1.97	1088
<i>n</i> -butyl	0.649 ± 0.020	0.295	1.27	1735
<i>n</i> -pentyl	1.26 ± 0.03	0.640	0.585	3369
<i>n</i> -hexyl	2.77 ± 0.13	1.23	0.305	7406
<i>n</i> -heptyl	8.64 ± 0.16	4.72	0.0792	23102
<i>n</i> -octyl	21.0 ± 0.7	11.5	0.0326	56150
<i>iso</i> -butyl	0.627 ± 0.017	0.276	1.35	1676
<i>iso</i> -pentyl	1.42 ± 0.05	0.623	0.601	3797
cyclopentyl	0.0855 ± 0.0077	0.157	2.38	229
cyclohexyl ^c	—	—	—	—

^a At 25 °C, in an aqueous carbonate buffer of pH 10.60, with $[\text{Br}^-]_{\text{total}} = 5.0 \text{ mM}$.

^b The values of K_{S} are taken from our earlier work (Table 6.2).⁵⁹

^c Experiments in the presence of CTAB were not successful because the variations of k_{obs} with [amine] were too shallow to be conducive to yield reliable or reproducible values for k_{cN} .

7.2.6 Third Order Reactivity (k_3)

By looking at the rate constants for the overall third order process, k_3 (Chapter VI, eq. [6.11]), an unbiased view of CTAB-mediated aminolysis can be obtained. Here, the third order rate is a measure of the Gibbs energy of the transition state composed of {amine + ester + CTAB} relative to the separate reactants in the initial state. With anionic nucleophiles this parameter was not that useful as it simply increased with ester chain length, however for aminolysis, variation of k_3 with the structure of the reactants might provide insight into the ter-molecular transition state. From Table 7.3, we see that the values of k_3 for the aminolysis of pNPA and pNPH by *n*-alkylamines in the presence of CTAB increase appreciably with amine chain length as well as with acyl chain length. This means that in order to probe transition state binding to CTAB we will have to assess how the catalysis depends on the amine chain as well as on the ester chain or the combination of the two.

7.2.7 The Aminolysis of a Series of Alkanoate Esters by *n*-Hexylamine

We just presented the systematic study on the effects of the variation of amine chain length and amine structure on the “catalysis” of the aminolysis of two esters (pNPA and pNPH) by CTAB micelles; but, in order to truly understand the puzzling effects of ester chain length on the catalysis, a necessary extension was to study a more complete series of esters. Thus, several other experiments were performed with the series of *p*-nitrophenyl alkanoate esters (acetate to decanoate) reacting with a one particular, relatively long, amine: *n*-hexylamine. The same kinetic analysis as used above is suitable for the data here, and the results are presented in Table 7.4. Plots of k_{obs} as a function of

$[n\text{-hexylamine}]_0$ in the absence and presence of CTAB are shown in Figures 7.5 and 7.6, respectively. Again, k_N and k_{cN} are estimated from the slopes of those plots (Chapter VI).

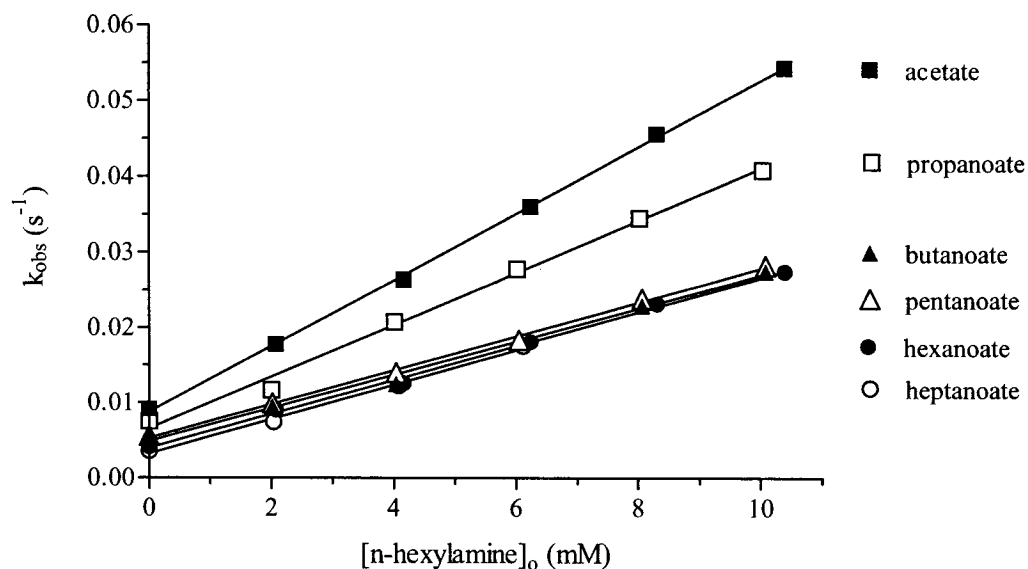


Figure 7.5 Variation of k_{obs} for ester aminolysis by n -hexylamine in the absence of CTAB. The slopes provide k_N .

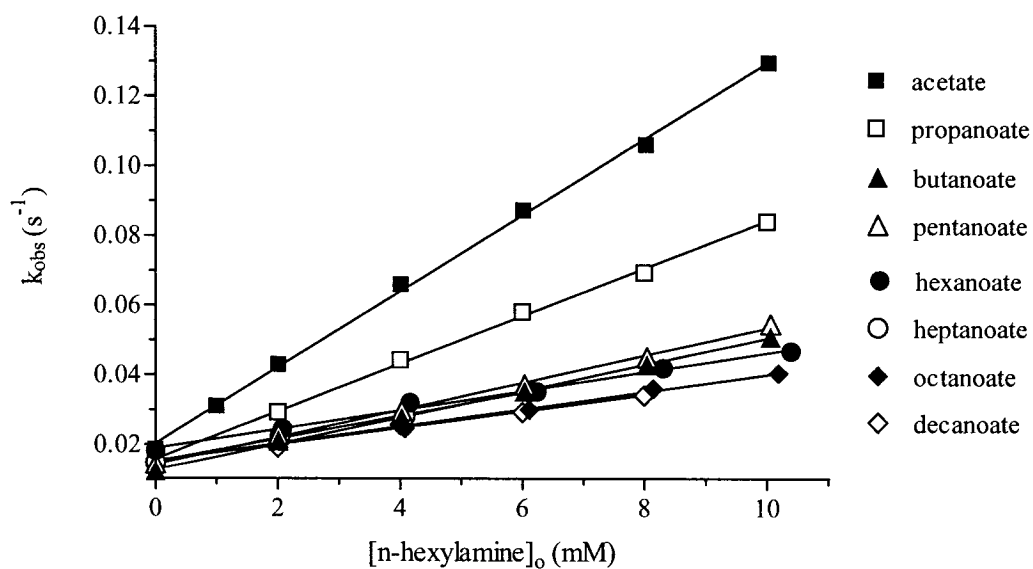


Figure 7.6 Variation of k_{obs} for ester aminolysis by n -hexylamine in the presence of 5.0 mM CTAB. The slopes provide k_{cN} .

Table 7.4 Constants for the reaction of *n*-hexylamine with *p*-nitrophenyl alkanoate esters in the absence and presence of CTAB.^a

Ester	k_N $M^{-1}s^{-1}$	k_{cN} $M^{-1}s^{-1}$	k_{cN}/k_N	K_S^c mM	K_{TS} mM
Acetate	4.38 ± 0.05	43.4 ± 1.0	9.91	24.6	2.48
Propanoate	3.33 ± 0.03	12.6 ± 0.4	3.78	8.11^c	2.14
Butanoate	2.21 ± 0.10	4.62 ± 0.09	2.09	2.60	1.24
Pentanoate	2.26 ± 0.05	4.26 ± 0.11	1.88	1.06	0.562
Hexanoate	2.26 ± 0.05	2.77 ± 0.13	1.23	0.374	0.305
Heptanoate	2.29 ± 0.11	3.34 ± 0.13	1.46	0.141	0.0967
Octanoate	2.29^b	2.47 ± 0.08	1.08	0.0539	0.0500
Decanoate	2.29^b	2.36 ± 0.12	1.03	0.00664^c	0.00644

^a At 25 °C, in aqueous carbonate buffer at pH 10.6.

^b Difficult to estimate and assumed to be very close to heptanoate.

^c The values of K_S are taken from our earlier work (Table 6.2).⁵⁹

^e Obtained by extrapolation of linear plot of pK_S vs. ester acyl chain length.

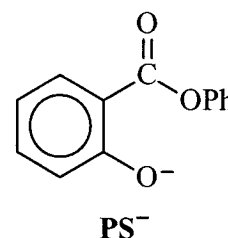
As seen in Figure 7.6, for aminolysis by *n*-hexylamine, unlike thiolysis of these esters (Chapter VI, Figure 6.3 and Table 6.1), the observed rate is greatest with the acetate ester in the presence of CTAB. The reactivity of *n*-hexylamine toward the CTAB.ester complex (k_{cN}) decreases as the ester chain lengthens (Table 7.4). This decrease results in the reactivity ratio (k_{cN}/k_N) to *decrease* from 9.91 (acetate) to 1.03 (decanoate). The transition state dissociation constant K_{TS} also *decreases* with ester chain length, but not monotonically, as will be discussed later on.

7.3 DISCUSSION

7.3.1 Amine Partitioning into the Micellar Pseudo-phase

The cleavage of esters by small, neutral nucleophiles, such as water²¹⁶ and imidazole,⁶² is generally *retarded* by both cationic and anionic micelles because hydrophobic esters enter easily into the micelles while the nucleophiles do not.³⁴³ One can expect the same to be true for small, hydrophilic amines, and apparently it is ($k_{cN}/k_N < 1$, Table 7.3). It has been shown that incorporation of very short alkylamines into SDS micelles is negligible³⁴³ and that such amines reside mainly in the aqueous phase. Since the incorporation of the neutral amines is not electrostatic in nature, amine incorporation into SDS and CTAB micelles should hardly differ. Thus, we attribute retardation of the ester aminolysis with *short* amines to be due to *dilution effects* by CTAB micelles, because the ester and the amine will be distributed in two different phases: the amine in the aqueous phase, and the ester in the micellar pseudo-phase.

In support of such an explanation, Khan *et al.*^{344,345} studied the effect of ionic micelles (CTAB and SDS) on the nucleophilic reaction of a number of amines (including piperidine and *n*-butylamine) with ionized phenyl salicylate (PS^-) (shown on the right). They concluded that “the hydrophilic amines remain in a more polar region while the less hydrophilic anions, PS^- , remain in the less polar region of the micelle (CTAB)”.^{344,345} As a consequence of the different average locations of the two reactants, the aminolysis of PS^- in the CTAB micellar pseudo-phase is slower than that in the aqueous phase.



In contrast to the retardation seen with short amines, for longer, more hydrophobic, *n*-alkylamines, aminolysis of pNPA and pNPH is *catalysed* by CTAB

micelles ($k_{\text{CN}}/k_{\text{N}} > 1$, Table 7.3). When amines with alkyl chains of medium length (C_5 - C_7) are used as co-surfactants, they are localized behind the head groups of micelles in the so-called “palisade layer”.^{344,346} Therefore, we suggest that catalysis of ester aminolysis is probably attributable to *concentration effects* by CTAB micelles, whereby the longer amines are *concentrated* in the micellar phase *proximal* to the ester-CTAB complex. In fact, for pNPA, the reactivity ratios increase monotonically with the amine chain length and a plot of $\log(\text{ratio})$ vs. chain length is linear with a slope of 0.49. Since hydrophobicity parameters are also linear in chain length, and with similar slopes, it is evident that the ratios also correlate with amine hydrophobicity.

After pioneering work of Hansch and coworkers, octanol/water partition coefficients ($P_{\text{o/w}}$) have generally been used as reliable indices of hydrophobicity.³⁴⁷⁻³⁵² It was during this work (and related studies) that it was shown that $\log P_{\text{o/w}}$ for alkyl derivatives correlate linearly with hydrocarbon chain length, with slopes of ~ 0.5 .^{351,352} Also, $P_{\text{o/w}}$ values are proportional to partition coefficients for the solubilization of solutes in biological membranes and in micelles.³⁵³⁻³⁵⁵ Treiner and coworkers,³⁵⁵ have shown that for straight, branched, and cyclic compounds (amines, alcohols, esters, and ketones) there is a good correlation between the logarithm (partition coefficients) for micelle/water (dodecyltrimethylammonium bromide, DTAB) micelles and for octanol/water, with a slope of the plot of $\log P_{\text{mic/w}}$ vs. $\log P_{\text{o/w}}$ being about 0.9 (Figure 7.7). For these reasons, we will use the $\log P_{\text{o/w}}$ for the amines, which are available in the literature,³⁴⁷ as a measure of the amines' hydrophobicity and of their ability to partition into CTAB micellar phase from the aqueous phase.

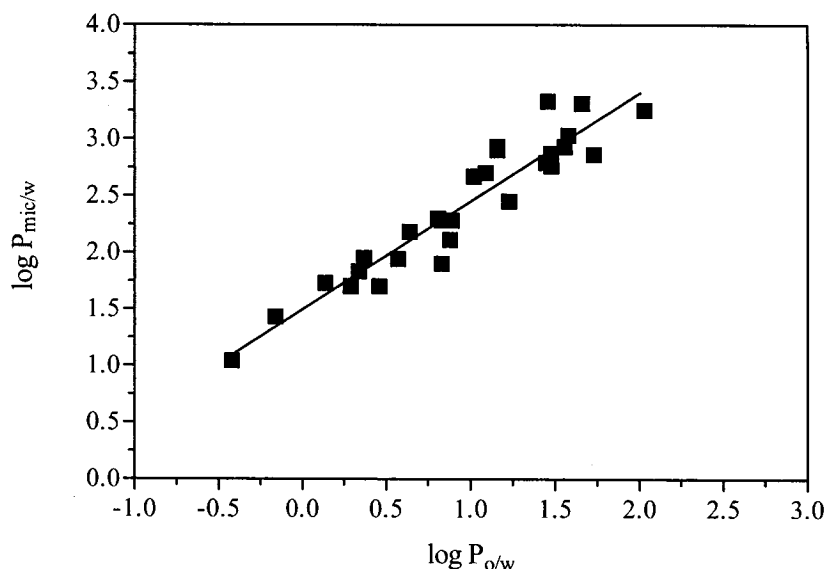


Figure 7.7 Correlation between log P in DTAB/water and octanol/water for 28 organic molecules. Data taken from Treiner *et al.*³⁵⁵

Figure 7.8 shows plots of $\log(k_{cN}/k_N)$ with the logarithms of octanol/water partition coefficients ($\log P_{o/w}$)^{347,356} for alkylamines as measures of amine hydrophobicity. There is a very good correlation for pNPA reacting with *n*-alkylamines ($r = 0.9983$, 6 points) and slope = 0.94 ± 0.03 , which indicates that amine hydrophobicity, and amine transfer into the micelles, greatly influence the magnitude of catalysis by CTAB micelles. However, for pNPH, the corresponding plot is biphasic: first there is an increase from *n*-propyl to *n*-hexylamine, with a slope of 0.53 ± 0.03 , and then a second, steeper increase for the longer amines, with a slope of 0.93 ± 0.1 . This behaviour suggests that the hydrophobicity of longer amines plays an integral role in determining the efficiency of aminolysis of pNPH, but the hydrophobicity of the short amine is not as vital in determining the magnitude of catalysis with the more hydrophobic hexanoate ester. Such a bend in the correlation plot with the longer pNPH ester (Figure 7.8) is indicative of a

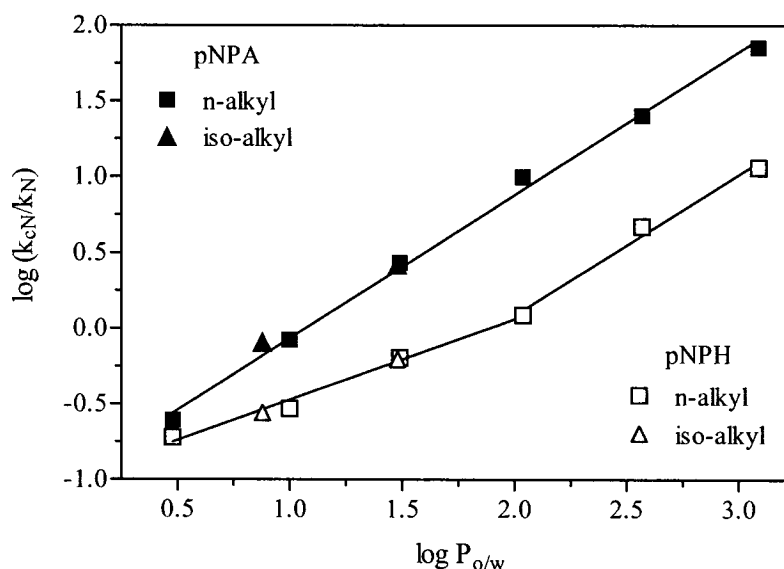


Figure 7.8 Dependence of the $\log (k_{cN}/k_N)$ on $\log P_{o/w}$, for *n*-alkyl and *iso*-alkyl-amines, and for pNPA and pNPH.

Table 7.5 The logarithms of amine octanol/water partition coefficients and catalytic ratios for aminolysis of pNPA and pNPH.^a

Amine	Log $P_{o/w}$	Log (k_{cN}/k_N) for pNPA	Log (k_{cN}/k_N) for pNPH
<i>n</i> -propyl	0.480	-0.607	-0.721
<i>n</i> -butyl	0.970 ^c	-0.077	-0.530
<i>n</i> -pentyl	1.49	0.432	-0.194
<i>n</i> -hexyl	2.04	0.996	0.0884
<i>n</i> -heptyl	2.57	1.40	0.674
<i>n</i> -octyl	3.08 ^b	1.85	1.06
<i>iso</i> -butyl ^c	0.880	-0.0932	-0.559
<i>iso</i> -pentyl ^c	1.51 ^b	0.419	-0.206
cyclopentyl	1.11 ^b	0.00370	-0.804
cyclohexyl	1.49	1.15	-

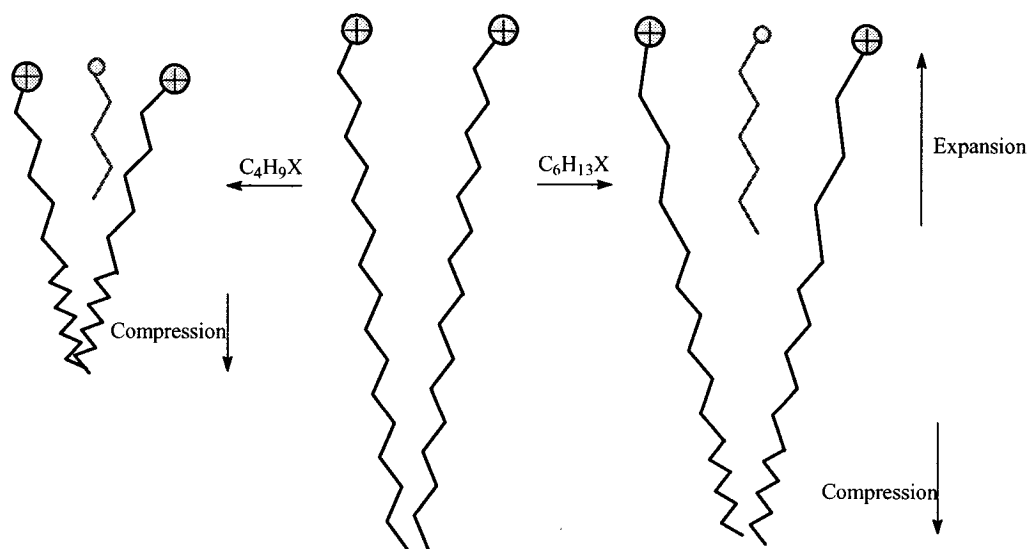
^a Most values $\log P_{o/w}$ are taken from Hansch, Leo and coworkers.³⁴⁷

^b Estimated values of $\log P_{o/w}$, see Experimental Section 7.5.

^c For *n*-butylamine average of two values by the same reference.

switch in the mechanism of the catalyzed reaction, and this switch occurs at an amine chain length of 6 carbons, which happens to be equal to the ester chain length (C_6). By contrast, for the shorter pNPA ester, there is only one mode of catalysis of aminolysis by CTAB micelles. As we will discuss in the sections to follow, the difference in the mechanisms of catalysis of the aminolysis of the two esters by the micelles depends on the mode of binding (and stabilization) of the transition states relative to the initial states.

In research which complements our explanation that amine hydrophobic partitioning into the micelles is a major factor affecting the magnitude of catalysis, Alonso and coworkers³⁵⁷ studied the solubilization of *n*-alkanols and *n*-alkylamines in CTAB micelles by NMR. They concluded that the dependence of the mole fraction of the solubilized additive on the alkyl chain is a direct consequence of the predominance of the hydrophobic effect. What they have shown additionally is that the “solubilized additives adopt more extended conformation than free ones, and their polar head groups are mainly located at the micellar surfaces,”³⁵⁷ as illustrated in Scheme 7.2.



Scheme 7.2 Conformational changes of the cetyl chains produced by solubilization of *n*-alkyl alcohols or amine additives in CTAB micelles.³⁵⁷

The longer chain *n*-hexanol and *n*-hexylamine were located more deeply in CTAB micelles than *n*-butanol and *n*-butylamine, leading to an extension of cetyl (hexadecyl) chains below the ionic head groups, counterbalanced by a compression at the chains ends (Scheme 7.2). In the case of the longer *cosurfactants*, penetration into the micelles leads to the formation of swollen aggregates larger than the initial CTAB micelles, while the shorter *cosolvents* result in the formation of smaller spherical micelles. It also seems that the longer alcohols penetrate deeper than the longer amines, and so there must be a greater hydrophilicity of the amino groups than the hydroxyl groups, which is expected from solubility measurements³⁵⁸ and octanol/water partition coefficients for the alcohols and amines (see Experimental Section 7.5). The explanation given for the greater hydrophilicity of amines is the presence of some protonated as well as non-protonated amino groups, at the micellar surface.

Mirgordshaya *et al.*^{336,337} have also observed catalysis (3 to 8 fold) for the aminolysis of pNPA by *n*-heptylamine in cetylpyridinium bromide (CPB) micelles. The magnitude of catalysis also increased with amine chain length, with a 14 fold catalysis with *n*-octylamine up to a 43 fold catalysis with *n*-cetylamine.³³⁷ Unlike our explanation, they suggested that part of the enhancement of reactivity with the long amines may be attributed to apparent pK_a shifts of the amines in the cationic micellar solution. In other words, there is more of the free base form of the longer chain amines than shorter chain amines at the same pH. In contrast to the reaction with pNPA, CPB micelles catalyzed the aminolysis of *p*-nitrophenyl octanoate (pNPO) by *n*-butylamine (30 to 65 fold) and by *n*-heptylamine (14 fold), but CPB micelles retarded (by a factor of 4 to 6) the reaction of pNPO with longer amines, *n*-decylamine and *n*-cetylamine. The retardation was assumed

to be due to micellization of the longer amines and to the formation of mixed micelles of them with CPB and pNPO, in which the amine and ester are localized in different regions.^{336,337} Based on our results with CTAB micelles (see Table 7.4), retardation by CPB micelles of the reaction between very long amines and the longer octanoate ester is reasonable; but, the high magnitude of catalysis reported when the amine is short is in contrast to our work (see Table 7.3). Nonetheless, we will be suggesting another explanation for the decrease in reactivity in the presence of cationic micelles when both amine and ester chain are long (*vide infra*).

In conclusion, our results indicate that the partitioning of the alkylamines into the micelles is governed largely by their hydrophobicities, even though amine binding never becomes strong enough to cause saturation kinetics at the amine concentrations used (Figures 7.3, 7.4 (b) and 7.6). Saturation behaviour is most likely with the long amines but, of course, they must be used at low concentrations because of their poor solubilities in water. The ease of partitioning of the amine from the aqueous phase into CTAB micelles dictates whether the aminolysis of the ester will be catalyzed or retarded, and this partitioning should be independent of the ester binding to CTAB micelles. For ester thiolysis (Chapter VI) and hydrolysis (Chapter V) the magnitude of catalysis afforded by CTAB micelles is indeed independent of the ester chain length, but this is not the case for aminolysis. So, the dissimilar magnitudes of “catalysis” and dissimilar plots for pNPA and pNPH in Figure 7.8 must reflect the different demands for ester (or amine) binding in the transition state. This last point will be discussed extensively in the next sections.

7.3.2 Transition State Binding Depends on Amine and Ester Hydrophobicity

For the aminolysis of both pNPA and pNPH in CTAB micelles, the strength of transition state binding (pK_{TS}) increases significantly with amine chain length (Figure 7.9) and thus with amine hydrophobicity. It is immediately obvious that pK_{TS} for each amine is decidedly larger for pNPH than for pNPA, which is expected due to additional stabilization of the longer acyl chain of the hexanoate ester by hydrophobic binding within the micelle. Furthermore, because of the relationship $pK_{TS} = \log (k_{cN}/k_N) + pK_S$, and since pK_S is a constant for each ester, the variations of pK_{TS} with the amine chain length and with partition coefficients (as $\log P_{o/w}$) follow the same pattern as shown by $\log (k_{cN}/k_N)$ (in Figure 7.8), although the plots for the two esters are vertically displaced relative to each other because of their different pK_S values.

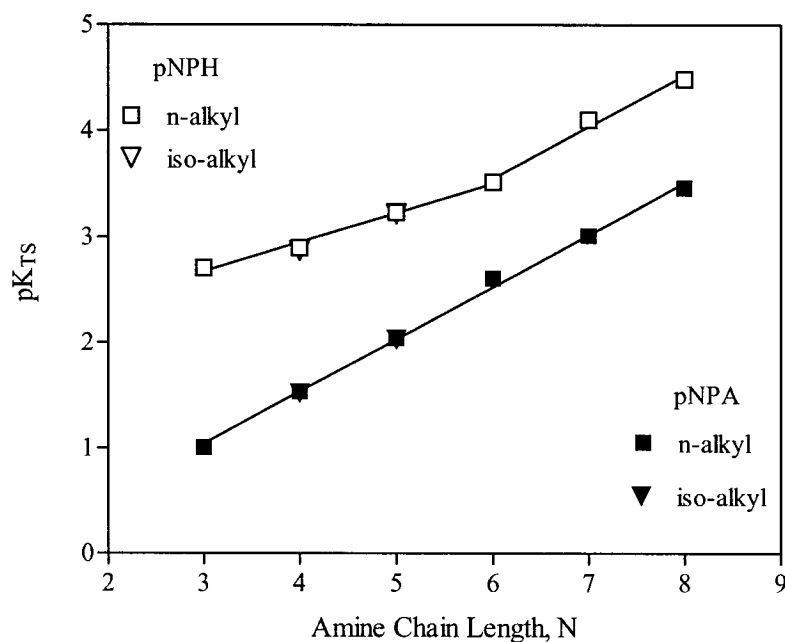


Figure 7.9 Dependence of the pK_{TS} on amine chain length, for *n*-alkyl and *iso*-alkyl amines, and for pNPA and pNPH.

Quantitatively, for pNPA the linearity in the plot of pK_{TS} vs. N (Figure 7.8), with a slope $= 0.49 \pm 0.01$ (with $r = 0.9997$, 6 points), implies that in the transition state there is one mode for amine-pNPA binding to CTAB micelles which is very sensitive to the amine. Since various measures of hydrophobicity are linear in alkyl chain length,^{65,68,75,175,215} this LFER (linear free energy relationship) is consistent with the variations in TS binding being determined by partially or largely hydrophobic interaction of the amine with the micelle. The slope of 0.49 corresponds to a free energy increment of 0.67 kcal/mol per methylene group, which is the middle of the range of values (0.4 to 0.9 kcal/mol) found for a variety of processes involving the transfer of alkyl derivatives from water to organic media, including transfers to micelles and micelle formation.⁶⁵

For the cleavage of pNPH, the plot in Figure 7.9 is biphasic: with the amines longer than *n*-hexylamine the slope of pK_{TS} vs. $N = 0.48 \pm 0.06$, which indicates that similar hydrophobic forces of the long amino chain are involved in binding the transition states with both pNPA and pNPH. However, with shorter amines ($N < 6$), reacting with pNPH, the slope $= 0.27 \pm 0.02$, which suggests that in the transition state the shorter alkylamino groups have a smaller influence on TS binding because of the longer chain of pNPH.

The corresponding correlation between TS binding strength for pNPH against pK_{TS} of pNPA is shown in Figure 7.10. This plot has the advantage that it allows direct comparison of the behaviour of the two esters without requiring the use of any parameter for the amines. The plot emphasises that transition state stabilisation is greater with pNPH than that with pNPA (by 1.0 - 1.7 pK units), implying a sizeable contribution from binding of the acyl chain of the ester. As with Figure 7.9, the non-linear nature of the

graph indicates that the binding of the amine chain and ester chain in the TS are not independent of one another.

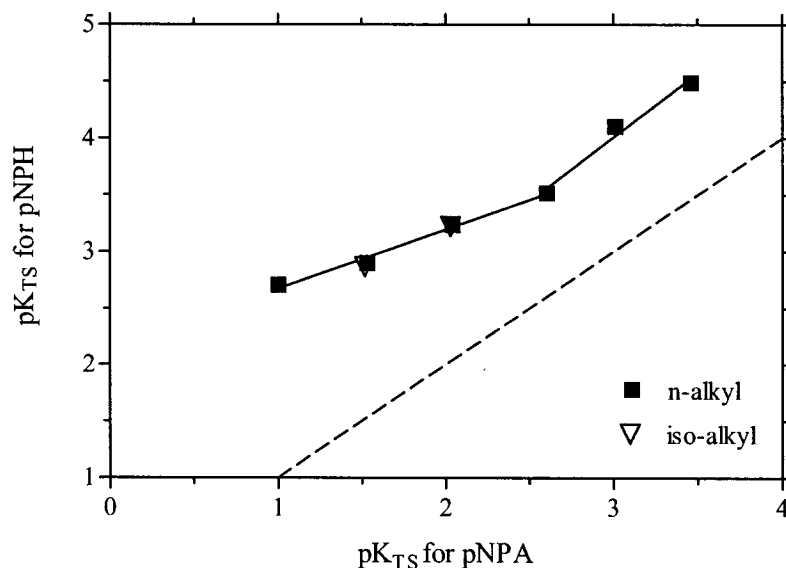


Figure 7.10 The corresponding relationship between TS stabilization for pNPA and pNPH with those same amines.

7.3.3 Probing Ester Acyl Chain Length Binding to CTAB Micelles

For the reaction between *n*-hexylamine and the series of esters in CTAB micelles (Table 7.4), we propose that the *decrease* in the catalytic ratio $k_{\text{cN}}/k_{\text{N}} = (K_{\text{S}}/K_{\text{TS}})$ arises because the ester chain length dependence of *transition state binding* and *substrate binding* are not parallel (Figure 7.11). The difference between $\text{p}K_{\text{TS}}$ and $\text{p}K_{\text{S}}$ *diminishes* as ester chain lengthens, indicating (again) that the effects of the ester and amine chain lengths on the transition state are not independent.

Quantitatively, the slope of $\text{p}K_{\text{TS}}$ vs. ester chain length is 0.37 ± 0.08 ($r = 0.998$, 6 points), not including the acetate or propanoate (Figure 7.11), while that of $\text{p}K_{\text{S}}$ is 0.44 ± 0.01 ($r = 0.999$, 8 points).⁵⁹ These values mean that hydrophobic interaction^{65,68,75} of the

ester acyl chains with the micelles is operative during TS binding (with butanoate to decanoate esters), but the overall ester binding in the initial state is more sensitive to the chain length. Actually, from the hexanoate ester and beyond there is hardly any difference between pK_{TS} and pK_S .

The correlation between pK_{TS} and pK_S (insert in Figure 7.11) has a slope 0.88 ($r = 0.9991$, for the 6 longer esters) which suggests that ester chain binding in the transition state is strong and *similar to* but *not exactly* the same as its binding in the initial state. For the shorter esters, acetate and propanoate, the points deviate appreciably from the linear correlation, implying that TS binding of their acyl chains are much less important.

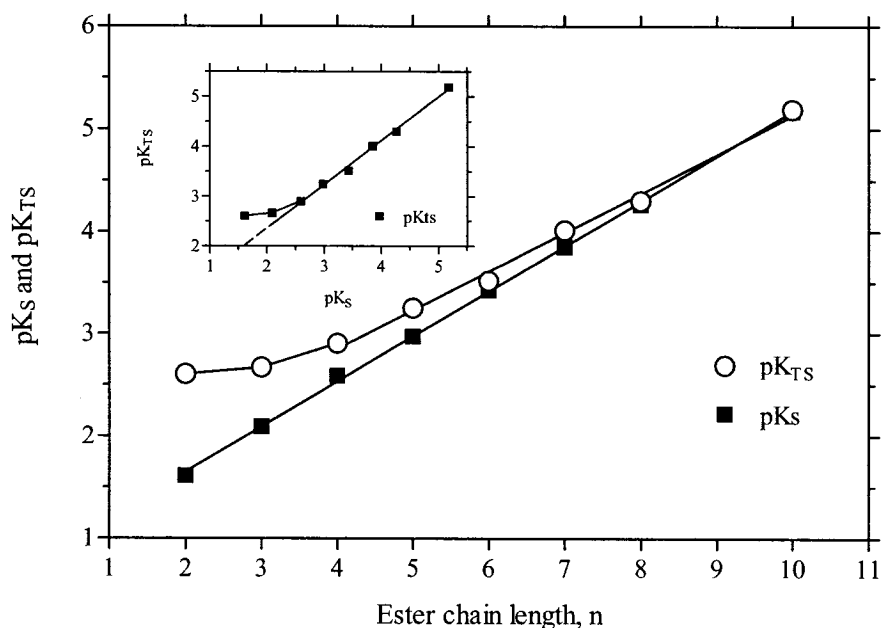
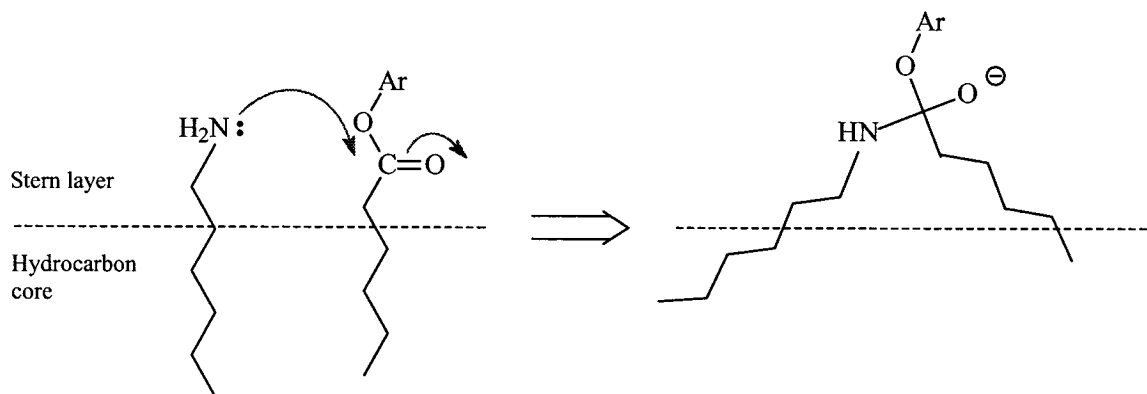


Figure 7.11 The dependence of transition state binding (pK_{TS}) and substrate binding (pK_S) to CTAB micelles on acyl chain length (n). The insert is a corresponding plot of transition state binding vs. ester binding.

The depth of penetration of substrates is often used to explain how catalysis relates to substrate selectivity by micelles and by microemulsions. Bhattacharya and Snehalathan studied the cleavage of *p*-nitrophenyl alkanoate esters of varying chain lengths mediated by (dialkylamino)pyridine functionalised amphiphile microemulsions.³⁵⁹ They also found that the shorter esters were more susceptible to catalyzed cleavage and that the reactivity decreased with increasing chain length. Also, 4-acetoxy-3-nitrobenzoic acid was found to react about 3 times faster than pNPA. They concluded that pNPA is concentrated more in the interface region and the longer chain esters are confined more deeply in the hydrophobic region of the oily microdroplets of the microemulsions.

At first glance, the *decrease* in the ability of CTAB to catalyze the aminolysis of the longer esters by *n*-hexylamine might have also been attributed to *deeper penetration* of the long chain esters into the micelle interior, rendering the carbonyl group less accessible to attack by a nucleophile. However, from our results with anionic nucleophiles,^{58,59} the *constancy* in the catalytic ratios (and the parallelism of pK_{TS} and pK_S) with varying ester chain length implies that the carbonyl group is not appreciably buried, which is consistent with the conclusions of Al-Awadi and Williams³⁰⁵ that the ester carbonyl group and the aryloxy leaving group are both in an aqueous environment.

A more probable explanation of the decrease in the catalytic efficiency with ester chain length is that strongly bound reactants (such as hexylamine and a long chain ester) in CTAB micelles cannot attain the *optimal geometry* for nucleophilic attack on the ester without losing some hydrophobic binding of either the alkylamino chain or ester acyl chain (Scheme 7.3).



Scheme 7.3 In the reaction of a long amine with a long ester, in CTAB micelles, the loss of some hydrophobic binding of the micellar-bound alkylamino and acyl chains is required to attain the transition state.

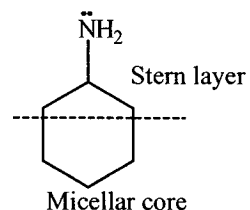
Because of the geometrical requirements of the addition step, the ester and amine chains must decrease their hydrophobic interactions with the micelle (to some extent) in order for the transition state to be reached, and for the reaction to proceed. By contrast, with hydrolysis^{58,59} and thiolysis^{58,59} of the esters, the anionic nucleophile is able to position itself appropriately in the Stern layer for attack at the carbonyl at an appropriate angle, regardless of how tightly the ester is bound.

7.3.4 Branched and Cyclic Amines

Up to this point we have not have discussed reaction with the branched and cyclic amines. Retardation of the aminolysis of pNPA and pNPH with *iso*-butyl and *iso*-pentyl amine ($k_{\text{CN}}/k_{\text{N}}$) can also be attributed to a “dilution effect” by CTAB, as with their *n*-alkyl counterparts. The *iso*-alkylamines have slightly lower partition coefficients due to their smaller surface area (Table 7.5), and correspondingly their reactivity ratios are slightly smaller than those of the *n*-alkyl derivatives. Thus, the two points for *iso*-alkylamines in

Figure 7.8 are very close to the correlation line between the logarithms of the reactivity ratios and *n*-alkylamine partition coefficients.

The two cyclic amines are less hydrophobic than their *n*-alkyl counterparts (Table 7.5), and correspondingly for cyclopentylamine the reactivity ratios are smaller than for *n*-pentylamine with both pNPA and pNPH (Table 7.3). However, whereas the reaction between pNPA and cyclohexylamine is greatly catalysed by CTAB, that with pNPH is not (see Table 7.3). To explain this difference we propose that cyclohexylamine is capable of stronger hydrophobic interaction with the micellar core (as shown on the right) and that this mode of binding in the transition state renders cyclohexylamine more reactive with a mobile acetate ester, but it makes it very unreactive with the tightly-bound hexanoate ester due to geometrically-restricted attack.



7.4 CONCLUSIONS

For many reactions the *concentration effect* arising from the partitioning of reactants into the micellar pseudo-phase is sufficient to explain micellar catalysis, but it is not here. We propose different modes of transition state binding to rationalize the different efficiencies of ester aminolysis in CTAB micelles. These modes are illustrated in Figure 7.12 (overleaf).

Mode (i): For the short esters (the acetate and propanoate) and *n*-alkylamines (Figure 7.12 (a) and (b)), the strength of TS binding strongly correlates with the hydrophobicity of the amine but is not greatly influenced by the hydrophobicity of the ester, which means that only the amine chain interacts with the hydrophobic core of the

micelle. Since the short amines (Figure 7.12 (a)) partition poorly into the micellar pseudo-phase, their reactions are retarded by CTAB micelles. However, the longer amines (Figure 7.12 (b)) partition much more easily so that both reactants are more concentrated in the pseudo-phase, their transition states are more tightly bound, and their reactions are catalyzed by CTAB.

Mode (ii): For the longer ester (pNPH) and short amines (*n*-propyl to *n*-pentyl), the TS binding involves additional hydrophobic interaction between the ester chain and the micellar core (Figure 7.12 (c)), and the strength of TS binding is less sensitive towards the hydrophobicity of the amine (Figure 7.8). Unlike mode (i), the amine chain is probably not as tightly bound to the core in the TS, and so these reactions are even more retarded by CTAB micelles.

Mode (iii): For longer esters (butanoate to decanoate) reacting with a long amine (*n*-hexylamine), both the acyl and alkylamino chains contribute to the TS binding through hydrophobic interactions with the micellar core (Figure 7.12 (d)) but there is a conflict in their binding for *geometric reasons*. Even though the CTAB micelles ‘concentrate’ both reactants into the pseudo-phase, there is a decrease in the catalytic efficiency with chain length because the combined TS binding of the acyl and amine chains, in the *optimal geometry* for nucleophilic attack, is weakened, relative to the initial state binding (Scheme 7.3).

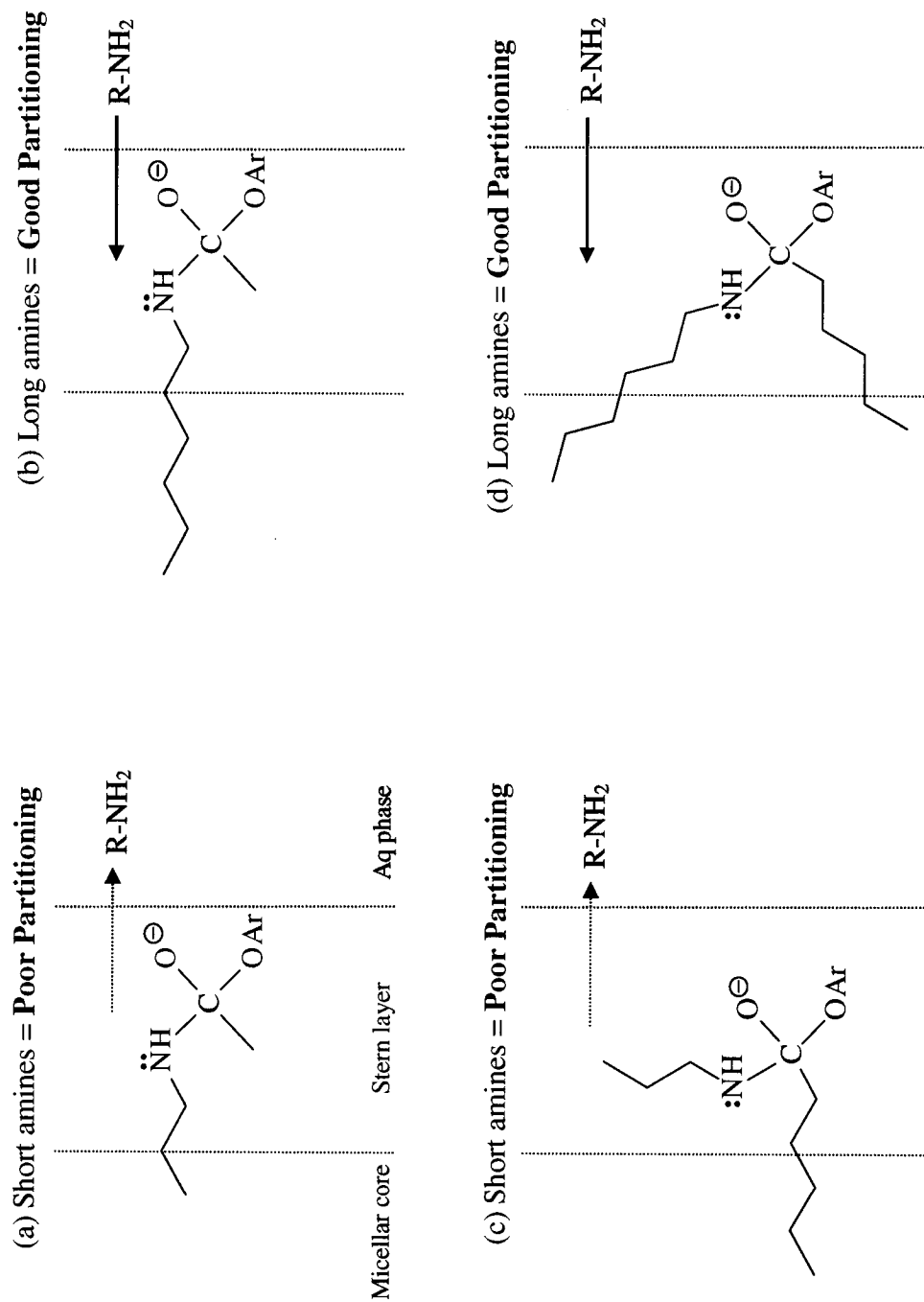


Figure 7.12 Transition State binding for the aminolysis of esters in CTAB micelles: (a, b) for a *weakly bound* short ester reacting with (a) short *n*-alkylamines and (b) long *n*-alkylamines; (c, d) for a *strongly bound* long ester reacting with (c) short *n*-alkylamines and (d) long *n*-alkylamines.

From this work we conclude that concentrating the reactants into the micellar pseudo-phase can lead to catalysis *provided* that the reactants are not held so rigidly that they cannot readily attain the appropriate transition state in the micellar environment. Enzymes, catalyzing bimolecular reactions, also bring reactants closer together, and generally orient them in such a way as to ease the formation and binding of the transition state.^{27,28,360}

7.5 EXPERIMENTAL

7.5.1 Materials

The amines were purchased as the best grades available from Aldrich Chemical Company. As earlier, most of the esters were obtained from Sigma Chemical Company; cetyltrimethylammonium bromide (CTAB) was obtained from ICN Biochemicals and purified as previously (Chapter VI). Aqueous buffers were made up from the best grades of the buffer reagents available and water that had been ion-exchanged and doubly distilled from glass.

7.5.2 Kinetic Measurements

As for the thiolysis studies, Chapter VI, three types of experiments were carried out. Details of the contents of each syringe of the stopped-flow apparatus are as follows:

a) For k_{obs} vs. [CTAB], in presence of amine (used to find K_S , Fig. 7.1):

Syringe A: amine + 0.2 M NaHCO_3 buffer, all together adjusted to pH = 10.6.

Syringe B: ester + varying [CTAB] + varying [NaBr] (total $[\text{Br}^-] = 10 \text{ mM}$).

b) For k_{obs} vs. [amine], with no CTAB (used to finding k_{N} , Fig. 7.2 and Fig. 7.5):

Syringe A: 10 mM NaBr + ester

Syringe B: varying [amine] + 0.2 M NaHCO_3 buffer, all together adjusted to pH = 10.6 (generally requiring drops of concentrated HCl).

(c) For k_{obs} vs. [amine], at fixed [CTAB] (used to find k_{cN} , Fig. 7.3 and Fig. 7.6):

Syringe A: 10 mM CTAB + ester

Syringe B: varying [amine] + 0.2 M NaHCO_3 buffer, pH = 10.6.

Stock solutions of the ester were prepared in 0.1 M spectral grade CH_3CN which were made up freshly and kept no longer than one week. The ester concentrations used in the experiments were the same as in the thiolysis studies (see Section 6.5), below that for ester aggregation and much less than [CTAB].

Kinetics were monitored using an Applied Photophysics Ltd. SX17MV stopped-flow Spectrophotometer, with the cell temperature maintained at 25.0 ± 0.1 °C. Rates of ester cleavage were measured by the first order appearance of the *p*-nitrophenolate ion at 405 nm. Normally 5-10 absorbance traces, whose rate constants deviated by no greater than 5%, were averaged for the estimation of k_{obs} by non-linear least square fitting of an exponential growth curve, taken to 10 half lives (where possible). With the least soluble esters, at low concentration, more traces were averaged.

The change in observed rate constant k_{obs} vs. [amine], in the presence and absence of CTAB, was fitted by the appropriately chosen kinetic model. Data analysis is briefly presented above in the results section; more details of the analysis were given previously

(in Chapter VI). The observed rate constants that were acquired from reproducible experiments were collected and tabulated in Appendix C.

7.5.3 The pH and Background Hydrolysis

The pHs of solutions were measured with an Accumet Model 25 pH/ion meter, with any required adjustments to pH being made with drops of concentrated NaOH or HCl. There are several reasons for our choice of buffer and pH. Under the reaction conditions chosen, 0.100 M carbonate buffer pH = 10.60 ± 0.01 , the background hydrolysis rate is relatively small. Tee and Fedortchenko⁵⁸ had previously determined rate constants for hydrolysis of *p*-nitrophenyl alkanoate esters (C2 to C8) in phosphate buffer at pH = 11.6, $k_u = 0.110 - 0.0591 \text{ s}^{-1}$ and $k_c = 0.301 - 0.147 \text{ s}^{-1}$. At the lower pH of 10.6, the rate of hydrolysis is slower by a factor of 10, so that it competes less with ester aminolysis and affords better kinetic data for analysis.

For alkylamines ($\text{pK}_a \sim 10.4 - 10.6$), at pH = 10.6, about half of the initial amine concentration are in the unprotonated, nucleophilic form and the other half are protonated. Protonation helps stabilize the amine solutions but then the rate of aminolysis is only half what it would be if all the amine was free. Long protonated alkylamines can form micelles themselves, although this is only significant for *n*-decylamine³³⁶ and beyond, and at higher concentrations than we have used.¹⁷⁵ Small amounts of protonated amines should not be unduly disruptive in the CTAB micelles.

Using a higher pH than 10.6, such as pH = 11.6, would solve the problem of having protonated amine in the solution, and it would also speed up the slow aminolysis reaction, but only by a factor of 2. However, at pH 11.6, both uncatalyzed and CTAB-

catalyzed hydrolysis are both faster by a factor of 10, and more competitive with aminolysis.

7.5.4 Concentration Range of Amines

The ranges of [amine] used were varied with the amine solubility (see Table 7.2), similar to those employed in other work on aminolysis, with the same amines.¹³¹ A very long chain amine, *n*-nonylamine, was tried but it proved to be problematic, due to its poor solubility. Experiments with it were discontinued because of the poor kinetic plots that it gave. For the readily soluble *n*-propylamine and *n*-butylamine, at very high concentrations (> 100 mM), k_{obs} were somewhat variable and irreproducible. This is likely attributable to inconstant pHs at high amine concentration, or volatilization of the amine. Therefore, experiments were conducted at a lower concentration ranges than that which is permitted by the limit of solubility.

In order for aminolysis to compete effectively with hydrolysis, and to detect a reasonable change in k_{obs} with [amine], it was found that the concentration range of amines should be kept fairly high. The observed rates of aminolysis of the esters in the absence and presence of CTAB were relatively slow at low concentrations of amine, and the absorbance curves were cut off before A_{∞} had been reached, rendering translation into reproducible k_{obs} values more difficult.

7.5.5 Partition Coefficients

As measures of amine hydrophobicity, we have followed tradition and used octanol/water partition coefficients ($P_{\text{o/w}}$).^{348,356,361,362} By consulting various literature

sources, we have assembled what seems to be the most reliable and consistent values of $\log P_{o/w}$ (Table 7.5) but we did not find values for *iso*-pentylamine or cyclopentylamine.³⁴⁷ Values for these two amines were estimated by a roundabout procedure, making use of the fact that $\log P$ values for different organic-water pairs generally correlate well with each other³⁶³ and also that $\log P_{o/w}$ values for amines and alcohols show a good linear correlation (Figure 7.13). For aliphatic alcohols distributed between 1-octanol and water, and between ether and water,¹¹³ the equation is: $\log P_{o/w} = (1.0048 \pm 0.0156) \cdot \log P_{e/w} - (0.2557 \pm 0.0161)$, $r = 0.9983$ (17 points), from which we estimated $\log P_{o/w} = 0.999$ for cyclopentanol. For twelve alkylamines and their cognate alcohols we found the correlation line: $\log P_{o/w}(\text{amine}) = (0.9339 \pm 0.0222) \cdot \log P_{o/w}(\text{alcohol}) - (0.1784 \pm 0.0328)$, $r = 0.9972$, which afforded estimates of $\log P_{o/w} = 1.505$ for *iso*-pentylamine and 1.111 for cyclopentylamine.

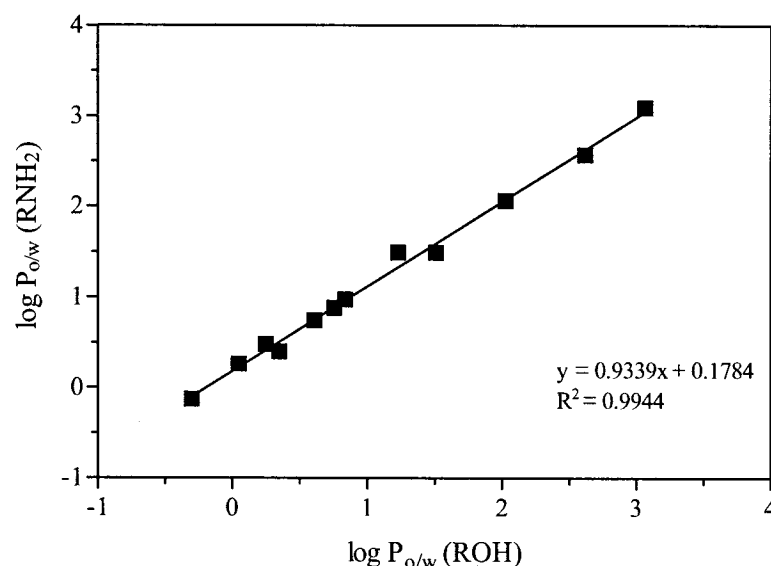


Figure 7.13 The correlation between $\log P_{o/w}$ values for amines vs. alcohols.

We also explored the feasibility of obtaining log $P_{o/w}$ values from prediction packages, using software available on the world-wide web,^a but we found the results to be quite variable, depending on the method of calculation, and that generally they give quite low for acyclic amines. Variability of "calculated" values and a pronounced dependence on the method are common problems in prediction of log P values.³⁵¹

^a See: <http://www.epa.gov/oppt/exposure/docs/episuitel.htm>, and pages linked thereto

CHAPTER VIII. CATALYSIS OF THE CLEAVAGE OF *p*-NITROPHENYL ALKANOATES BY AMINO ACID ANIONS IN CTAB MICELLES

8.1 INTRODUCTION

Hydrophobic and electrostatic interactions such as those between reactants and micelles are also evident in enzyme-substrate recognition.^{27,28,31,53} With the idea of using micelles as enzymes mimics,²⁸ it may be useful to study amino acid reactivity in micelles, to look for another link between micellar and enzymatic catalysis.

Following work on the catalysis by cetyltrimethylammonium bromide (CTAB) micelles of the hydrolysis⁵⁸ (Chapter V), thiolysis⁵⁹ (Chapter VI) and aminolysis (Chapter VII) of *p*-nitrophenyl alkanoate esters, we chose to study the aminolysis of these esters by amino acid anions ($\text{R-CH(NH}_2\text{)CO}_2^-$). These nucleophiles were chosen to probe the combined effect of their negative charge and hydrophobicity. The entry of the amino acid anions into the cationic CTAB micellar pseudo-phase should be facilitated by their anionic charge, as well as by the alkyl group R- *if it is hydrophobic*. These two features, ion exchange and hydrophobicity, should therefore affect the magnitude of catalysis by the micelles for ester cleavage by the amino acid anions. In support of this proposal, we point out that we have found that the cleavage of *p*-nitrophenyl acetate (pNPA) by glycinate anion ($\text{NH}_2\text{CH}_2\text{CO}_2^-$) has a catalytic ratio, $k_{\text{cN}}/k_{\text{N}}$, of 1.7, as compared with a value of 0.25 for neutral *n*-propylamine ($\text{NH}_2\text{CH}_2\text{CH}_2\text{CH}_3$). This difference seems to indicate a significant enhancement due to the negative charge. We have also found that increasing the chain length of *n*-alkylamines (NH_2R) leads to greater catalysis of pNPA cleavage in CTAB micelles (Chapter VII), and we have attributed this improvement to

increased amine hydrophobicity, leading to better amine partitioning into the micellar pseudo-phase.

We also saw in the study of aminolysis by a long amine (*n*-hexylamine) of longer esters in CTAB micelles, the hydrophobic binding of the alkylamino and/or the acyl chain is *decreased* in the transition state, relative to their micellar binding in the initial state, causing the magnitude of catalysis to decrease with ester chain length. We now would like to see if these results extend to amino acid anions ($\text{R-CH(NH}_2\text{)CO}_2^-$) with varying R- groups, and what effect, if any, does the anionic charge have? Will the magnitude of catalysis for amino acid ion cleavage of the esters be independent of the acyl chain length, as it was for the hydrolysis and thiolysis studies, or will catalysis be affected by the chain length of the ester, as it was for the aminolysis study?

The mechanism of ester cleavage by amino acid anions is not appreciably different from the mechanism of aminolysis of the esters (Scheme 7.1, page150). For all cases, except cysteine, under basic conditions, the deprotonated amino group of the amino acid is the nucleophile. Here also, the nucleophilic attack of the amine on the ester bearing a good leaving *p*-nitrophenoxide ion is rate limiting.^{38,332}

Briefly, introducing some work by other researchers, about the interaction of amino acids with CTAB micelles and other colloids, such as “reverse micelles” (below), will help later on in the discussion of our own results. Forgacs and coworkers^{364,365} studied the binding of amino acids to CTAB, using charge-transfer, reversed-phase thin-layer chromatography, and they concluded that “the hydrophobicity of the amino acid side chains significantly influenced the strength of interaction”. In relation to enzyme binding Subramanian *et al.*³⁶⁶ studied the binding of the enzyme lysozyme to CTAB at

various surfactant concentrations, and they concluded that hydrophobic interactions between the detergent and the aromatic amino acid residues in lysozyme contribute more to the binding strength than electrostatic interactions, which play only a minor role. Yamashita and coworkers³⁶⁷ showed that micelles shift the equilibrium constants for the ionization of amino acids, and the shifts depends on the total charge of the amino acid; however, this micellar effect is weaker than that found for amines. Cardoso *et al.*³⁶⁸ and Leodidis *et al.*³⁶⁹⁻³⁷¹ discussed the driving forces involved in amino acid solubilization in cationic “reverse micelles”, and they found that with small amino acids it depends on the charge (because of ion-exchange) but with more hydrophobic amino acids, their hydrophobicity is important.

To elaborate further on these studies, which we will discuss in more detail later, we determined the effect of CTAB micelles on the reactivity of amino acid anions (AA^-) towards *p*-nitrophenyl acetate (pNPA) and its hexanoate (pNPH). We studied the extent of ‘catalysis’ and its correlation to structural variations of a homologous series of amino acid anions, varying the group R in $R-CH(NH_2)CO_2^-$. To the best of our knowledge, the reaction of AA^- with alkanoate esters, their transition state binding, and interactions with CTAB micelles have not been studied systematically before. However, a study of the reaction mediated by cyclodextrins was conducted before in this laboratory⁵⁶ and in another.³⁷²

8.2 RESULTS

Kinetic experiments and data analysis for the cleavage of pNPA and pNPH by a number of amino acid anions (AA^-) were conducted in much the same way as for

micelle-mediated ester cleavage by thiolate anions (Chapter VI) and *n*-alkylamines (Chapter VII). Pseudo-first order rate constants obtained at various concentrations of amino acids in the presence and absence of CTAB (see Appendix D), were analysed, as before, to yield rate constants for the reaction of the AA^- with free and CTAB-bound ester (see Chapter VI, Section 6.2, for the detailed kinetic model). For comparative purposes, the bulk medium was the same aqueous carbonate buffer of pH 10.6, with constant total bromide ion concentration of 5.0 mM, as used for the thiolysis and aminolysis studies. The pK_{a} s of the acid groups of the amino acids are between 1.7 and 3, and the pK_{a} s of the ammonium groups range from 8.6 to 10, and so at pH = 10.6 the amino acids are largely ionized, as their anions, $\text{NH}_2\text{CHRCO}_2^-$.

The cleavage of pNPA and pNPH by AA^- in the absence of CTAB show a linear dependence of k_{obs} on $[\text{amino acid}]_0$ (eg. Figure 8.1), as required by equation [6.6] (as

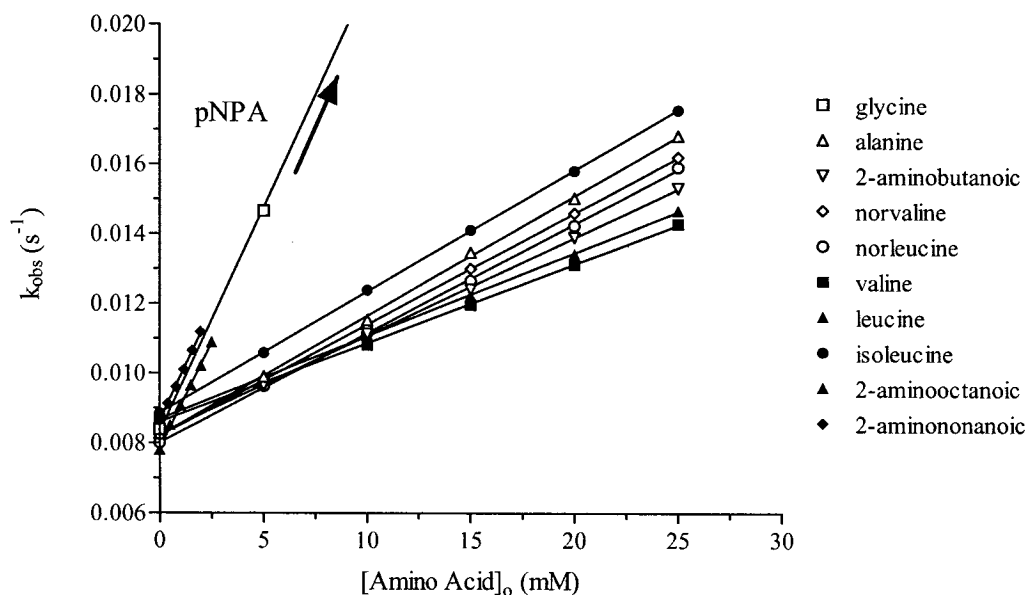


Figure 8.1 Observed rate constants for pNPA cleavage vs. the $[\text{amino acid}]$ in the absence of CTAB. The data for glycine extend up to $k_{\text{obs}} = 0.0403 \text{ s}^{-1}$ at $[\text{amino acid}] = 25 \text{ mM}$. Similar data were found for pNPH.

derived in Chapter VI, page 127). The second order rate constants (k_N) for the cleavage of the free esters by the amino acid and the first order rate constants (k_u) for ester cleavage in the buffer are presented in Table 8.1.

Table 8.1 First order rate constants (k_u) and second order rate constants (k_N) for cleavage of *p*-nitrophenyl acetate (pNPA) and *p*-nitrophenyl hexanoate (pNPH) by the buffer solution and by the amino acid anions (AA^-) respectively. ^{a, b}

Amino Acid	$k_u, (s^{-1})$		$k_N, (M^{-1} s^{-1})$	
	pNPA	pNPH	pNPA	pNPH
Cysteine	0.00900	0.00528	9.78 ± 0.08	5.70 ± 0.03
Serine	0.00936	0.00488	0.0825 ± 0.006	0.0361 ± 0.0017
Histidine	0.00790	0.00418	0.486 ± 0.15	0.307 ± 0.011
Glycine	0.00839	0.00406	1.29 ± 0.01	0.552 ± 0.006
Alanine	0.00827	0.00429	0.343 ± 0.004	0.134 ± 0.004
2-Aminobutanoic	0.00829	0.00461	0.281 ± 0.002	0.107 ± 0.007
Norvaline	0.00824	0.00477	0.319 ± 0.001	0.121 ± 0.003
Valine	0.00866	0.00494	0.226 ± 0.002	0.0786 ± 0.0028
Norleucine	0.00801	0.00457	0.313 ± 0.003	0.156 ± 0.004
Leucine	0.00875	0.00463	0.238 ± 0.003	0.0909 ± 0.0044
Isoleucine	0.00885	0.00470	0.348 ± 0.001	0.144 ± 0.028
2-Aminooctanoic	0.00782	0.00414	1.21 ± 0.019	0.577 ± 0.031
2-Aminononanoic	0.00872	0.00473	1.28 ± 0.033	0.551 ± 0.024

^a At 25 °C, in 0.10 M aqueous carbonate buffer of pH 10.6, with $[NaBr] = 5.00$ mM.

^b The structures of the amino acids are given in Table 8.2.

At pH 10.6, the k_u values are as expected knowing that the second order rate constant for hydroxide ion attack on pNPA ranges from $11 - 13 M^{-1} s^{-1}$. The k_N values found for reaction of the pNPA and pNPH with the amino acid anions ($NH_2CHRCO_2^-$) are comparable to those found earlier by our research group under different conditions (at

pH = 9.88 borate buffer).⁵⁶ Note that the k_N values are much higher for cysteine ($R = CH_2SH$) than the other amino acids because cysteine reacts through its thiolate ion ($R = CH_2S^-$) which is a more reactive nucleophile than an amine. For serine ($R = CH_2OH$), k_N is around 4 times smaller than for alanine ($R = CH_3$), presumably due to the electron-withdrawing inductive effect of the hydroxyl group, making the amine lone-pair less nucleophilic. As for histidine ($R = CH_2$ -Imidazolyl) reacting with pNPA, the k_N value at pH = 10.6 is much higher than the value found in a previous study at pH = 8.00 ($k_N = 0.0741 \text{ M}^{-1}\text{s}^{-1}$).⁵⁶ The large difference indicates that when both the α -ammonium group ($pK_a \sim 9$) and the imidazole moiety ($pK_a = 6.5$) are deprotonated, ester cleavage involves attack by the α -amino group and not the imidazolyl group. In support of this assertion, the k_N values for histidine with pNPA and pNPH are comparable to those for most of the other amino acids.

The k_N values for amino acids ions with simple alkyl substituents, in a homologous series, show little variation with structure and chain length, and their k_N values are about 5 times smaller than k_N for glycine, due to normal steric factors. More noticeably with pNPH, the branched AA^- react slower than their *n*-alkyl counterparts. As observed with various other nucleophiles (Chapters V, VI, and VII), the k_N values for aminolysis of pNPH are roughly half those for pNPA for steric reasons.^{59,131}

We found that the k_N values for the 2-aminooctanoate and 2-aminononanoate anions are unexpectedly higher (about 4 times) than those with shorter alkyl chains. It is reasonable to initially assume that these two amino acid anions might be forming micelles, especially at the higher concentration.³⁷³ However, if that were the case, we would have expected to see a greater increase in the observed rate constant as the amino

acid concentration rises (upward curvature), but we did not. Since these two amino acids are uncommon, NMR studies were conducted to establish that they were the right compounds, and indeed it was confirmed that they were. A series of ^1H -NMR spectra was also taken with different concentrations of the pure form of 2-aminooctanoic acid (0.01 – 2.0 mM) in D_2O in order to monitor changes in the chemical shift that would be expected to occur at the critical micelle concentration (*cmc*). But, the ^1H -NMR chemical shifts did not show any significant change with concentration, which leads us to believe that micellization is not taking place. In the presence of pNPA, the NMR chemical shifts for 2-aminooctanoic acid did not change. In the presence of pNPH, it was hard to detect change because the chemical shifts of the amino acid alkyl group and the ester hexanoyl group overlapped. Another possible explanation for the higher than expected rate constant for the reaction between the esters and the longer chain AA^- is that these reactants are brought closer together in solution by hydrophobic interactions between them. Such interaction may occur either between the aromatic group of the ester and the alkyl chain of the AA^- or between the alkyl chains of both reactants.

In the presence of a fixed concentration of CTAB ($= 5.0 \text{ mM}$), the variation of k_{obs} with $[\text{amino acid}]_0$ is also linear over the concentration range used for the amino acid anions (AA^-) reacting with pNPA (Figure 8.2), as it is for some of them reacting with pNPH (Figure 8.3). However, for pNPH and AA^- of 5 carbons and more, the observed rate constants showed little variance with the concentration of the amino acid (Figure 8.3). Where possible, the second order rate constants (k_{cN}) for the AA^- cleavage of the CTAB-bound ester were estimated as before (Chapter VI), and these values are collected in Table 8.2 and 8.3, along with other parameters.

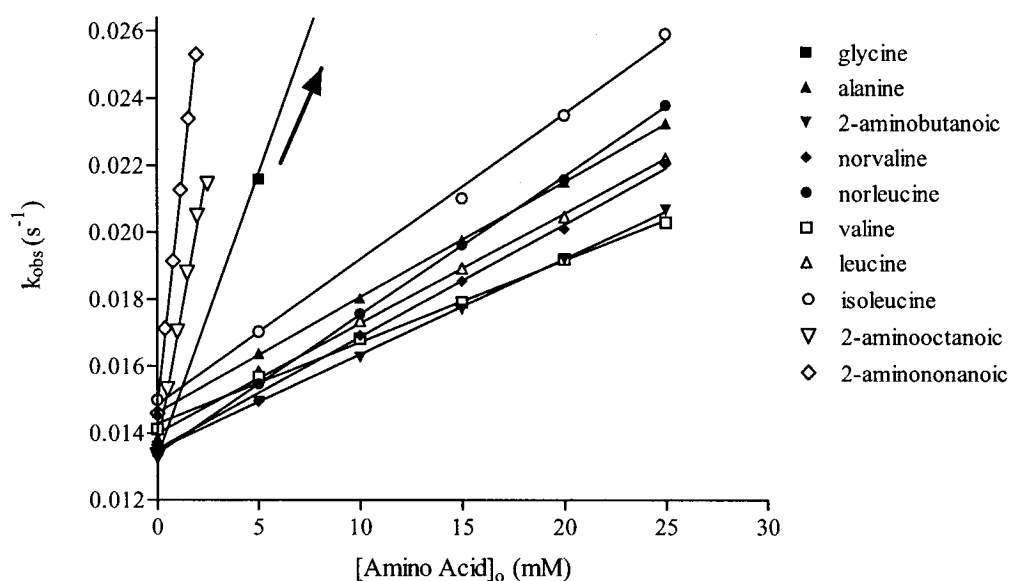


Figure 8.2 Observed rate constants for pNPA cleavage vs. [amino acid] in the presence of 5.0 mM CTAB. The data for glycine extend to $k_{\text{obs}} = 0.0553 \text{ s}^{-1}$ at [amino acid] = 25 mM.

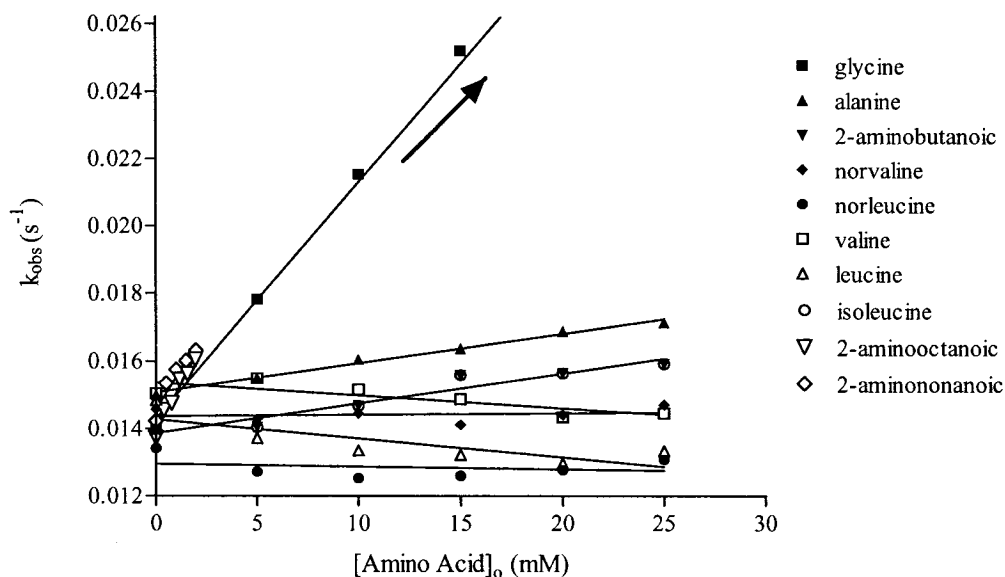


Figure 8.3 The observed rate constant for pNPH cleavage vs. [amino acid] in the presence of 5.0 mM CTAB. The data for glycine extend to $k_{\text{obs}} = 0.0315 \text{ s}^{-1}$ at an [amino acid] = 25 mM. Unlike in Fig. 8.2, k_{obs} did not vary much or even decreased somewhat for a few amino acids reacting with pNPH.

Table 8.2 Constants for the cleavage of *p*-nitrophenyl acetate (pNPA) by amino acids in the presence of CTAB.^a

Amino Acid, NH ₂ CH(R)COOH	R-	k _{cN} M ⁻¹ s ⁻¹	k _{cN} /k _N	K _{TS} mM
Cysteine	HSCH ₂ -	812 ± 17	83.0 ± 1.0	0.296
Serine	HOCH ₂ -	0.0764 ± 0.036	0.926 ± 0.400	27
Histidine	Im-CH ₂ -	3.47 ± 0.15	7.23 ± 0.15	3.40
Glycine	H-	2.12 ± 0.08	1.64 ± 0.01	15.0
Alanine	CH ₃ -	0.349 ± 0.01	1.02 ± 0.02	24.2
2-Aminobutanoic	CH ₃ CH ₂ -	0.298 ± 0.023	1.06 ± 0.07	23.2
Norvaline	CH ₃ (CH ₂) ₂ -	0.411 ± 0.052	1.29 ± 0.16	19.1
Valine	(CH ₃) ₂ CH-	0.330 ± 0.039	1.46 ± 0.16	16.8
Norleucine	CH ₃ (CH ₂) ₃ -	0.913 ± 0.015	2.92 ± 0.02	8.43
Leucine	(CH ₃) ₂ CHCH ₂ -	0.778 ± 0.032	3.27 ± 0.15	7.53
Isoleucine	CH ₃ CH ₂ (CH ₃)CH-	0.878 ± 0.102	2.52 ± 0.28	9.75
2-Aminooctanoic	CH ₃ (CH ₂) ₅ -	13.8 ± 0.9	11.4 ± 0.6	2.16
2-Aminononanoic	CH ₃ (CH ₂) ₆ -	26.2 ± 0.6	20.5 ± 0.1	1.20

^a At 25 °C, in an aqueous carbonate buffer of pH 10.6, with [Br⁻]_{total} = 5.00 mM.

^b The value of the dissociation constant for pNPA-CTAB complex, K_S = 24.6 mM, are taken from earlier work (Table 6.2).⁵⁹

^c K_{TS} = (k_N/k_{cN}) K_S

A few experiments were conducted with the amino acid tryptophan, and a distinct downward curvature of the data was observed each time for reaction in the presence of CTAB. This means that tryptophan is binding strongly and more deeply to CTAB micelles than the other amino acids,³⁷⁴ and so a different and more complex kinetic model, which allows for tryptophan binding, is required to analyze its kinetic data.

Table 8.3 Constants for the cleavage of *p*-nitrophenyl hexanoate (pNPH) by amino acid anions in the presence of CTAB.^a

Amino Acid	Number of carbons	k_{cN} $M^{-1} s^{-1}$	k_{cN}/k_N	K_{TS} mM
Cysteine	-	357 ± 8	62.6 ± 1.0	0.006
Serine	-	0.0164 ± 0.0028	0.454 ± 0.006	0.82
Histidine	-	2.23 ± 0.09	7.26 ± 0.04	0.051
Glycine	2	0.712 ± 0.017	1.29 ± 0.02	0.290
Alanine	3	0.0833 ± 0.005	0.622 ± 0.019	0.602
2-Aminobutanoic	4	0.0873 ± 0.0133	0.819 ± 0.68	0.457
Norvaline	5	ND ^c	-	-
Valine	5	ND	-	-
Norleucine	6	ND	-	-
Leucine	6	ND	-	-
Isoleucine	6	ND	-	-
2-Aminooctanoic	8	0.918 ± 0.095	1.59 ± 0.08	0.252
2-Aminononanoic	9	1.19 ± 0.19	2.17 ± 0.25	0.161

^a At 25 °C, in an aqueous carbonate buffer of pH 10.6, with $[Br^-]_{total} = 5.00$ mM.

^b The value of the dissociation constant for pNPH-CTAB complex, $K_S = 0.374$ mM, are taken from earlier work (Table 6.2).⁵⁹

^c The k_{cN} values were not determined (ND) because of the insufficient changes in k_{obs} with [amino acid].

^d $K_{TS} = (k_N/k_{cN}) K_S$

In order to get a better appreciation for the data, Figures 8.4 to 8.6 present a clearer view of the effects of CTAB micelles on the observed rates of the reaction of the esters with some representative amino acid anions. Figure 8.4 shows data for the cleavage of pNPA and pNPH by the anion of histidine in the presence and absence of CTAB. For both esters, it is clear that the CTAB-bound form of ester is more reactive than the unbound form ($k_{cN} > k_N$). Similar trends in the data were obtained for cleavage by cysteine (see Appendix B).

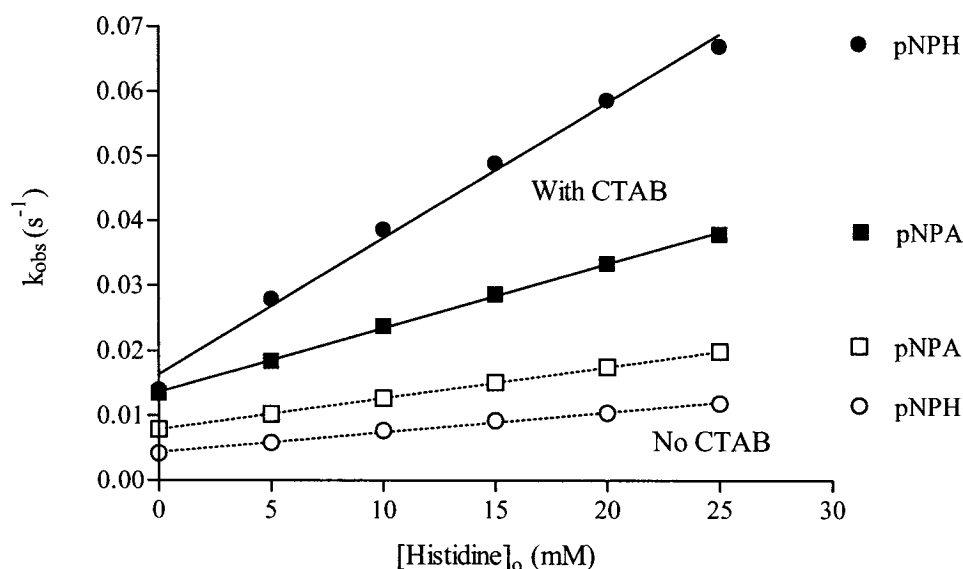


Figure 8.4 CTAB catalyzes the reaction between pNPA or pNPH with histidine. The slope of the lines through the open symbols (no CTAB) equals to k_N . The slope of the lines through the solid symbols (5.0 mM added CTAB) are $(k_N K_S + k_{cN}[\text{Surf}]) / (K_S + [\text{Surf}])$. For both pNPA and pNPH, $k_{cN} > k_N$.

Figure 8.5 illustrates the effect of CTAB on the reaction between pNPA and the amino acids: norleucine (2-aminohexanoic acid), norvaline (2-aminopentanoic acid), and 2-aminobutanoic acid. Without CTAB, there is very little difference in the rate constants k_N for the three amino acids (their plots overlap), but with CTAB the observed rate constants increase with alkyl chain length of the amino acid, reflecting an increase in the rate constants k_{cN} . A small amount of catalysis is observed ($k_{cN}/k_N \geq 1$) and it increases moderately in proportion to k_{cN} , since k_N is basically constant.

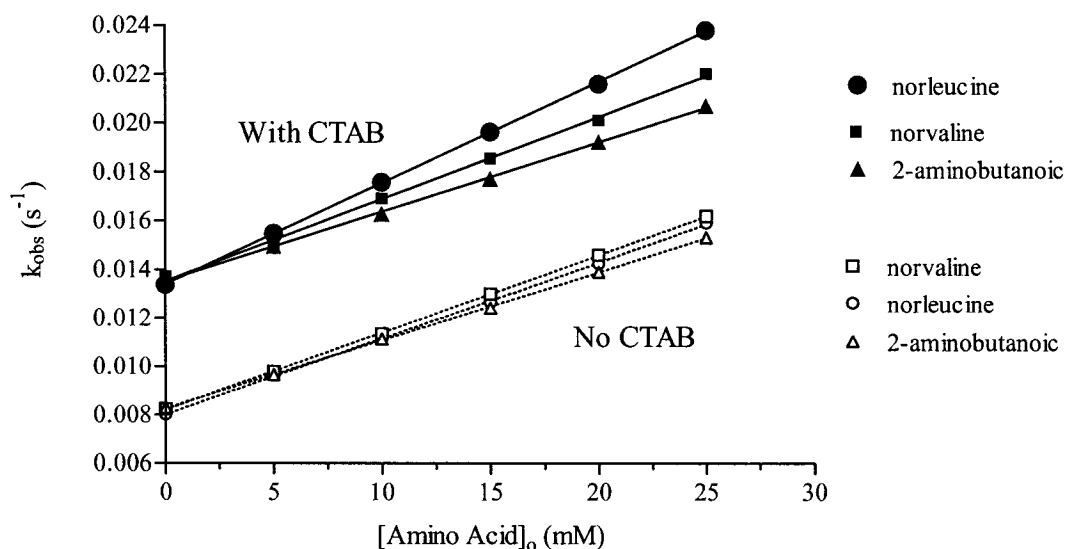


Figure 8.5 CTAB catalyzes the reaction between pNPA and the anions of the amino acids: norleucine (2-aminohexanoic acid), norvaline (2-aminopentanoic acid), and 2-aminobutanoic acid. The ratio $k_{cN}/k_N (\geq 1)$ increases moderately with chain length.

Figure 8.6 shows data for the cleavage of the two esters, pNPA and pNPH, by just norvaline, in the presence and absence of CTAB. For pNPA, the lines are parallel and thus $k_{cN} \approx k_N$. In the case of the reaction of pNPH in the presence of CTAB, there is a hardly a change in the observed rate constant with [norvaline], and so k_{cN} cannot be accurately estimated. Similar results were obtained for valine, norleucine, leucine, isoleucine reacting with pNPH. Our interpretation of the results in Figure 8.4 to 8.6 will be discussed in detail in the next section.

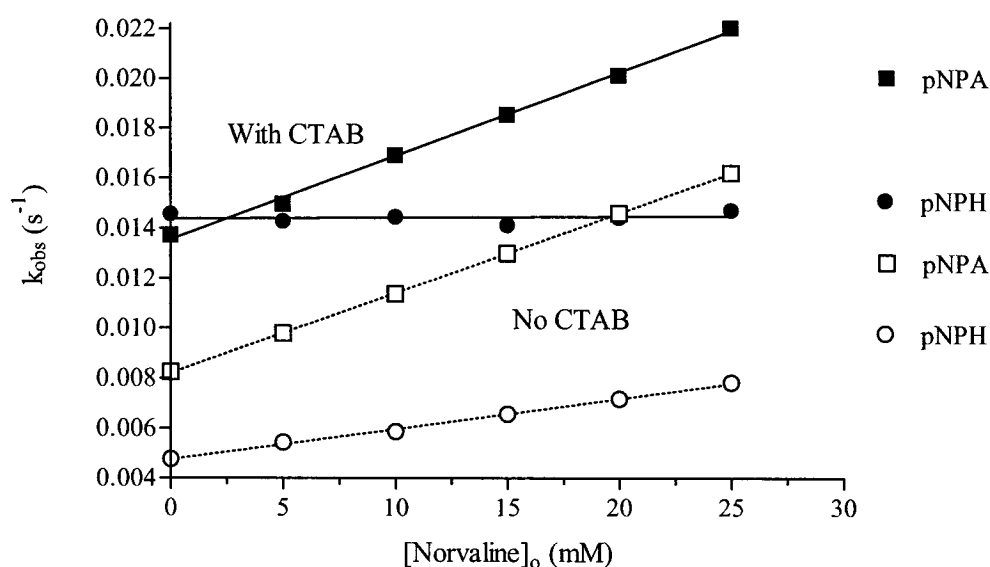


Figure 8.6 The change in the observed rate constant vs. [norvaline], for the cleavage of pNPA and pNPH in the presence of CTAB (closed symbols) and in the absence of CTAB (open symbols).

8.3 DISCUSSION

8.3.1 Amino Acid Anions Ion-Exchange and Partition into CTAB Micelles

Under the basic reaction conditions, the amino acids are anionic ($\text{NH}_2\text{CHR}\text{CO}_2^-$), and ion exchange between them and bromide ions, which are in the Stern layer of CTAB micelles, contributes to their transfer into the micelles. In support of this idea, CTAB retards the aminolysis of pNPA by *n*-propylamine ($k_{\text{cN}}/k_{\text{N}} = 0.25$) and by *n*-butylamine ($k_{\text{cN}}/k_{\text{N}} = 0.83$) but it does not retard the reaction of pNPA with $\text{CH}_3\text{CH}_2\text{CH}(\text{COO}^-)\text{NH}_2$ ($k_{\text{cN}}/k_{\text{N}} = 1.1$) or $\text{CH}_3(\text{CH}_2)_2\text{CH}(\text{COO}^-)\text{NH}_2$ ($k_{\text{cN}}/k_{\text{N}} = 1.3$). It is reasonable, therefore, to conclude that the presence of the carboxylate anion group is assisting the entry of the AA^- into the micellar pseudo-phase proximal to where the ester is bound. But that is not the only factor that determines the magnitude of catalysis as the results clearly show that amino acid *hydrophobicity* also plays a major role, as with amines.

As mentioned in Chapter VII, coefficients for the partitioning or distribution of organic solutes between micelles and water correlate well for those between octanol and water, with slopes ~ 0.9 in log-log plots (e.g. Figure 7.7, page 166), although exceptions do exist.^{353-355,369,375} Recall also that for the reaction of pNPA with alkylamines in CTAB micelles, we found that the slope of the line between the $\log k_{cN}/k_N$ and $\log P_{o/w}$ is 0.94 for *all* the *n*-alkylamines (Figure 7.8, page 167). These good correlations, with slopes near 1.0, mean that the hydrophobicities of the amines and/or their solubilities in the micelles are dominant factors that determine the magnitude of catalysis. With the amino acids in this Chapter, there is only a moderate correlation between catalysis of their reactions and their partition coefficients (Figure 8.7). The difference in the $\log (k_{cN}/k_N)$ vs. $\log P_{o/w}$ plots for the amines and amino acid anions reacting with pNPA must in some way reflect the charge effect.

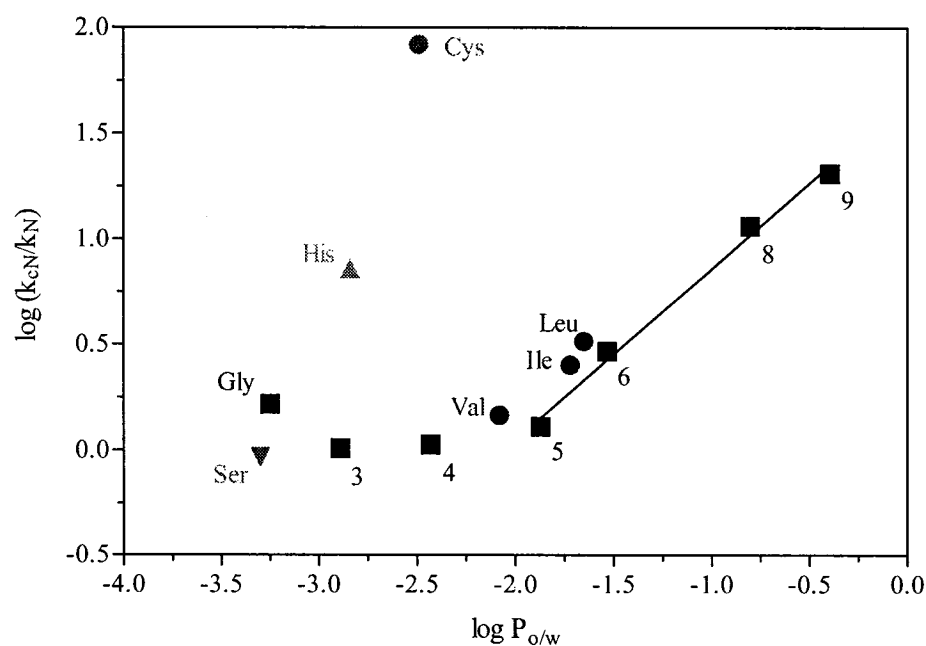


Figure 8.7 The reactivity ratio for pNPA cleavage depends on amino acid hydrophobicity ($\log P_{o/w}$) and charge effects.

Table 8.4 Derived constants for the cleavage of *p*-nitrophenyl acetate (pNPA) and hexanoate (pNPH) by amino acids in the presence of CTAB.

Amino Acid	Log $P_{o/w}$ for amino acids ^a	pNPA		pNPH	
		log k_{cN}/k_N	pK_{TS}	log k_{cN}/k_N	pK_{TS}
Cysteine	-2.49	1.92	3.53	1.80	5.22
Serine	-3.30	-0.0334	1.58	-0.343	3.08
Histidine	-2.84	0.859	2.47	0.861	4.29
Glycine	-3.25	0.216	1.82	0.111	3.54
Alanine	-2.89	0.00753	1.62	-0.206	3.22
2-Aminobutanoic	-2.43	0.0255	1.63	-0.0867	3.34
Norvaline	-1.87	0.110	1.72	-	-
Valine	-2.08	0.164	1.77	-	-
Norleucine	-1.53	0.465	2.07	-	-
Leucine	-1.65	0.514	2.12	-	-
Isoleucine	-1.72	0.402	2.01	-	-
2-Aminooctanoic	-0.801	1.06	2.67	0.202	3.60
2-Aminononanoic	-0.393	1.31	2.92	0.336	3.79

^a Values for Log $P_{o/w}$ are taken from Pliska *et al.*,³⁷⁶ except for 2-aminooctanoic, and 2-aminononanoic acid. See the Experimental section 8.5 for a discussion of the controversy of log $P_{o/w}$ for the amino acids.

The logarithms of the reactivity ratio (log k_{cN}/k_N) for pNPA reacting with the AA^- are proportional to log $P_{o/w}$ (Table 8.4) only for the longer amino acids (Figure 8.7). The slope of the line for amino acids having 5 carbons and higher, is 0.811 ± 0.048 ($r = 0.996$, $n = 4$) but the acceleration is essentially *independent* of log $P_{o/w}$ for the three AA^- with an alkyl group shorter than 4 carbon atoms. This means that there is a point at which there is a change-over in what factor plays a dominant role in determining the magnitude of catalysis by CTAB. For the longer amino acids, since the log (k_{cN}/k_N) correlate with log

$P_{o/w}$, with a slope of ~ 0.8 , their partitioning and hydrophobicity play a dominant role in the catalysis by CTAB micelles whereas for the shorter AA^- (eg. glycine) other factors, including steric factors and ion exchange, play a more vital role in the catalysis. In Figure 8.7, the points for the branched amino acids (Val, Ile, Leu) lie very close to the line defined by their linear counterparts which means that the catalytic ratios are not greatly affected by their branching, just their hydrophobicity. The situation with histidine, cysteine and serine will be considered separately, later.

In a series of papers, Leodidis and coworkers³⁶⁹⁻³⁷¹ studied the solubilization of amino acids in AOT (sodium di-(2-ethylhexyl)-sulfosuccinate) reverse micelles, and estimated partition coefficients for transfer between the micellar and aqueous phases. They stressed the importance of hydrophobic effects as the main driving force for interfacial solubilization of the amino acids. Comparing the free energy of transfer of amino acids from water to the micelle interface with a variety of existing amino acid hydrophobicity scales,^{377,378} they found the best correlation with $\log P_{o/w}$ values from Yunger³⁷⁹ and Pliska³⁷⁶, with slopes of about 0.9 but only for the more hydrophobic amino acids. From their studies Leodidis *et al.*³⁶⁹ concluded that for homologues of alanine “the amino acid side chain, even when it is completely hydrophobic, must contain at least three carbon atoms beyond the α -carbon for partition coefficients to be significantly larger than unity”.³⁶⁹ In a comparable way, we have found a good correlation between the magnitude of catalysis and $\log P_{o/w}$ values for the more hydrophobic amino acids. In our work, we note that the hydrophobicity of the amino acid starts to have a significant effect on catalysis when there are three carbon atoms in the alkyl chain (Figure 8.7). Leodidis *et al.*³⁶⁹ indicate that the order of amino acid binding

to AOT reverse micelles is tryptophan > phenylalanine > norleucine > leucine > norvaline > valine > 2-amino- butanoic acid; glycine, alanine and threonine are not in the order because they are so soluble in water that it was hard to quantify their binding. This order agrees with that which we found for the magnitude of catalysis for pNPA cleavage by the amino acid anions. Thus, binding of the amino acids to micelles and catalysis by CTAB are closely linked.

Our results are also comparable to those of Imamura and Konishi,³⁷⁴ who examined the influence of the hydrophobicity of the side chain residues and of charge on the binding affinities of tryptophan dipeptides (X-Trp, X-Trp-NH₂, where X = an amino acid residue) to sodium dodecylsulfate (SDS) micelles (Figure 8.8). The authors first pointed out that the tryptophan ring (indole) in SDS micelles, as in the membrane bilayers, is localized near the micelle-water interface. They found that the free energies of

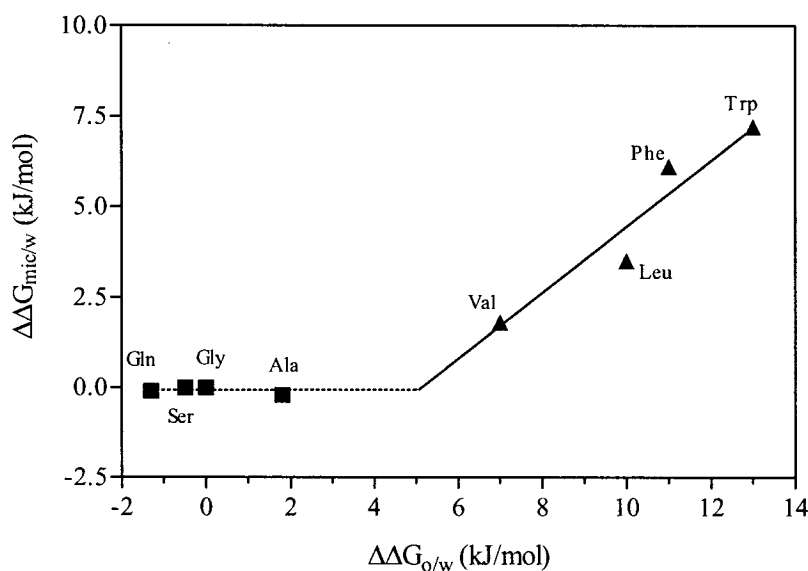


Figure 8.8 The relationship between the change in free energies ($\Delta\Delta G$) of transfer from SDS micellar to aqueous phase for X-Trp-NH₂ at pH 10.7, relative to X = Gly and those ($\Delta\Delta G_{o/w}$) of transfer from 1-octanol to water for acetyl-X-NH₂. The amino acid residues, X, are indicated on the figure.³⁷⁴

transfer of the more hydrophobic amino acids (such as X = Val, Leu) from SDS micelles to aqueous solution correlate with the free energies of transfer from 1-octanol to water for acetyl-X-NH₂, and the correlation line had a slope of unity (Figure 8.8).³⁷⁴ Like our results in Figure 8.7, the relationship between the free energies indicated that hydrophilic residues (such as Ser and Ala) apparently do not contribute to the binding ability of the dipeptides to the micelles.³⁷⁴

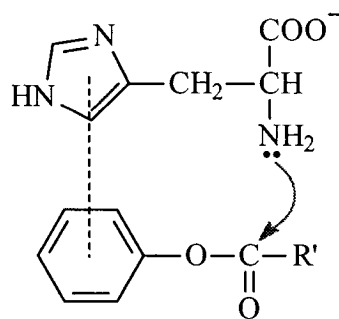
Now we will look at the cases of cysteine, serine, and histidine. These amino acid ions are at the lower end of the octanol/water partition scale (Figure 8.7), being very hydrophilic, and thus ion exchange must be the main force for the amino acid ion transfer into the micelles. The $\log (k_{cN}/k_N)$ with these amino acid ions are more or less independent of the ester (pNPA or pNPH, Table 8.4), as was the case in the thiolysis and hydrolysis studies (Chapter V, VI), and the reasons for this will be discussed when we look at the transition state binding.

For cysteine, good ion exchange results in the much higher magnitude of catalysis by micelles. At pH = 10.6 cysteine exists and reacts as its *dianion* (thiolate ion and carboxylate ion). This dianion exchanges very well with bromide ions of Stern layer of CTAB micelles because it involves a hydrophobic thiolate ion, and its double negative charge leads to added columbic attractions to the ammonium cationic head groups of the CTAB micelles (Chapter VI).

With serine, the CTAB-bound form of the ester is much less reactive than the unbound form, and the overall reaction is retarded ($\log k_{cN}/k_N < 0$). Presumably, because serine is more hydrophilic than alanine, with a hydroxymethyl group in place of the methyl group, it is partitioned more poorly into the micelle. Unlike the -SH group of

cysteine ($pK_a = 8.3$), the -OH group of serine ($pK_a \sim 16$) is not ionized under the reaction conditions, and so there are no additional coulombic attractions contributing to the binding to the CTAB micelles.

Williams' research group has recently studied the reactivity of imidazole towards pNPA and pNPH in CTAB (and SDS) micelles, in a buffer of pH 7.04.⁶² They concluded that because imidazole is hydrophilic ($\log P_{o/w} = -0.08$) it partitions poorly into the micelles and so the reaction, which takes place in the Stern layer, is overall *retarded* by CTAB micelles.⁶² By contrast, in our work, where the buffer pH = 10.6, the reactions of pNPA and pNPH with histidine are *catalyzed* by CTAB micelles. As we noted before, these reactions are with the histidine *anion* and take place on its α -amino group, not on its imidazole moiety. Consequently, we conclude that the negative charge on the histidine anion helps its transport into the CTAB micellar pseudo-phase. However, this argument does not explain why the catalytic ratio, which is ~ 7 for both pNPA and pNPH, is higher than for almost all other amino acid anions, regardless of hydrophobicity. Since the reaction is taking place in the Stern layer with the alkyl group of ester oriented (or bound) in the micellar core, the micelles may be assisting in the alignment of the aromatic ring and the imidazole ring in such a way that π - π interactions are possible (as illustrated below).



CTAB micelles have different effects on the reaction between pNPH and the AA^- , and these depend on the amino acid side chain. The reaction is catalyzed when the nucleophile is the anion of cysteine, histidine, or glycine, and the two longest alkyl chain AA^- (Tables 8.3 and 8.4), whereas it is retarded ($k_{cN}/k_N < 1$) when it is with short alkyl chain AA^- . Furthermore, the reaction with AA^- of intermediate chain lengths (5 to 7 carbons) was not detected in the presence of CTAB micelles. If we are merely looking at partitioning of the amino acids into the micelles as the determining factor for catalysis, then we would have expected the reaction with the more hydrophobic long chain amino acids to be even more catalyzed by CTAB (as it is with alkylamines), because the pNPH ester is relatively tightly bound to the micelle and so both the ester and the amino acid are concentrated and confined in the micelle pseudo-phase. We believe these results can be best described by looking at the attainment of the transition state for the reaction and the mode of transition state binding to CTAB micelles, as will be discussed in the next section (Section 8.3.2).

8.3.2 Transition State Binding (pK_{TS}) varies with Amino Acid Anion Chain and Ester Chain

Our usual approach to discussing the mechanism of reactions in micelle-mediated processes involves explicit consideration of transition state (TS) binding and its variation with structure of the reactants. The strength of transition state binding (measured by pK_{TS}) for pNPA reacting with the series of anions of amino acids, ranging from alanine (C3) up to 2-aminononanoic (C9), increases with the number of carbon atoms in the chain but the increase is *biphasic* (Figure 8.9). The slope of the line with the shorter AA^- is only 0.050 ± 0.023 ($r = 0.908$, $n = 3$). This means that the strength of transition state

stabilization (pK_{TS}) is almost independent of the length of the carbon chain for the short AA^- , which indicates that in the TS, the alkyl group (R) of those amino acids is not bound to the micellar core.

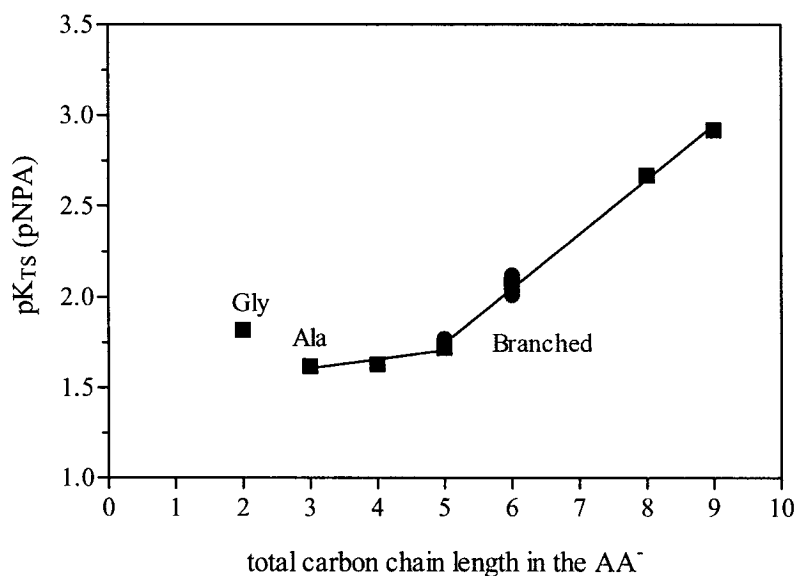


Figure 8.9 The transition state binding for pNPA + amino acid anions. The values of pK_{TS} is almost independent of the short amino acid chains (C3 - C5) but is directly proportional to the chain length of the longer amino acids (C5 - C9).

By contrast, the slope of the line for the longer amino acid anions (5 or more carbons) is 0.300 ± 0.011 ($r = 0.998$, $n = 4$), with the points for the three branched AA^- falling directly on the line. This means that there is a greater dependence of pK_{TS} on the chain length of the longer AA^- , but the slope of the line is lower than those normally corresponding to the free energy of stabilization due to hydrophobic effects.^{65,75} For example, for the aminolysis of pNPA, the slope of pK_{TS} vs. amine chain length is 0.49 (Figure 7.9, page 171), and for the hydrolysis and thiolysis studies, the slopes of pK_{TS} vs. ester chain length are about 0.4 for all nucleophiles (Table 6.3, page 137). These slopes fall in the range expected for the free energy of hydrophobic stabilization per methylene

group (Chapter VII).^{65,75} The differences in the slopes indicates that not only hydrophobic interactions between the alkyl chain (R) of the longer AA⁻ and the micellar core contribute to TS stabilization, but also that the negative charge of the carboxylate group of the amino acids attenuates this stabilization. It is plausible that by increasing the alkyl length of the side chain of the amino acid far enough from the carboxylate group, which is strongly solvated, hydrophobic interactions will become dominant and, perhaps, eventually mask the charge effect.

The strength of transition state binding for the reaction with pNPH is greater than that with pNPA for *all* AA⁻ that we were able to measure k_{cN} values (Table 8.4, Figure 8.10). This is due to the stronger binding of the acyl chain of the hexanoate ester to the micellar hydrophobic core providing additional stabilization in the TS as it does in the initial state. From the solid diagonal line in Figure 8.10, whose slope is equal to 0.998,

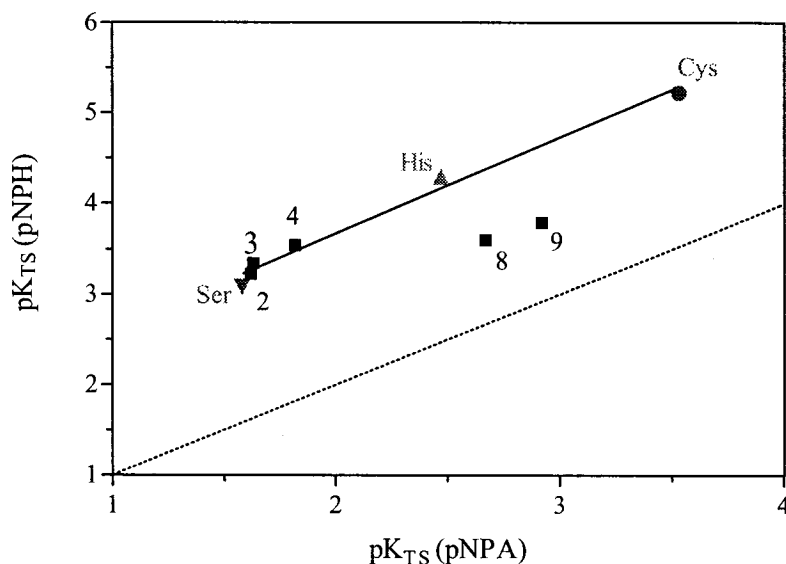


Figure 8.10 Relation between the strength of transition state binding (pK_{TS}) for the reaction of amino acid anions with pNPH and pNPA in CTAB micelles. The slope is essentially one and the values of pK_{TS} with pNPH are greater than those with pNPA (all points are above the dotted line $pK_{TS}(pNPA) = pK_{TS}(pNPH)$).

one can suggest that for the two esters (pNPA and pNPH) reacting with the *shorter* AA⁻ (along with cysteine, histidine and serine) the mode of TS binding is essentially *independent* of the amino acid.

It should be recalled that in the hydrolysis and thiolysis studies (Chapters V and VI) the strength of transition state binding (pK_{TS}) varied linearly with ester chain length (n), and the line is *parallel* to the variation of initial state binding (pK_S) with n (see Figure 6.4, page 136). From this finding it was concluded that the mode of TS binding is *similar* to that of initial state binding, with the acyl chain of the ester bound in the CTAB micellar core while the carbonyl group and aromatic ring remain in the Stern layer. Moreover, the anionic nucleophiles are freely mobile in the Stern layer and able to attack the bound esters easily, not significantly altering the mode of binding of the ester. We believe that the results with the *shorter* AA⁻ reacting with pNPA and with pNPH also fit this model in which the TS binding of the acyl chain of the two esters is similar to initial state binding of these esters, and *independent* of the loosely-bound nucleophile.

As in the aminolysis studies (Chapter VII), the reactivity and mode of transition state binding of pNPA and pNPH differ from one another when the esters are reacting with longer, more hydrophobic amino acid anions. We propose that for pNPH to react with the hydrophobic AA⁻ which are also bound to the micelle in the initial state, either the hexanoyl chain of pNPH or the n -alkyl chain of the AA⁻ must unbind (to some extent) in order to achieve the *optimal geometry* for the reaction to proceed and for the TS to form in the micelle (cf. Scheme 7.3 in Chapter VII, page 176). In the case of average length amino acids (C5 – C7), linear or branched, it was difficult to estimate k_{CN} , or outright inhibition occurs, probably because both reactants are bound to the micelle

with similar strengths in the initial state, such that neither acyl nor the alkyl chain of the amino acid wants to forfeit hydrophobic binding to the micellar core. In the case of the two longest AA⁻ (C8 and C9), where catalysis is again seen: $k_{cN}/k_N = 1.6$ and 2.2, it is possible that the hydrophobic interaction of these AA⁻ with the micellar core is stronger than that of pNPH, and the reaction can proceed because the contribution to transition state stabilization from the hexanoyl chain of pNPH is diminished (Figure 8.10). In these cases, the mode of binding of pNPH in the TS is *not the same* as it is in the initial state, and it is *not independent* of the AA⁻.

8.3.3 Comparison of Amines and Amino Acid Anions

Here we take a closer look at the ratios k_{cN}/k_N for the amino acid anions (AA⁻) relative to those we found earlier for alkylamines. The logarithm of the reactivity ratio (k_{cN}/k_N) for short chain AA⁻ are higher than short amines (Figure 8.11) which we previously attributed to the anionic charge of the AA⁻ assisting in the transfer of the nucleophile into the micelles. However, the ratios k_{cN}/k_N are larger for the longer amines than for the longer AA⁻ (Figure 8.11). It is reasonable that when the nucleophile has a long chain that hydrophobic effects play a larger role in determining the magnitude of catalysis than electrostatic (ion exchange) effects. Alkylamines are more hydrophobic than amino acid anions of comparable size, and so they are expected to partition more effectively from the aqueous phase into CTAB micelles, as indeed they do (compare log $P_{o/w}$ values in Tables 7.5 and 8.4). Consequently, the reaction of long chain amines with CTAB-bound pNPA is catalyzed to a greater extent.

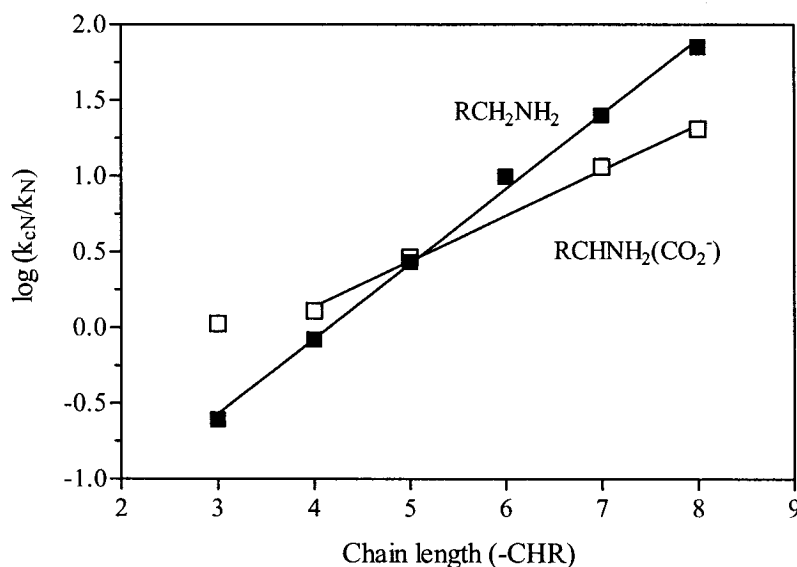


Figure 8.11 Comparison of the $\log(k_{cN}/k_N)$ for the cleavage of pNPA by amines ($R-CH_2-NH_2$) and amino acid anions ($R-CH(NH_2)(CO_2^-)$) of the same alkyl carbon chain length ($R-C-$).

The cross over between the two effects (hydrophobic effects and electrostatic/ion exchange effects) occurs at about 5 carbon atoms in the alkyl chain. It has been suggested that the side chains of glycine and alanine are smaller in size than a carboxyl group, while the *iso*-butyl group of leucine is larger than a carboxyl group.³⁷⁰ Therefore, it is also possible that with the larger amino acid anions, and especially the branched ones, the side chains shield the charge, such that hydrophobicity dominates over electrostatic effects. In conclusion, when hydrophobic effects govern nucleophile transfer into the micelles, the cleavage of pNPA by the amines is catalyzed more than is cleavage by AA^- , but when electrostatic effects control the transport then catalysis is greater for the AA^- .

Comparison of the catalytic ratios for the cleavage of pNPH by amines and amino acid anions in CTAB micelles is more complicated. While the ratios for amines show an overall gradual trend with increasing chain length (Table 7.3, Figure 7.8) those for AA^-

do not. It is unclear why for the reaction of pNPH with AA^- having 5 – 7 carbons, both branched and linear, the values of k_{cN} are essentially zero,^a whereas for the corresponding amines the k_{cN} values increase with chain length (Chapter VII). There may well be a difference in the way that the amines and the amino acid anions are held in the Stern layer of CTAB micelles, and this difference must be such that the hexanoate ester is readily attacked by micelle-bound amines but not by the AA^- , however they are bound. Presumably, the reactivity in CTAB micelles depends greatly on the *geometric demands* dictated by the formation of the transition state (cf. Scheme 7.3 in Chapter VII) and these demands may well be different for the two types of nucleophile.

8.4 CONCLUSIONS

The cleavage of pNPA and (to a lesser extent) of pNPH by amino acid anions (AA^-) is catalyzed by CTAB micelles because the AA^- can be transferred from the aqueous phase to micellar pseudo-phase. When the anions have short side chains, electrostatic effects (i.e. ion exchange) determines their transport into the Stern layer, and the reactions occur without altering the binding of the ester in the transition state (Figure 8.12 (a) and (c)). For amino acid anions with longer side chains, there exists a *threshold hydrophobicity* dictating the binding of the alkyl chain of the nucleophile to the core of CTAB micelles. This hydrophobic binding may assist in the transition state binding in the case of the short, weakly-bound acetate ester (Figure 8.12 (b)), but it hinders TS binding in the case of the longer, more strongly-bound hexanoate ester (Figure 8.12 (d)).

^a There was no significant variation of k_{obs} vs. $[\text{AA}^-]$ in the presence of CTAB (See Results and Fig. 8.6).

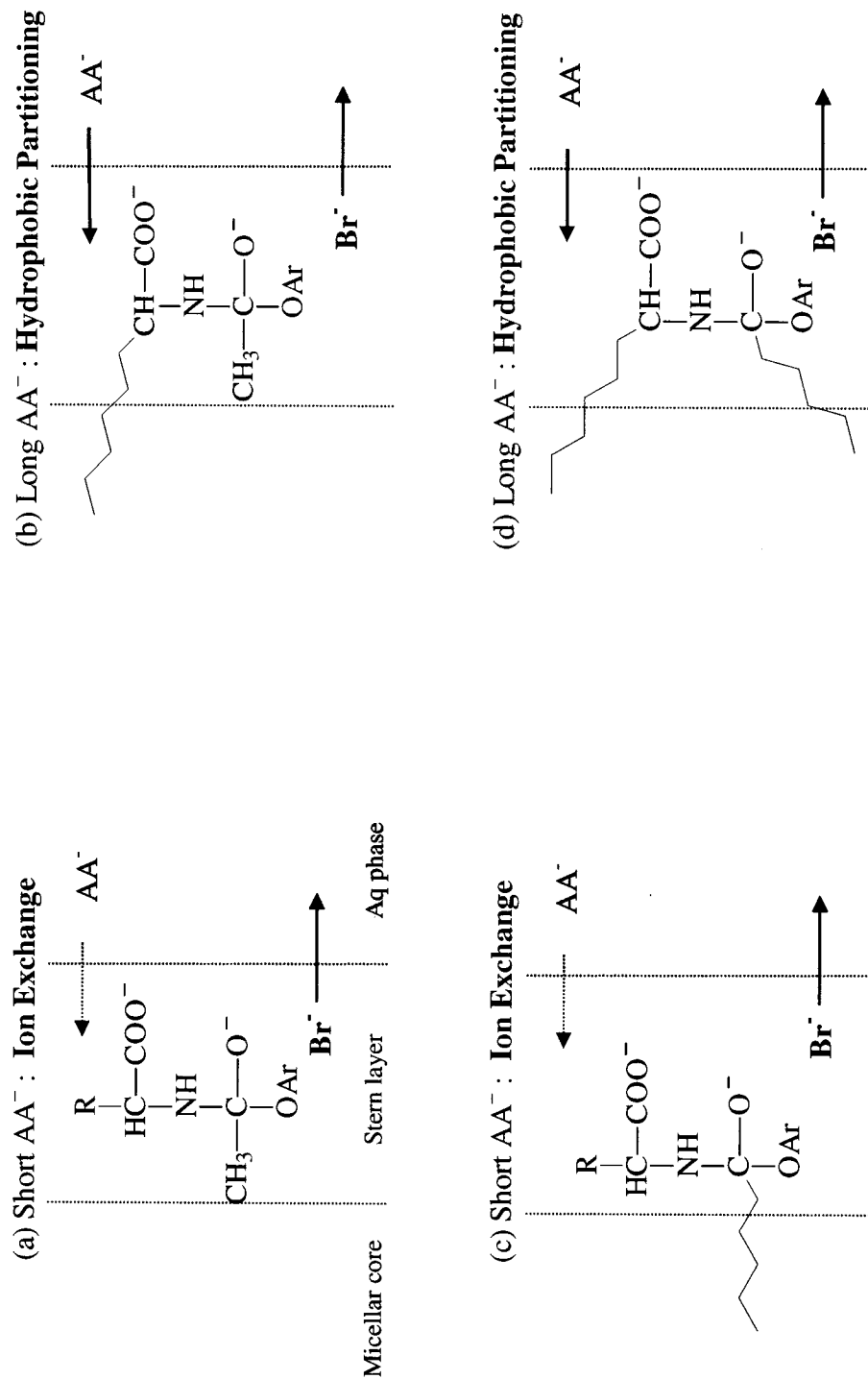


Figure 8.12 Transition State binding for the reaction of pNPA and pNPH with n-alkyl amino acid anions in CTAB micelles: (a, b) for a *weakly bound* short ester reacting with (a) short AA^- and (b) long AA^- , (c, d) for a *strongly bound* long ester reacting with (c) short AA^- and (d) long AA^- .

We recall Kirby's⁵³ proposal for the recognition of transition state by enzymes, which he divided into two components, "*passive binding*" and "*dynamic binding*" (see Chapter VI, Section 6.3.3). Such a framework can be used in the present discussion also.

(i) If the nucleophiles do not bind to the micellar core, as in the case of hydroxide ion, thiolate anions, and short chain amino acid anions, then the *passive component* of TS binding is *similar* to ester acyl chain binding, *independent* of the nucleophile, and it involves *hydrophobic interaction* of the *TS acyl chain* with the *hydrocarbon core* of CTAB micelle (Figure 8.12 (a) and (c)). (ii) If the nucleophiles do bind to the micellar core in the initial state, as in the case of long chain *n*-alkylamines and long chain amino acid anions, then the *passive component* of TS binding is *not similar* to ester acyl chain binding, and it is *dependent* on the nucleophile hydrophobicity. (iii) The *dynamic component* of TS binding is primarily associated with interactions accompanying *acyl transfer* in the *Stern layer*, and this component varies with the nucleophile since the ease of nucleophilic attack on the micelle-bound ester is greatly influenced by the extent of *ion exchange* or *hydrophobic partitioning* of the nucleophiles into the micelles.

8.5 EXPERIMENTAL

8.5.1 Materials, Kinetic Measurements, and pH

The regular racemic mixture D/L amino acids were purchased as the best grades available from Aldrich Chemical Company or Sigma Chemical Company. The two long chain amino acids, 2-aminooctanoic acid and 2-aminononanoic acid, were bought from Fluka. The other chemicals were the same as in previous chapters (VI and VII).

The solution mixtures were prepared as in the aminolysis studies (Chapter VII), and the data analysis was the same as in the thiolysis studies (Chapter VI). The reaction medium was a carbonate buffer of pH 10.6, as with the thiolysis and aminolysis studies.

The amino acids have both acid and basic groups, and so the stock solutions of amino acids in buffer required a variable amount of added concentrated NaOH or HCl to bring them to the required pH of 10.6. The pH of each solution flask (of 50 mL) having a different concentration of amino acid (by dilution with buffer) was measured separately and standardized individually. A difference of 0.1 in buffer pH dramatically influences the k_u and k_N values and consistency is critical for these experiments. In the case of histidine, reproducibility is a problem because it is difficult to keep the pH buffered constantly due to number of acidic and basic groups in histidine. As a reminder, using the overall reaction ratio k_{cN}/k_N as the basis for comparison and discussion of catalysis is critical in eliminating buffer and pH effects.

8.5.2 Hydrophobicity Scales and $P_{o/w}$ Values of Amino Acids

There are significant differences between various scales of the hydrophobicity of amino acids and amino acid side chains,³⁷⁷⁻³⁸³ due principally to the fundamentally different methods used for constructing the scales. The scales may be divided into two major types: (1) Scales constructed by examining proteins with known 3-D structures and defining hydrophobic character by the frequency for the amino acid residue to be found *inside* of a protein,^{380,382} (2) Scales derived from the physicochemical properties of the amino acids themselves (eg. solubility in water, partition between water and an organic solvent) and which more clearly follow the trends that would be expected on the

inspection of amino acid structures.^{378,381} Charton and Charton³⁸³ offer some insight onto the dependence of amino acid hydrophobicity parameters on structure and concluded that “no single hydrophobicity parameter and log P values (which show variable dependence on intermolecular forces and steric effects) can represent the complete range of amino acid behavior.” Cornette *et al.*³⁷⁷ reviewed and evaluated various hydrophobicity scales (37 of them) that have been used to estimate amino acid hydrophobicity, and the authors attempted to extract correlations between the scales.

Generally, the logarithms of octanol-water partition coefficients are taken as reliable indicators of hydrophobicity.^{347,348} Also, the solubilization of organic solutes into micelles correlates with log $P_{o/w}$ values (Figure 7.7).^{354,355} However, while the aqueous phase of the 1-octanol/water system contains almost no octanol at equilibrium, the octanol phase dissolves an appreciable amount of water (2.3 M, corresponding to a molar ratio of 1-octanol/water \approx 4/1 in that phase).³⁵¹ Therefore, polar groups need not to be totally dehydrated on their transfer from aqueous phase to the octanol (organic) phase. Also, it is noted that hydrophilic solutes are able to carry water molecules from the aqueous phase into the organic phase, a process known as the “water dragging effect”.^{351,352}

The octanol-water system is not the most suitable one for the direct partitioning of amino acids, owing to their low solubility of the amino acids in the organic phase, especially if they are charged. Another problem with literature data is that log $P_{o/w}$ values are often determined at a fixed pH, without regard to the state of ionization of the CO_2H and NH_2 groups. The log $P_{o/w}$ values estimated by most researchers are at neutral pH, or near the isoelectric points of the amino acid, where most of the amino acids are

zwitterionic. It appears that the amino acids bearing ionizable side-chains (e.g. cysteine, histidine, arginine) display pH dependent $P_{o/w}$ values, whereas this phenomenon is generally absent in other amino acids.³⁸⁴

Determination of $P_{o/w}$ values by the conventional “shake-flask method” does not work in the case of amino acids because they are too soluble in water. For this reason, various experimental techniques, such as the radiometric method used by Yunger *et al.*,³⁷⁹ thin-layer chromatography used by Pliska *et al.*,³⁷⁶ reversed-phase HPLC used by Chmelik *et al.*,³⁸⁵ and centrifugal partition chromatography used by El-Tayar *et al.*³⁸⁴ have been employed for the purpose of finding $P_{o/w}$ for amino acids. Hansch and coworkers³⁴⁹ have compiled some of the log $P_{o/w}$ values for amino acids from the above-mentioned studies. Sangster’s group has collected a databank of log $P_{o/w}$ for many organics, including most amino acids, which can be accessed directly on the Internet: (<http://logkow.cisti.nrc.ca>). As well as measured values, there are also log $P_{o/w}$ values that are calculated from molecular structure on the basis of the simple addition of the hydrophobicities of smaller segments of the solute.^{349,356,362} Such calculations of partition coefficients³⁵¹ have been greatly aided by the use of computer programs, some of which are available from the Internet: (<http://www.epa.gov/oppt/exposure/docs/episuitd1.htm>).

To plot log k_{cN}/k_N vs. log $P_{o/w}$ in Figure 8.7 we have chosen the values of $P_{o/w}$ obtained by Pliska *et al.*³⁷⁶ because they had values for most of the amino acids which we studied (Table 8.4), and their method is reliable.^{351,352} Nonetheless, using log $P_{o/w}$ values found by the other researchers^{379,384,385} would not have changed the results, giving similar slopes for the plots as in Figure 8.7, with only minor differences for the values of cysteine and the branched amino acids.

Values of $\log P_{o/w}$ for 2-aminooctanoic acid and 2-aminononanoic acid were not found in the literature. From a correlation of Pliska's $\log P_{o/w}$ values versus the chain length (N) of alkyl-substituted amino acids, $\log P_{o/w} = (0.408 \pm 0.043).N - (4.06 \pm 0.18)$, we find extrapolated values for 2-aminooctanoic acid of $\log P_{o/w} = -0.801$ and -0.393 for 2-aminononanoic acid.

CHAPTER IX. CONCLUSIONS AND FUTURE PERSPECTIVES

9.1 CONCLUSIONS

It is hard to overstate the importance of “catalysis” to industry, as well as to biological systems. Just as enzymes catalyze biochemical reactions, supramolecular hosts (Chapter I), such as cyclodextrins (Chapter II) and colloidal micelles (Chapter IV), can catalyze organic reactions. The analysis of catalytic mechanisms based on the *transition state stabilization/pseudo-equilibrium approach* (Chapter I, Section 1.2),^{42,43} may be applied to micelle-catalyzed reactions, in the same way that it has been applied to catalysis by enzymes.²⁴ The analysis of micellar catalysis from the point of view of transition state stabilization marks the principal contribution of this thesis.

Stemming from earlier research by various workers on the catalysis of the alkaline hydrolysis of phenyl esters by micelles (Chapter V), we continued the study of the basic cleavage of *p*-nitrophenyl alkanoate (p-NPAlk) esters, with varying chain length, by a number of different nucleophiles in cetyltrimethylammonium bromide (CTAB) micelles (Chapters VI - VIII). The use of a reaction medium with a “constant ionic atmosphere” was initiated by other researchers,^{62,297,305} and in our work we have done the same,^{58,59} keeping the total concentration of the counterion of CTAB constant, as well as the pH and ionic strength of the buffer constant. As anticipated, under such conditions, we observed that rate *versus* surfactant profiles followed simple *saturation kinetic behaviour*, making the kinetic analysis of the bimolecular acyl transfer reactions in the micelles much easier.

As we alluded to in Chapter IV, there has been some disagreement with respect to the loci of solubilization of specific solutes, and the amount of their penetration into

micelles, because the micellar pseudo-phase offers a variety of different solubilizing environments from quite polar (at the Stern layer) to quite non-polar (in the micellar core). From earlier work and our own results, the phenyl esters are oriented with the aromatic ring and carbonyl group located at the aqueous regions of the Stern layer of CTAB micelles,³⁰⁵ and the acyl chain in the hydrophobic regions of the Stern layer or bound in the micellar core depending on its length.^{58,59} Regardless of the exact modes of initial state and transition state binding, the acyl transfer reaction takes place in a decidedly aqueous region of the Stern layer of CTAB micelles.

From our studies, we conclude that as a rule the partitioning of reactants into the micellar pseudo-phase and the resultant *concentration effect* is sufficient to explain catalysis by micelles. The exceptions to this rule occur when both the reactants (ester and nucleophile) are tightly bound to the micelles. Increasing ester hydrophobicity accelerates the CTAB-mediated reactions by increasing the transfer of ester between the aqueous phase and micellar pseudo-phase (K_S), but the acceleration is not due to a change in the reactivity of the ester in the micellar medium, as was previously believed.^{180,241,246,247} In fact, when simple ionic nucleophiles react with the pNPAlk esters the magnitude of catalysis hardly varies with acyl chain length but it does vary greatly with the nucleophile's ability to transfer into the micelles (Chapter VI).

In most cases, ester cleavage by anionic nucleophiles is *catalyzed* by CTAB micelles, and the amount of catalysis depends on the ability of the anions to exchange with bromide anions in the Stern layer. Ester cleavage by short chain alkylamines is, however, *retarded* by CTAB micelles because those amines are not hydrophobic enough to partition well into the micelles. With longer, more hydrophobic alkylamines, catalysis

of ester cleavage occurs because those amines can bind tightly to the micellar core; such binding assists in the transition state stabilization with pNPA but conflicts with the binding of pNPH in the TS. In the case of amino acid anion nucleophiles, there is a switch in mechanism from *ion exchange*, bringing the less hydrophobic amino acid anions into the Stern layer, to *hydrophobicity* dictating the partitioning and binding of the more hydrophobic amino acid anions to the micellar core.

We have noted earlier how the dissection of TS binding into *passive* and *dynamic* binding, developed by Kirby for application to enzymatic reactions,⁵³ can also be practical for discussing transition state stabilization in ester cleavage mediated by micelles. In the case of ionic nucleophiles, such as hydroxide ion (Chapter V), thiolates (Chapter VI), and short amino acid anions (Chapter VIII), the passive TS binding is *independent* of the nucleophile binding and it involves hydrophobic interactions between the ester acyl chain and the micellar core, in much the *same* way as the ester binding in the initial state. With non-ionic alkylamines, as well as with long chain amino acid anions, the passive TS binding is *not independent* of the chain length of the nucleophile, and the binding of the acyl chain is *decreased* in the transition state, as compared to the initial state. The dynamic TS binding is greatly dependent on the nucleophile, since it takes place in the immediate region where bonds are made and broken. In the case of ionic nucleophiles, the dynamic TS binding depends on the ability of the nucleophile to *ion exchange* with bromide ions in the Stern layer of CTAB micelles, whereas in the case of non-ionic alkylamines, as well as the more hydrophobic amino acid anions, it depends on the hydrophobicity of the nucleophile.

We have seen cases where there is a decrease in magnitude of catalysis when both reactants are concentrated into the micellar pseudo-phase and they bind well to the micellar core in the initial state, as in the case of long chain alkylamines and amino acid anions reacting with *p*-nitrophenyl hexanoate. We had no evidence of pK_a shifts of the nucleophiles, micellization of the esters or nucleophile, or deeper penetration of the carbonyl group of the ester into the micellar core. Our explanation of the reduced catalysis found with strongly micelle-bound ester and nucleophile is that the *optimal geometry* for acyl transfer is not readily accessible because of the conflicting demands of binding both the alkyl chain of the nucleophile and the acyl chain of the ester in the transition state, as compared to the initial state.

Since our studies were started, other researchers have also concluded that a major contributor to the “catalysis” of the cleavage of *p*-nitrophenyl alkanoate esters by microemulsions³⁸⁶ and colloidal polymer dispersions³⁸⁷ is the partitioning of the esters and the nucleophile into the supramolecular “host”.

9.2 FUTURE PERSPECTIVES

The kinetic model used in this thesis to analyze the results for *p*NPAlk ester cleavage by ionic nucleophiles in CTAB micelles did not include an ion-exchange constant K_Y^X . This means that these constants are imbedded into the second order rate constants for nucleophilic attack on the CTAB bound ester, k_{cN} , which were derived from the results. It is possible to estimate relative K_Y^X for the ionic nucleophiles by studying ester cleavage in other CTAX micelles having different counterions. Thus far, the studies in this thesis have been restricted to CTAB micelles anticipating high catalysis of ester

cleavage by them. Commercially available cetyltrimethylammonium hydroxide (CTAOH),^{294,388} tosylate (CTATs), and chloride (CTACl) will also likely be good catalysts.³⁸⁹ Previous work with CTAOH surfactants is scarce because the surfactants are expensive and because rate-surfactant profiles with CTAOH micelles do not adhere to the pseudo-phase ion exchange model.²⁹⁴ Comparison of ester cleavage by these CTAX surfactants can provide a counterion effect on the catalytic ratios, from which kinetic estimates of relative ion-exchange constant K_X^Y can be made.²⁴⁸ Such an elaboration of the studies already conducted will probably not result in a great difference in the conclusions about the mode of ester and TS binding in CTAX micelles, though more quantitative values of micellar rate constants (k_{cN}) can be estimated. Also, one may see if the counterion plays any role in solubilization of the non-polar ester.

For *p*-NPAIk ester cleavage, the passive TS binding has been shown to involve *hydrophobic interaction* of the acyl chains of esters with the CTAB micellar core, but it still remains questionable how much *electrostatic interactions* contribute to the dynamic TS stabilization for the reaction. By comparing ester cleavage reactions within micelles of varying head groups, ionic and non-ionic, and in the presence of model compounds resembling the surfactant Stern layer (below), one may be able to address the extent of involvement of the head group of the micelles in determining the rate and the electrostatic contribution to TS stabilization for catalyzed ester cleavage. For comparison with cetyltrimethylammonium surfactants (CTAX), other surfactants of interest would be (a) mono, di-, and tri-alkylsubstituted cetylammmonium surfactants, (b) sodium dodecylsulfate (SDS), (c) Brij-30 ($C_{12}H_{25}(OCH_2CH_2)_4OH$), and (d) Brij-56 ($C_{16}H_{33}(OCH_2CH_2)_4OH$). Engberts and coworkers²¹⁶ recently looked at identifying non-covalent interactions in the

Stern region determining micellar catalysis by studying organic reactions in an “electrolyte solution mimicking the local environment in the Stern region of the micelle”.²¹⁶ Similarly, it would be interesting to study ester cleavage in concentrated solution of tetramethylammonium bromide (TMAB, $\text{Me}_4\text{N}^+ \text{Br}^-$) to compare with CTAB, and in sodium methylsulfate (SMS, $\text{MeSO}_4^- \text{Na}^+$) to compare with SDS.

In many cases, as seen in the survey of micellar reactions in Chapter IV, the rate constants for bimolecular processes in the micellar phase are similar to those in the aqueous phase and so some authors have automatically assumed that the binding of the reactants are at or near the interface of the micelle.²³⁰ In some cases, it has been shown that a reactant might bind in one area of the micelle, though the reaction takes place in another. Unless explicit binding studies (using NMR) is done to see where the reactants are bound, the difference between the rate constants in the micellar and in the aqueous phase cannot be used to determine accurately binding locations within micellar aggregates. From our studies, the intrusion of the short acyl chain esters past the Stern layer into the micellar core is arguable. It would be valuable to conduct NMR studies in order to probe ester binding to CTAB micelles and see if the results agree with those we found using kinetics.

As shown in the thesis, keeping a constant counterion concentration simplifies the analysis of rate-surfactant profiles for ester cleavage, but could this methodology be applied to other organic reactions? To our knowledge no other bimolecular reactions have been studied under such conditions. Nucleophilic aromatic substitution ($\text{S}_{\text{N}}\text{Ar}$),³⁹⁰ which has been extensively studied within micellar systems,^{269,271,391} showed kinetics which are greatly complicated by the salt effects of counterions, such that rate-maxima were

observed with rate-surfactant profiles.^{270,272,392,393} Studying this reaction under constant “ionic atmosphere” would be of interest in future work.

Enzyme mimics, such as cyclodextrins and micelles, have yet to approach the complexity, substrate-recognition capability, and information-storage ability of the natural archetype. Inevitably, a move towards the design of more complex (structural and functional) supramolecular systems (hosts and guests) should be a direction for future development. Micelles bearing “simple” head groups generally foster a modest rate and no selectivity with chiral reactants. *Functional micelles* act not only as media or “host” for reactions but they are also reactants by virtue of having a reactive functionality in the head group of the surfactant.²⁴⁰ So far, the most frequently studied functional micelles have reactive hydroxyl, mercapto, imidazolyl,³⁹⁴ and pyridyl groups.³⁹⁵ The catalytic activity of these micelles exceeds that of non-functional ones which makes them more valuable for study. *Chiral micelles* with chiral amino-acids as functional groups have been synthesized,^{189,191} but they have yet to be extensively studied. Selective and chiral recognition of reagents¹⁸² has been effectively achieved by chiral surfactants¹⁹⁵ and by the incorporation of a ‘receptor’ molecule, as rigid binding site (such as a porphyrin) inside a micelle.³⁹⁶ Research in this area has been limited, probably because such chiral surfactants are not commercially available.¹⁹⁴ Future emphasis will be to study *functional chiral micelles*, which may be superior *enzyme mimics* because 1) they might achieve rate enhancements comparable to those of enzymes; 2) they can be synthesized to be structurally more similar to enzymes; and 3) they might show stereo-control over reactions. Chiral selectivity can be expressed in functional micelles only when the substrates are also chiral.^{182,191,192,397} A widely studied enantioselective reaction is the

hydrolysis of *p*-nitrophenyl esters of N-protected D- or L- amino acids,^{105,193} and it may well be a good start up reaction to study in chiral micelles.

Finally, the ability to determine supramolecular geometries, similar to the way in which covalent structures are determined, remains one of the great challenges in the fields of supramolecular and colloidal chemistry. This challenge remains because the all-important “non-covalent bond”, for example a “hydrophobic bond”, is far from being understood and mastered. In the absence of an ability to detect and measure non-covalent interactions, success with catalytic hosts often relies on intuition and good fortune.

REFERENCES

- (1) Atwood, J. L.; Davies, J. E. D.; MacNicol, D. D.; Vögtle, F. *Comprehensive Supramolecular Chemistry*; Pergamon: Oxford, 1996; Vol. 1-11.
- (2) Vögtle, F. *Supramolecular Chemistry*; Wiley: Chichester, 1991.
- (3) Lehn, J.-M. *Supramolecular Chemistry: Concepts and Perspectives*; VCH: Weinheim, 1995; Lehn, J.-M. *Angew. Chem., Int. Ed. Engl.* **1988**, *112*, 90; Whitesides, G. M.; Simanek, E. E.; Mathias, J. P.; Seto, C. T.; Chin, D. N.; Mammen, M.; Gordon, D. M. *Acc. Chem. Res.* **1995**, *28*, 37; Fyfe, M. C. T.; Stoddart, J. F. *Acc. Chem. Res.* **1997**, *30*, 393; Edelmann, F. T.; Haiduc, I. *Supramolecular Organometallic Chemistry*; Wiley/VCH: New York, 1999; Schneider, H.-J. *Angew. Chem.* **1991**, *103*, 1419; Schneider, H.-J. *Angew. Chem., Int. Ed. Engl.* **1991**, *30*, 1417; Reinhoudt, D. N. Dance, I. In *The Crystal as a Supramolecular Entity*; Desiraju, G. R., Ed.; Wiley: Chichester, UK, 1996; pp 137; Sauvage, J.-P. In *Transition Metals in Supramolecular Chemistry*; Sauvage, J.-P., Ed.; Wiley: New York, 1999;; Crego-Calama, M. *Science* **2002**, *295*, 2403; Lehn, J.-M. *Proc. Natl. Acad. Sci.* **2002**, *99*, 4763; Turro, N.J. *Proc. Natl. Acad. Sci.* **2002**, *99*, 4805.
- (4) Lehn, J.-M. *Science* **1985**, *227*, 849.
- (5) Lehn, J.-M. *Angew. Chem., Int. Ed. Engl.* **1990**, *29*, 1304.
- (6) Whitesides, G. M.; Mathias, J. P.; Seto, C. T. *Science* **1991**, *254*, 1312; Lowe, C. R. *Curr. Opin. Struct. Biol.* **2000**, *10*, 428; Merkle, R. C. *Trends Biotechnol.* **1999**, *17*, 271.
- (7) Philp, D.; Stoddart, J. F. *Angew. Chem., Int. Ed. Engl.* **1996**, *35*, 1154; Stoddart, J. F. *Nature* **1988**, *334*, 10; Lieinniger, S. ; Olenyuk, B.; Stang, P.J. *Chem. Rev.* **2000**, *100*, 853; Swieger, G. F.; Malefetse, T. J. *Chem. Rev.* **2000**, *100*, 3483.
- (8) Menger, F. M.; Caran, K. L. *J. Am. Chem. Soc.* **2000**, *122*, 11679.
- (9) Menger, F. M. *Proc. Natl. Acad. Sci.* **2002**, *99*, 4818.
- (10) Cram, D. J. *Angew. Chem., Int. Ed. Engl.* **1988**, *27*, 1009.
- (11) Lawrence, D. S.; Jiang, T.; Levett, M. *Chem. Rev.* **1995**, 2229.
- (12) Benddle, C. R. *Chem. Soc. Rev.* **1984**, *13*, 279.
- (13) Cram, D. J.; Cram, J. M. *Container Molecules and Their Guests*; Royal Society of Chemistry: Cambridge, England, 1994.
- (14) Cram, D. J.; Cram, J. M. *Acc. Chem. Res.* **1978**, *11*, 7; Cram, D. J. *Nature* **1992**, *29*, 356; Cram, D. J. *Angew. Chem., Int. Ed. Engl.* **1986**, *25*, 1039; Bryant, J. A.; Knobler, C. B.; Cram, D. J. *J. Am. Chem. Soc.* **1990**, *112*, 1254; Cram, D. J.; Trueblood, K. N. In *Host Guest Complex Chemistry Macrocycles*; Vögtle, F., Weber, E., Eds.; Springer-Verlag: Berlin Heidelberg, 1985; pp 127.
- (15) Schmidtchen, F. P.; Berger, M. *Chem. Rev.* **1997**, *97*, 1609.

- (16) Hayward, R. C. *Chem. Soc. Rev.* **1993**, 285; Dietrich, B. In *Inclusion Compounds*; Atwood, J. L., Davies, J. E. D., MacNichol, D. D., Eds.; Academic Press: Oxford, 1984; Vol. 2, pp 373.
- (17) Izatt, R. M.; Christensen, J. J., Eds. *Synthesis of Macrocycles: The Design of Selective Complexing Agents*; John Wiley & Sons: New York, 1987; Vol. 3.
- (18) Schmidtchen, F. P. In *Supramolecular Chemistry of Anions*; Bianchi, A., Bowman-James, K., Garcia-España, E., Eds.; Wiley-VCH: New York, 1997.
- (19) Tee, O. S. *Adv. Phys. Org. Chem.* **1994**, 29, 1.
- (20) Atwood, J. L. *Inclusion Phenomena and Molecular Recognition*; Plenum Press: New York, 1990.
- (21) Rebek, J. *New Shapes for Catalysis and Molecular Recognition*; Plenum Press: New York, 1990.
- (22) Moyer, B. E.; Bonnesen, P. V. In *Supramolecular Chemistry of Anions*; Bianchi, A., Bowman-James, K., Garcia-España, E., Eds.; Wiley-VCH: New York, 1997.
- (23) Martell, A. E.; Moteikatis, R. J. *Determination and Use of Stability Complexes*; VCH: New York, 1998; Braibanti, A.; Ostacoli, G.; Paoletti, P.; Pettit, L. D.; Sanmartano, S. *Pure. Appl. Chem.* **1987**, 59, 1721; Connor, K. A. *Binding Constants, the Measurements of Molecular Complex Stability*; John Wiley & Sons: New York, 1987; Legget, D. J., Ed. *Computational Methods for Determination of Stability Constants*; Plenum Press, New York, 1985; Gans, P. *Data Fitting in Chemical Sciences*; Wiley: Chichester, 1992; Izaat, R. M.; Pawlak, K.; Bradshaw, J. S.; Bruening, R. L. *Chem. Rev.* **1991**, 91, 1721; Schneider, H.-J.; Blatter, T.; Kramer, R.; Kumar, S.; Schneider, U.; Theis, I. In *Inclusion Phenomena and Molecular Recognition*; Atwood, J. L., Ed.; Plenum Press: New York, 1990; pp 65.
- (24) Kraut, J. *Science* **1988**, 242, 533.
- (25) Engel, P. C. In *The Chemistry of Enzyme Action*; Page, M. I., Ed.; Elsevier: Amsterdam, 1984.
- (26) Tipton, K. F. In *Enzymology: LABFAX*; Engel, P. C., Ed.; Academic Press: San Diego, 1996; Vol. Chap. 4.
- (27) Fersht, A. *Enzyme Structure and Mechanism*; second ed.; Freeman: New York, 1985.
- (28) Dugas, H. In *Bioorganic Chemistry: A Chemical Approach to Enzyme Action*; second ed.; Springer-Verlag Inc: New York, 1989.
- (29) Jarvo, E. R.; Copeland, G. T.; Papaioannou, N.; Jr, P. J. B.; Miller, S. J. *J. Am. Chem. Soc.* **1999**, 121, 11638.
- (30) Hollfelder, F.; Kirby, A.J.; Tawfik, D. S. *J. Org. Chem.* **2001**, 66, 5866; Hollfelder, F.; Kirby, A. J.; Tawfik, D. S. *J. Am. Chem. Soc.* **1997**, 119, 9578.
- (31) Fersht, A. R. *Enzyme Structure and Mechanism*; first ed. Freeman: New York, 1977.
- (32) Haldane, J. B. S. *Enzymes*; Longmans, Green & Co.: London, 1930.
- (33) Pauling, L. *Chem. Eng. News* **1946**, 24, 1375; Pauling, L. *Am. Sci.* **1948**, 36, 51.
- (34) Laidler, K. J. *Chemical Kinetics*; third ed.; Haper & Row: New York, 1987.

- (35) Lowry, T. H.; Richardson, K. S. *Mechanism and Theory in Organic Chemistry*; second ed.; Harper & Row: London, 1981
- (36) Moore, J. W.; Pearson, R. G. *Kinetics and Mechanism*; Wiley: New York, 1981.
- (37) Kreevoy, M. M.; Truhlar, D. C. *Investigation of Rates and Mechanism of Reactions*; fourth ed.; Wiley-Interscience: New York, 1986; Vol. VI; Hammett, L. P. *Physical Organic Chemistry*; second ed.; McGraw-Hill: New York, 1970.
- (38) Page, M.; Williams, A. *Organic and Bio-organic mechanisms*; Addison Wesley Longman Ltd.: Singapore, 1997.
- (39) Albery, W. J. *Adv. Phys. Org. Chem.* **1993**, 139; Berne, B. J.; Borkovec, M. J. *Chem. Soc., Faraday Trans.* **1998**, 94, 2717.
- (40) Truhlar, S. G.; Garrett, B. C.; Klippenstein, S. J. *J. Phys. Chem* **1996**, 100, 12771.
- (41) Eyring, H. *J. Chem. Phys.* **1935**, 3, 107.
- (42) Kurz, J. L. *J. Am. Chem. Soc.* **1963**, 84, 987.
- (43) Kurz, J. L. *Acc. Chem. Res.* **1972**, 5, 1.
- (44) Wolfenden, R. *Nature* **1969**, 223, 704; Wolfenden, R.; Frick, L. In *Enzyme Mechanism*; Page, M. I., William, A. Eds.; Royal Society of Chemistry: London, 1987.
- (45) Wolfenden, R. *Acc. Chem. Res.* **1972**, 5, 10.
- (46) Wolfenden, R.; Kati, W. M. *Acc. Chem. Res.* **1991**, 24, 209.
- (47) Lienhard, G. E. *Science* **1973**, 180, 149.
- (48) Tee, O. S. *Carbohydr. Res.* **1989**, 192, 181.
- (49) Maskill, H. *The Physical Basis of Organic Chemistry*; Oxford University Press: Oxford, 1985.
- (50) Jencks, W. P. *Adv. Enzymol.* **1975**, 43, 219.
- (51) Schowen, R. L. In *Transition States in Biochemical Processes*; Gandour, R. D., Schowen, R. L., Eds.; Plenum: New York, 1978; Wong, C.-H.; Shen, G.-J.; Pederson, R. L.; Wang, Y.-F.; Hennen, W. J. *Methods in Enzymology* **1991**, 202, 591; Cacciapaglia, R.; Mandolini, L. *Chem.Soc. Rev.* **1993**, 22, 221.
- (52) Jahangiri, G. K.; Reymond, J.-L. *J. Am. Chem. Soc.* **1994**, 116, 11264; Thomas, N. R. *Nat. Prod. Rep.* **1996**, 13, 479; Mader, M. M.; Bartlett, P. A. *Chem. Rev.* **1997**, 97, 1281.
- (53) Kirby, A. J. *Angew. Chem. Int. Ed. Engl.* **1996**, 35, 707.
- (54) Tee, O. S.; Gadosy, T. A. *J. Chem. Soc. Perkin Trans. 2* **1994**, 2304.
- (55) Gadosy, T. A.; Tee, O. S. *J. Chem. Soc. Perkin Trans. 2* **1995**, 71.
- (56) Tee, O. S.; Gadosy, T. A.; Giorgi, J. B. *Can. J. Chem.* **1997**, 75, 83.
- (57) Tee, O. S.; Boyd, M. J. *Can. J. Chem.* **1999**, 77, 950.
- (58) Tee, O. S.; Fedortchenko, A. A. *Can. J. Chem.* **1997**, 75, 1434.
- (59) Tee, O. S.; Yazbeck, O. J. *Can. J. Chem.* **2000**, 78, 1100.
- (60) Davies, D. M.; Gillitt, N. D.; Paradis, P. M. *J. Chem. Soc. Perkin Trans. 2* **1996**, 659.

- (61) Davies, D. M.; Foggo, S. J.; Paradis, P. M. *J. Chem. Soc. Perkin Trans. 2* **1998**, 1597; Davies, D. M.; Foggo, S. J. *J. Chem. Soc. Perkin Trans. 2* **1998**, 247.
- (62) Pirinccioglu, N.; Zaman, F.; Williams, A. *J. Org. Chem.* **2000**, 65, 2537.
- (63) Bunton, C. A.; Yatsimirsky, A. K. *Langmuir* **2000**, 16, 5921.
- (64) Dill, K. A. *Biochemistry* **1990**, 29, 7133.
- (65) Tanford, C. *The Hydrophobic Effect: Formation of Micelles and Biological Membranes*; second ed.; Wiley: New York, 1980.
- (66) Pratt, L. R.; Pohorille, A. *Chem. Rev.* **2002**, 102, 2671.
- (67) Davis, A. M.; Teague, S. J. *Angew. Chem., Int. Ed. Engl.* **1999**, 38, 736.
- (68) Blokzijl, W.; Engberts, J. B. F. N. *Angew. Chem., Int. Ed. Engl.* **1993**, 32, 1545.
- (69) Hummer, G.; Garde, S.; Garcia, A. E.; Paulaitis, M. E.; Pratt, L. R. *J. Phys. Chem. B* **1998**, 102, 10469.
- (70) Muller, N. *Acc. Chem. Res.* **1990**, 23, 23.
- (71) Dill, K. A. *Science* **1990**, 250, 297.
- (72) Hartley, G. *Aqueous Solutions of Paraffin-Chain Salts*; Hermann & Cie.: Paris, 1963.
- (73) Sharp, K. A.; Madan, B. *J. Phys. Chem. B* **1997**, 101, 4343.
- (74) Frank, H. S.; Evans, M. W. *J. Chem. Phys.* **1945**, 13, 507.
- (75) Abraham, M. H. *J. Am. Chem. Soc.* **1982**, 104, 2085.
- (76) Hummer, G.; Garde, S.; Garica, A. E.; Pohorille, P.; Pratt, L. R. *Proc. Natl. Acad. Sci.* **1996**, 93, 8951.
- (77) Huang, D. M.; Chandler, D. *J. Phys. Chem. B* **2002**, 106, 2047; Huang, D. M.; Geissler, P. L.; Chandler, D. *J. Phys. Chem. B* **2001**, 105, 6704.
- (78) Silverstein, K. A. T.; Haymet, A. D. J.; Dill, K. A. *J. Am. Chem. Soc.* **2000**, 122, 8037.
- (79) Engberts, J. B. F. N.; Blandamer, M. J. *Chem. Commun.* **2001**, 1701.
- (80) Lehninger, A. A. *Lehninger Principles of Biochemistry*; Nelson, D. L.; Cox, M., Eds.; third ed.; Worth Publishers: New York, 2000; Chapter 4.
- (81) Huang, D. M.; Chandler, D. *Proc. Natl. Acad. Sci.* **2000**, 97, 8324; Silverstein, K. A. T.; Haymet, A. D. J.; Dill, K. A. *J. Am. Chem. Soc.* **1998**, 120, 3166.
- (82) Kauzmann, W. *Adv. Protein Chem.* **1959**, 14, 1.
- (83) Bender, M. L.; Komiyama, M. *Cyclodextrin Chemistry*; Springer-Verlag: Berlin, 1978.
- (84) Cramer, F.; Saenger, W.; Spatz, H.-C. *J. Am. Chem. Soc.* **1967**, 89, 14.
- (85) Wenz, G. *Angew. Chem. Int. Ed. Engl.* **1994**, 33, 803.; Atwood, J. L.; Davies, J. E. D.; MacNicol, D. D.; Vögtle, F.; Lehn, J.-M., Eds. *Comprehensive Supramolecular Chemistry*; Pergamon: Oxford, 1996; Vol. 3.
- (86) Szejtli, J. *Chem. Rev.* **1998**, 98, 1743.
- (87) Bergeron, R. J. In *Inclusion Compounds*; Atwood, J. L., Davies, J. E. D., MacNicol, D. D., Eds.; Academic Press: Montreal, 1984; Vol. 3.

- (88) Breslow, R. In *Inclusion Compounds*; Atwood, J. L., Davies, J. E. D., MacNicol, D. D., Eds.; Academic Press: Montreal, 1984, Vol. 3.
- (89) Connors, K. A. *Chem. Rev.* **1997**, 97, 1325.
- (90) Szejtli, J. *Cyclodextrins and their Inclusion Complexes*; Akademiai Kiado: Budapest, 1982.
- (91) Szejtli, J. *Cyclodextrin Technology*; Kluwer Academic Publishers: Dordrecht, 1988.
- (92) Klein, C.; Schulz, G. E. *J. Mol. Biol.* **1991**, 217, 737.
- (93) Szejtli, J. In *Inclusion Compounds*; Atwood, J. L., Davies, J. E. D., MacNicol, D. D., Eds.; Academic Press: Montreal, 1984, Vol. 3.
- (94) Sundararajan, P. R.; Rao, V. S. *Carbohydr. Res.* **1970**, 13, 351.
- (95) Diaz, D.; Vargas-Baca, I.; Garcia-Mora, J. *J. Chem. Ed.* **1994**, 71, 703.
- (96) Gelb, R. I.; Schwartz, L. M.; Bradshaw, J. J.; Laufer, D. A. *Bioorg. Chem.* **1980**, 9, 299; Gelb, R. I.; Schwartz, L. M.; Laufer, D. A. *Bioorg. Chem.* **1982**, 11, 274.
- (97) Hamai, S. *Bull. Chem. Soc. Jpn.* **1982**, 55, 2721.
- (98) Cox, G. S.; Turro, N. J.; Yang, N. C.; Chen, M. J. *J. Am. Chem. Soc.* **1984**, 106, 422; Heredia, A.; Requena, G.; Sanchez, F. G. *J. Chem. Soc. Chem. Commun.* **1985**, 1814.
- (99) Fraiji, E. K. J.; Cregan, T. R.; Werner, T. C. *Appl. Spec.* **1994**, 63, 2924.
- (100) Inoue, Y.; Okuda, T.; Miyata, Y.; Chujo, R. *Carbohydr. Res.* **1984**, 125, 65; Nishimura, M.; Deguchi, T.; Sanemasa, I. *Bull. Chem. Soc. Jpn.* **1989**, 62, 3718.
- (101) Palepu, R.; Reinsborough, V. C. *Can. J. Chem.* **1988**, 66, 325.
- (102) Palepu, R.; Richardson, J. E.; Reinsborough, V. C. *Langmuir* **1989**, 5, 218.
- (103) Fujiki, M.; Deguchi, T.; Sanemasa, I. *Bull. Chem. Soc. Jpn.* **1988**, 61, 1163.
- (104) Tee, O. S.; Du, X.-X. *J. Org. Chem.* **1988**, 53, 1837; Tee, O. S.; Du, X.-X. *J. Am. Chem. Soc.* **1992**, 114, 620; Giorgi, J. B.; Tee, O. S. *J. Am. Chem. Soc.* **1995**, 117, 3633.
- (105) Loncke, P. G. *Hydrolytic Cleavage of p-Nitrophenyl Ester of N-Protected Amino Acids in the Presence of Cyclodextrins : Transition State Stabilization*; M.Sc. Thesis, Concordia University: Montreal, 1998.
- (106) Davies, D. M.; Deary, M. E. *J. Chem. Soc. Perkin Trans. 2* **1999**, 1027.
- (107) Inoue, Y.; Hakushi, T.; Lui, Y.; Tong, L.-H.; Shen, B.-J.; Jin, D.-S. *J. Am. Chem. Soc.* **1993**, 115, 475.
- (108) Hamai, S. *J. Am. Chem. Soc.* **1989**, 111, 3954.
- (109) Tee, O. S.; Bozzi, M. *J. Am. Chem. Soc.* **1990**, 112, 7815.
- (110) Sanemasa, I.; Akamine, Y. *Bull. Chem. Soc. Jpn.* **1987**, 60, 3440; Sanemasa, I.; Takuma, T.; Deguchi, T. *Bull. Chem. Soc. Jpn.* **1989**, 62, 3102.
- (111) Gadosy, T. A. *Stabilization by Natural and Unnatural Cyclodextrins of the Transition State of Acyl Transfers of Nitrophenyl Alkanoate Esters*; Ph.D. Thesis, Concordia University: Montreal, 1995.
- (112) Rekharsky, M. V.; Inoue, Y. *Chem. Rev.* **1998**, 98, 1875.

- (113) Matsui, Y.; Nishioka, T.; Fujita, T. *Topics Curr. Chem.* **1985**, 128, 61.
- (114) Ross, P. D.; Rekharsky, M. V. *Biophys. J.* **1996**, 71, 2144.
- (115) Rüdiger, V.; Eliseev, A.; Simova, S.; Schneider, H.-J.; Blandamer, M. J.; Cullis, P. M.; Meyer, A. J. *J. Chem. Soc., Perkin Trans. 2* **1996**, 726.
- (116) Schneider, H.-J.; Hacket, F.; Rüdiger, V.; Ikeda, H. *Chem. Rev.* **1998**, 98, 1755.
- (117) Kamiya, M.; Mitsuhashi, S.; Makino, M.; Yoshioka, H. *J. Phys. Chem.* **1992**, 96, 95; Marconi, G.; Monti, S.; Mayer, B.; Köhler, G. *J. Phys. Chem.* **1995**, 99, 3943.
- (118) Park, J. H.; Nah, T. H. *J. Chem. Soc., Perkin Trans. 2* **1994**, 1359.
- (119) Manor, P. C.; Saenger, W. *J. Am. Chem. Soc.* **1974**, 96, 3630; Fayos, J.; Saenger, W.; McMullan, R. K.; Mootz, D. *Carbohydr. Res.* **1973**, 31, 211.
- (120) Lindner, K.; Saenger, W. *Carbohydr. Res.* **1982**, 99, 103.
- (121) MacLennan, J. M.; Stezowski, J. J. *Biochem. Biophys. Res. Commun.* **1980**, 92, 926.
- (122) Tutt, D. E.; Schwartz, M. A. *J. Am. Chem. Soc.* **1971**, 93, 767.
- (123) Hennrich, N.; Cramer, F. *J. Am. Chem. Soc.* **1965**, 87, 1121.
- (124) Breslow, R. *Acc. Chem. Res.* **1995**, 28, 146.
- (125) Straub, T. S.; Bender, M. L. *J. Am. Chem. Soc.* **1972**, 94, 8881.
- (126) Tee, O. S.; Bennett, J. M. *J. Am. Chem. Soc.* **1988**, 110, 269; Tee, O. S.; Bennett, J. M. *J. Am. Chem. Soc.* **1988**, 110, 3226.
- (127) Tee, O. S.; Paventi, M.; Bennett, J. M. *J. Am. Chem. Soc.* **1989**, 111, 4172; Ruasse, M.-F. *Acc. Chem. Res.* **1990**, 28, 87; Ruasse, M.-F. *Adv. Phys. Org. Chem.* **1992**, 28, 207.
- (128) Griffith, D.W.; Bender, M. L. *J. Am. Chem. Soc.* **1973**, 95, 1679.
- (129) VanEtten, R. L.; Sebastian, J. F.; Clowes, G. A.; Bender, M. L. *J. Am. Chem. Soc.* **1967**, 89, 3242; VanEtten, R. L.; Sebastian, J. F.; Clowes, G. A.; Bender, M. L. *J. Am. Chem. Soc.* **1967**, 89, 3253.
- (130) Ghadiali, D. *Aminolysis of the 4-Acetoxybenzoate Anion Catalyzed by Cyclodextrins*; M.Sc. Thesis, Concordia University: Montreal, 2000.
- (131) Tee, O. S.; Gadosy, T. A.; Boyd, M. *J. Org. Chem.* **2000**, 65, 6879.
- (132) Kodaka, M. *J. Am. Chem. Soc.* **1993**, 115, 3702; Kodaka, M. *J. Phys. Chem.* **1998**, 102, 8101.
- (133) Ueno, A.; Takahashi, K.; Osa, T. *Chem. Commun.* **1980**, 921.
- (134) Connors, K. A. *J. Pharm. Sci.* **1995**, 82, 843.
- (135) Matsui, Y.; Mochida, K. *Bull. Chem. Soc. Jpn.* **1979**, 52, 2808.
- (136) Tee, O. S.; Bozzi, M.; Hoeven, J. J.; Gadosy, T. A. *J. Am. Chem. Soc.* **1993**, 115, 8990.
- (137) Segel, I. H. *Enzyme Kinetics: Behavior and Analysis of Rapid Equilibrium and Steady State Enzyme Systems*; Wiley-Interscience: New York, 1975.
- (138) Tee, O. S.; Gadosy, T. A.; Giorgi, J. B. *J. Chem. Soc. Perkin Trans. 2* **1993**, 1707.
- (139) Tee, O. S.; Gadosy, T. A.; Giorgi, J. B. *Can. J. Chem.* **1996**, 74, 736.

- (140) Tee, O. S.; Fedortchenko, A. A.; Loncke, P. G.; Gadosy, T. A. *J. Chem. Soc. Perkin Trans. 2* **1996**, 1243.
- (141) Tee, O. S.; Giorgi, J. B. *J. Chem. Soc. Perkin Trans. 2* **1997**, 1013.
- (142) Cooper, A.; Dryden, D. In *The Enzyme Catalysis Process: Energetics, Mechanism, and Dynamics*; Cooper, A., Houben, J. L., Chien, L. C., Eds.; Plenum Press: New York, 1989.
- (143) Tee, O. S.; Fedortchenko, A. A.; Soo, P. L. *J. Chem. Soc. Perkin Trans. 2* **1998**, 123.
- (144) Tee, O. S.; Hussein, S. M. I.; Turner, I. E.; Yazbeck, O. J. *J. Chem. Soc. Perkin Trans. 2* **2000**, 436.
- (145) Jencks, W. P. *Chem. Rev.* **1972**, 72, 705; Brown, C. J.; Kirby, A. J. *J. Chem. Soc. Perkin Trans. 2* **1997**, 1081; Buckley, N.; Oppenheimer, N. J. *J. Org. Chem.* **1996**, 61, 8048; Jensen, J. L.; Wuhrman, W. B. *J. Org. Chem.* **1983**, 4686; Jensen, J. L.; Jenks, W. P. *J. Am. Chem. Soc.* **1979**, 1476; Fife, T. H. *J. Am. Chem. Soc.* **1967**, 89, 3228.
- (146) Cordes, E. H.; Bull, H. G. *Chem. Rev.* **1974**, 74, 518.
- (147) Fife, T. H.; Jao, L. K. *J. Org. Chem.* **1964**, 30, 1492.
- (148) Jensen, J. L.; Herold, L. R.; Lenz, P. P.; Trusty, S.; Sergi, V.; Bell, K.; Rogers, P. *J. Amer. Chem. Soc.* **1979**, 101, 4672.
- (149) Jensen, J. L.; Martinez, A. B.; Shimazu, G. L. *J. Org. Chem.* **1983**, 4175; Wiberg, K. B.; Squires, R. S. *J. Am. Chem. Soc.* **1981**, 103, 4473; Wiberg, K. B.; Squires, R. S. *J. Am. Chem. Soc.* **1979**, 101, 5512.
- (150) McClelland, R. A.; Sørensen, P. *Acta Chem. Scand.* **1990**, 44, 1082.
- (151) Belarmino, A. T. N.; Froehner, S.; Zanette, D.; Farah, J. P. S.; Bunton, C. A.; Romsted, L. S. *J. Org. Chem.* **2003**, 68, 706.
- (152) Jensen, J. L.; Lenz, P. A. *J. Am. Chem. Soc.* **1978**, 100, 1291.
- (153) DeWolfe, R. H.; Jensen, J. L. *J. Am. Chem. Soc.* **1963**, 85, 3264.
- (154) Capon, B. *Pure & Appl. Chem.* **1977**, 49, 1001.
- (155) Turner, I. *The Study of β -Cyclodextrin Interactions with Sugars using "Inhibition Kinetics" and Bromination of Pyrimidine Derivatives*. M.Sc. Thesis, Concordia University: Montreal, 1999.
- (156) Fedortchenko, A. *Stabilization of Transition States of Organic Reactions by Cyclodextrins, Micelles and Dendrimers*; M.Sc. Thesis, Concordia University: Montreal, 1997.
- (157) Taraszewska, J. *J. Inclusion Phenom.* **1991**, 10, 69.
- (158) Rekharsky, M. V.; Schwartz, F. P.; Tewari, Y.; Goldberg, R. N.; Yamashoji, Y. J. *Phys. Chem.* **1994**, 98, 4098.
- (159) Gadre, A.; Rüdiger, V.; Schneider, H.-J.; Connors, K. A. *J. Pharm. Sci.* **1997**, 86, 236.
- (160) Buvari, A.; Barcza, L. *J. Chem. Soc. Perkin Trans. 2* **1988**, 543.
- (161) Tawarah, K. M.; Khouri, S. J. *Carbohydr. Res.* **1993**, 245, 165; Toki, A.; Yonemura, H.; Matsuo, T. *Bull. Chem. Soc. Jpn.* **1993**, 66, 3382.

- (162) Johnson, M. D.; Reinsborough, V. C.; Ward, S. *Inorg. Chem.* **1992**, *31*, 1087; Johnson, M. D.; Reinsborough, V. C. *J. Solution Chem.* **1994**, *23*, 185.
- (163) Iglesias, E. *J. Am. Chem. Soc.* **1998**, *120*, 13057.
- (164) Iglesias, E.; Ojea-Cao, V.; Garcia-Rio, L.; Leis, J. R. *J. Org. Chem.* **1999**, *64*, 3954.
- (165) Dunlap, R. B.; Ghanim, G. A.; Cordes, E. H. *J. Phys. Chem.* **1969**, *73*, 1898.
- (166) Bull, H. G.; Koehler, K.; Pletcher, T. C.; Ortiz, J. J.; Cordes, E. H. *J. Am. Chem. Soc.* **1971**, *93*, 3002.
- (167) Jensen, J. L.; Yamaguchi, K. S. *J. Org. Chem.* **1984**, *49*, 2613.
- (168) March, J. *Advanced Organic Chemistry*; third ed.; John Wiley & Sons: New York, 1985.
- (169) Wells, P. R. *Chem. Rev.* **1963**, *63*, 171.
- (170) Satake, I.; Ikenoue, T.; Takashita, T.; Hayakawa, K.; Meda, T. *Bull. Chem. Soc. Jpn.* **1985**, *58*, 2746; Satake, I.; Yoshida, S.; Hayakawa, K.; Meda, T.; Kusumoto, Y. *Bull. Chem. Soc. Jpn.* **1986**, *59*, 3991; Sanemasa, I.; Osajima, T.; Deguchi, T. *Bull. Chem. Soc. Jpn.* **1990**, *63*, 22814.
- (171) Schneider, H.-J. *Angew. Chem. Int. Ed. Engl.* **1991**, *30*, 1417; Schneider, H.-J. *Chem. Soc. Rev.* **1994**, *23*, 227.
- (172) Hamasaki, K.; Ikeda, H.; Nakamura, A.; Ueno, A.; Toda, F.; Suzuki, I.; Osa, T. *J. Am. Chem. Soc.* **1993**, *115*, 5035; Ikeda, H.; Nakamura, A.; Ise, N.; Oguma, N.; Nakamura, A.; Ikeda, T.; Toda, F.; Ueno, A. *J. Am. Chem. Soc.* **1996**, *118*, 10980; Corradini, R.; Dossena, A.; Galaverna, G.; Marchelli, R.; Panagia, A.; Sartor, G. *J. Org. Chem.* **1997**, *62*, 6283; Lipkowitz, K. B.; Raghothama, S.; Yang, J.-A. *J. Am. Chem. Soc.* **1992**, *114*, 1554.
- (173) Liu, Y.; Han, B.-H.; Sun, S.-X.; Wada, T.; Inoue, Y. *J. Org. Chem.* **1999**, *64*, 1487.
- (174) Bevington, P. R. *Data Reduction and Error Analysis for the Physical Sciences*; McGraw-Hill: New York, 1969; Draper, N. R.; Smith, H. *Applied Regression*; second ed.; Wiley: New York, 1981; Bates, D. M.; Watts, D. G. *Nonlinear Regression Analysis and its Application*; Wiley: New York, 1988; Seber, G. A. F.; Wild, C. J. *Nonlinear Regression*; Wiley: New York, 1989; Mezei, L. M. *Practical Spreadsheet Statistics and Curve Fitting for Scientists and Engineers*; Prentice-Hall: Englewood Cliffs, NJ, 1990.
- (175) Rosen, M. J. *Surfactants and Interfacial Phenomena*; second ed.; John Wiley & Sons: New York, 1989.
- (176) Wiedmann, T. S.; Kamel, L. *J. Pharm. Sci.* **2000**, *91*, 1743.
- (177) Overdeest, P. E. M.; Schutyser, M. I.; Bruin, T. J.; Riet, K.; Keurentjes, J. T. F.; Padt, A. *Ind. Eng. Chem. Res.* **2001**, *40*, 5998.
- (178) Fendler, J. H.; Fendler, E. J. *Catalysis in Micellar and Macromolecular Systems*; Academic Press: New York, 1975.
- (179) Fendler, J. H. *Ann. Rev. Phys. Chem.* **1985**, *35*, 137.
- (180) Bunton, C. A.; Savelli, G. *Adv. Phys. Org. Chem.* **1986**, *22*, 213.

- (181) Cordes, E. H. *Pure App. Chem.* **1978**, 50, 617.
- (182) Taşciolğlu, S. *Tetrahedron* **1996**, 52, 11113.
- (183) Rathman, J. F. *Curr. Opin. Colloid Interface Sci.* **1996**, 1, 514.
- (184) Fendler, J. H. *Membrane Mimetic Chemistry - Characterizations and Applications of Micelles, Microemulsions, Monolayers, Bilayers, Vesicles, Host-Guest Systems and Polyions*; John Wiley: New York, 1982; Fendler, J. H. *Acc. Chem. Res.* **1980**, 9, 7; Fendler, J. H. In *Handbook of Surface of Colloid Chemistry*; Birdi, K. S., Ed.; CRC Press, New York, 1997, Chapter 16. Liang, Y.; Zhang, Z. *J. Dispersion Sci. Technol.* **1995**, 16, 339; Ringsdorf, H.; Schlarb, B.; Venzmer, J. *Angew. Chem., Int. Ed. Engl.* **1988**, 27, 113; Kunitake, T. *Angew. Chem., Int. Ed. Engl.* **1992**, 31, 709; Fuhrhop, J. H.; Helfrich, W. *Chem. Rev.* **1993**, 93, 1565.
- (185) Kamlet, M. J.; Abboud, J. L. M.; Abraham, M. H.; Taft, R. W. *J. Org. Chem.* **1983**, 48, 2877.
- (186) Jennings, K.; Marshall, I.; Birrell, H.; Edwards, A.; Haskins, N.; Södermann, O.; Kirby, A. J. *J. Chem. Soc., Chem. Commun.* **1998**, 1951.
- (187) McGregor, C.; Perrin, C.; Monck, M.; Camilleri, P.; Kirby, A. J. *J. Am. Chem. Soc.* **2001**, 123, 6215; Menger, F. M.; Littau, C. A. *J. Am. Chem. Soc.* **1991**, 113, 1451; Menger, F. M.; Littau, C. A. *J. Am. Chem. Soc.* **1991**, 115, 10083; Menger, F. M.; Peresyphin, A. V. *J. Am. Chem. Soc.* **2001**, 123, 5614; Menger, F. M.; Keiper, J. S. *Angew. Chem., Int. Ed. Engl.* **2000**, 39, 1906.
- (188) Menger, F. M.; Seredyuk, V. A.; Apkarian, R. P.; Wright, E. R. *J. Am. Chem. Soc.* **2002**, 124, 12408.
- (189) Moss, R. A.; Mhas, G. G.; Lukas, T. J. *Tetrahedron Lett.* **1978**, 45, 507.
- (190) Moss, R. A.; Lukas, T. J.; Nahas, R. C. *Tetrahedron Lett.* **1977**, 44, 3851.
- (191) Moss, R. A.; Lee, Y.-S.; Lukas, T. J. *J. Am. Chem. Soc.* **1979**, 101, 2499.
- (192) Weijnen, J. G. J.; Koudjis, A.; Engbersen, J. F. J. *J. Org. Chem.* **1992**, 1994, 7258; Scrimin, P.; Tecilla, T.; Tonellato, U. *J. Org. Chem.* **1994**, 59, 4194; Brown, J. M.; Bunton, C. A. *Chem. Comm.* **1974**, 969.
- (193) Bunton, C. A.; Robinson, L.; Stam, M. F. *Tetrahedron Lett.* **1971**, 121.
- (194) Diego-Castro, M. J.; Hailes, H. C. *Chem. Commun.* **1998**, 1549.
- (195) Tickle, D.; George, A. *J. Chem. Soc. Perkin Trans. 2* **1998**, 467474.
- (196) Menger, F. M. *Acc. Chem. Res.* **1979**, 12, 111.
- (197) Professor Alexander Mackerell, Department of Pharmaceutical Chemistry, School of Pharmacy, University of Maryland, Baltimore, U.S.A.
- (198) El-Khadi, N.; Nartins, F.; Clausse, D.; Schulz, P. C. *Colloid Polym. Sci.* **2003**, 281, 353.
- (199) Asakawa, T.; Kitano, H.; Ohta, A.; Miyagishi, S. *J. Colloid Interface Sci.* **2001**, 242, 284.
- (200) Bhairi, S. M. "A Guide to the Properties and Uses of Detergents in Biology and Biochemistry," CALBIOCHEM, 1997.

- (201) Lindman, B.; Puyal, M.-C.; Kamenka, N.; Rymden, R. *J. Phys. Chem.* **1984**, *88*, 5048.
- (202) Zana, R. *Adv. Colloid Interface Sci.* **1995**, *57*, 1; Eads, C. D.; Robosky, L. C. *Langmuir* **1999**, *15*, 2661.
- (203) Kawashima, N. *J. Colloid Interface Sci.* **1985**, *103*, 459.
- (204) Reif, I.; Mulqueen, M.; Blankshtein, D. *Langmuir* **2001**, *17*, 5801.
- (205) Mysels, K. J.; Mukerjee, P. *Pure Appl. Chem.* **1979**, *51*, 1083.
- (206) Singh, H. N.; Saleem, S. M.; Singh, R. P.; Birdi, K. S. *J. Phys. Chem.* **1980**, *84*, 2191.
- (207) Mukerjee, P.; Chan, C. C. *Langmuir* **2002**, *18*, 5375.
- (208) Wennerstorm, H.; Lindman, B. *J. Phys. Chem.* **1979**, *23*, 2931.
- (209) Moroi, Y. *Micelles: Theoretical and Applied Aspects*; Plenum Press: New York, 1992.
- (210) Blandamer, M. J.; Cullis, P. M.; Engberts, J. B. F. N. *J. Chem. Soc. Faraday Trans.* **1998**, *94*, 2261.
- (211) MacInnis, J. A.; Marangoni, D. G.; Palepu, R. *Can. J. Chem.* **2000**, *78*, 1222.
- (212) Chatterjee, A.; Moulik, S. P.; Sanyal, S. K.; Mishra, B. K.; Puri, P. M. *J. Phys. Chem. B* **2001**, *105*, 12823.
- (213) Blandamer, M. J.; Cullis, P. M.; Soldi, L. G.; Engberts, J. B. F. N.; Kacperska, A.; Os, N. M. V.; Subha, M. C. S. *Adv. Colloid Interface Sci.* **1995**, *58*, 171.
- (214) Muller, N. *Langmuir* **1993**, *9*, 96; Islam, M. N.; Kato, T. *J. Phys. Chem. B* **2003**, *107*, 965.
- (215) Abraham, M. H. *J. Chem. Soc. Faraday Trans. 1* **1984**, *80*, 153.
- (216) Buurma, N. J.; Herranz, A. M.; Engberts, J. B. F. N. *J. Chem. Soc. Perkin Trans. 2* **1999**, 113; Buurma, N. J.; Serena, P.; Blandamer, M. J.; Engberts, J. B. F. N. *J. Org. Chem.* **2004**, *69*, 3899.
- (217) Gruen, D. W. R. *Progr. Colloid Polym. Sci.* **1985**, *70*, 6; Böcker, J.; Brickmann, J.; Bopp, P. *J. Phys. Chem.* **1994**, *98*, 712.
- (218) Laaksonen, L.; Rosenholm, J. B. *Chem. Phys. Lett.* **1993**, *216*, 42.
- (219) Lin, C.-C.; Jafvert, C. T. *Langmuir* **2000**, *16*, 2450.
- (220) Rathman, J. F.; Scamehorn, J. F. *J. Phys. Chem.* **1984**, *88*, 5807.
- (221) Benjamin, L. *J. Phys. Chem.* **1966**, *70*, 3790.
- (222) Menger, F. M. In *Surfactants in Solution*; Mittal, K. L., Lindman, B., Eds.; Plenum Press, 1984; Vol. 1, p 347.
- (223) Soler-Illia, G. J. A.; Sanchez, C.; Lebeau, B.; Patarin, J. *Chem. Rev.* **2002**, *102*, 4093.
- (224) Michels, B.; Waton, G. *J. Phys. Chem. A* **2003**, *107*, 1133; Hassan, P. A.; Yakhmi, J. V. *Langmuir* **2000**, *16*, 7187.
- (225) Broxton, T. J.; Nasser, A. *Can. J. Chem.* **1997**, *75*, 202; Froehner, S. J.; Nome, F.; Zanette, S.; Bunton, C. A. *J. Chem. Soc. Perkin Trans. 2* **1996**, 673.
- (226) Iglesias, E.; Montenegro, L. *J. Chem. Soc. Faraday Trans.* **1995**, *91*, 1349.

- (227) Khan, M. N.; Arifin, Z. *Langmuir* **1996**, *12*, 261.
- (228) Davies, D. M.; Foggo, S. J. *J. Chem. Soc. Perkin Trans. 2* **1998**, 247.
- (229) Iglesias, E. *J. Phys. Chem. B* **2001**, *105*, 10295.
- (230) Couderc, S.; Toullec, J. *Langmuir* **2001**, *17*, 3819.
- (231) Seoud, O. A.; Ruasse, M.-F.; Possidonio, S. *J. Phys. Org. Chem.* **2001**, *14*, 526; Possidonio, S.; Siviero, F.; Seoud, O. A. *E. J. Phys. Org. Chem.* **1999**, *12*, 325.
- (232) Profio, P. D.; Germani, R.; Savelli, G.; Cerichelli, G.; Spreti, N.; Bunton, C. A. *J. Chem. Soc. Perkin Trans. 2* **1996**, 2162; Corria, V. R.; Cuccovia, I. M.; Stelmo, M.; Chaimovich, H. *J. Am. Chem. Soc.* **1992**, *114*, 2144.
- (233) Iglesias, E. *Langmuir* **2001**, *17*, 6871.
- (234) Brinchi, L.; Profio, P. D.; Germani, R.; Savelli, G.; Spreti, N.; Bunton, C. A. *J. Chem. Soc. Perkin Trans. 2* **1998**, 361.
- (235) Profio, P. D.; Brinchi, L.; Germani, R.; Savelli, G.; Cerichelli, G.; Bunton, C. A. *J. Chem. Soc. Perkin Trans. 2* **2000**, 2162.
- (236) Blagoeva, I. B.; Toteva, M. M.; Quarti, N.; Ruasse, M.-F. *J. Org. Chem.* **2001**, *66*, 2123.
- (237) Rispen, R.; Engberts, J. B. F. N. *J. Org. Chem.* **2002**, *67*, 7369.
- (238) Brinchi, L.; Profio, P. D.; Germani, R.; Savelli, G.; Tugliani, M.; Bunton, C. A. *Langmuir* **2000**, *16*, 10101.
- (239) Engberts, J. B. F. N. *Pure App. Chem.* **1992**, *64*, 1653; Ruasse, M.-F. *Pure App. Chem.* **1997**, *69*, 1923; Li, Y.; Li, G.; Ma, C. *J. Disp. Sci. Technol.* **2000**, *21*, 409.
- (240) Zeng, X.; Chen, Y. *J. Disp. Sci. Technol.* **2000**, *21*, 449.
- (241) Bunton, C. A. *J. Mol. Liq.* **1997**, *72*, 231.
- (242) Cordes, E. H.; Dunlap, R. B. *Acc. Chem. Res.* **1969**, 329.
- (243) Fendler, E. J.; Fendler, J. H. *Adv. Phys. Org. Chem.* **1970**, *8*, 271.
- (244) Bunton, C. A. *Pure App. Chem.* **1977**, *49*, 969.
- (245) Funasaki, N. *J. Phys. Chem.* **1979**, *83*, 1998.
- (246) Romsted, L. S. In *Surfactants in Solution*; Mittal, K. L., Lindman, B., Eds.; Plenum Press: New York, 1984; Vol. 2, pp 1015.
- (247) Bunton, C. A.; Nome, F.; Quina, F. H.; Romsted, L. S. *Acc. Chem. Res.* **1991**, *24*, 357.
- (248) Bartet, D.; Gamoa, C.; Sepulveda, L. *J. Phys. Chem.* **1980**, *84*, 272.
- (249) Bunton, C. A.; Moffatt, K. R. *J. Phys. Chem.* **1986**, *90*, 538.
- (250) Jansson, M.; Stilbs, P. *J. Phys. Chem.* **1987**, *93*, 113.
- (251) Bunton, C. A. *J. Phys. Chem.* **1989**, *93*, 7851.
- (252) Bunton, C. A.; Fendler, E. J.; Sepulveda, L.; Yang, K.-U. *J. Am. Chem. Soc.* **1968**, *90*, 5512.
- (253) Bunton, C. A.; Foroudian, H. J.; Gillitt, N. D.; Whiddon, C. R. *Can. J. Chem.* **1998**, *76*, 946.
- (254) Dunlap, R. B.; Cordes, E. H. *J. Am. Chem. Soc.* **1968**, *90*, 4395; Dunlap, R. B.; Cordes, E. H. *J. Phys. Chem.* **1969**, *73*, 361.

- (255) Behme, M. T. A.; Fullington, J. G.; Noel, R.; Cordes, E. H. *J. Am. Chem. Soc.* **1965**, *87*, 265.
- (256) Ghosh, K. K.; Roy, S. *Bull. Chem. Soc. Jpn.* **1996**, *69*, 3417.
- (257) Otto, S.; Engberts, J. B. F. N.; Kwak, J. C. T. *J. Am. Chem. Soc.* **1998**, *120*, 9517.
- (258) Hawrylak, B. E.; Marangoni, D. G. *Can. J. Chem.* **1999**, *77*, 1241; Cang, H.; Brace, D. D.; Fayer, M. D. *J. Phys. Chem. B* **2001**, *105*, 10007.
- (259) Moroi, Y. *J. Phys. Chem.* **1980**, *84*, 2186.
- (260) Zhang, Y.-H.; Guo, L.; Ma, C.; Li, Q.-S. *Phys. Chem. Chem. Phys.* **2001**, *3*, 583; Riisager, A.; Hanson, B. E. *J. Molecular Catalysis A* **2002**, *189*, 195.
- (261) Hilczer, M.; Barzykin, A. V.; Tachiya, M. *Langmuir* **2001**, *17*, 4196; Rharbi, Y.; Li, M.; Winnik, M. A.; Hahn, K. G. *J. Am. Chem. Soc.* **2000**, *122*, 6242; Rharbi, Y.; Li, M.; Winnik, M. A.; Hahn, K. G. *Adv. Colloid Interface Sci.* **2001**, *90*, 25.
- (262) Rharbi, Y.; Chen, L.; Winnik, M. A. *J. Am. Chem. Soc.* **2004**, *126*, 6025.
- (263) Okahata, Y.; Ando, R.; Kunitake, T. *J. Am. Chem. Soc.* **1977**, *99*, 3067.
- (264) Kunitake, T.; Shinkai, S.; Okahata, Y. *Bull. Chem. Soc. Jap.* **1976**, *49*, 540.
- (265) Cerichelli, G.; Luchetti, L.; Mancini, G.; Muzzioli, M. N.; Germani, R.; Ponti, P. P.; Spreti, N.; Savelli, G.; Bunton, C. A. *J. Chem. Soc. Perkin Trans. 2* **1989**, 1081; Gustavsson, H.; Lindman, B. *J. Am. Chem. Soc.* **1975**, *97*, 3923; Oakes, J. *J. Chem. Soc. Faraday Trans. 2* **1973**, *69*, 1321; Robb, I. D.; Smith, J. *J. Chem. Soc. Faraday Trans. 2* **1974**, *70*, 287.
- (266) Buchner, R.; Holzl, C.; Stauber, J.; Barthel, J. *Phys. Chem. Chem. Phys.* **2002**, *4*, 2169.
- (267) Chaimovich, H.; Zanette, D.; Bonilha, J. B. S.; Cucovia, I. M. In *Surfactants in Solutions*; Mittal, K. L., Lindman, B., Eds.; Plenum Press: New York, 1984; Vol. 2, pp 1121; Chaimovich, H.; Blanco, A.; Chayet, L.; Costa, L. M.; Monteiro, P. M.; Bunton, C. A.; Paik, C. *Tetrahedron* **1975**, *31*, 1139.
- (268) Correia, V. R.; Cuccovia, I. M.; Chaimovich, H. *J. Phys. Org. Chem.* **1993**, *6*, 7.
- (269) Broxton, T. J.; Marcou, V. *J. Org. Chem.* **1991**, *59*, 1041; Broxton, T. J.; Christie, J. R.; Theodoris, D. *J. Phys. Org. Chem.* **1993**, *6*, 535.
- (270) Bunton, C. A.; Robinson, L. *J. Am. Chem. Soc.* **1968**, *90*, 5965.
- (271) Bunton, C. A.; Robinson, L. *J. Am. Chem. Soc.* **1970**, *92*, 356; Bunton, C. A.; Robinson, L. *J. Am. Chem. Soc.* **1968**, *34*, 780; Bunton, C. A.; Robinson, L. *J. Am. Chem. Soc.* **1968**, *90*, 5972; Bunton, C. A.; Robinson, L.; Schaak, J.; Stam, M. F. *J. Am. Chem. Soc.* **1971**, *36*, 2349.
- (272) Bunton, C. A.; Moffatt, J. R. *J. Phys. Chem.* **1988**, *92*, 2897.
- (273) Gandler, J. R.; Setiarahardjo, I. U.; Tufon, C.; Chen, C. *J. Org. Chem.* **1992**, *54*, 4169; Forlani, L. *J. Chem. Soc. Perkin Trans. 2* **1993**, 1525; Liou, J.-Y.; Huang, T.-M.; Chang, G.-G. *J. Chem. Soc. Perkin Trans. 2* **1999**, 2171; Montanari, S.; Paradisi, C.; Scorrano, G. *J. Org. Chem.* **1993**, *58*, 5628; Correa, N. M.; Durantini, E. N.; Silber, J. J. *J. Org. Chem.* **1999**, *64*, 5757.

- (274) Cerichelli, G.; Gramde C.; Luchetti, L.; Mancini, G. *J. Org. Chem.* **1991**, *56*, 3025. Ruasse, M.-F.; Moro, G. L.; Galland, B.; Bianchini, R.; Chiappe, C.; Bellucci, G. *J. Am. Chem. Soc.* **1997**, *119*, 2492.
- (275) Tee, O. S.; Javed, B. C. *J. Chem. Soc. Perkin Trans. 2* **1994**, 23.
- (276) Menger, F. M.; Portnoy, C. E. *J. Am. Chem. Soc.* **1967**, *89*, 4698.
- (277) Bunton, C. A.; Romsted, L. S.; Savelli, G. *J. Am. Chem. Soc.* **1979**, *101*, 1253.
- (278) Neves, M. F. S.; Zanette, D.; Quina, F.; Moretti, M. T.; Nome, F. *J. Phys. Chem.* **1989**, *93*, 1502.
- (279) Ferreira, L. C. M.; Zucco, C.; Zanette, D.; Nome, F. *J. Phys. Chem.* **1992**, *96*, 9058.
- (280) Soldi, V.; Keiper, J.; Romsted, L. S.; Cuccovia, I. M.; Chaimovich, H. *Langmuir* **2000**, *16*, 59.
- (281) Khan, N. M.; Ismail, E. *J. Chem. Soc. Perkin Trans. 2* **2001**, 1346.
- (282) Romsted, L. S. In *Micellization, Solubilization, and Microemulsions*; Mittal, K. L., Ed., 1977; Vol. 2, p 509.
- (283) Romsted, L. S. *J. Phys. Chem.* **1985**, *89*, 5107.
- (284) Romsted, L. S. *J. Phys. Chem.* **1985**, *89*, 5113.
- (285) Berzin, I. V.; Martinek, K.; Yatsimirskii, A. Y. *Russ. Chem. Rev. (Engl.)* **1973**, *41*, 787.
- (286) Martinek, K.; Osipov, A. P.; Yatsimirskii, A. Y.; Dahali, V. A.; Berzin, I. V. *Tetrahedron Lett.* **1975**, 1279; Martinek, K.; Osipov, A. P.; Yatsimirskii, A. Y.; Berzin, I. V. *Tetrahedron Lett.* **1973**, *29*, 963.
- (287) Quina, F. H.; Chaimovich, H. *J. Phys. Chem.* **1979**, *83*, 1844.
- (288) Quina, F. H.; Politi, M. J.; Cuccovia, I. M.; Baumgarten, E.; Martins-Franchetti, S. M.; Chaimovich, H. *J. Phys. Chem.* **1980**, *84*, 361.
- (289) Chaudhuri, A.; Loughlin, J. A.; Romsted, L. S.; Yao, J. J. *J. Am. Chem. Soc.* **1993**, *115*, 8351.
- (290) Bunton, C. A.; Moffat, J. R. *J. Phys. Chem.* **1988**, *92*, 2896.
- (291) Marin, M. A. B.; Nome, F.; Zanette, S.; Zucco, C.; Romsted, L. *J. Phys. Chem.* **1995**, *99*, 10879.
- (292) Rubio, D. A. R.; Zanette, S.; Nome, F.; Bunton, C. A. *Langmuir* **1994**, *10*, 1155.
- (293) Wei, L.; Lucas, A.; Yue, J.; Lennox, R. B. *Langmuir* **1991**, *7*, 1336.
- (294) Bunton, C. A.; Gan, L.-H.; Moffatt, J. R.; Romsted, L. S.; Savelli, G. *J. Phys. Chem.* **1981**, *85*, 4118.
- (295) Toullec, J.; Couderc, S. *Langmuir* **1997**, *13*, 1918.
- (296) Rathman, J. F.; Scamehorn, J. F. *Langmuir* **1987**, *3*, 372; Rathman, J. F.; Scamehorn, J. F. *J. Phys. Chem.* **1984**, *88*, 5807.
- (297) Romsted, L. R.; Cordes, E. H. *J. Am. Chem. Soc.* **1968**, *90*, 4404.
- (298) Almgren, M.; Rydholm, R. *J. Phys. Chem.* **1979**, *83*, 360.

- (299) Quina, F. H.; Politi, M. J.; Cuccovia, I. M.; Martins-Franchetti, S. M.; Chaimovich, H. In *Surfactants in Solution*; Mittal, K. L., Lindman, B., Eds.; Plenum Press: New York, 1984; Vol. 2, pp 1125.
- (300) Jencks, W. P.; Carriuolo, J. J. *Am. Chem. Soc.* **1960**, 1778; Jencks, W. P.; Gilchrist, M. J. *Am. Chem. Soc.* **1962**, 2910; Colthurst, M. J.; William, A. J. *Chem. Soc. Perkin Trans. 2* **1997**, 1493; Neuvonen, H.; Neuvonen, K. J. *Chem. Soc. Perkin Trans. 2* **1999**, 1497; Hess, R. A.; Hengge, A. C.; Cleland, W. W. *J. Am. Chem. Soc.* **1998**, 120, 2703; Tagaki, W.; Kobayashi, S.; Kurihara, K.; Kurashima, A.; Yoshida, Y.; Yano, Y. *J. Chem. Soc. Chem. Comm.* **1976**, 843-844.
- (301) Hupe, D. J.; Jencks, W. P. *J. Am. Chem. Soc.* **1977**, 99, 451.
- (302) Menger, F. M.; Ladika, M. J. *Am. Chem. Soc.* **1987**, 109, 3145.
- (303) Quina, F. H.; Politi, M. J.; Cuccovia, I. M.; Baumgarten, E.; Martins-Franchetti, S. M.; Chaimovich, H. *J. Phys. Chem.* **1977**, 81, 2000.
- (304) Bobica, C.; Anghel, D. F.; Voicu, A. *Colloids and Surfaces A: Physiochem. Eng. Aspects* **1995**, 105, 305.
- (305) Al-Awadi, N.; Williams, A. *J. Org. Chem.* **1990**, 55, 2001.
- (306) Williams, A. *Adv. Phys. Org. Chem.* **1992**, 27, 1.
- (307) Quarti, N.; Marques, A.; Blagoeva, I.; Ruasse, M.-F. *J. Disp. Sci. Technol.* **2000**, 16, 2157.
- (308) Chaimovich, H.; Bonihla, J. B. S.; Politi, M. J.; Quina, F. H. *J. Phys. Chem.* **1979**, 83, 1851.
- (309) Cuccovia, I. M.; Schroter, E. H.; Monteiro, P. M.; Chaimovich, H. *J. Org. Chem.* **1978**, 43, 2248.
- (310) Tagaki, W.; Amada, T.; Yamashita, Y.; Yano, Y. *J. Chem. Soc. Chem. Comm.* **1972**, 1131.
- (311) Williams, A. *Acc. Chem. Res.* **1989**, 22, 387.
- (312) Guthrie, J. P. *Can. J. Chem.* **1973**, 51, 3494; Guthrie, J. P. *J. Chem. Soc. Chem. Comm.* **1972**, 897.
- (313) Birdi, K. S. *Micellization, Solubilization and Microemulsions*; Plenum Press: New York, 1977; Vol. 1.
- (314) O'Connor, C. J.; Mitha, A. S. H.; Walde, P. *Aust. J. Chem.* **1986**, 39, 249.
- (315) Loupy, A.; Tchoubar, B. *Salt Effects in Organic and Organometallic Chemistry*; VCH: Weinheim, 1992.
- (316) Pearson, R. G. *Science* **1966**, 151, 172.
- (317) Kawamuro, M. K.; Chaimovich, H.; Albumin, E. B.; Lissi, E. A.; Cuccovia, I. M. *J. Phys. Chem.* **1991**, 95, 1458.
- (318) Chaimovich, H.; Blanco, A.; Chayet, L.; Costa, L. M.; Monteiro, P. M.; Bunton, C. A.; Paik, C. *Tetrahedron* **1975**, 31, 1139.
- (319) Perrin, D. D.; Armarego, W. L. F.; Perrin, D. R. *Purification of Laboratory Chemicals*; second ed.; Pergamon Press: Oxford, 1980.

- (320) Seoud, O. A. E.; Ruasse, M.-F.; Rodrigues, W. A. *J. Chem. Soc. Perkin Trans. 2* **2002**, 1053; O'Connor, C. J.; Wallace, R. G. *Aust. J. Chem.* **1984**, 37, 2559.
- (321) Machado, V. G.; Bunton, C. A.; Zucco, C.; Nome, F. *J. Chem. Soc. Perkin Trans. 2* **2000**, 169.
- (322) Sudholter, E. J. R.; Engberts, J. B. F. N. *J. Phys. Chem.* **1979**, 83, 1854.
- (323) Warthall, D. P.; Izatt, R. M.; Christiansen, J. J. *J. Am. Chem. Soc.* **1964**, 86, 4779.
- (324) Irving, R. J.; Nelander, L.; Wadso, I. *Acta Chem. Scand.* **1964**, 18, 769.
- (325) Hupe, D. J.; Jencks, W. P. *J. Am. Chem. Soc.* **1977**, 99, 454.
- (326) King, E. J. *J. Am. Chem. Soc.* **1951**, 73, 155.
- (327) Arrowsmith, C. H.; Kresge, A. J.; Tang, Y. C. *J. Am. Chem. Soc.* **1991**, 113, 179.
- (328) Adalsteinsson, H.; Bruice, T. C. *J. Am. Chem. Soc.* **1998**, 120, 3440; Hess, R. A.; Hengge, A. C.; Cleland, W. W. *J. Am. Chem. Soc.* **1997**, 119, 6980; Bruice, T. C.; Donzel, A.; Huffman, R. W.; Butler, A. R. *J. Am. Chem. Soc.* **1967**, 89, 2106; Henge, A. C.; Hess, R. A. *J. Am. Chem. Soc.* **1994**, 116, 11256.
- (329) Bruice, T. C.; Katzhendler, J.; Fedor, L. R. *J. Am. Chem. Soc.* **1968**, 90, 1333.
- (330) Jencks, W. P.; Gilchrist, M. *J. Am. Chem. Soc.* **1968**, 90, 2622.
- (331) Satterthwait, A. C.; Jencks, W. P. *J. Am. Chem. Soc.* **1974**, 96:22, 7018.
- (332) Williams, A. *Concerted Organic and Bio-organic Mechanisms*; CRC Press: Boca Raton, 2000.
- (333) Perrin, C. L.; Chem, J.-H.; Ohta, B. K. *J. Am. Chem. Soc.* **1999**, 121, 2448; Perez-Juste, J.; Hollfeder, F.; Kirby, A. J.; Engberts, J. B. F. N. *Organic Lett.* **2000**, 2, 127.
- (334) Menger, F. M.; Lynn, J. L. *J. Am. Chem. Soc.* **1975**, 97, 948.
- (335) Müller, P. *Pure Appl. Chem.* **1994**, 66, 1077; Hammond, G. S. *J. Am. Chem. Soc.* **1955**, 77, 334.
- (336) Mirgodskaya, A. B.; Kudryavtseva, L. A.; Ivanov, B. E. *Russ. Chem. Bull.* **1996**, 45, 351.
- (337) Mirgorodshaya, A. B.; Kudryavtseva, L. A.; Zakharova, L. Y.; Bel'skii, V. E. *Russ. Chem. Bull.* **1998**, 47, 1296.
- (338) Mirgodskaya, A. B.; Kudryavtseva, L. A. *Russ. Chem. Bull.* **1997**, 46, 258.
- (339) Oakenfull, D. G.; Fenwick, D. E. *Aust. J. Chem.* **1974**, 27, 2149; Oakenfull, D. G. *J. Chem. Soc. Perkin Trans. 2* **1973**, 1006; Blyth, C. A.; Knowles, J. R. *J. Am. Chem. Soc.* **1971**, 93, 3021; Knowles, J. R.; Parsons, C. A. *Chem. Commun.* **1967**, 755; Knowles, J. R.; Parsons, C. A. *Nature* **1969**, 53, 221; Blyth, C. A.; Knowles, J. R. *J. Am. Chem. Soc.* **1971**, 93, 3017.
- (340) Gitler, C.; Ochoa-Solano, A. *J. Am. Chem. Soc.* **1968**, 90, 5004.
- (341) Funasaki, N. *J. Colloid Interface Science* **1978**, 64, 461.
- (342) Gallo, R. *Prog. Phys. Org. Chem.* **1983**, 14, 115; Williams, A. In *The Chemistry of Enzyme Action*; Page, M. I., Ed.; Elsevier: Amsterdam, 1984; Chapter 5.
- (343) Harada, S.; Okada, H.; Sano, T.; Yamashita, T.; Yano, H. *J. Phys. Chem.* **1990**, 94, 7648.

- (344) Khan, M. N.; Arifin, Z.; Ismail, E.; Ali, S. F. M. *J. Org. Chem.* **2000**, 65, 1331.
- (345) Khan, M. N. *J. Phys. Org. Chem.* **1999**, 112, 1.
- (346) Zana, R.; S. Yiv; C. Strazielle; Lianos, P. *J. Colloid Interface Sci.* **1981**, 80, 208.
- (347) Hansch, C.; Leo, A. *Substituent Constants for Correlation Analysis in Chemistry and Biology*; John Wiley: New York, 1979.
- (348) Fujita, T.; Isawa, J.; Hansch, C. *J. Am. Chem. Soc.* **1964**, 86, 5175.
- (349) Hansch, C.; Leo, A. *Exploring QSAR: Fundamentals and Applications in Chemistry and Biology*; American Chemical Society: Washington, 1995.
- (350) Hansch, C.; Leo, A.; Hoekman, D. *Exploring QSAR: Hydrophobic, Electronic and Steric Constants.*; A.C.S. Publications: Washington. D.C., 1995; Sangster, J. *Octanol-water Partition Coefficients: Fundamentals and Physical Chemistry*; John Wiley & Sons: Chichester, 1997.
- (351) Kubinyi, H. *QSAR: Hansch Analysis and Related Approaches*; VCH: Weinheim, 1993; Vol. 1.
- (352) Taylor, P. J. In *Comprehensive Medicinal Chemistry: The Rational Design, Mechanistic Study & Therapeutic Application of Chemical Compounds.*; Hansch, C., Sammes, P. G., Taylor, J. B., Eds.; Pergamon Press: Oxford, 1990; Vol. 4.
- (353) Treiner, C. *J. Colloid Interface Sci.* **1983**, 93, 33.
- (354) Treiner, C.; Chattopadhyay, A. K. *J. Colloid Interface Sci.* **1986**, 109, 101.
- (355) Treiner, C.; Manneback, M.-H. *J. Colloid Interface Sci.* **1987**, 118, 243.
- (356) Leo, A.; Hansch, C.; Elkins, D. *Chem. Rev.* **1971**, 71, 525.
- (357) Alonso, B.; Harris, R. K.; Kenwright, A. M. *J. Colloid Interface Sci.* **2002**, 251, 366.
- (358) Kamlet, M. J.; Doherty, R. M.; Abboud, J.-L.; Abraham, M. H.; Taft, R. W. *J. Pharm. Sci.* **1986**, 75, 338; Kamlet, M. J.; Doherty, R. M.; Abraham, M. H.; Carr, P. W.; Doherty, R. F.; Taft, R. W. *J. Phys. Chem. B* **1987**, 91, 1966; Kamlet, M. J.; Doherty, R. H.; Abraham, M. H.; Marcus, Y.; Taft, R. W. *J. Phys. Chem. B* **1988**, 92, 5244; Sangster, J. *J. Phys. Chem. Ref. Data.* **1989**, 18, 1111.
- (359) Bhattacharya, S.; Snehlatha, K. *J. Chem. Soc. Perkin Trans. 2* **1996**, 2021.
- (360) Mock, W. L. *Bioorganic Chem.* **1976**, 5, 403.
- (361) Hansch, C. *Acc. Chem. Res.* **1993**, 26, 147; Fujita, T. *Prog. Phys. Chem.* **1983**, 14, 75; Leo, A. *Methods in Enzymology* **1991**, 202, 544; Hansch, C. *J. Am. Chem. Soc.* **1964**, 86, 5175.
- (362) Leo, A. *Chem. Rev.* **1993**, 93, 1281.
- (363) Leo, A.; Hansch, C. *J. Org. Chem.* **1971**, 36, 1539.
- (364) Cserhati, T.; Hollo, J.; Forgacs, E. *Hungarian Acad. Sci.* **1994**, 34, 275; Forgacs, E. *Biochem. Molec. Biol. Int.* **1993**, 30, 1.
- (365) Cserhati, T.; Forgacs, E. *Biochem. Molec. Biol. Int.* **1995**, 37, 555.
- (366) Subramanian, M.; Shershadri, B. S.; M.P.Venkatappa *J. Biochem.* **1984**, 95, 413.

- (367) Yamashita, T.; Yamasaki, M.; Sano, T.; Harada, S.; Yano, H. *Langmuir* **1995**, *11*, 1477; Yamashita, T.; Tanaka, K.; Yano, H.; Harada, S. *J. Chem. Soc.* **1991**, 87, 1857.
- (368) Cardoso, M. M.; Barrada, M. J.; Carrondo, M. T.; Kroner, K. H.; Crespo, J. G. *Bioseparations* **1998**, *7*, 65; Cardoso, M. M.; Barrada, M. J.; Kroner, K. H.; Crespo, J. G. *J. Chem. Technol. Biotechnol.* **1999**, *74*, 801.
- (369) Leodidis, E. B.; Hatton, T. A. *J. Phys. Chem.* **1990**, *94*, 6400.
- (370) Leodidis, E. B.; Hatton, T. A. *J. Phys. Chem.* **1990**, *94*, 6411.
- (371) Leodidis, E. B.; Bommarius, A. S.; Hatton, T. A. *J. Phys. Chem.* **1991**, *95*, 5943; Leodidis, E. B.; Hatton, T. A. *J. Phys. Chem.* **1991**, *95*, 5957.
- (372) Barra, M.; Rossi, R. H. D. *Can. J. Chem.* **1991**, *69*, 1124.
- (373) Miyagishi, S.; Akasohu, W.; Hashimoto, T.; Asakawa, T. *J. Colloid Interface Sci.* **1996**, *184*, 527; Miyagishi, S.; Akasohu, W.; Hashimoto, T.; Asakawa, T. *J. Colloid Interface Sci.* **1983**, *103*, 164; Tabohashi, T.; Tobita, K.; Sakamoto, K.; Kouchi, J.; Yokoyama, S.; Sakai, H.; Abe, M. *Colloids and Surfaces B: Biointerfaces* **2001**, *20*, 79.
- (374) Imamura, T.; Konishi, K. *J. Colloid Interface Sci.* **1998**, *198*, 300.
- (375) Treiner, C. *J. Colloid Interface Sci.* **1982**, *90*, 444; Sepulveda, L.; Lissi, E.; Wuina, F. *Adv. Colloid Interface Sci.* **1986**, *25*, 1.
- (376) Pliska, V.; Schmidt, M.; Fauchere, J. L. *J. Chromatogr.* **1981**, *216*, 79.
- (377) Cornette, J.; Cease, K. B.; Margalit, H.; Spouge, J. L.; Berzofsky, J. A.; DeLisi, C. *J. Mol. Biol.* **1987**, *195*, 659.
- (378) Wolfenden, R.; Andersson, L.; Cullis, P.; Southgate, C. *Biochemistry* **1981**, *20*, 849.
- (379) Yunger, L. M.; Cramer, R. D. *Mol. Pharmacol.* **1981**, *20*, 602.
- (380) Janin, J. *Nature* **1979**, *277*, 491.
- (381) Kyte, J.; Doolite, R. *J. Mol. Biol.* **1982**, *157*, 105.
- (382) Rose, G.; Geselowitz, A.; Lesser, G.; Lee, R.; Zehfus, M. *Science* **1985**, *229*, 834.
- (383) Charton, M.; Charton, B. I. *J. Theor. Biol.* **1982**, *99*, 629.
- (384) Tayar, N. E.; Tsai, R.-S.; Vallat, P.; Altomare, C.; Testa, B. *J. Chromatogr.* **1991**, *556*, 181; Tayar, N. E.; Tsai, R.-S.; Carrupt, P.-A.; Testa, B. *J. Chem. Soc. Perkin Trans. 2* **1992**, 79.
- (385) Chmelik, J.; Hudecek, J.; Putyera, K.; Makovicka, J.; Kalous, V.; Chmelikova, J. *Coll. Czech. Chem. Commun.* **1991**, *56*, 2030.
- (386) Bhattacharya, S.; Snehathatha, K. *Langmuir* **1997**, *13*, 378; Bhattacharya, S.; Snehathatha, K. *J. Chem. Soc. Perkin Trans. 2* **1996**, 2021.
- (387) Miller, P. D.; Spivey, H. O.; Copeland, S. L.; Sanders, R.; Woodruff, A.; Gearhart, D.; Ford, W. T. *Langmuir* **2000**, *16*, 108.
- (388) Kenley, R. A.; Lee, G. C.; Winterle, J. S. *J. Org. Chem.* **1985**, *50*, 40; Toullec, J.; Moukawim, M. *J. Chem. Soc. Chem. Comm.* **1996**, 221.
- (389) Marin, M. A. B.; Nome, F.; Zanette, D.; Zucco, C.; Romsted, L. S. *J. Phys. Chem.* **1995**, *99*, 10879.

- (390) Terrier, F. *Nucleophilic Aromatic Displacement*; VCH Publishers: New York, 1991.
- (391) Broxton, T. J.; Chung, R. R.-T. *J. Org. Chem.* **1990**, *55*, 3886.
- (392) Bunton, C. A.; Robinson, L.; Sepulveda, L. *J. Org. Chem.* **1970**, *35*, 108.
- (393) Cipiciani, A.; Germani, R.; Savelli, G.; Bunton, C. A.; Mhala, M.; Moffatt, J. R. *J. Chem. Soc. Perkin Trans. 2* **1987**, 541; Cipiciani, A.; Fracassini, M. C.; Germani, R.; Savelli, G.; Bunton, C. A. *J. Chem. Soc. Perkin Trans. 2* **1987**, 547; Al-Lohedan, H. A. *J. Chem. Soc. Perkin Trans. 2* **1995**, *8*, 1707.
- (394) Moss, R. A.; Nahas, R. C.; Ramaswami, S.; Sanders, W. J. *Tetrahedron Lett.* **1975**, *39*, 3379.
- (395) Anoardi, L.; Fornasier, R.; Tonellato, U. *J. Chem. Soc. Perkin Trans. 2* **1981**, 260.
- (396) Bonar-Law, R. P. *J. Am. Chem. Soc.* **1995**, *117*, 12397.
- (397) Shinitzk, M.; Haimovitz, R. *J. Am. Chem. Soc.* **1993**, *115*, 12545.

APPENDIX A - Data Relevant to Chapter III

Table A.1 Rate constants for the cleavage of PhCH(OMe)_2 in the presence of β -CD and various concentrations of ketone (G), and the calculation of K_G values for β -CD-Ketone complexes.^a

$[\text{G}]_0$ (mM)	k_{obs} (s ⁻¹)	$[\text{CD}]^b$ (mM)	$[\text{G} \cdot \text{CD}]^c$ (mM)	$[\text{G}]^d$ (mM)	K_G^e (mM)
Guest: acetone (# Jen 08)					
0.0	1.18	5.00	---	---	---
20.4	1.26	4.56	0.44	20.0	208
40.1	1.37	4.01	0.99	39.1	159
60.1	1.50	3.44	1.56	58.6	129
80.2	1.64	2.98	2.02	78.1	115
100.2	1.79	2.53	2.47	97.7	100
Average K_G					142 ± 38
Guest: cyclohexanone (# Jen 02)					
0.0	1.16	5.00	---	---	---
10.0	2.25	1.47	3.53	6.47	2.68
20.0	2.78	0.762	4.24	15.8	2.83
30.0	2.96	0.582	4.42	25.6	3.37
40.0	3.18	0.382	4.62	35.4	2.93
50.0	3.26	0.317	4.68	45.3	3.06
Average K_G					2.88 ± 0.14
Guest: 2-butanone (# Jen 03)					
0.0	1.14	5.00	---	---	---
20.0	1.29	4.16	0.838	19.2	95.4
40.0	1.51	3.21	1.787	38.2	68.7
60.1	1.74	2.50	2.49	57.6	57.7
80.2	2.04	1.80	3.19	76.9	43.3
100	2.19	1.51	3.48	96.7	42.1
Average K_G					61.4 ± 19.6
Guest: 2-butanone (# Jen 04)					
0.0	1.19	5.00	---	---	---
20.0	1.39	3.96	1.04	19.0	72.1
40.0	1.60	3.14	1.86	38.1	64.5
60.0	1.78	2.58	2.42	57.6	61.5
80.0	2.47	1.23	3.77	76.2	25.0
100.0	2.71	0.92	4.08	95.9	21.7
Average K_G					48.9 ± 21.2

Guest: 2-butanone (# Jen 07)					
0.0	1.19	5.00	---	---	---
20.7	1.39	3.96	1.04	19.6	74.5
41.2	1.60	3.12	1.88	39.3	65.3
61.8	1.84	2.42	2.58	59.2	55.7
82.4	2.11	1.83	3.17	79.3	45.8
103	2.35	1.40	3.60	99.4	38.8
Average K _G					56.0 ± 12.9
Guest: 2-pentanone (# Jen 05)					
0.0	1.23	5.00	---	---	---
10.0	1.41	4.09	0.91	9.09	40.7
20.0	1.62	3.26	1.74	18.26	34.3
30.0	1.79	2.72	2.28	27.72	33.2
40.0	1.94	2.34	2.66	37.34	32.8
50.0	2.10	1.99	3.01	46.99	31.0
Average K _G					34.4 ± 3.3
Guest: 2-pentanone (# Jen 11)					
0.0	1.16	5.00	---	---	---
10.0	1.38	3.83	1.17	8.83	28.7
20.0	1.53	3.21	1.79	18.2	32.8
30.0	1.77	2.47	2.53	27.5	26.9
40.0	1.92	2.10	2.90	37.1	26.9
50.0	2.15	1.64	3.36	46.6	22.7
Average K _G					27.6 ± 3.4
Guest: 2-hexanone (# Jen 06)					
0.0	1.19	5.00	---	---	---
5.0	1.39	3.94	1.06	3.94	14.7
10.0	1.63	3.04	1.96	8.04	12.4
15.0	1.97	2.13	2.87	12.1	8.99
20.0	2.25	1.59	3.41	16.6	7.70
25.0	2.53	1.15	3.85	21.2	6.32
Average K _G					10.0 ± 3.1

Guest: 2-hexanone (# Jen 9)					
0.0	1.12	5.00	---	---	---
5.0	1.34	3.80	1.20	3.94	12.06
10.0	1.67	2.59	2.41	8.04	8.17
15.0	2.14	1.54	3.46	12.1	5.15
20.0	2.37	1.17	3.83	16.6	4.93
25.0	2.75	0.69	4.31	21.2	3.33
Average K_G					6.73 ± 3.9
Guest: 2-hexanone (# Jen 10)					
0.0	1.15	5.00	---	---	---
5.06	1.38	3.82	1.18	3.88	12.5
10.1	1.66	2.77	2.23	7.89	9.81
15.2	1.80	2.39	2.61	12.6	11.5
20.2	2.02	1.89	3.11	17.1	10.4
25.3	2.37	1.27	3.73	21.6	7.35
Average K_G					10.3 ± 1.8

^a In 0.10 M aqueous HCl, at 25.0 °C. The $[\beta\text{-CD}]_0 = 5.00$ mM, and $[\text{BDMA}] = 50$ μM .

^b Calculated using equation [3.7], ^c eq. [3.8], ^d eq.[3.9], ^e eq.[3.10] in Chapter 3, Section 3.2.3.

Table A.2 Rate constants for the cleavage of PhCH(OMe)_3 in the presence of β -CD and various concentrations of ketone (G), and the calculation of K_G values for β -CD-Ketone complexes.^a

$[\text{G}]_0$ (mM)	k_{obs} (s^{-1})	$[\text{CD}]^b$ (mM)	$[\text{G} \cdot \text{CD}]^c$ (mM)	$[\text{G}]^d$ (mM)	K_G^e (mM)
Guest: 2-butanone (# Jen 13)					
0.0	2.19	1.00	---	---	---
20.0	2.42	0.844	0.156	19.8	107
40.0	2.67	0.708	0.292	39.7	96.4
60.0	2.90	0.611	0.389	59.6	93.4
79.9	3.18	0.514	0.486	79.4	84.1
99.9	3.40	0.452	0.548	99.4	82.0
Average K_G					92.6 ± 9.0
Guest: 2-pentanone (# Jen 14)					
0.0	2.16	1.00	---	---	---
10.3	2.51	0.769	0.231	10.0	33.5
20.6	2.84	0.617	0.383	20.2	32.5
30.8	3.14	0.513	0.487	30.4	31.9
41.1	3.39	0.442	0.558	40.6	32.1
51.4	3.67	0.377	0.623	50.8	30.7
Average K_G					32.1 ± 0.9
Guest: 2-hexanone (# Jen 15)					
0.0	2.15	1.00	---	---	---
5.0	2.54	0.747	0.253	4.75	14.0
10.0	3.03	0.541	0.459	9.54	11.2
15.0	3.51	0.408	0.592	14.4	9.92
20.0	3.88	0.330	0.670	19.3	9.51
25.0	4.55	0.227	0.773	24.2	7.12
Average K_G					10.4 ± 2.2
Guest: 2-heptanone (# Jen 24)					
0.00	2.22	1.000	---	---	---
1.04	2.43	0.856	0.144	0.891	5.31
2.07	2.62	0.747	0.253	1.82	5.37
3.11	2.82	0.657	0.343	2.76	5.30
4.14	3.10	0.552	0.448	3.69	4.56
5.18	3.25	0.507	0.493	4.68	4.81
Average K_G					5.07 ± 0.32

Guest: 2-octanone (# Jen 25)					
0.0	2.22	1.000	---	---	---
0.156	2.29	0.945	0.0555	0.101	1.72
0.313	2.35	0.906	0.0944	0.218	2.10
0.469	2.43	0.852	0.148	0.321	1.84
0.626	2.49	0.813	0.187	0.439	1.91
0.782	2.58	0.765	0.235	0.547	1.78
Average K _G					1.87 ± 0.13
Guest: 3-hexanone (# Jen 20)					
0.0	2.20	1.00	---	---	---
4.0	2.42	0.846	0.154	3.85	21.1
8.0	2.69	0.701	0.299	7.70	18.1
12.0	2.92	0.604	0.396	11.6	17.7
16.0	3.14	0.528	0.472	15.5	17.4
20.0	3.33	0.472	0.528	19.5	17.4
Average K _G					18.3 ± 1.40
Guest: 3-heptanone (# Jen 22)					
0.00	2.24	1.00	---	---	---
2.01	2.49	0.829	0.171	1.84	8.90
4.03	2.79	0.680	0.320	3.71	7.87
6.03	3.06	0.575	0.425	5.61	7.58
8.04	3.30	0.499	0.501	7.54	7.52
10.05	3.51	0.443	0.557	9.49	7.54
Average K _G					7.88 ± 0.52
Guest: 3-octanone (# Jen 23)					
0.00	2.21	1.00	---	---	---
0.138	2.25	0.970	0.0299	0.108	3.50
0.276	2.30	0.933	0.0670	0.209	2.91
0.414	2.32	0.918	0.0824	0.332	3.69
0.552	2.37	0.887	0.113	0.439	3.46
0.690	2.41	0.857	0.143	0.547	3.27
Average K _G					3.37 ± 0.27
Guest: cyclopentanone (# Jen 16)					
0.0	2.12	1.00	---	---	---
10.0	2.78	0.620	0.380	9.65	15.7
20.1	3.31	0.447	0.553	19.5	15.8
30.1	3.64	0.367	0.633	29.5	17.1
40.1	4.09	0.285	0.715	39.4	15.7
50.2	4.29	0.255	0.745	49.4	16.9
Average K _G					16.2 ± 0.6

Guest: cyclohexanone (# Jen 17)					
0.0	2.20	1.00	---	9.24	---
10.0	4.78	0.214	0.786	19.2	2.51
20.1	5.78	0.119	0.881	29.2	2.59
30.1	6.39	0.077	0.923	39.2	2.45
40.2	6.71	0.058	0.942	49.2	2.43
50.2	6.89	0.049	0.951	9.24	2.53
Average K _G				2.50 ± 0.06	
Guest: cycloheptanone (# Jen 18)					
0.00	2.22	1.00	---	---	---
1.04	3.10	0.555	0.445	0.596	0.743
2.01	3.87	0.358	0.642	1.37	0.763
3.12	4.49	0.257	0.743	2.38	0.822
4.17	4.96	0.199	0.801	3.36	0.838
5.21	5.33	0.161	0.839	4.37	0.839
Average K _G				0.801 ± 0.040	
Guest: cyclooctanone (# Jen 21)					
0.00	2.20	1.000	---	---	---
0.40	2.56	0.771	0.229	0.171	0.576
0.83	3.02	0.572	0.428	0.402	0.538
1.21	3.40	0.458	0.542	0.668	0.564
1.61	3.97	0.334	0.666	0.944	0.474
2.01	4.29	0.280	0.720	1.29	0.501
Average K _G				0.530 ± 0.038	

^a In 0.10 M aqueous HCl, at 25.0 °C. The $[\beta\text{-CD}]_0 = 1.00$ mM, and $[\text{TMOB}] = 50$ μM .

^b Same as in table A.1

APPENDIX B - Data Relevant to Chapter VI

Table B.1 Rate constants for the cleavage of *p*-nitrophenyl alkanoates in varying concentration of CTAB, with constant $[\text{Br}^-]$ and constant mercaptoethanol $([\text{ME}]_0)^a$

[CTAB] ₀ (mM)	$k_{\text{obs}} (\text{s}^{-1})$	
	acetate (# Jen 30)	acetate (# Jen 33)
0.00	0.228	0.233
1.00	0.465	0.476
2.00	0.708	0.714
3.00	0.910	0.931
4.00	1.12	1.14
5.00	1.26	1.34
$K_S =$	19.7 ± 3.2 (not constant $[\text{Br}^-]$, <i>cmc</i> variable)	17.2 ± 4.91 (not constant $[\text{Br}^-]$)

[CTAB] ₀ (mM)	$k_{\text{obs}} (\text{s}^{-1})$	
	acetate (# Jen 38)	acetate (# Jen 62)
0.00	0.246	0.208
0.25	0.295	0.265
0.50	0.367	0.324
0.75	0.431	-
1.00	0.492	0.462
2.00	0.747	0.691
3.00	0.975	0.891
4.00	1.17	1.07
5.00	1.37	1.22
$K_S =$	15.6 ± 3.0 (constant $[\text{Br}^-]$, <i>cmc</i> constant)	12.7 ± 0.5 (constant $[\text{Br}^-]$, <i>cmc</i> constant))

[CTAB] ₀ (mM)	k_{obs} (s ⁻¹)	
	butanoate (# Jen 50)	hexanoate (# Jen 43)
0.00	0.140	0.138
0.05	-	0.156
0.10	0.168	0.358
0.25	0.267	0.723
0.50	0.465	1.24
0.75	0.605	1.37
1.00	0.732	1.63
2.00	1.07	1.89
3.00	1.27	1.98
4.00	1.40	2.04
5.00	1.51	2.08
$K_S =$	2.34 ± 0.10	0.465 ± 0.030

[CTAB] ₀ (mM)	k_{obs} (s ⁻¹)	
	pentanoate (# Jen 56)	heptanoate (# Jen 59)
0.00	0.141	0.130
0.05	0.146	0.160
0.25	0.478	1.49
0.50	0.792	1.83
0.75	0.995	1.93
1.00	1.16	1.99
2.00	1.50	-
3.00	1.67	2.11
4.00	1.77	-
5.00	1.86	2.14
$K_S =$	0.975 ± 0.015	0.0995 ± 0.004

[CTAB] ₀ (mM)	k_{obs} (s ⁻¹) octanoate (# Jen 53 & 85)
0.0	0.111
0.0137	0.114
0.0343	0.128
0.0500	0.298
0.0686	0.638
0.100	1.63
0.137	1.90
0.150	1.69
0.200	1.87
0.206	2.09
0.253	1.93
0.274	2.14
0.300	2.01
0.343	2.17
0.500	2.13
1.000	2.17
5.000	2.28
$K_S =$	0.0323 ± 0.0065

[CTAB] ₀ (mM)	k_{obs} (s ⁻¹) decanoate (# Jen 91 & 94)
0	0.00546
0.0630	0.00647
0.0810	0.0398
0.0940	1.05
0.100	2.17
0.112	1.93
0.200	2.19
0.214	2.14
0.300	2.15
0.318	2.20
0.400	2.15
0.500	2.38
1.00	2.37
2.00	2.38
3.00	2.40
4.00	2.46
5.00	2.43
5.00	2.52
$K_S =$	0.00585^c

^a The total [Br⁻] = 5.0 mM, kept constant. The buffer is 0.1 M NaHCO₃, standardized to a pH = 10.6. The nucleophile is hydroxide ion from the buffer and added [ME] = 20 mM. Concentration of the esters are: [acetate - pentanoate] = 50 μM, [hexanoate] = 25 μM, [octanoate] = 2.5 μM, [decanoate] = 1.5 μM.

^b The values of K_S are found using equation 6.7 (Chapter VI, section 6.2), with the *cmc* found kinetically to average 0.050 mM, and kept constant throughout.

^c Obtained by extrapolation of the linear plot of pK_S vs. *n*, the ester chain length.

Table B.2 Rate constants for the cleavage of *p*-nitrophenyl alkanoates in varying concentration of mercaptoethanol (ME) in the absence or presence of CTAB.^a

[ME] _o (mM)	k _{obs} (s ⁻¹) [CTAB] _o = 0 mM [Br ⁻] _o = 5.0 mM	k _{obs} (s ⁻¹) [CTAB] _o = 5.0 mM [Br ⁻] _o = 0 mM
	Ester: acetate	
	(# Jen 60)	(# Jen 61)
5.0	0.0568	0.241
10.0	0.114	0.619
15.0	0.173	0.957
20.0	0.232	1.29
25.0	0.291	1.61
40.0	0.465	2.58
50.0	0.581	3.19
	Ester: butanoate	
	(# Jen 44)	(# Jen 45)
5.0	0.0390	0.326
10.0	0.0798	0.803
15.0	0.116	1.17
20.0	0.155	1.67
25.0	0.192	2.04
40.0	0.311	3.23
50.0	0.390	4.04
	Ester: pentanoate	
	(# Jen 54)	(# Jen 55)
5.0	0.0367	0.411
10.0	0.0781	0.923
15.0	0.117	1.43
20.0	0.158	1.96
25.0	0.204	2.51
40.0	0.320	3.95
50.0	0.395	4.87

^a The total [Br⁻] = 5.0 mM, kept constant. The buffer is 0.1 M NaHCO₃, standardized to a pH = 10.6. In the data analysis to find k_{cN} values, the fixed [CTAB] was set to be [CTAB]_o - cmc = 4.95 mM. Concentration of the esters are: [acetate - pentanoate] = 50 μM, [hexanoate] = 25 μM, [octanoate] = 2.5 μM, [decanoate] = 1.5 μM. See Chapter VI, Section 6.2, for data analysis.

Ester: hexanoate		
	(# Jen 40)	(# Jen 41)
5.0	0.0351	0.433
10.0	0.0784	1.09
12.5	0.0970	1.41
20.0	0.159	2.23
25.0	0.196	2.78
30.0	0.230	-
40.0	0.311	4.43
50.0	0.376	5.40
Ester: heptanoate		
	(# Jen 57)	(# Jen 58)
5.0	0.0357	0.446
10.0	0.0733	1.09
15.0	0.116	1.73
20.0	0.155	2.30
25.0	0.192	2.84
40.0	0.307	4.40
50.0	0.379	5.36
Ester: octanoate		
	(# Jen 47)	(# Jen 48)
5.0	0.0315	0.327
10.0	0.0673	1.07
15.0	0.0948	1.76
20.0	0.118	2.27
25.0	0.163	2.92
40.0	0.279	4.54
50.0	0.374	5.73
Ester: decanoate ^b		
	(# Jen 93)	
5.0	0.459	
10.0	1.16	
15.0	1.94	
20.0	2.58	
25.0	3.13	
40.0	4.88	
50.0	5.89	

^b For *p*-nitrophenyl decanoate k_{obs} values in the absence of CTAB cannot be measured accurately. In the data analysis, the k_N is taken to be the same as for the octanoate ester.

Table B.3 Rate constants for the cleavage of *p*-nitrophenyl alkanoates in the presence of varying concentration of CTAB, with constant $[\text{Br}^-]$ and constant mercaptoacetic acid ($[\text{MAA}]_0$).^a

$[\text{CTAB}]_0$ (mM)	$k_{\text{obs}} (\text{s}^{-1})$	
	acetate (# Jen 101)	butanoate (# Jen 102)
0.00	0.346	0.219
0.30	-	1.22
0.50	0.806	2.07
1.00	1.32	3.58
2.00	2.37	5.62
3.00	3.31	6.66
4.00	4.17	7.46
5.00	4.91	8.51
$K_S =$	24.6 ± 4.0	2.60 ± 0.23

$[\text{CTAB}]_0$ (mM)	$k_{\text{obs}} (\text{s}^{-1})$	
	pentanoate (# Jen 103)	hexanoate (# Jen 107)
0.00	0.220	0.214
0.10	-	1.70
0.30	2.70	6.07
0.50	4.19	8.12
1.00	6.94	10.6
2.00	9.44	12.3
3.00	10.3	12.9
4.00	11.3	13.4
5.00	11.5	13.6
$K_S =$	1.06 ± 0.07	0.374 ± 0.009

^a The total $[\text{Br}^-] = 5.0 \text{ mM}$, kept constant. The buffer is 0.1 M NaHCO_3 , standardized to a $\text{pH} = 10.6$. Concentration of the esters are: [acetate - pentanoate] = $50 \mu\text{M}$, [hexanoate] = $25 \mu\text{M}$, [octanoate] = $2.5 \mu\text{M}$, [decanoate] = $1.5 \mu\text{M}$.

The nucleophile is hydroxide ion from the buffer and added $[\text{MAA}] = 20 \text{ mM}$.

^b The values of K_S are found using equation 6.7 (Chapter VI, section 6.2), with the *cmc* found kinetically to average 0.050 mM , and kept constant throughout.

[CTAB] _o (mM)	k_{obs} (s ⁻¹)	
	heptanoate (# Jen 114)	octanoate (# Jen 106)
0.00	0.203	0.0867
0.05	0.320	0.331
0.10	3.63	4.08
0.2	-	6.81
0.30	10.2	7.22
0.50	11.8	7.62
0.80	13.0	7.71
1.00	13.5	7.87
2.00	14.0	8.30
3.00	14.5	8.61
4.00	14.7	
5.00	14.9	
$K_S =$	0.141 ± 0.008	0.0493 ± 0.013

[CTAB] _o (mM)	k_{obs} (s ⁻¹)
	octanoate (# Jen 107)
0.00	0.180
0.05	0.796
0.10	7.15
0.20	10.65
0.30	12.13
0.50	13.00
0.80	13.13
1.00	13.68
2.00	14.02
3.00	14.26
4.00	14.44
5.00	14.60
$K_S =$	0.0539 ± 0.0032

[CTAB] _o (mM)	k_{obs} (s ⁻¹)
	decanoate (# Jen 111)
0	0.00
0.05	3.95
0.06	3.86
0.08	7.51
0.15	12.4
0.10	11.7
0.20	12.5
0.30	13.2
0.40	13.6
0.50	13.5
1.00	13.6
2.00	13.6
3.00	14.6
4.00	14.2
5.00	14.1
$K_S =$	0.00664^c

^c Obtained by extrapolation of the linear plot pK_S vs. n , where n is the ester chain length.

Table B.4 Rate constants for the cleavage of *p*-nitrophenyl alkanoates in varying concentrations of mercaptoacetic acid (MAA) in the absence or presence of CTAB.^a

[MAA] _o (mM)	k _{obs} (s ⁻¹) [CTAB] _o = 0 mM [Br ⁻] _o = 5.0 mM	k _{obs} (s ⁻¹) [CTAB] _o = 5.0 mM [Br ⁻] _o = 0 mM
	Ester: acetate	
	(# Jen 95)	(# Jen 95)
0.0	0.00808	0.0170
5.0	0.0803	1.93
10.0	0.156	3.36
15.1	0.242	4.75
20.1	0.320	5.78
25.1	0.405	6.79
Ester: butanoate		
	(# Jen 96)	(# Jen 99)
0.0	0.00509	0.0171
5.2	0.0419	2.93
10.4	0.0928	5.33
15.7	0.147	7.76
20.9	0.199	9.66
26.1	0.261	11.40
Ester: pentanoate		
	(# Jen 97)	(# Jen 100)
0.0	0.00447	0.0204
5.02	0.0301	3.42
10.0	0.0788	6.03
15.1	0.143	9.88
20.1	0.196	12.29
25.1	0.257	14.65
Ester: hexanoate		
	(# Jen 104)	(# Jen 105)
0.0	0.00453	0.0169
5.01	0.0495	3.17
10.0	0.103	7.04
15.0	0.155	10.80
20.1	0.215	12.89
25.1	0.269	15.31

Ester: heptanoate		
	(# Jen 112)	(# Jen 113)
0.0	0.00441	0.0194
5.0	0.0464	4.81
10.0	0.100	9.19
15.0	0.157	13.4
20.0	0.210	15.6
25.0	0.271	18.2
Ester: octanoate		
	(# Jen 108)	(# Jen 109)
0.0	0.0367	0.0173
5.0	0.0493	4.3
10.0	0.0976	8.7
15.0	0.147	13.2
20.1	0.199	16.3
25.1	0.251	19.0
Ester: decanoate ^b		
	(# Jen 110)	
0.0	0.0166	
5.0	4.18	
10.0	8.46	
15.0	13.1	
20.1	16.5	
25.1	19.6	

^a The total $[\text{Br}^-] = 5.0 \text{ mM}$, kept constant. The buffer is 0.1 M NaHCO_3 , standardized to a $\text{pH} = 10.6$. Concentration of the esters are: [acetate - pentanoate] = $50 \text{ }\mu\text{M}$, [hexanoate] = $25 \text{ }\mu\text{M}$, [octanoate] = $2.5 \text{ }\mu\text{M}$, [decanoate] = $1.5 \text{ }\mu\text{M}$. In the data analysis to find k_{cN} values, the fixed [CTAB] was set to be $[\text{CTAB}]_0 - \text{cmc} = 4.95 \text{ mM}$. See Chapter VI, Section 6.2, for data analysis.

^b For *p*-nitrophenyl decanoate k_{obs} values in the absence of CTAB cannot be measured accurately. In the data analysis, the k_{N} is taken to be the same as for the octanoate ester.

Table B.5 Rate constants for the cleavage of *p*-nitrophenyl alkanoates in varying concentration of 3-mercaptopropanoic acid (MPA) in the absence or presence of CTAB.^a

[MPA] _o (mM)	k _{obs} (s ⁻¹) [CTAB] _o = 0 mM [Br ⁻] _o = 5.0 mM	k _{obs} (s ⁻¹) [CTAB] _o = 5.0 mM [Br ⁻] _o = 0 mM
	Ester: acetate	
	(# Jen 89a)	(# Jen 89b)
0.0	0.00802	0.0143
4.01	0.0501	0.310
8.03	0.101	1.22
12.1	0.149	1.86
16.1	0.196 ^b	2.08 ^b
20.1	0.240 ^b	2.51 ^b
Ester: butanoate		
	(# Jen 121)	(# Jen 115)
0.0	0.00653	0.147
4.01	0.0310	1.25
8.03	0.0750	2.11
12.1	0.115	2.90
16.1	0.164 ^b	3.69 ^b
20.1	0.203 ^b	4.44 ^b
Ester: pentanoate		
	(# Jen 118)	(# Jen 116)
0.0	0.00513	0.0132
1.00	-	0.230
2.49	0.0231	0.970
4.98	0.0437	2.09
10.0	0.0886	3.96
15.0	0.130	5.19
20.0	0.173 ^b	6.79 ^b
24.9	0.216 ^b	7.04 ^b

Ester: hexanoate		
	(# Jen 120)	(# Jen 122)
0.0	0.00568	0.0183
1.00	-	0.217
2.50	0.0122	0.746
5.00	0.0323	1.68
10.0	0.0779	4.09
15.0	0.122	6.32
20.0	0.150 ^b	7.54 ^b
25.0	0.196 ^b	8.05 ^b

Ester: heptanoate		
	(# Jen 119)	(# Jen 117)
0.0	0.00508	0.0144
1.00	-	0.101
2.49	0.0179	0.961
4.98	0.0361	2.18
10.0	0.0778	4.31
15.0	0.119	5.88
20.0	0.162 ^b	7.77 ^b
24.9	0.197 ^b	7.82 ^b

Ester: octanoate		
	(# Jen 124)	(# Jen 123)
0.0	0.00557	0.0185
1.00	-	0.149
2.49	0.0128	0.496
4.98	0.0324	1.19
10.0	0.0772	3.47
15.0	0.119	5.75
20.0	0.145 ^b	6.82 ^b
24.9	0.189 ^b	8.15 ^b

^a As in Table B.4.

^b Data points excluded in the analysis. Observed curvature at higher concentrations due to saturation of the mercaptopropanoate dianions in CTAB micelles.

Table B.6 Rate constants for the cleavage of *p*-nitrophenyl alkanoates in varying concentration of cysteine (Cys) in the absence or presence of CTAB.^a

[Cys] _o (mM)	k _{obs} (s ⁻¹) [CTAB] _o = 0 mM [Br ⁻] _o = 5.0 mM	k _{obs} (s ⁻¹) [CTAB] _o = 5.0 mM [Br ⁻] _o = 0 mM
	Ester: acetate	
	(# Jen 142)	(# Jen 143)
0.0	0.00900	0.0145
2.5	0.0325	0.373
5.0	0.0553	0.773
10.0	0.103	1.51
15.0	0.153	2.16
20.0	0.202 ^b	2.74 ^b
25.0	0.254 ^b	3.18 ^b
	Ester: butanoate	
	(# Jen 144)	(# Jen 145)
0.0	0.00471	0.0140
2.5	0.0162	0.666
5.0	0.0305	1.32
10.0	0.0613	2.64
15.0	0.0921	3.56
20.0	0.123 ^b	4.75 ^b
25.0	0.153 ^b	5.39 ^b
	Ester: hexanoate	
	(# Jen 146)	(# Jen 147)
0.0	0.00528	0.0152
2.5	0.0197	0.804
5.0	0.0350	1.70
10.0	0.0619	3.47
15.0	0.0899	5.04
20.0	0.119 ^b	6.42 ^b
25.0	0.149 ^b	7.54 ^b

Ester: octanoate		
	(# Jen 148)	(# Jen 149)
0.0	0.00420	0.0165
2.5	0.0187	0.794
5.0	0.0339	1.74
10.0	0.0701	3.75
15.0	0.102	5.40
20.0	0.139 ^b	6.99 ^b
25.0	0.177 ^b	8.15 ^b

^a As in Table B.4.

^b Data points excluded in the analysis. Observed curvature at higher concentrations due to saturation of the cysteine dianions in CTAB micelles.

Table B.7 Rate constants for the cleavage of *p*-nitrophenyl alkanoates in varying concentration glycine (Gly) in the absence or presence of CTAB.^a

[Gly] _o (mM)	k _{obs} (s ⁻¹) [CTAB] _o = 0 mM [Br ⁻] _o = 5.0 mM	k _{obs} (s ⁻¹) [CTAB] _o = 5.0 mM [Br ⁻] _o = 0 mM
	Ester: acetate	
	(# Jen 135)	(# Jen 134)
0.0	0.00603	0.0135
2.5	0.0116	0.0174
5.0	0.0150	0.0216
10.0	0.0220	0.0300
15.0	0.0290	0.0385
20.0	0.0373	0.0473
25.0	0.0448	0.0553
Ester: butanoate		
	(# Jen 138)	(# Jen 137)
0.0	0.00447	0.0128
5.0	0.0076	0.0161
10.0	0.0100	0.0191
15.0	0.0131	0.0224
20.0	0.0167	0.0258
25.0	0.0181	0.0294

Ester: hexanoate		
	(# Jen 139)	(# Jen 136)
0.0	0.00498	0.0144
2.5	-	0.0164
5.0	0.00776	0.0187
10.0	0.01068	0.0218
15.0	0.01375	0.0240
20.0	0.01623	0.0303
25.0	0.01934	0.0366

Ester: octanoate		
	(# Jen 141)	(# Jen 140)
0.0	0.00285	0.0158
5.0	0.00461	0.0183
10.0	0.00867	0.0238
15.0	0.01022	0.0241
20.0	0.01131	0.0281
25.0	0.01519	0.0321

^a As in Table B.4.

Table B.8 Rate constants for the cleavage of *p*-nitrophenyl alkanoates in varying concentration of 2,2,2-trifluoroethanol (TFE) in the absence or presence of CTAB.^a

[TFE] _o (mM)	k _{obs} (s ⁻¹) [CTAB] _o = 0 mM [Br ⁻] _o = 5.0 mM	k _{obs} (s ⁻¹) [CTAB] _o = 5.0 mM [Br ⁻] _o = 0 mM
	Ester: acetate	
	(# Jen 131)	(# Jen 125)
0.00	0.0820	0.132
2.51	-	0.608
5.02	0.147	1.08
10.0	0.214	1.93
15.1	0.280	2.74
20.1	0.343	3.44
25.1	0.410	4.06

Ester: butanoate		
	(# Jen 132)	(# Jen 127)
0.00	0.0524	0.108
2.51	-	0.486
5.02	0.0910	0.871
10.0	0.129	1.58
15.1	0.164	2.26
20.1	0.201	2.82
25.1	0.234	3.34

Ester: hexanoate		
	(# Jen 130)	(# Jen 126)
0.00	0.0519	0.121
2.53	-	0.625
5.06	0.0892	1.10
10.1	0.129	1.94
15.2	0.166	2.71
20.2	0.205	3.37
25.3	0.243	3.81

Ester: octanoate		
	(# Jen 133)	(# Jen 128)
0.00	0.0467	0.133
2.51	-	0.611
5.02	0.0871	1.07
10.0	0.126	1.95
15.1	0.155	2.79
20.1	0.212	3.49
25.1	0.224	4.05

^a The total $[\text{Br}^-] = 5.0 \text{ mM}$, kept constant. Reaction medium in a 0.2 M phosphate buffer ($\text{H}_2(\text{PO}_3)^-$), standardized to a $\text{pH} = 11.6$. In the data analysis to find k_{CN} values, the fixed $[\text{CTAB}]$ was set to be $[\text{CTAB}]_0 - \text{cmc} = 4.95 \text{ mM}$

APPENDIX C - Data Relevant to Chapter VII

Table C.1 Rate constants for the cleavage of *p*-nitrophenyl acetate (pNPA) in varying concentration of amines in the absence or presence of CTAB.^a

	$k_{\text{obs}} (\text{s}^{-1})$	
	[Amine] _o	
	(mM)	
	[CTAB] _o = 0 mM	[CTAB] _o = 5.00 mM
	[Br ⁻] _o = 5.00 mM	[Br ⁻] _o = 0 mM
(a) butylamine	(# Jen 195)	(# Jen 194)
0.0	0.00966	0.0161
10.0	0.0466	0.0574
20.0	0.0952	0.101
30.1	0.137	0.146
40.1	0.190	0.191
50.1	0.238	0.241
(b) pentylamine	(# Jen 82)	(# Jen 83)
0.0	0.00803	0.0138
5.0	0.0268	0.0407
10.0	0.0448	0.0669
15.0	0.0593	0.0933
20.1	0.0750	0.117
25.1	0.108	0.143
(c) hexylamine	(# Jen 197)	(# Jen 196)
0.00	0.00911	0.0153
2.08	0.0178	0.0380
4.16	0.0264	0.0584
6.24	0.0360	0.0782
8.31	0.0456	0.0959
10.4	0.0543	0.113
(d) heptylamine	(# Jen 67)	(# Jen 68)
0.00	0.00848	0.0131
0.50	0.0102	0.0231
1.00	0.0121	0.0349
2.00	0.0160	0.0538
3.00	0.0199	0.0739
4.00	0.0233	0.0919
5.00	0.0268	0.105

(e) octylamine ^b		(# Jen 170)	
0.00		0.0144	
0.21		0.0216	
0.41		0.0297	
0.83		0.0509	
1.24		0.0691	
1.66		0.0921	
2.07		0.110	
(f) propylamine		(# Jen 75)	
0	0.00791		
5.0	0.0231		
25.0	0.0939		
50.0	0.205		
100	0.459		
150	0.708		
200	0.958		
250	1.21		
(f) propylamine ^c		(# Jen 190)	
0.0		0.0157	
10.0		0.0507	
19.9		0.0906	
29.9		0.133	
39.8		0.175	
49.8		0.229	
(g) isobutylamine		(# Jen 202)	(# Jen 203)
0.0	0.00968		0.0154
9.92	0.0469		0.047
19.9	0.0827		0.082
29.8	0.132		0.123
39.7	0.178		0.168
49.6	0.227		0.215
(h) isopentylamine		(# Jen 162)	
0	0.00962		
2.5	0.0208		
5.0	0.0317		
10.0	0.0538		
15.0	0.0767		
20.0	0.0996		
25.0	0.122		

<hr/>		
(h) isopentylamine	(# Jen 200)	
0		0.0151
5		0.0433
9.9		0.0703
14.9		0.0993
19.9		0.128
24.8		0.158
<hr/>		
(i) cyclopentylamine	(# Jen 173)	(# Jen 174)
0.0	0.00929	0.0140
2.62	0.0126	0.0161
5.25	0.0155	0.0202
10.5	0.0226	0.0251
15.7	0.0291	0.0291
21.0	0.0336	0.0385
26.2	0.0401	0.0442
<hr/>		
(j) cyclohexylamine	(# Jen 176)	(# Jen 178)
0.0	0.00925	0.0141
2.0	0.0103	0.0186
5.0	0.0122	0.0227
10.0	0.0161	0.0358
15.0	0.0201	0.0495
20.0	0.0236	0.0554
25.0	0.0270	0.0583
<hr/>		

^a Reaction conducted at 25 °C. The reaction buffer is 0.1 M sodium hydrogen carbonate standardized to pH = 10.6. The [pNPA] = 50.0 μM. The concentration of amines used is limited to their solubility.

^b Octylamine is insoluble in aqueous medium such that the rate constants in the absence of CTAB cannot be measured accurately.

^c At very high concentrations of propylamine the pH greatly affects the k_{obs} values, especially in the presence of CTAB.

Table C.2 Rate constants for the cleavage of *p*-nitrophenyl hexanoate (pNPH) in varying concentration of amine in the absence or presence of CTAB.^a

	$k_{\text{obs}} (\text{s}^{-1})$	
	[Amine] _o (mM)	[CTAB] _o = 0 mM
		[Br ⁻] _o = 5.00 mM
		[CTAB] _o = 5.00 mM
		[Br ⁻] _o = 0 mM
<hr/>		
(a) butylamine	(# Jen 193)	(# Jen 192)
0.0	0.00445	0.0174
10.0	0.0262	0.0257
20.1	0.0504	0.0339
30.1	0.0652	0.0418
40.1	0.0924	0.0477
50.2	0.116	0.0558
<hr/>		
(b) pentylamine	(# Jen 79)	(# Jen 77)
0.0	0.00334	0.0142
5.0	0.0144	0.0209
10.0	0.0236	0.0284
15.0	0.0315	0.0351
20.0	0.0426	0.0404
25.0	0.0537	0.0472
<hr/>		
(c) hexylamine	(# Jen 199)	(# Jen 198)
0.00	0.00410	0.0151
2.08	0.00898	0.0244
4.16	0.0126	0.0319
6.24	0.0181	0.0352
8.31	0.0231	0.0418
10.4	0.0274	0.0468
<hr/>		
(d) heptylamine	(# Jen 70)	(# Jen 71)
0.00	0.00442	0.0140
0.50	0.00563	0.0180
1.00	0.00647	0.0227
2.00	0.00697	0.0309
3.00	0.00995	0.0389
4.00	0.0107	0.0463
5.00	0.0144	0.0510
<hr/>		

(e) octylamine ^b		(# Jen 171)	
0.00		0.0178	
0.21		0.0191	
0.41		0.0228	
0.83		0.0318	
1.24		0.0411	
1.66		0.0490	
2.07		0.0563	
(f) propylamine		(# Jen 76)	
0	0.00514		
5.0	0.0125		
25.0	0.0449		
50.0	0.101		
100	0.217		
150	0.269		
200	0.395		
250	0.597		
(f) propylamine ^c		(# Jen 191)	
0.0		0.0164	
10.0		0.0214	
19.9		0.0256	
29.9		0.0314	
39.8		0.0372	
49.8		0.0426	
(g) isobutylamine		(# Jen 159)	(# Jen 161)
0.0	0.00516		0.0168
10.0	0.0207		0.0228
20.0	0.0380		0.0293
40.1	0.0945		0.0440
60.1	0.144		0.0606
80.2	0.150		0.0753
100	0.224		0.0532

(h) isopentylamine (# Jen 163)		
0	0.00516	
2.5	0.0114	
5.0	0.0170	
10.0	0.0287	
15.0	0.0407	
20.0	0.0519	
25.0	0.0618	

(h) isopentylamine (# Jen 165)		
0		0.0166
5		0.0228
9.9		0.0302
14.9		0.0376
19.9		0.0459
24.8		0.0484

(i) cyclopentylamine (# Jen 172)		(# Jen 175)
0.00	0.00475	0.0142
2.62	0.00613	0.0145
5.25	0.00724	0.0151
10.5	0.0110	0.0155
15.7	0.0137	0.0161
21.0	0.0161	0.0167
26.2	0.0188	0.0168

(j) cyclohexylamine (# Jen 178)		(# Jen 205)
0.0	0.00481	0.0157
2.0	0.00513	0.0158
5.0	0.00632	0.0163
10.0	0.00752	0.0162
15.0	0.00868	0.0163
20.0	0.00974	0.0164
25.0	0.0120	0.0163

^a Reaction conducted at 25 °C. The reaction buffer is 0.1 M sodium hydrogen carbonate standardized to pH = 10.6. The [pNPH] = 25.0 μM. The concentration of amines used is limited to their solubility.

^b Octylamine is insoluble in aqueous medium such that the rate constants in the absence of CTAB cannot be measured accurately.

^c At very high concentrations of propylamine the pH greatly affects the k_{obs} values, especially in the presence of CTAB.

Table C.3 Rate constants for the cleavage of *p*-nitrophenyl acetate (pNPA) in the presence of varying concentration of CTAB, constant $[\text{Br}^-]$, and constant amine concentration.^a

$[\text{CTAB}]_0$ (mM)	$[\text{Br}^-]_0$ (mM)	<i>n</i> -heptylamine ^b (# Jen 69)	<i>n</i> -propylamine ^b (# Jen 75)
0.00	5.00	0.0285	1.43
0.50	4.50	0.0373	1.39
1.00	4.00	0.0463	1.36
2.00	3.00	0.0619	1.32
3.00	2.00	0.0770	1.21
4.00	1.00	0.0907	1.19
5.00	0	0.105	1.13
		$K_S =$	22.3 ± 3.1^c
			$-^d$

^a $[\text{Br}^-]_0 = 5.0 - [\text{CTAB}]_0$, such that the total $[\text{Br}^-]$ is constant at 5.0 mM. The buffer is 0.1 M NaHCO_3 , standardized to a pH = 10.6. Concentration of pNPA = 50 μM . The nucleophile is hydroxide ion from the buffer and added amine.

^b The constant $[\text{amine}]_0$ are 5.0 mM for *n*-heptylamine, 250 for mM *n*-propylamine.

^c The values of K_S are found using equation 6.7 (Chapter VI, section 6.2), with the *cmc* found kinetically to average 0.050 mM, and kept constant throughout.

^d There is insufficient change in the rate constant to estimate K_S .

Table C.4 Rate constants for the cleavage of *p*-nitrophenyl hexanoate (pNPH) in the presence of varying concentration of CTAB_o, constant total [Br⁻], and constant amine concentration.

[CTAB] _o (mM)	[Br ⁻] _o (mM)	<i>n</i> -heptylamine ^b (# Jen 69b)	<i>n</i> -propylamine ^b (# Jen 75b)	<i>n</i> -pentylamine ^b (# Jen 81b)
0.00	5.00	0.0157	0.616	0.0562
0.25	4.75	0.0259	0.455	0.0506
0.50	4.50	0.0340	0.347	0.0514
1.00	4.00	0.0390	0.241	0.0504
2.00	3.00	0.0494	0.196	0.0460
3.00	2.00	0.0533	0.174	0.0480
4.00	1.00	0.0556	0.156	0.0482
5.00	0	0.0554	0.156	0.0471

$$K_S = 0.911 \pm 0.113^c \quad 0.388 \pm 0.025^c \quad -^d$$

^a [Br⁻]_o = 5.0 – [CTAB]_o, such that the total [Br⁻] is constant at 5.0 mM. The buffer in 0.1 M NaHCO₃, standardized to a pH = 10.6. Concentration of pNPH = 25 μM. The nucleophile is hydroxide ion from the buffer and added amine.

^b The constant [amine]_o are 5.0 mM for *n*-heptylamine, 25.0 mM for *n*-pentylamine, 250 mM for *n*-propylamine.

^c The values of K_S are found using equation 6.7 (Chapter VI, section 6.2), with the *cmc* found kinetically to average 0.050 mM, and kept constant throughout. This analysis works for inhibition or catalysis of the reaction.

^d There is insufficient change in the rate constant to estimate K_S.

Table C.5 Rate constants for the cleavage of *p*-nitrophenyl alkanoates in varying concentration of *n*-hexylamine in the absence or presence of CTAB.^a

[<i>n</i> -hexylamine] _o (mM)	k_{obs} (s ⁻¹)	
	[CTAB] _o = 0 mM	[CTAB] _o = 5.00 mM
	[Br ⁻] _o = 5.00 mM	[Br ⁻] _o = 0 mM
Ester: acetate		
	(# Jen197)	(# Jen196)
0.00	0.00911	0.0153
2.08	0.0178	0.0380
4.16	0.0264	0.0584
6.24	0.0360	0.0782
8.31	0.0456	0.0959
10.4	0.0543	0.113
Ester: propanoate		
	(# Jen 188)	(# Jen 189)
0.00	0.00753	0.0149
2.00	0.01165	0.0293
4.00	0.02075	0.0443
6.00	0.02779	0.0581
8.00	0.0345	0.0694
10.0	0.04081	0.0841
Ester: butanoate		
	(# Jen 180)	(# Jen 182)
0.00	0.00545	0.0122
2.01	0.00946	0.0209
4.02	0.0125	0.0276
6.04	0.0153	0.0352
8.05	0.0229	0.0428
10.1	0.0274	0.0509
Ester: pentanoate		
	(# Jen 155)	(# Jen 157)
0.00	0.00556	0.0142
2.01	0.00992	0.0228
4.02	0.0140	0.0297
6.04	0.0183	0.0371
8.05	0.0239	0.0450
10.1	0.0282	0.0545

Ester: hexanoate		
	(# Jen 199)	(# Jen 198)
0.00	0.00410	0.0151
2.08	0.00898	0.0244
4.16	0.0126	0.0319
6.24	0.0181	0.0352
8.31	0.0231	0.0418
10.4	0.0274	0.0468
Ester: heptanoate		
	(# Jen 187)	(# Jen 185)
0.00	0.00357	0.0147
2.04	0.00745	0.0223
4.08	0.0123	0.0280
6.11	0.0176	0.0353
8.15	0.0261	0.0387
10.2	0.0216	0.0406
Ester: octanoate ^b		
	(# Jen 186)	
0.00	0.0152	
2.04	0.0210	
4.08	0.0246	
6.11	0.0299	
8.15	0.0360	
10.2	0.0404	
Ester: decanoate ^b		
	(# Jen 187)	
0.00	0.0156	
2.00	0.0191	
4.00	0.0257	
6.00	0.0292	
8.00	0.0341	
10.0	0.0360	

^a Concentration of the esters are: [acetate - pentanoate] = 50 μ M, [hexanoate] = 25 μ M, [octanoate] = 2.5 μ M, [decanoate] = 1.5 μ M. The buffer is 0.1 M NaHCO₃, standardized to a pH = 10.6.

^b Rate constants in the absence of CTAB for the octanoate and decanoate esters cannot be measured accurately, and in the analysis the k_N values are taken to be the same as those for the heptanoate ester.

APPENDIX D - Data Relevant to Chapter VIII

Table D.1 Rate constants for the cleavage of *p*-nitrophenyl acetate (pNPA) by amino acid (AA) anions in the absence or presence of CTAB.^a

	$k_{\text{obs}} (\text{s}^{-1})$	
[AA] _o (mM)	[CTAB] _o = 0 mM [Br ⁻] _o = 5.00 mM	[CTAB] _o = 5.00 mM [Br ⁻] _o = 0 mM
<hr/>		
(a) serine	(# Jen 290)	(# Jen 291)
0.0	0.00936	0.0157
5.0	0.00963	0.0162
10.0	0.00993	0.0163
15.0	0.0103	0.0168
20.0	0.0109	0.0173
25.0	0.0114	0.0178
<hr/>		
(b) histidine	(# Jen 256)	(# Jen 257)
0.0	0.00790	0.0134
5.0	0.0103	0.0184
10.0	0.0127	0.0238
15.0	0.0151	0.0286
20.0	0.0175	0.0333
25.0	0.0199	0.0378
<hr/>		
(c) cysteine *	(# Jen 142)	(# Jen 143)
* The data for cysteine are the same as that in the thiolysis studies (Appendix B, Table A.6).		
<hr/>		
(d) glycine	(# Jen 286)	(# Jen 287)
0.0	0.00839	0.0135
5.0	0.0147	0.0216
10.0	0.0211	0.0300
15.0	0.0276	0.0385
20.0	0.0343	0.0473
25.0	0.0403	0.0553

(e) alanine	(# Jen 236)	(# Jen 238)
0.0	0.00827	0.0146
5.0	0.00990	0.0164
10.0	0.0115	0.0180
15.0	0.0135	0.0198
20.0	0.0150	0.0215
25.0	0.0168	0.0232
(f) 2-aminobutanoic acid	(# Jen 261)	(# Jen 262)
0.0	0.00829	0.0136
5.0	0.00965	0.0150
10.0	0.0111	0.0163
15.0	0.0124	0.0177
20.0	0.0139	0.0192
25.0	0.0153	0.0207
(g) norvaline	(# Jen 248)	(# Jen 250)
0.0	0.00824	0.0137
5.0	0.00978	0.0150
10.0	0.0114	0.0169
15.0	0.0130	0.0185
20.0	0.0146	0.0201
25.0	0.0162	0.0220
(h) valine	(# Jen 240)	(# Jen 241)
0.0	0.00866	0.0141
5.0	0.00974	0.0157
10.0	0.01082	0.0168
15.0	0.01197	0.0179
20.0	0.01312	0.0192
25.0	0.0143	0.0203
(i) norleucine	(# Jen 252)	(# Jen 255)
0.0	0.00801	0.0134
5.0	0.00963	0.0155
10.0	0.0112	0.0176
15.0	0.0127	0.0196
20.0	0.0142	0.0216
25.0	0.0159	0.0238

(j) leucine	(# Jen 244)	(# Jen 245)
0.0	0.00875	0.0138
5.0	0.00980	0.0158
10.0	0.0111	0.0174
15.0	0.0122	0.0189
20.0	0.0134	0.0205
25.0	0.0147	0.0222
(k) isoleucine	(# Jen 264)	(# Jen 267)
0.0	0.00885	0.0150
5.0	0.0106	0.0170
10.0	0.0124	0.0186
15.0	0.0141	0.0210
20.0	0.0158	0.0235
25.0	0.0176	0.0259
(l) 2-aminooctanoic acid	(# Jen 278)	(# Jen 279)
0	0.00782	0.0133
0.50	0.00851	0.0153
1.00	0.00907	0.0170
1.49	0.00965	0.0188
1.99	0.0102	0.0205
2.49	0.0109	0.0215
(m) 2-aminononanoic acid	(# Jen 282)	(# Jen 283)
0	0.00872	0.0146
0.390	0.00913	0.0171
0.781	0.00960	0.0191
1.17	0.0101	0.0213
1.56	0.0107	0.0234
1.95	0.0112	0.0253
(n) tryptophan ^b	(# Jen 268)	(# Jen 269)
0.0	0.0104	0.0168
5.0	-	0.0337
10.0	0.0120	0.0387
20.0	0.0140	0.0436
25.0	0.0150	0.0452

^a Reaction conducted at 25 °C. The reaction buffer is 0.1 M sodium hydrogen carbonate standardized to pH = 10.6. The [pNPA] = 50.0 μM.

^b Data for tryptophan could not be analyzed by the kinetic model.

Table D.2 Rate constants for the cleavage of *p*-nitrophenyl hexanoate (pNPH) by amino acid (AA) anions in the absence or presence of CTAB.^a

	$k_{\text{obs}} (\text{s}^{-1})$	
	[CTAB] ₀ = 0 mM	[CTAB] ₀ = 5.00 mM
	[Br ⁻] ₀ = 5.00 mM	[Br ⁻] ₀ = 0 mM
[AA] ₀ (mM)		
(a) serine	(# Jen 292)	(# Jen 293)
0.0	0.00488	0.0161
5.0	0.00507	0.0162
10.0	0.00522	0.0162
15.0	0.00548	-
20.0	0.00557	0.0164
25.0	0.00579	0.0165
(b) histidine	(# Jen 259)	(# Jen 258)
0.0	0.00418	0.0140
5.0	0.00578	0.0279
10.0	0.00770	0.0386
15.0	0.00920	0.0489
20.0	0.0104	0.0586
25.0	0.0119	0.0669
(c) cysteine *	(# Jen 146)	(# Jen 147)
* The data for cysteine are the same as that in the thiolysis studies (Appendix B, Table A.6).		
(d) glycine	(# Jen 289)	(# Jen 288)
0.0	0.00406	0.0140
5.0	0.00681	0.0178
10.0	0.00961	0.0215
15.0	0.0124	0.0252
20.0	0.0153	0.0282
25.0	0.0177	0.0316

(e) alanine	(# Jen 237)	(# Jen 239)
0.0	0.00429	0.0150
5.0	0.00506	0.0155
10.0	0.00576	0.0161
15.0	0.00646	0.0164
20.0	0.00705	0.0169
25.0	0.00764	0.0171
(f) 2-aminobutanoic acid	(# Jen 260)	(# Jen 263)
0.0	0.00461	0.01396
5.0	0.00528	0.01404
10.0	0.00578	0.0147
15.0	0.00622	0.0156
20.0	0.00649	0.0156
25.0	0.00672	0.0159
(g) norvaline	(# Jen 249)	(# Jen 251)
0.0	0.00477	0.0146
5.0	0.00543	0.0143
10.0	0.00586	0.0145
15.0	0.00656	0.0141
20.0	0.00717	0.0144
25.0	0.00782	0.0147
(h) valine	(# Jen 242)	(# Jen 243)
0.0	0.00494	0.0150
5.0	0.00541	0.0155
10.0	0.00577	0.0152
15.0	0.00626	0.0149
20.0	0.00653	0.0143
25.0	0.00692	0.0145
(i) norleucine	(# Jen 254)	(# Jen 253)
0.0	0.00457	0.0134
5.0	0.00496	0.0127
10.0	0.00556	0.0125
15.0	0.00624	0.0126
20.0	0.00672	0.0128
25.0	0.00737	0.0131

(j) leucine	(# Jen 247)	(# Jen 246)
0.0	0.00463	0.0148
5.0	0.00515	0.0137
10.0	0.00564	0.0134
15.0	0.00589	0.0132
20.0	0.00657	0.0130
25.0	0.00691	0.0133
(k) isoleucine	(# Jen 265)	(# Jen 266)
0.0	0.00470	0.0157
5.0	0.00484	0.0152
10.0	0.00584	0.0150
15.0	0.00676	0.0149
20.0	0.00770	0.0152
25.0	0.00825	0.0154
(l) 2-aminooctanoic acid	(# Jen 280)	(# Jen 281)
0.00	0.00426	0.0137
0.50	0.00470	0.0146
1.00	0.00488	0.0148
1.49	0.00522	0.0155
1.99	0.00542	0.0156
2.49	0.00577	0.0161
(m) 2-aminononanoic acid	(# Jen 284)	(# Jen 285)
0	0.00473	0.0142
0.390	0.00493	0.0154
0.781	0.00510	0.0158
1.17	0.00538	0.016
1.56	0.00558	0.0163
1.95	0.00601 ^c	0.0167

(n) tryptophan ^b	(# Jen 274)	(# Jen 272)
0.0	0.00492	0.0150
5.0	0.00581	0.0288
10.0	0.00682	0.0330
15.0	0.00746	0.0360
20.0	0.00791	0.0363
25.0	0.00833	0.0375

^a Reaction conducted at 25 °C. The Buffer is sodium hydrogen carbonate standardized to pH = 10.6. The [pNPH] = 25.0 μM.

^b Data for tryptophan in the presence of 5.0 mM CTAB could not be analyzed by the kinetic model.

^c Data excluded from the analysis because of curvature at higher [2-aminononanoic acid].